

**Taxonomic Utility and  
Phylogenetic Signal of  
Bone Microstructure within Sauropoda**

**Sarah-Jane Strachan**

**UCL**

**Thesis submitted for the degree of Doctor of Philosophy**

**May 2022**

# Declaration

I, Sarah-Jane Strachan, confirm that the work presented in this thesis is my own. Where information has been derived from other sources, I confirm this has been indicated in the thesis.

*“And if the microscope be thus essential to the full and true interpretation of the vegetable remains of a former world, it is not less indispensable to the investigator of the fossilized parts of animals.”*

Owen - first annual address 1841 (Quekett, 1849a)

# Abstract

Bone microstructural data can offer insight into the reconstruction of evolutionary histories of extinct taxa, the micro and histological level features within bone often being well preserved. However, to date, few papers have specifically explored the topic in this field, and we are not aware of any studies that have incorporated bone microstructure data formally into phylogenetic analyses for non-avian dinosaurs. To use this data in phylogenies, the presence and strength of a phylogenetic signal within the traits needs to be established. Therefore, the phylogenetic signal in various macro, micro, and histological variables in homologous regions of adult sauropod femora, one of the most widely sampled non-avian dinosaur taxa, was explored. The morphometry of secondary osteons and their canals, osteocytes from woven and parallel-fibered bone and from within secondary osteons, and several indices of robusticity, were tested for phylogenetic signal using Blomberg's  $K$ , Pagel's  $\lambda$ , Moran's  $I$  and Abouheif's  $C_{\text{mean}}$ . Osteocyte aspect ratio, circularity, and minimum diameter from all three bone types showed a strong phylogenetic signal according to Blomberg's  $K$  and were identified as suitable for coding and incorporating into phylogenetic analyses, thus improving our understanding of evolutionary patterns in deep time. In addition, three indices of robusticity,  $Rd/CT$ ,  $TI$ , and  $RI(CT)$ , showed a moderate phylogenetic signal according to Abouheif's  $C_{\text{mean}}$ . Secondary osteon and canal morphometrics, bone area and cortical thickness did not show a significant phylogenetic signal and were found to be positively correlated with body mass. Although not recommended for inclusion in phylogenetic analyses, these variables may still prove useful for species' identification and discrimination, particularly when used in a 'combined approach' with other data, such as gross morphology and stratigraphy, a recommended approach.

# Impact statement

Interest in non-avian dinosaurs and how they lived remains a fascinating topic to the public, often a child's first introduction to the study of science, helping to develop a love and curiosity of natural history. An under-researched area in this field is the use of palaeohistological data to explore evolutionary relationships and trajectories in deep time. With the advent of increasingly sophisticated, non-destructive imaging techniques, information is increasingly available, but so far, few papers have specifically explored this topic. Further, we are not aware of any studies that have formally incorporated palaeohistological data into phylogenetic analyses for non-avian dinosaurs. Therefore, bone microstructure data that could be used to inform phylogenetic research, clarify relationships, and the development of these taxa, is entirely absent.

The purpose of this research is to establish, within the taxonomic group, Sauropoda, whether the morphometry of various palaeohistological, micro-level variables, and indices of robusticity, display a phylogenetic signal, in which case these variables may be suitable for inclusion in phylogenetic analyses, and if so, to suggest how this might best be done. This will increase the resolution and accuracy of phylogenetic trees, increase understanding of evolutionary relationships within these taxa, and may provide additional data to help resolve problem taxa. This study will also explore whether bone microstructure data can be used to discriminate between, identify, or discount species. This is particularly challenging when dealing with fragmented material using standard morphological techniques, but possible due to the often-excellent preservation of biological structures at the microscopic level within fossilised bone.

Additionally, a novel method for calculating cortical thickness, that also illustrates bone compactness, is described, which is applicable to a variety of bone types of irregular shape. Further, a theoretical framework which helps position palaeohistology within broader evolutionary concepts is presented. Finally, a case study is used to demonstrate a recommended 'combined

approach' that utilises several lines of evidence, including bone microstructure data.

The information in this study will be of use to biologists, anthropologists, forensic scientists, and palaeontologists interested in the application of histological data to taxonomic and evolutionary questions, and the methodologies applicable to a wide range of taxa. Outside academia, it is hoped the application of the techniques and approaches outlined will increase the information available to excite and inform the public and future generations about non-avian dinosaurs, and further embed palaeontology as an inspiring gateway to science in general.

The theoretical framework was presented at ISPH 2017 by the author, and the alternative method for calculating cortical thickness at ISPH 2019. The combined approach case study is taken from a paper recently published by the author in *Nature Ecology and Evolution*, available in the supplementary materials.

# Contents

|  |             |
|--|-------------|
| <b>Abstract</b>                              | <b>i</b>    |
| <b>Impact statement</b>                      | <b>ii</b>   |
| <b>Contents</b>                              | <b>iv</b>   |
| <b>List of Tables</b>                        | <b>vii</b>  |
| <b>List of Figures</b>                       | <b>viii</b> |
| <b>Chapter 1 Introduction</b>                | <b>1</b>    |
| 1.1 Overview.....                            | 1           |
| 1.2 Palaeohistology .....                    | 3           |
| 1.3 Phylogenetic signal.....                 | 7           |
| 1.4 Phylogenetic and taxonomic utility ..... | 9           |
| 1.5 Secondary osteons .....                  | 9           |
| 1.6 Osteocytes.....                          | 11          |
| 1.7 Robusticity .....                        | 14          |
| 1.8 Bone matrix.....                         | 15          |
| 1.9 Vascular canals .....                    | 19          |
| 1.10 Non-avian dinosaur bone histology.....  | 22          |
| 1.11 Sauropod bone histology .....           | 23          |
| <b>Chapter 2 Signals in bone histology</b>   | <b>30</b>   |
| 2.1 The signals in bone.....                 | 30          |
| 2.2 Ontogeny and growth.....                 | 30          |
| 2.3 Mechanics.....                           | 37          |
| 2.4 Environment.....                         | 41          |

|                  |   |           |
|------------------|---|-----------|
| 2.5              | Taxonomy and Phylogeny .....  | 43        |
| 2.6              | Summary .....   | 46        |
| <b>Chapter 3</b> | <b>Materials and methods</b>  | <b>48</b> |
| 3.1              | Sauropod specimens .....  | 48        |
| 3.2              | Phylogenetic tree .....   | 52        |
| 3.3              | Specimen histology.....   | 53        |
| 3.4              | Definition of adult .....   | 54        |
| 3.5              | Skeletal element .....  | 55        |
| 3.6              | Measuring phylogenetic signal.....  | 55        |
| 3.7              | Imaging and analysis .....  | 61        |
| 3.8              | List of variables.....  | 65        |
| 3.9              | Statistical analysis.....   | 66        |
| 3.10             | Abbreviations .....   | 67        |
| 3.11             | Terminology .....   | 67        |
| <b>Chapter 4</b> | <b>A Novel Method to Quantify Cortical Thickness</b>                      | <b>69</b> |
| 4.1              | Introduction .....  | 69        |
| 4.2              | Materials and methods.....  | 71        |
| 4.3              | Results.....  | 72        |
| 4.4              | Discussion .....  | 78        |
| 4.5              | Conclusion.....   | 80        |
| <b>Chapter 5</b> | <b>Phylogenetic Signal of Bone Microstructure traits Within Sauropoda</b> | <b>82</b> |
| 5.1              | Introduction .....  | 82        |
| 5.2              | Materials and Methods.....  | 86        |
| 5.3              | Results.....  | 92        |
| 5.4              | Discussion .....  | 98        |

|                                  |  |            |
|----------------------------------|--|------------|
| 5.5                              | Limitations.....   | 109        |
| 5.6                              | Conclusion .....   | 110        |
| 5.7                              | Recommendations .....                                      | 111        |
| <b>Chapter 6</b>                 | <b>Correlation of Bone Histology Traits with Body Mass</b> | <b>114</b> |
| 6.1                              | Introduction .....   | 114        |
| 6.2                              | Materials and Methods.....                                 | 115        |
| 6.3                              | Results.....   | 118        |
| 6.4                              | Discussion .....   | 122        |
| 6.5                              | Conclusion .....   | 126        |
| <b>Chapter 7</b>                 | <b>Theoretical Framework</b>                               | <b>128</b> |
| 7.1                              | Introduction .....   | 128        |
| 7.2                              | Interrelatedness of signals .....                          | 128        |
| 7.3                              | Theoretical framework .....                                | 131        |
| 7.4                              | Adding the four 'signals'.....                             | 138        |
| 7.5                              | Conclusion .....   | 140        |
| <b>Chapter 8</b>                 | <b>Taxonomic Utility; a Combined Approach</b>              | <b>141</b> |
| 8.1                              | Introduction .....   | 141        |
| 8.2                              | A case study .....   | 142        |
| 8.3                              | Discussion .....   | 145        |
| 8.4                              | Conclusion .....   | 148        |
| <b>Chapter 9</b>                 | <b>Conclusions and future work</b>                         | <b>149</b> |
| <b>References</b>                | Error! Bookmark not defined.                               |            |
| <b>Supplementary information</b> |  | <b>199</b> |

# List of Tables

|  |     |
|--|-----|
| <b>Table 3.1</b> List of specimens in the current study.....                   | 49  |
| <b>Table 3.2</b> List of variables used in current study.....                  | 65  |
| <b>Table 4.1</b> Cortical thickness measurements estimated from CP and CB .... | 77  |
| <b>Table 5.1</b> Phylogenetic signal in osteocyte morphometrics.....           | 94  |
| <b>Table 5.2</b> Phylogenetic signal in femoral robusticity .....              | 97  |
| <b>Table 6.1</b> Spearman's correlation of variables with scale.....           | 119 |
| <b>Table 6.2</b> PGLS correlation of macro and micro variables with scale..... | 121 |

# List of Figures

|                   |   |     |
|-------------------|---|-----|
| <b>Figure 1.1</b> | Schematic diagram illustrating the hierarchical levels of bone. . .           | 5   |
| <b>Figure 1.2</b> | Bone histology materials.....   | 6   |
| <b>Figure 1.3</b> | Haversian bone tissue and secondary osteon..                                  | 11  |
| <b>Figure 1.4</b> | Osteocytes in fossilised and human bone.....                                  | 12  |
| <b>Figure 1.5</b> | Bone matrix types..   | 16  |
| <b>Figure 1.6</b> | Fibrolamellar bone. ....  | 19  |
| <b>Figure 1.7</b> | Orientation of vascular canals in primary bone matrix.....                    | 21  |
| <b>Figure 1.8</b> | Sauropod cortical bone. ....  | 25  |
| <b>Figure 1.9</b> | Schematic comparison of Tendaguru sauropod long bone histology.....           | 26  |
| <b>Figure 2.1</b> | The four signals of palaeohistology.....                                      | 31  |
| <b>Figure 2.2</b> | Cyclical growth marks. ....   | 36  |
| <b>Figure 3.1</b> | Cladogram of Neosauropoda. ....   | 52  |
| <b>Figure 3.2</b> | Osteocyte lacunae within the cortical bone of <i>Dicraeosaurus</i> ... ..     | 62  |
| <b>Figure 3.3</b> | Workflow process for histomorphometric analysis. ....                         | 63  |
| <b>Figure 4.1</b> | Image processing workflow of CP and CB images. ....                           | 73  |
| <b>Figure 4.2</b> | Image processing of compactness bar of <i>Ampelosaurus atacis</i> C3 638..... | 75  |
| <b>Figure 4.3</b> | Image processing of CP and CB without thresholding. ....                      | 76  |
| <b>Figure 4.4</b> | Comparison of CPs across two sauropod taxa. ....                              | 79  |
| <b>Figure 5.1</b> | Phylogenetic signal in osteocyte morphometrics. ....                          | 93  |
| <b>Figure 5.2</b> | Box and whisker plots showing comparison of osteocyte morphometry.....        | 96  |
| <b>Figure 5.3</b> | Osteocyte morphometrics mapped onto phylogeny. ....                           | 101 |
| <b>Figure 5.4</b> | PCA analysis of bone histology morphometrics. ....                            | 104 |
| <b>Figure 7.1</b> | Constructional morphology. ....   | 130 |

|   |     |
|---|-----|
| <b>Figure 7.2</b> Three principal components of bone growth rate. ....                          | 131 |
| <b>Figure 7.3</b> Theoretical framework linking form, function, behaviour, and morphology. .... | 133 |
| <b>Figure 7.4</b> Theoretical framework extended. ....  | 135 |
| <b>Figure 7.5</b> Constraints and correlations within the framework. ....                       | 137 |
| <b>Figure 7.6</b> Theoretical framework with four 'signals' overlaid. ....                      | 139 |
| <b>Figure 8.1</b> Images of <i>Spicomellus afer</i> . ....                                      | 144 |
| <b>Figure 8.2</b> Histology of <i>Spicomellus afer</i> . ....                                   | 145 |

# Chapter 1 Introduction

## 1.1 Overview

Relationships between extinct taxa are traditionally explored using morphological traits at the macroscopic level, but in some cases this data is insufficient or inconclusive. Bone microstructure traits, as with other phenotypic traits, tend to be associated with phylogenetic relatedness (Gould, 1977), and may therefore offer additional insight into the evolutionary history of extinct taxa (de Ricqlès, 2021 and references therein).

However, few phylogenetic analyses incorporate bone microstructure data. This is in part due to the interrelatedness and complex nature of factors that influence the development of these tissues (see Padian & Lamm, 2013 and Chapter 2), the historically destructive nature of the process, and challenges inherent in quantifying microscopic structures in fossilised material. Although the use of this data for taxonomic purposes, to identify or discriminate between taxa, is enjoying something of a revival (de Ricqlès, 2011), the lack of inclusion of bone microstructure data in evolutionary studies means that a potentially informative data source is largely absent.

Phylogenetic signal has previously been identified in micro and histological data in sauropsids (Cubo et al., 2005), amniotes (Legendre et al., 2013) and palaeognathus birds (Legendre et al., 2014). However, the signal is inconsistent and affected by a variety of factors such as sample size, calculation method, tree topology, and body mass (Felder et al., 2017; Münkemüller et al., 2012; Revell, 2010). In addition, there is general agreement that it is important to compare homologous skeletal elements, comparable developmental stage, and locomotor style (de Ricqlès et al., 2008a; Padian & Lamm, 2013).

This study looks at the morphometry of various histological and micro-level traits within fossilised sauropod femora, to see if, within a constrained

taxonomic group, a phylogenetic signal (Blomberg & Garland, 2002; Klingenberg & Gidaszewski, 2010) is present. Further, to consider whether these traits could be considered suitable for inclusion in phylogenetic analyses to increase our understanding of the relationships between these taxa in deep time. In addition, the utility of bone microstructure data is assessed for taxonomic purposes.

Sauropods are one of the most widely sampled non-avian dinosaur taxa (Sander, 2000a) and large bone size and a graviportal locomotor style means that more cellular data can be gathered, and variance due to biomechanics can be limited. We are not aware of any studies that have compared homologous sections of homologous bones of closely related taxa at a similar developmental stage.

This study will address the following questions:

- Is there a phylogenetic signal in the morphometry of secondary osteons, canals and osteocytes?
- Is there phylogenetic signal in cortical thickness, bone area and indices of robusticity that utilise micro-level variables?
- If there is a phylogenetic signal, are these variables suitable to include in phylogenetic analyses?
- If so, how might this be achieved?
- Is there size dependent variation?
- Do these variables have taxonomic utility?
- If so, how might they best be incorporated into palaeontological research?

Chapter 1 begins by introducing the basic terms and concepts used in this study. Chapter 2 summarises and reviews the literature on the signals that influence bone microstructure. Chapter 3 describes the main materials and methods used in the study, and Chapter 4 describes a novel method developed to quantify cortical width in sauropods. Chapter 5 explores phylogenetic signal in various micro and histological traits in sauropod femora,

and Chapter 6 explores correlation with scale. In Chapter 7 a theoretical framework is proposed which attempts to visualise the various complex influences on bone histology and positions them within broader macroevolutionary themes. Chapter 8 explores the taxonomic use of palaeohistology, and conclusions and future work are summarised in Chapter 9.

## 1.2 Palaeohistology

Structures within the body can be studied at various levels of the biological hierarchy, defined as macrostructural (~1 m – 1 mm), microstructural (1 mm – 100 µm), and sub microstructural (100 µm – 1 µm, **Figure 1.1**) (Francillon-Vieillot et al., 1990; Rho et al., 1998). Palaeohistology is the study of ancient tissues and organs of the body at the sub microstructural level, although in practice micro-scale structures are often included (de Buffrénil et al., 2021; Pawlina, 2016). The material under investigation in palaeontological studies is usually shell, teeth, scales, osteoderms and skeletal bone from vertebrates and invertebrates, and is often remarkably well preserved at the cellular level. For vertebrate studies in deep time, palaeohistology often becomes synonymous with osteo-histology, the study of microscopic structures within bone (de Buffrénil et al., 2021; Padian & Lamm, 2013).

Palaeohistology is a rapidly expanding area of study and has been used to test hypotheses in extinct taxa as widely ranging as: gender in *Tyrannosaurus* (Schweitzer et al., 2005), *Dysalotosaurus* (Hubner, 2012) and *Confuciusornis* (Chinsamy et al., 2013); growth rates in sauropods (Griebeler et al., 2013; Sander, 2000b) and *Archaeopteryx* (Erickson et al., 2009); ankylosaur tail club mechanics (Arbour, 2009); and precociality in the titanosaur *Rapetosaurus* (Curry Rogers et al., 2016). Palaeohistology can offer insights that may not be possible via any other analytical method for extinct taxa, for example: age; metabolism; growth strategies; life history or developmental stage (Horner & Padian, 2004; Klein & Sander, 2008; Legendre et al., 2016; Padian et al., 2001, 2004; Scheyer et al., 2010; Stein et al., 2010).

There are several seminal texts on fossil bone histology, notably by Armand de Ricqlès (de Ricqlès, 1975; 1976; 1977; 1978) and Francillon-Vieillot et al. (1990), which are often referenced regarding terminology. Reid (1996) provides a good summary, and work by Enlow (Enlow, 1955; Enlow & Brown, 1956, 1957, 1958) provides a useful comparative reference of fossil and bone tissue types from a variety of organisms. Advances, discoveries and approaches in vertebrate palaeohistology were summarised by Houssaye (2014), demonstrating the value and breadth of the contribution that palaeohistology can make to understanding biological traits in extinct taxa. A review of dinosaur palaeohistology by Bailleul et al. (2019) summarised further developments in the field, including the relatively new application of biomolecular and biochemical techniques to preserved soft tissue in fossil specimens. Work by Padian and Lamm (2013), Chinsamy-Turan (2005), and recently, de Buffrénil et al. (2021), provide broad coverage of the subject and illustrate the rapid development and application of novel techniques.

Palaeohistological analysis is traditionally carried out via microscopic analysis of thin sections using a standard petrological microscope, although increasingly Micro-CT scanning, SEM and 3D synchrotron imaging is used (see summaries by Curtin et al., 2012; Houssaye, 2014; Sanchez et al., 2012; Urino et al., 2013; Wood & de Pietri, 2015). For standard petrological microscope preparation, transverse slices are cut from the bone, or, for very large bones, a cylindrical core is extracted (Sander, 2000a). Drill coring has some limitations (see Erickson, 2014) but is the only practical way of taking samples of very large bones such as sauropod long bones. Samples are stabilised, measured, cast, and thin sections prepared as for geological samples for viewing under transmitted plane polarised (PPL) and cross polarised light (XPL) (**Figure 1.2**). This is currently the cheapest method that offers a suitable level of resolution for most histological study, and therefore the most common technique employed. As it involves a destructive process, access to material can be limited, and thin sections are a precious resource that are frequently re-examined by different researchers, as with much of the material in this study.

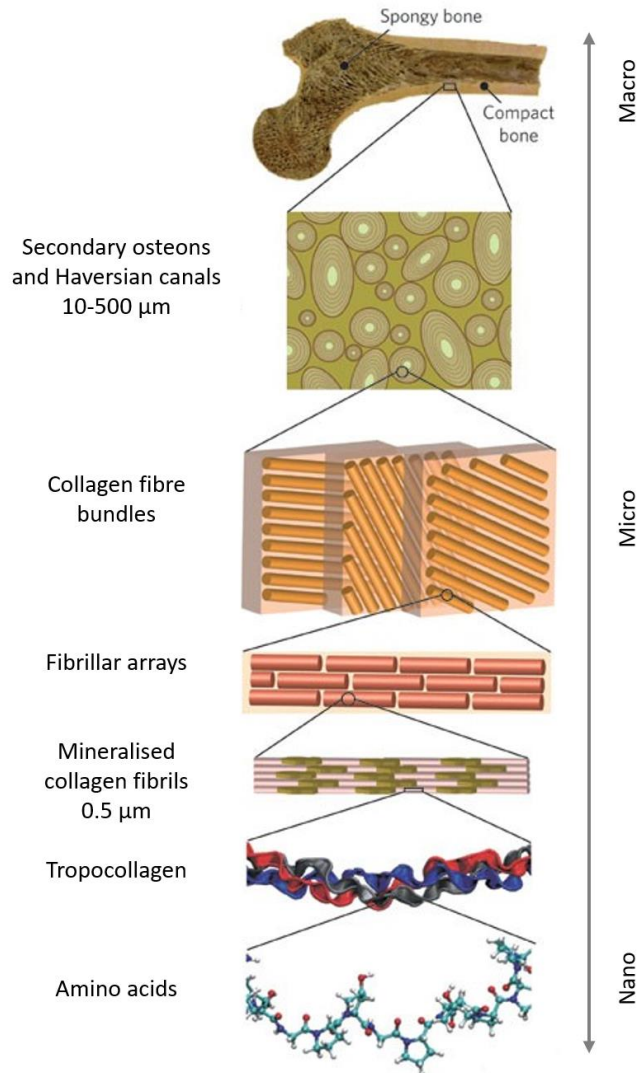


**Figure 1.1 Schematic diagram illustrating the hierarchical levels of bone.**

At the macro-level, compact bone surrounds a central core of spongy bone. The microstructure of bone contains structures such as secondary osteons. Blood vessels and nerve fibres are housed within the central canal. Individual collagen fibrils form arrays, which are packaged together to form fibre bundles, and in turn are arranged in various orientations to form the lamellae of the secondary osteon. Modified from Launey et al. (2010).



**Figure 1.2 Bone histology materials.** From top left, cast and mold of section, embedded section of bone, original (repaired) bone of *Tyrannosaurus rex*, and preparatory and ground thin section slides. Materials from Museum of the Rockies, Montana, photograph by S. Strachan.

Traditionally, palaeohistological study has focussed on three objectives: to accurately describe and record observations; to understand and explain the underlying biological mechanisms; and to interpret what those observations might mean, including functional interpretations and evolutionary patterns. Throughout, reference to homologous features in extant organisms and actualistic reasoning (inference of the unknown from the known) is applied. Growth rates in fossil taxa, for example, are inferred from bone accretion rates and associated vascular canal orientation from extant organisms in which growth rates are known (Castanet et al., 1996, 2000; de Margerie et al., 2002, 2004; Starck & Chinsamy, 2002). There are a number of bone histology structures available to the palaeohistologist to study, including: the degree of spatial organisation of the bone matrix; size and orientation of vascular canals; primary and secondary osteons; and osteocyte lacunae. Structures visible in extinct vertebrate bone are considered analogous to those observed in modern

organisms. These structures can be studied qualitatively or quantitatively, in terms of density, shape and size.

Over time, palaeohistological study has generally moved from qualitative to quantitative analysis due to the availability of technology and advanced software, and increasingly sophisticated statistical methods are now routinely used to test underlying assumptions. De Ricqlès commented on the trend of early histologists (including himself) “towards an *a priori* taxonomic interpretation of the histological data” (de Ricqlès, 2011), and on the emphasis of identifying characters with a systematic value. Subsequently, there has been a focus on trying to understand growth trajectories, mechanics, and life history traits of extinct organisms from bone histology (Cubo et al., 2008; de Ricqlès et al., 2004; 2011). More recently, attention has returned to exploring the significance of a phylogenetic signal at the histological level, as in this study.

### **1.3 Phylogenetic signal**

The strict meaning of phylogenetic signal in systematics refers to secondary homology, similarity arising from shared common ancestry (Münkemüller et al., 2012). This is often considered synonymous with synapomorphy, a shared derived character or trait that distinguishes a clade (de Pinna, 1991). There are, however, very few examples of discrete histological character states that are unique to, and therefore diagnostic of, a particular clade, the acellular bone of some teleost fish (Moss, 1961; Meunier, 2011), and endochondral bone tissue in Osteichthyes (Janvier, 1996) being two of the few examples. Therefore, histological features are generally uninformative in this context (Cubo et al., 2021), and, particularly for fossil taxa, a slightly more relaxed definition of phylogenetic signal is more practical. Therefore, we define phylogenetic signal as the “tendency for related species to resemble each other more than they resemble species drawn at random from the tree” (Blomberg & Garland, 2002), or “the degree to which phylogenetic relatedness among taxa is associated with their phenotypic similarity” (Klingenberg & Gidaszewski, 2010). When a phylogenetic signal is present and said to be

strong, closely related taxa are more similar than distantly related taxa, and as phylogenetic distance increases, similarity decreases, resulting in divergent phylogenetic trees. This is expected under genetic drift and natural selection, as these processes should approximate a Brownian Motion model of evolution (Revell et al., 2008). Brownian Motion (BM) is a gradual, random, non-directional trait change through time (Felsenstein, 1985; Harvey & Pagel, 1991). According to a BM model, trait divergence among species is expected to increase proportionally with the phylogenetic distance between them. Evolutionary distance between taxa is therefore proportional to tree branch lengths. Stochastic evolution along a hierarchical tree will also show the presence of a phylogenetic signal as evolutionary change is not independent, resulting in recently diverged lineages being more similar than more distantly related lineages (Münkemüller et al., 2012).

Phylogenetic signal has been observed in a variety of microanatomical and palaeohistological traits, including: vascular density and canal orientation; bone size; cortical thickness; compactness; secondary osteon area; osteocyte lacunae size and cell density (Cubo et al., 2005; Felder et al., 2017; Houssaye et al., 2016; Legendre et al., 2013; Legendre et al., 2014; Marín-Moratalla et al., 2014; Mitchell et al., 2017; Ponton et al., 2007; Stein & Werner, 2013 - see Chapter 6 for more details). It should be noted, however, that the significance and strength of phylogenetic signal is influenced by many factors, including: taxonomic level; sample size; topology; calculation method; skeletal element; and the biological variable under investigation (Losos, 2008; Pearman et al., 2008).

A central debate in the literature, is the degree to which bone histology represents a plastic response to intrinsic and extrinsic influences (e.g., the environment, ontogeny, and mechanical stress) as opposed to a predetermined, phylogenetic signal (Laurin et al., 2004; Cubo et al., 2008; Marín-Moratalla et al., 2014). De Ricqlès' opinion, expressed in several studies, is that a phylogenetic signal in bone histology is present, but likely to be weakly expressed (de Ricqlès et al., 2004, 2008; de Ricqlès, 2011). However, he does conclude that "bone tissue phenotypes can reflect a

phylogenetic signal at supraspecific levels if homologous elements are used, and if ontogenetic trajectories and size-dependent differences are taken into consideration” (de Ricqlès et al., 2008). Padian (2013) also agrees that “the phylogenetic ‘signal’ in bone is persistent, but it is never the strongest signal”.

## 1.4 Phylogenetic and taxonomic utility

Discussion of the phylogenetic ‘signal’ within bone (sensu Padian, 2013, see Chapter 2), covers observable differences between taxonomic groups. As such, it encompasses both a taxonomic and phylogenetic purpose. For clarity, we propose a distinction is made here between ‘taxonomic utility’, and ‘phylogenetic utility’. A trait with taxonomic utility is defined in the current study as one that is: uniquely present, or lacking in, or highly typical of a species or taxonomic group; and can be used to classify or differentiate between taxa. A trait with phylogenetic utility is here defined as one that: arises from shared ancestry; contains a strong, but not overly strong, phylogenetic signal; is not correlated strongly with other variables; is comparable across species and taxonomic groups. Therefore, a trait with phylogenetic utility can be used to construct evolutionary relationships between taxa, and taxonomic utility can be thought of as a more relaxed state than phylogenetic utility and may be more strongly influenced by external factors such as the environment.

Phylogenetic utility is therefore distinct from phylogenetic signal, which for the current study, refers to the degree of correlation with an established phylogenetic tree, using various calculation methods (see Chapter 5).

## 1.5 Secondary osteons

Mature sauropod long bones often show a high degree of reworking by secondary osteons in the bone cortex (**Figure 1.3**). A secondary osteon, also called a Haversian system, is a cylindrical structure of lamellar bone that replaces primary bone, and (unlike primary osteons), is surrounded by a cement sheath that marks the bone resorption boundary (Reid, 1983). In histological thin sections, secondary osteons are visible as circular features

enclosed by a dark line. They are formed via the 'basic multicellular unit of bone' (BMU), which consists of osteoclasts (cells that break down bone tissue), and osteoblasts (bone building cells) working in tandem to dig a tunnel through existing bone (a 'cutting cone'), and subsequently filling the tunnel with new bone (a 'closing cone'). A central channel is left which houses nerves, lymph, and blood vessels. This vascular canal is also called a Haversian canal. New bone is laid down by the osteoblasts concentrically from the tunnel wall towards the centre, and some osteoblasts flatten and become embedded in the lining cells of the canal, forming osteocytes (Parfitt, 1994; van Oers et al., 2014). The Haversian canal is typically oriented along the longitudinal direction of the diaphysis of long bones (Petrtyl et al., 1996). Multiple generations of overlapping secondary osteons are described as Haversian bone (**Figure 1.3**). Dense Haversian bone tissue contains closely packed Haversian systems with reduced or absent interstitial systems or lamellae (Hillier & Bell, 2007).

Within vertebrates, only birds and mammals show extensive Haversian remodelling which is partly related to body size, being more extensive in larger birds and mammals of over 2kg mass (Currey, 2002). Secondary osteons serve a variety of functions including periosteal resorption and remodelling in response to mechanical stress (Riggs et al., 1993); repair or limitation of microcracks (Bentolila et al., 1998); regulating mineral homeostasis (Cullinane, 2002; Teti & Zallone, 2009); and regeneration of necrotic bone tissue (Enlow, 1962) and pathologies (Annè et al., 2015). They also appear within cancellous endosteal bone, at muscle relocation sites, and in response to ageing (Currey, 1964; Enlow, 1962).

Enlow (1962) noted "When secondary Haversian systems do occur, they are always found in predictable locations and patterns of distribution." For example, extensive secondary remodelling associated with ageing in sauropods (as well as extant animals and humans) advances from the inner cortex of the bone outwards (Boskey & Coleman, 2010; Erickson, 2005; Klein & Sander, 2008; Sander, 2000a), whereas pathological remodelling clusters around the injured area of bone (Annè et al., 2015). The pattern of remodelling may be useful in distinguishing between species or clades, such as the

distinctive pattern of secondary osteons seen in sauropods (Sander, 2000a), (see also **Figure 1.9**). However, it is not always easy to discern the specific cause, as the resulting Haversian systems are mechanically the same, and different influences can cause remodelling in the same bone area.

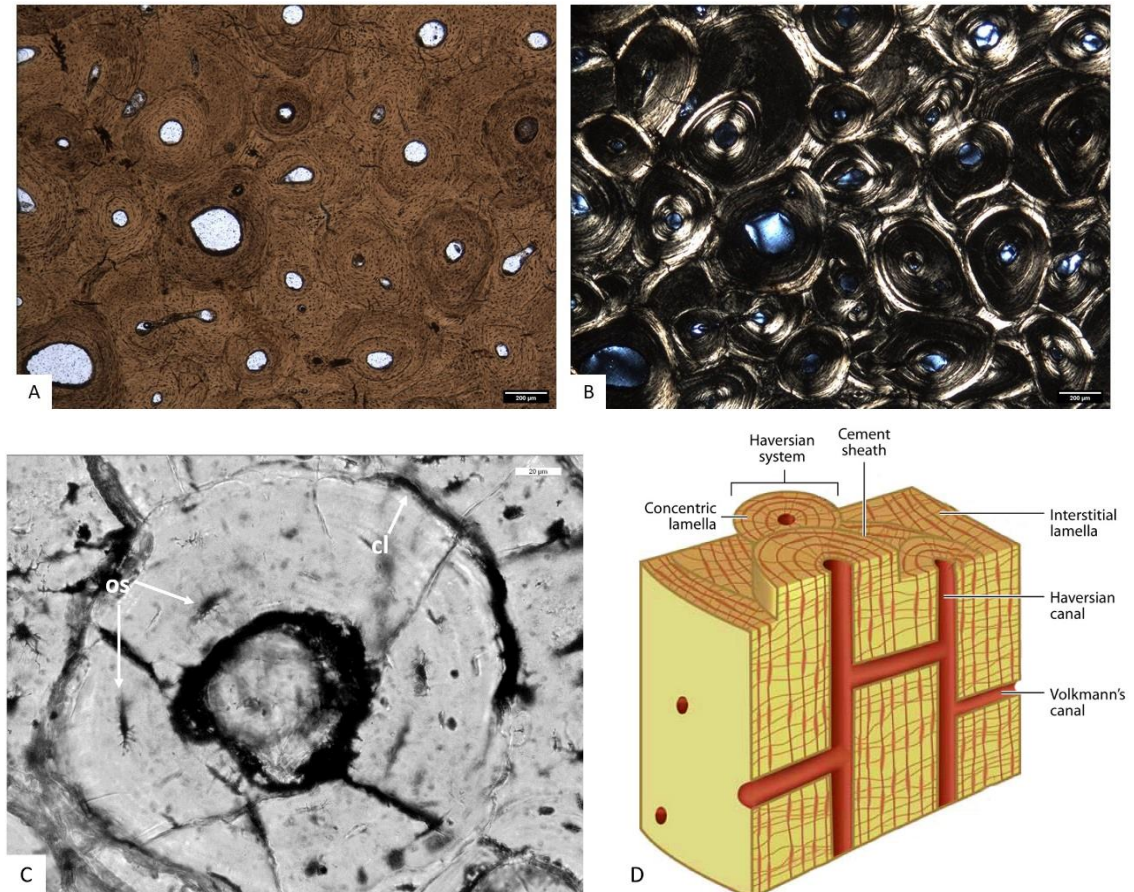


**Figure 1.3 Haversian bone tissue and secondary osteon.** **A)** Cortical bone of the Ankylosaur *Euoplocephalus*, showing at least 3 generations of overlapping secondary osteons in heavily remodelled Haversian bone. Image taken in plane polarised light (PPL). **B)** Same field of view as A) under cross polarised light (XPL), which enhances the cement lines and lamellar structure of the Haversian system. **C)** Secondary osteon, or 'Haversian system' from *Giraffatitan*, showing cement line (cl) and osteocyte lacunae (ol). **D)** Schematic diagram illustrating the central canal structure within the Haversian system, from Launey et al. (2010). Photographs by S. Strachan.

## 1.6 Osteocytes

Osteocytes are the most numerous cells in mature bone and arise from osteoblast cells, the result of osteoblast differentiation of mesenchymal stem

cells (Hall, 2015). Osteoblasts secrete unmineralised bone material called osteoid, and some become encased in the bone matrix where they become osteocytes. They then create a complex network of interconnected cytoplasmic processes which sit in channels called canaliculi, surrounded by extracellular fluid (Bonewald, 2011; Freemont, 1993; Parfitt, 1994) (**Figure 1.4**).

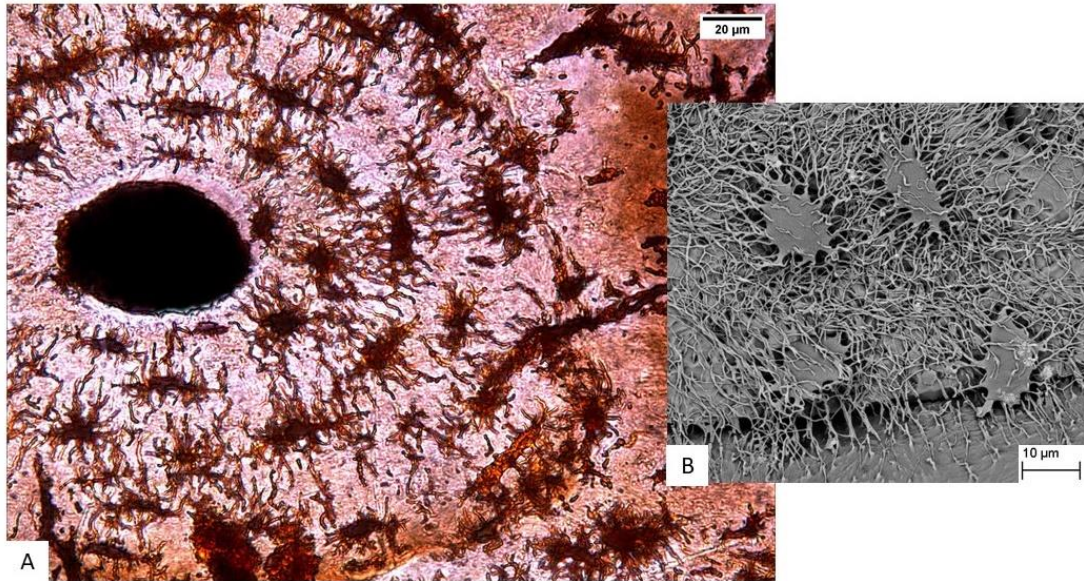


**Figure 1.4 Osteocytes in fossilised and human bone. A)** Osteocyte lacunae within secondary osteon in an *Apatosaurus* femur. The canalicular network is often more heavily developed on the side of the osteocyte facing the central canal (PPL). **B)** SEM image of human osteocytes. Image A) by S. Strachan, and B) by K. Mackenzie, University of Aberdeen.

Osteocytes play a role in communication and mineral homeostasis. In addition, they perform a mechanosensing function; signalling bone building and resorption in response to mechanical loading experienced by the skeleton (Aarden et al., 1994; Bonewald & Johnson, 2008; Bonewald, 2011; van Oers et al., 2014); and repairing microcracks by inducing osteocyte apoptosis and subsequent bone resorption (Enlow, 1962; Bentolila et al., 1998; Verborgt et al., 2000).

Osteocytes are not generally found in fossilised specimens due to cellular degradation and the process of permineralisation that destroys the original

cellular structure. However, the lacuno-canalicular spaces that an osteocyte and its processes would have resided in are often clearly preserved in fossilised bone (visible as dark ovate shapes under a microscope in **Figure 1.4**), and it is accepted that these are representative of the size, shape and orientation of the original cell (Padian & Lamm, 2013; Hall, 2015). As such, they are measured as a proxy for the original bone cell and its processes. Strictly speaking therefore, 'osteocytes' in fossil bone usually refer to lacunae, or lacuno-canalicular spaces; however, in practice (as in the current study), they are often called osteocytes, even though the cellular structure is not present.

It has been shown in studies of vertebrates that osteocyte morphology is associated with different types of bone fibre matrix, and hence rates of bone deposition. Volumetrically larger and more rounded osteocytes are typically present in the faster growing and more disorganised matrix of woven bone, and smaller, more ovate, and regularly arranged osteocytes are found in more organised, slower growing lamellar and parallel-fibered bone (Cadena & Schweitzer, 2012; Canè et al., 1982; Davesne et al., 2020; Ferretti & Palumbo, 2021; Grunmeier & D'Emic, 2019; Remaggi et al., 1998; Sanchez et al., 2013; although see Houssaye et al., 2013). Marotti (1979) suggests this is due to osteoblasts that deposit bone faster under static osteogenesis (in woven bone) being larger and giving rise to larger osteocytes.

It is important to understand the interrelated nature of osteocytes, secondary osteons, remodelling, and bone development. Bone matrix is laid down by osteoblasts, some of which turn into osteocytes. Bone renewal, repair and remodelling involves the development of secondary osteons, which contain osteocytes within their lamellae. Therefore, osteocytes and osteons are relevant to bone development and growth and are influenced by extrinsic as well as intrinsic factors (for more on these factors see Chapters 2 and 7).

## 1.7 Robusticity

Some micro-anatomical data, such as cortical thickness, can be used to calculate skeletal robusticity. Robusticity is a measure of bone strength, as described by its size and shape (Stock & Shaw, 2007). Measures of long bone robusticity (or the opposite, gracility) have previously been explored in extant and extinct taxa for a variety of purposes: to investigate sexual size dimorphism (Riesenfeld, 1978); functional adaptation (Riesenfeld, 1972; Habib & Ruff, 2008; Miskiewicz & Mahoney, 2016); growth (Carrano, 2001; Christiansen, 2007; Kilbourne & Makovicky, 2010; Kokshenev & Christiansen, 2010; Griebeler et al., 2013); and weight (Anderson et al., 1985). Robusticity has been used to explore species differentiation (Bonnar, 2004; Swanepoel, 2003; Swanepoel & Steyn, 2011; Taylor, 2009); to distinguish between human and non-human bone (Phatsara et al., 2016); and study phylogenetic trends (Chan, 2017).

Various different measures have been used to calculate robusticity such as: Riesenfeld's total robusticity quotient (TRQ), which is bone length  $^{1/3}$  bone weight (Riesenfeld, 1972); diaphyseal thickness standardised to bone length (Martin & Saller, 1957); relative cortical thickness (K), the ratio of inner to outer bone diameter (Currey & Alexander, 1985); and Gracility index (GI), the ratio between bone length and minimum diameter (Taylor, 2009). Others have applied beam theory by determining periosteal and endosteal contours to quantify cross-sectional geometries (for a review of different methods see Stock & Shaw, 2007). When calculating robusticity in fossilised specimens some methods, such as measuring ash content to estimate bone weight, as used by Riesenfeld (1972), are not possible due to almost complete mineralisation of the material. In addition, when using slides of core samples, cortical bone area may not be known, and it may not be possible to ascertain true bone or medullary centre of the section. Measures of robusticity that use circumference, however, are possible to calculate in most cases, and are therefore a popular choice for fossilised material.

Few of the studies exploring species differentiation and robusticity mentioned above have tested their results statistically, instead they have looked at the overlap in raw data. Therefore, we cannot be sure whether a significant difference exists, and whether differences are due to evolutionary relationships or some other factor. Variation in locomotor style, for example, influences bone histology through remodelling by secondary osteons within the cortex, as well as impacting the external shape and circumference of the long bones as a result of varying mechanical stresses. Further analysis is needed to conclude that differences are not due to these, or similar biomechanical influences.

## **1.8 Bone matrix**

Establishing bone matrix type, (lamellar, parallel-fibered, or woven) is one of the first broad categories used to describe a specimen in most palaeohistological studies and as such is worth more attention here.

### **Cortical bone matrix types**

There are three main types of cortical bone matrix: lamellar bone (LB); parallel-fibered bone (PFB), sometimes called pseudolamellar bone (de Ricqlès, 1975; Enlow, 1969), non-lamellated bone, or non-lamellar PFB (Prondvai et al., 2014); and woven bone (WB), sometimes called fibrous bone (Francillon-Vieillot et al., 1990). These cortical bone matrices are types of primary bone, and may be avascular, or contain simple vascular canals, primary or secondary osteons.

Levels of vascularity and organisation of the collagen fibres within bone indicate growth rates (Amprino, 1947). For example, higher levels of vascularity and lower levels of organisation of collagen fibres, typical of woven bone, are indicative of faster rates of growth (**Figure 1.5**).

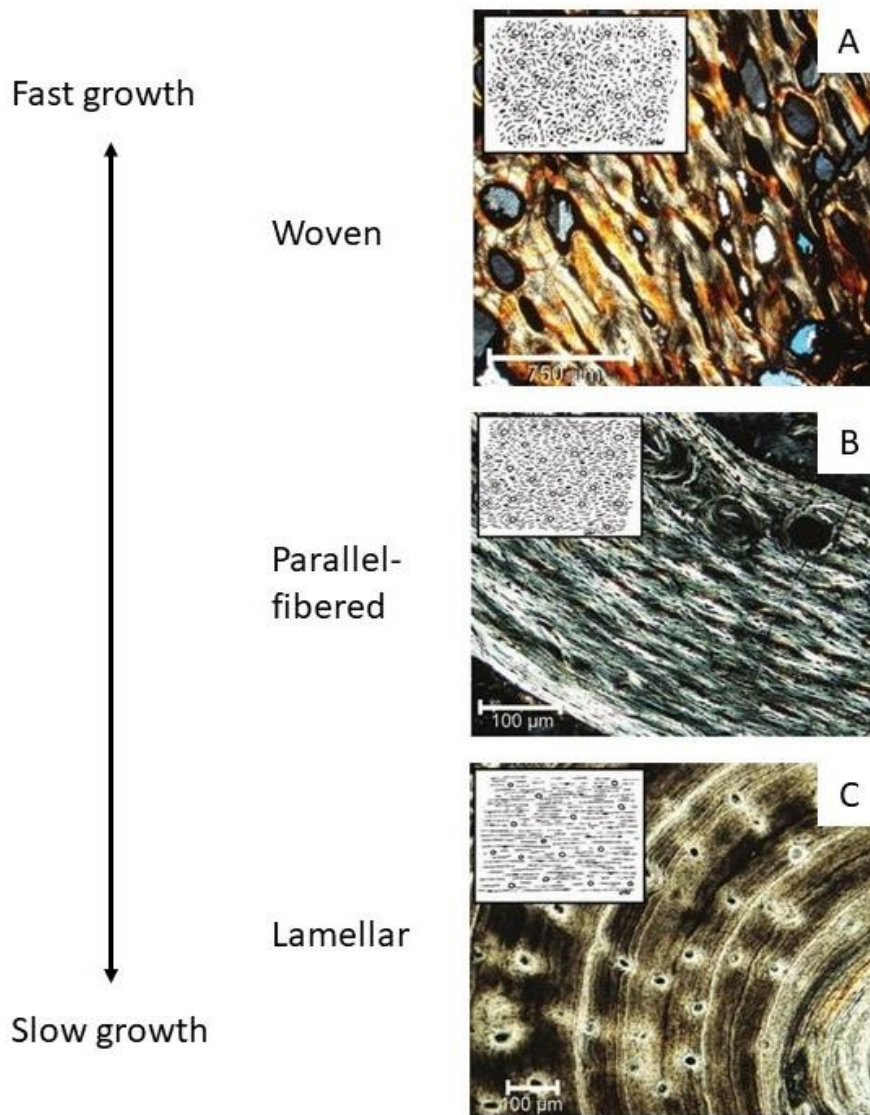


**Figure 1.5 Bone matrix types.** From top to bottom A - C: woven bone; parallel-fibered bone; and lamellar bone matrix types. These can be distinguished by the degree of organisation of the collagen fibres, visible as lighter and darker areas here, and arrangement of vascular canals. Woven bone, for example, is the result of relatively faster rates of osteogenesis, typical of juvenile bone. Lamellar bone shows collagen fibres in an ordered, circumferential pattern and relatively slower rates of growth. Photographs by J. Horner (MOR), modified from Huttenlocker et al. (2013).

### **Bone matrix formation**

For the internal skeleton, the different bone matrix types are produced by one of two processes - static or dynamic osteogenesis. Parallel-fibered and lamellar bone is produced by dynamic osteogenesis (DO) in which the

osteoblasts form a sheet of cells that are arranged on a firm, pre-existing surface (such as bone or cartilage). Some osteoblasts secrete osteoid in a uniformly oriented manner, occasionally ceasing production of osteoid and becoming buried in the bone matrix (Ferretti et al., 2002; Ferretti & Palumbo, 2021 and references therein). Hydroxyapatite crystals in the osteoid align along a fibril of bone collagen (Landis et al., 1996) to which the long axis of the osteocyte is parallel. The osteocytes in this more ordered matrix are spindle shaped and have dendrites in more regular arrangement extending from the main cell body perpendicular to the collagen fibril (Kerschnitzki et al., 2011; Hall, 2015).

Woven bone is produced by a different process, static osteogenesis (SO), where randomly arranged osteoblasts secrete osteoid, burying themselves and turning into osteocytes in situ (Prondvai et al., 2014 and references therein). The osteocytes are larger than those formed by dynamic osteogenesis, being more rounded and globular, with irregular and more randomly oriented dendrites extending from the cell body (Hall, 2015).

Many authors have traditionally described parallel-fibered bone as an intermediary between lamellar and woven bone (Currey, 2002). However, as mentioned by Prondvai et al., (2014), research into the origin of production of bone matrix types in extant taxa, shows that both lamellar and parallel-fibered bone are formed by dynamic osteogenesis, and parallel-fibered bone may in fact be more spatially organised than some lamellar bone. As mode of production is not visible in fossil bone, there is not always a clear distinction between lamellar, parallel-fibered, and woven bone. Rather, they form a continuum, and all three may be found within the same bone sample.

While acknowledging the critical distinction between lamellar or parallel-fibered and woven bone in terms of formation, this study maintains the use of the three terms lamellar bone, parallel-fibered bone, and woven bone.

### **Bone matrix identification**

The spatial organisation of collagen fibres and the size, shape, and orientation of lacunocanalicular spaces are used to identify bone matrix type in fossil bone (Francillon-Vieillot et al., 1990; Padian & Lamm, 2013). Although the collagen content will usually have degraded, in living bone, hydroxyapatite crystals align along the organic compound of the bone; therefore, the orientation of the preserved crystalline structure (which seems unaffected by the fossilisation process) can be used as a proxy for the alignment of the original collagen fibres (Marotti, 1979). A polarising light microscope is used to examine the pattern of birefringence resulting from the alignment of hydroxyapatite crystals along the original (now degraded) organic component of the bone. When the orientation of the crystals (and thus the collagen fibres) is transverse to the long bone axis and parallel to the thin section cut, the bone appears bright or lighter under cross-polarised light. Longitudinally oriented crystals perpendicular to the section cut appear darker under cross-polarised light (Bromage et al., 2003). Due to the irregular arrangement of fibres in woven bone, this bone matrix will appear dark with no extinction phase (isotropic) under cross-polarised light.

As osteocytes tend to align with their long axis along the collagen fibre matrix (Kerschnitzki et al., 2011), orientation of the preserved lacunocanalicular spaces is also indicative of the organisational level of the original bone matrix in fossil bone. In addition, these spaces are generally more globular and irregular for woven bone, and spindle shaped in more organised bone matrices (Davesne et al., 2020; Stein & Prondvai, 2013).

### **Bone complexes**

Two bone complexes are recognised by Huttenlocker et al. (2013), and are distinguished by a combination of types of bone matrix, vascular canals, and features such as growth lines. Fibrolamellar bone (FLB, or fibrolamellar complex, FLC) consists of a primary woven bone scaffold onto which either lamellar, or parallel-fibered bone is subsequently deposited to surround the vascular canals and form primary osteons (Francillon-Vieillot et al., 1990). High levels of vascularity are typical in FLB (**Figure 1.6**).

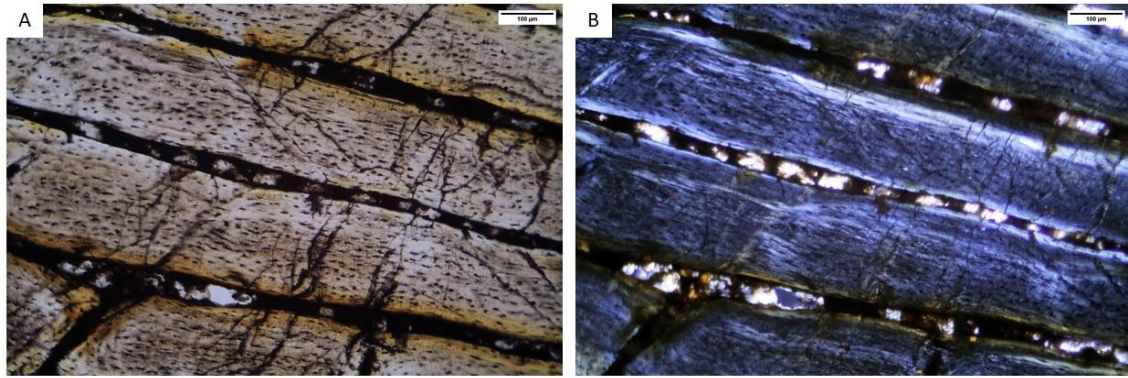


**Figure 1.6 Fibrolamellar bone.** **A)** Laminar fibrolamellar bone in *Giraffatitan* femur, composed of a woven bone matrix that surrounds the blood vessels, and lamellar bone infill. Image taken in PPL. **B)** Same as A) but in XPL. Note the lamellar bone surrounding the primary osteons is visible as a lighter area, called a 'bright line' (sensu Sander, 2000a). Scale bar = 100 µm. Images by S. Strachan.

Haversian bone contains many secondary osteons surrounded by cement lines, which appear in secondary, or remodelled bone, and may show several generations of overlapping or cross-cutting structures (**Figure 1.3**). In addition, a further complex could be added; lamellar-zonal bone (LZB), which consists of primary bone matrix with cyclical growth marks (**2.2**), or concentric zones (de Ricqlès & Horner, 2003; Padian et al., 2001). The zones may be distinguished in various ways, such as subtle changes in bone microstructure, resting lines, or circumferential orientation of flattened osteocytes. The matrix in between the zonal boundaries may range from fine lamellar, to woven bone (Reid, 1984).

## 1.9 Vascular canals

Primary bone can be avascular, contain simple vascular canals, or contain primary osteons where the central canal is surrounded by concentric lamellations (or a combination of these). Primary osteons may display a 'Maltese cross' pattern (Bromage et al., 2003) under cross polarised light (as can secondary osteons), but are not surrounded by a cement line, as in secondary osteons.

There are five patterns of vascular canal orientation within primary osteons (Francillon-Vieillot et al., 1990):

- Longitudinal - longitudinal vascular canals
- Laminar - circumferential vascular canals
- Plexiform - circumferential vascular canals connected by a radial or oblique anastomosing network
- Reticular - oblique or varying orientation of vascular canals
- Radial - radial vascular canals

A single vascular canal would be described as 'circumferential' or 'circular', whereas bone matrix with predominantly circumferential canals would be described as displaying laminar vascular canal orientation (**Figure 1.7**).

These descriptors were applied to fibrolamellar bone (FLB) by de Ricqlès (1975) as: laminar bone (FLB with longitudinal and circumferential primary osteons); reticular bone (FLB with oblique primary osteons); radial bone (FLB with radially and longitudinal primary osteons); longitudinal (FLB with longitudinal primary osteons); additionally, pseudo-laminar bone (lamellar bone with longitudinal and circumferential primary osteons). This can lead to confusion (for example, 'laminar' referring to vascular canal orientation as opposed to 'laminar bone'), which is why Padian & Lamm (2013) propose reserving the use of the terms longitudinal, reticular, laminar, and radial to describing vascular canal orientation patterns. These terms can then be applied as an additional descriptor to any bone matrix type, such as 'laminar fibrolamellar bone'.

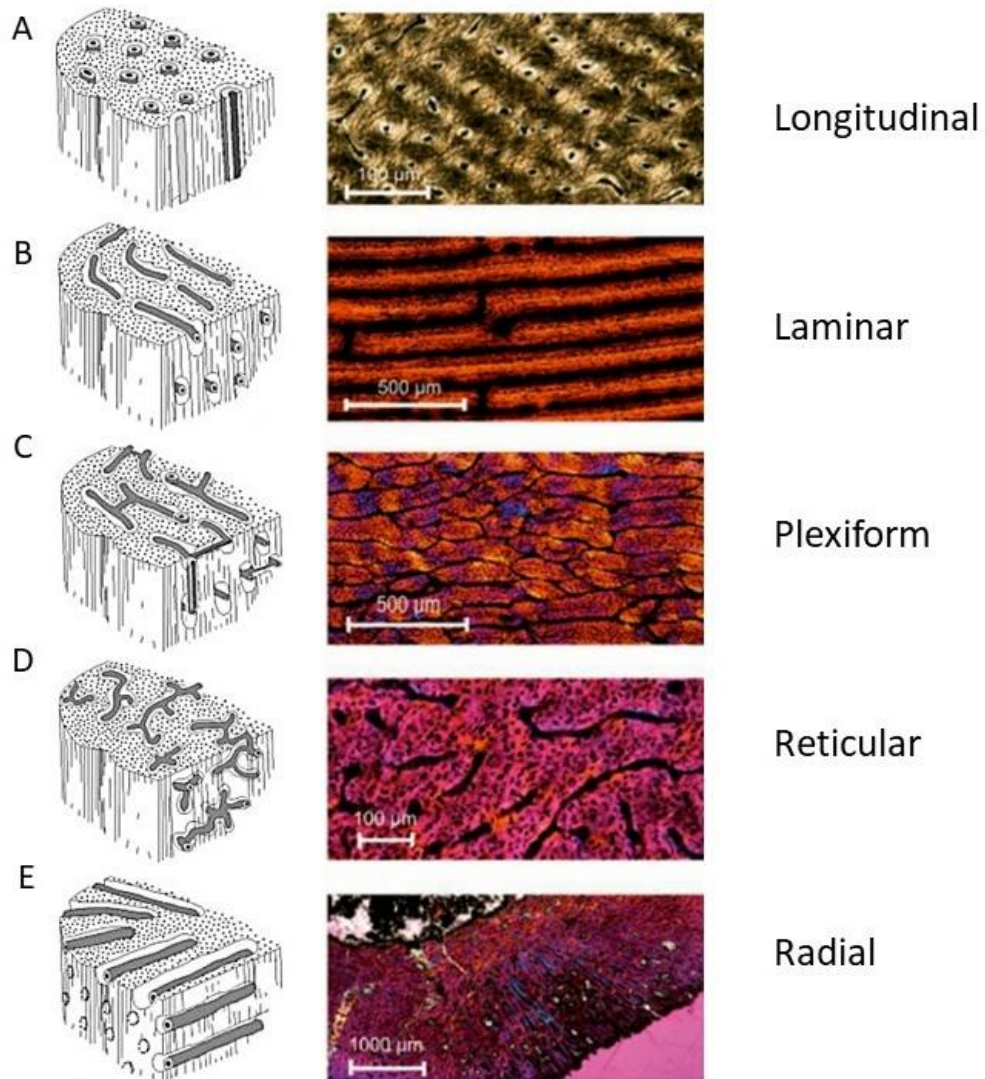


**Figure 1.7 Orientation of vascular canals in primary bone matrix.** Images **A) – D)**, show transverse micrographs. Vascular canal architecture varies according to whether bone is sectioned along the transverse (top of schematic drawing) or longitudinal (side of schematic drawing) axis of the bone. **A)** Longitudinal vascularisation. **B)** Laminar vascularisation with circumferential canals, sometimes also called circular or transverse canals. **C)** Plexiform vascularisation, with a mixture of radial and oblique anastomoses. **D)** Reticular vascularisation with oblique vascular canals, sometimes also called irregular canals. **E)** Radial vascularisation. Schematic diagrams from Erickson (2005), after Francillon-Vieillot et al. (1990). Photographs J. Horner (MOR) modified from Huttenlocker et al. (2013).

## 1.10 Non-avian dinosaur bone histology

The typical bone fibre matrix of reptiles is 'lamellar-zonal' bone (de Ricqlès & Horner, 2003; Padian et al., 2001), with low to medium vascularity, and a repeated pattern of (usually) parallel-fibred bone with well aligned collagen fibres, interspersed with an annulus of almost avascular bone, and a line, or lines, of arrested growth (LAGs) marking the pause, or cessation of growth (Curry, 1999; Reid, 2012; Hall, 2015). By contrast, modern birds and mammals typically display a woven fibered bone matrix with disorganised collagen fibres, laminar and reticular vascular canal orientation, medium to high levels of vascularity, and generally no LAGs or annuli (Padian et al., 2001).

As members of Archosauria, non-avian dinosaurs might be expected to show similar bone histology to that of reptiles and other ectotherms. Zones and annuli were noted in a sauropod pelvis (Reid, 1981), structures usually only seen in the histology of slow growing reptile bones. However, typical dinosaur bone histology shows a predominance of fibrolamellar bone (Prondvai et al., 2014; Reid, 1996; Sander, 2000a), most similar to that of large, extant mammals (Curry, 1999; Sander, 1999, 2000a), suggesting a fast rate of growth more typical of endotherms. This 'mixed message' in non-avian dinosaur bone appears less surprising when viewed in the context of the broad range of bone histology types that have been noted in reptiles as well as modern birds and mammals. Woven bone matrix, in the form of fibrolamellar complex is often laid down in most groups early in ontogeny (Padian et al., 2004). However, primary woven bone matrix and fibrolamellar bone have occasionally been reported in the bones of Crocodylia (Lee, 2004). For example, extensive fibrolamellar bone has been noted in young and mature wild alligators (Tumarkin-deratzian, 2007) and, woven bone appears in mature alligator specimens, suggesting that it is not a feature restricted to fast growing juveniles as has previously been suggested. Further, patches of woven bone were noted in the long bones of young wild and captive alligators, unusually, containing simple primary canals, a feature very rarely seen in well-developed fibrolamellar bone (Woodward et al., 2014). An extensive study in large and small mammals, including marsupials and island placental mammals,

concluded that mammalian palaeohistology also varies widely (Kolb et al., 2015). Mammalian bone displays all three bone matrix types (lamellar, parallel-fibered and woven), and a variety of vascularisation patterns which are visible in the different bone tissue types depending on taxon and individual age. Therefore, the presence of particular bone fibre types or complexes is not a definitive marker of non-avian dinosaurs; rather, the prevailing type and combination of histological features, often in combination with macro-level variables such as bone length, are used to characterise dinosaur bone (see Chapter 8).

It is also important to consider that non-avian dinosaur bone histology encompasses a very wide range of lifestyles and sizes. Non-avian dinosaurs ranged in scale by five orders of magnitude (Alexander, 1997) and, by comparison with mammals which demonstrate similar size range, it is expected that bone tissue would encompass a broad range of characteristics. Padian et al. (2004) illustrates this with comparative images of thin sections of the long bones of large dinosaurs and pterosaurs which show 'typical' fibrolamellar bone; small dinosaurs and pterosaurs with slower growing bone matrix types; and crocodylians that show the slowest growing bone matrix. Lamellar, parallel-fibered, and woven bone (in the form of fibrolamellar complex) has been found in endotherms and ectotherms and there is agreement in the literature that there is no definitive bone matrix type relating to either of these metabolic categories (Padian & Lamm, 2013). Rather, bone matrix types are informative about general rates of growth, although aspects of physiology may be inferred from growth rates (Carballido et al., 2017; Sander et al., 2011; Upchurch et al., 2004).

## **1.11 Sauropod bone histology**

Sauropods are giant, herbivorous, quadrupedal non-avian dinosaurs, famous for their size, with body mass estimates of between 6 to over 60 tonnes (Carballido et al., 2017; Sander et al., 2011; Upchurch et al., 2004). They include the largest terrestrial animals ever discovered, and are one of the most widespread and diverse lineages, their remains having been found on every

continent (Mannion et al., 2012, 2019; Sander et al., 2011; Sander & Clauss, 2008). Sauropods originated in the Late Triassic, peaking in diversity in the Late Jurassic, until their demise at the end of the Cretaceous, spanning 140 million years (Mannion et al., 2017; Wilson et al., 2012). Studies of bone histology and bone matrix type, have shown that their tremendous body size was achieved relatively quickly due to fast rates of growth (rather than growing slowly for a long time), facilitated by a high basal metabolic rate, a pneumatized skeleton, and an avian-style respiratory system (Klein & Sander, 2008; Sander et al., 2004; 2011; Sander, 2000a; Sander & Clauss, 2008; Wedel, 2003). There are over 230 genera (Upchurch pers. comm. 2022) and although they vary in scale, all share the same Bauplan of a long neck with relatively small skull, a long tail, and a large body supported by four columnar legs, and thus are considered truly graviportal (Sander et al., 2011; Sander & Clauss, 2008).

Sauropods are one of the most extensively sampled non-avian dinosaur taxa histologically. Sauropod bone histology typically shows fast rates of growth, a predominance of well-vascularised laminar fibrolamellar bone (**Figure 1.8**), extensive remodelling, and a lack of open medullary cavity in limb bones (Company, 2011; Curry, 1999; de Buffrénil et al., 2021; Díez Díaz et al., 2018; Enlow & Brown, 1956, 1957, 1958; Erickson, 2005; Erickson et al., 2001; Klein et al., 2009; Klein & Sander, 2008; Lehman & Woodward, 2008; Sander et al., 2004; 2006; 2011; Rogers & Erickson, 2005; Sander, 1999, 2000a; Sander & Tückmantel, 2003).

Sander (2000a) took 38 cores from basal Macronarian and Diplodocoid sauropods from Tendaguru in Africa and noted patterns in the cortical bone fibre and vascularity that could be used to estimate ontogenetic stage, as well as differences between taxa. Polish lines were observed (growth lines visible under transmitted light) in some skeletal elements, and a reduction in polish line spacing was used to indicate a reduction in growth rate and hence the onset of sexual maturity. The reduction in vascularity throughout the radius of the bone was also used to indicate the transition from juvenile to adult (Sander, 2000a). Differences in bone histology and growth rates were used to construct

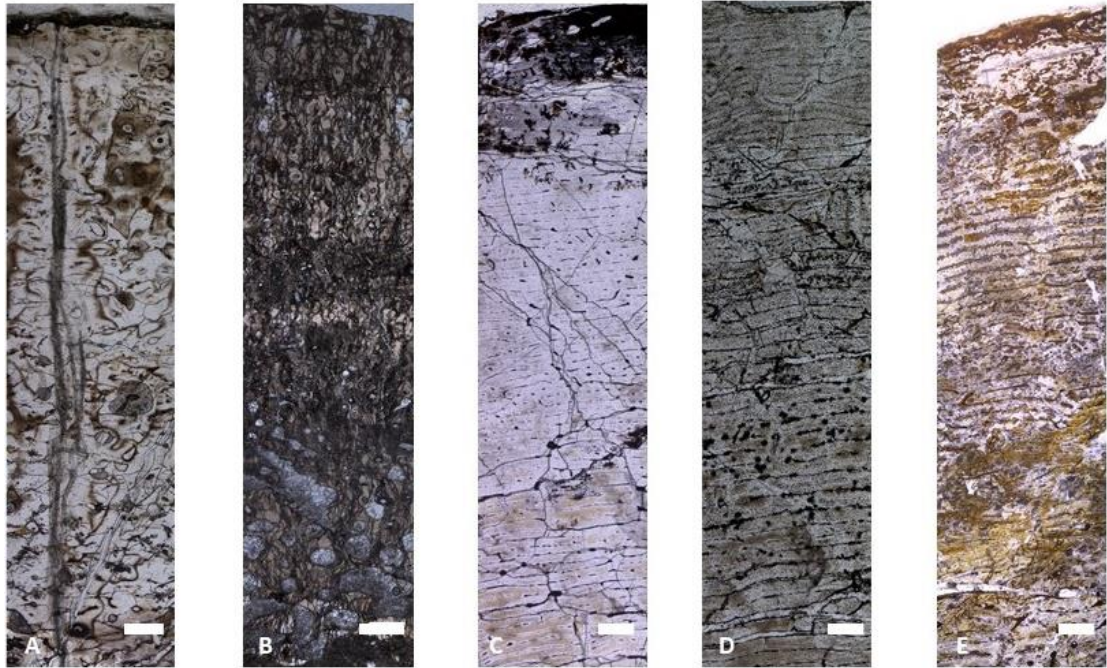


**Figure 1.8 Sauropod cortical bone.** Composite micrograph images showing heavy remodelling in **A**) *Ampelosaurus* (C3 174) and, **B**) *Magyarosaurus* (r1220), where secondary osteons have reached the bone's periphery (top of image) and have overlaid the primary bone matrix. In **C**) *Phuwiangosaurus* (No no.), **D**) *Giraffatitan* (dd452), and **E**) *Dicraeosaurus* (UK PV unreg\*), there is a predominance of laminar fibrolamellar bone. Some degree of diagenetic alteration can be seen in all specimens in the form of streaks, cracks, or stellate blotches (most noticeable in *Magyarosaurus*). Bone surface is at the image top. Scale bar = 500  $\mu\text{m}$ , photographed under PPL. Images by S. Strachan.

a timeline of life history events which were then compared across taxa. Further, the descriptions of typical bone histology for a variety of sauropods, across different ontogenetic stages, can be used as a reference for taxonomic comparison (**Figure 1.9**).

In general, juvenile sauropods display highly vascularised woven bone with longitudinal canals and wide lumina. This progresses during ontogeny to laminar fibrolamellar bone with circumferential canals at the outer cortex where new bone is laid down. In subadults, increasing amounts of lamellar bone surround primary osteons and line vascular canals; canal orientation may be

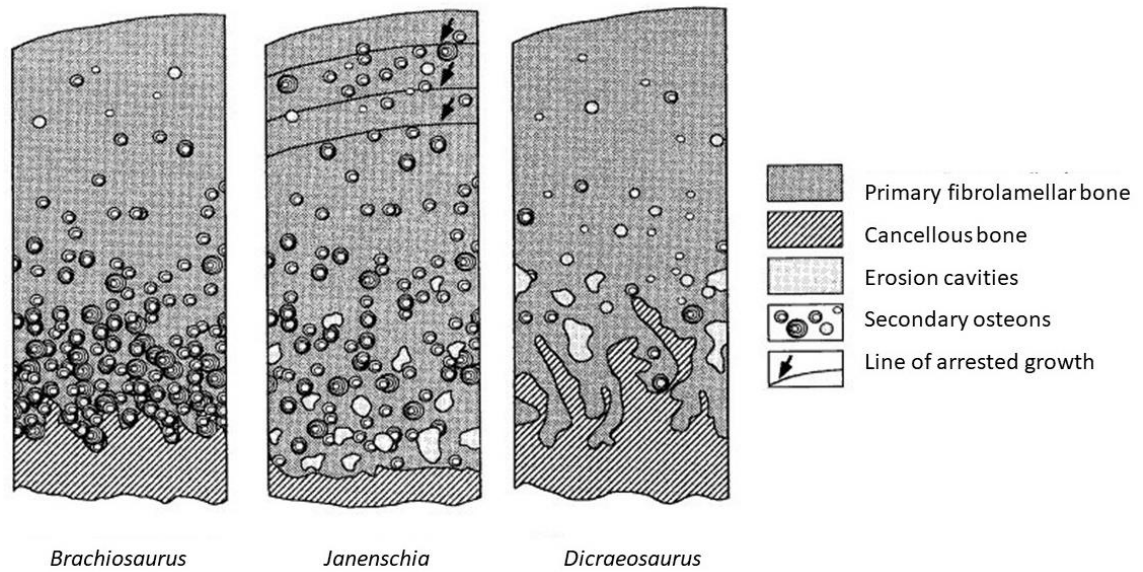


**Figure 1.9 Schematic comparison of Tendaguru sauropod long bone histology.** *Brachiosaurus*, *Janenschia*, and *Dicraeosaurus*. The specimens vary in degree of remodelling (most advanced in *Brachiosaurus*), presence of growth lines (*Janenschia*), and evenness of transition from the medullary cavity (less even in *Dicraeosaurus*). The central medullary cavity is mostly filled with cancellous bone in sauropods. The development of large erosion cavities, as can be seen in *Janenschia*, and remodelling by secondary osteons, both proceed from the inner to the outer region of the cortex. The bone surface is at the image top. Modified from Sander (2000a).

reticular, and remodelling may begin near the medullary cavity. Post sexual maturity, sauropod bone is less highly vascularised in the outer cortex due to the increase in thickness of lamellar bone lining the vascular canals creating narrow lumina, primary osteons are clearly differentiated, and remodelling may progress as far as the bone centre. Rarely, growth lines may also be found. As maximum size is reached, growth slows, and cortical bone vascularity is further reduced as secondary osteons are infilled with lamellar bone. Lamellar-zonal bone may be present in addition to high levels of remodelling, rarely growth marks, and possibly a closely packed series of growth marks at the bone surface marking the cessation of growth (see Chapter 2 and **Figure 2.2**). Eventually Haversian bone may overprint almost all the primary bone matrix with increasing numbers of generations of overlapping secondary osteons

(Klein & Sander, 2008; Mitchell et al., 2017; Sander et al., 2011; Stein et al., 2010).

Although there is some variation between taxa, the general principles relating to faster growth in juveniles and subadults, slowing of growth around sexual maturity and further slowing into adulthood, are consistent in sauropods. Growth rates are inferred from the bone fibre matrix and organisation of vascular canals. For example, woven bone is laid down significantly faster than lamellar bone, and radial vasculature is indicative of significantly faster growth rates than longitudinal vasculature (Castanet et al., 1996; de Margerie et al., 2002, 2004). Sander concluded that “the Tendaguru sauropods show a common growth pattern in which growth is determinate but sexual maturity is achieved well before maximum size is reached” (Sander, 2000a).

Based on these observations, thirteen histologic ontogenetic stages (HOS) were identified in basal macronarian and diplodocoid sauropods (Klein & Sander, 2008) and have subsequently been applied to a wide range of sauropod taxa (Carballido & Sander, 2014; Company, 2011; Ghilardi et al., 2016; Griebeler et al., 2013; Klein et al., 2009, 2012; Stein et al., 2010; Woodward & Lehman, 2009). Using the HOS system, bone tissue types are categorised (A to G) according to tissue type, orientation, degree, margin and infilling of vascular canals, presence and type of osteons, growth marks, remodelling, and presence of an external fundamental system (EFS, a series of closely packed growth marks at the bone’s periphery) (**Figure 2.2**). An advanced HOS stage (typical of a large adult) found in a small sized specimen would therefore suggest a small adult rather than a juvenile (although see Sander & Klein, 2005). A further stage was added by Stein et al., (2010), and similarity of histological indicators of maturity seen in large sauropods were used to provide evidence that *Magyarosaurus dacus* of Romania was an island dwarf form rather than the juvenile of a larger sauropod taxon (Stein et al., 2010). A further development was to align HOS stages with Biological Ontogenetic Stages (BOS) of development, ranging from embryo (equivalent to HOS 1) to Adult III (commensurate with HOS 13) (Klein & Sander, 2008). The Histo-morph Ontogeny Scale (H-MOS), comprising four stages, was

developed to incorporate morphological features in addition to histological ones, and applied to diplodocids (*Apatosaurus* and *Diplodocus*) by Woodruff et al., (2017) as remodelling starts earlier in ontogeny in these taxa. A combination of skeletal elements (neural spines, centra), LAGs in the ribs, morphological indicators (such as post parietal foramen) and femoral HOS stages were used to establish ontogenetic stage. Sexual maturity, H-MOS stage 3, being commensurate with HOS 8 (Woodruff et al., 2017).

Extensive remodelling by secondary osteons is characteristic within the long bones of animals that have reached asymptotic size, and particularly extensive in many sauropod taxa, overprinting nearly all the primary bone matrix in some mature specimens (Enlow & Brown, 1956, 1957, 1958). This feature was the inspiration for the description of 15 remodelling stages (RS) by Mitchell et al. (2017), based on the number of cross cutting generations of secondary osteons. This can be used to extend the HOS stages into senescence for Sauropoda. Remodelling stages correlated well with femoral length, although not strongly with specific HOS stages. Differences in degree of Haversian remodelling at different ontogenetic stages (as well as variation in type and spacing of growth lines) was used previously to distinguish between different Tendaguru taxa (Sander, 2000a).

A thick cortex with wide transition zone between the cortex and medullary cavity, and a spongiouse medullary cavity are typical in Neosauropoda (Cerde et al., 2017). These are adaptations observed in graviportal taxa, such as elephants (Nganvongpanit et al., 2017), which may help resist compressive loading (Oxnard, 1993; Houssaye, Waskow, et al., 2016). A filled medullary cavity has even been reported in perinatal young sauropods (Curry Rogers et al., 2016; González et al., 2020), and used to distinguish between sauropod and other dinosaurian taxa (Nikolov et al., 2020).

### **Sauropod variation**

Variations between taxa in Sauropod bone are observed in fibre matrix type, degree of remodelling, and type and degree of vascularity (Klein et al., 2009, 2012; Klein & Sander, 2008; Sander et al., 2006; Mitchell et al., 2017; Sander,

1999, 2000a; Sander & Tückmantel, 2003; Stein et al., 2010). When comparing the Tendaguru sauropods, Sander asserts “The histology of the long bones, primarily humerus and femur, of the four Tendaguru sauropod genera is comparable in some respects but there are surprising differences in others. These differences allow taxon recognition based on bone histology, especially if bones of the same size are compared” (Sander, 2000a). Differences in vascularity and degree of remodelling between taxa were noted, as well as the prevalence, or lack of features such as growth lines. However, bone fibre matrix, vascularity and remodelling are known to alter in response to growth rates throughout ontogeny, and it is likely that this is a primary influence on many histological features in sauropod bone, rather than phylogeny.

Few of these studies are quantitative, in part due to the challenges inherent in quantifying characters such as bone fibre matrix, the definition of which incorporates combinations of multiple individual characteristics. Nonetheless, these taxon-specific differences, when combined with additional data such as size, can be used to differentiate between taxa, as two bones of the same length displaying very different ontogenetic stages and features are considered unlikely to be from the same taxonomic group (Klein & Sander, 2008; Sander, 2000a; Wiersma-Weyand et al., 2021).

# Chapter 2 Signals in bone histology

## 2.1 The signals in bone

Bone tissue composition and structure are influenced by a variety of factors. As expressed by de Ricqlès (2011) “the variability of bone tissues expresses a highly complex, multifactorial causality that can be deciphered, and hence can bring us a very rich amount of biological (and palaeobiological) information” (de Ricqlès, 2011). The influences on bone histology fall into several non-exclusive areas, or four ‘signals’ according to Padian (2013); ontogeny, mechanics, phylogeny, and environment (**Figure 2.1**). The current study focuses on phylogeny, however there is a strong degree of overlap in each of these areas. Therefore, each of these influences is summarised here. Chapter 7 provides the introduction of a theoretical framework to position the four signals within a broader evolutionary context.

## 2.2 Ontogeny and growth

As stated by Scheyer et al. (2010): *“the analysis of bone microstructures still remain the most important and most reliable tool for determining the absolute ontogenetic age of fossil vertebrates”*. Reviews by Padian et al. (2001) and Erickson (2014) highlight the importance of histology as a technique in understanding growth rates throughout ontogeny and the minimum absolute age of dinosaurs. Erickson (2014) gives a useful summary of the strengths and weaknesses of some histological methods (see also Griebeler et al., 2013), and Padian et al. (2001) includes a cladogram summarising bone growth rates across archosaurian taxa. Both papers mention the use of histology to infer rates of growth in fossil taxa using tissue typing and growth lines.

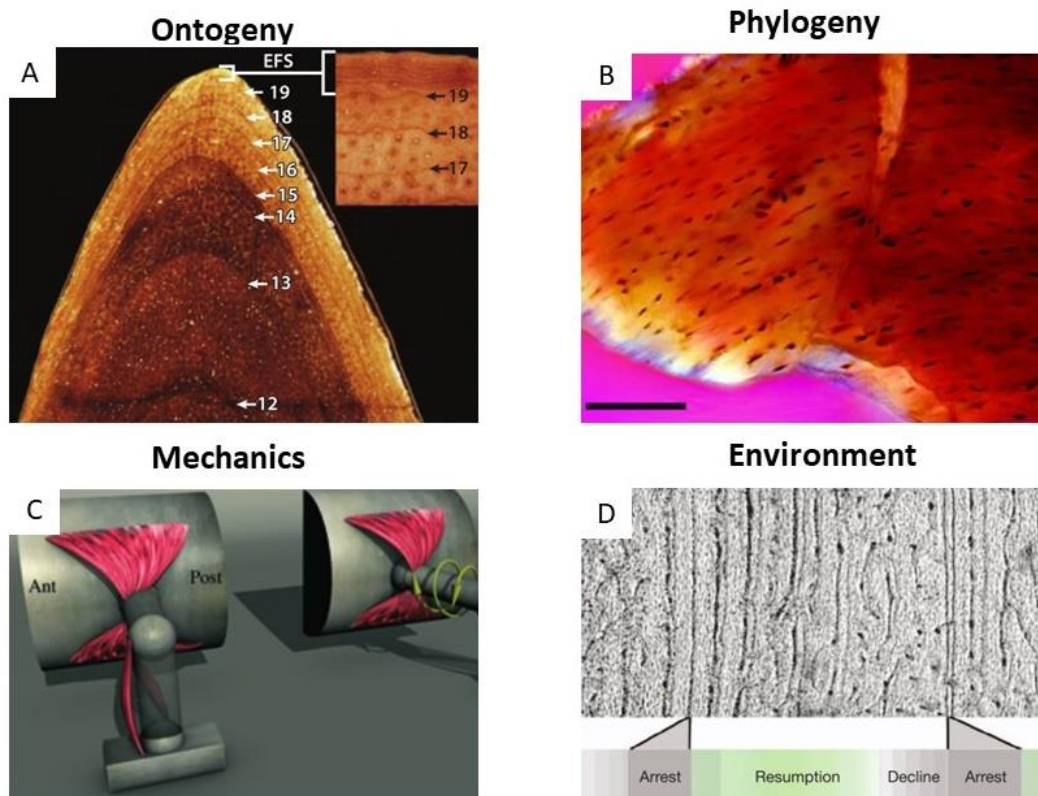


**Figure 2.1 The four signals of palaeohistology.** The information within a bone can be seen as falling into four non-exclusive categories; ontogeny, phylogeny, mechanics, and environment (Padian, 2013). **A**) Decreasing width between growth rings in a *Tyrannosaurus* rib indicate a slowing of growth (Erickson, 2014). **B**) The nearly avascular parallel-fibered bone of *Archaeopteryx* indicates slow growth rates, typical of ectothermic reptiles (Erickson et al., 2009). **C**) Histological indicators of strain were used to infer locomotor behaviours in a study of temnospondyls (Sanchez et al., 2010). **D**) Seasonal, cyclical growth was inferred from the slowing and cessation of bone deposition in an impala femur (Köhler et al., 2012).

### Growth from bone matrix type

In tissue typing in fossil specimens, the radial thickness of the cortex is divided by a daily rate of osteogenesis to estimate growth rates, or minimum chronological age. The rate of osteogenesis is estimated from a homologous bone matrix type of known growth rate from extant organisms (Cubo et al., 2012; Horner & Padian, 2004; Padian et al., 2001). According to “Amprino’s rule”, rates of osteogenesis correlate with the level of organisation of periosteal bone tissue and degree of vascularisation (Amprino, 1947). Specifically, highly vascularised bone with disorganised woven bone matrix grows faster than less

vascularised and more spatially organised parallel-fibred or lamellar matrix (Amprino, 1947; Hall, 2015). Therefore, rates of growth can be estimated from the type of bone fibre matrix present.

### **Testing of Amprino's rule**

There is strong agreement in the literature regarding Amprino's rule, but with some important qualifications because absolute measures of bone apposition rate vary across different skeletal elements and taxa.

Castanet et al. (2000) found reduced growth rates were commensurate with a decrease in bone vascular density, and the highest growth rates were linked to bone tissue types with oblique and circumferential oriented vascular canals (reticular and laminar bone respectively). Fluorescent markers were used to measure growth rates in young emus and ostriches and combined these measurements with a qualitative assessment of the orientation of the vascular canals observed across a range of skeletal elements. (Castanet et al., 2000). It was noted that rates of bone accretion of these two types of vascular canal orientation overlap, and, therefore, are only indicative of a range of values. A later study (using the same method and various statistical tests) by de Margerie et al. (2002) explored the relationship between growth rates and various histological observations across a variety of skeletal elements in mallard ducks of different ages. Fibrolamellar bone showed the fastest deposition rates and avascular lamellar bone the slowest, in agreement with Amprino's rule. The authors found that faster growth rates were indicated by greater presence and diameter of primary osteons, and importantly, no significant relationship was found between growth rates and vascular canal orientation which, it is suggested, may be more closely related to biomechanics (de Margerie et al., 2002). Castanet's study did not apply any statistical test, or include the diameter of primary osteons, so it is difficult to directly compare these studies. Oblique, and circumferential vascular canals predominate in woven bone (fast growing) which also tends to have larger primary osteons in diameter, therefore the results are not incompatible. A further study carried out on king penguin chicks (de Margerie et al., 2004), however, found that radially oriented vascular canals within fibrolamellar bone

are associated with the highest growth rates, but also (contra Castanet et al., 2000), that laminar vascularity was associated with the slowest rates of growth. Therefore, it seems the relationship between vascular canal orientation and rates of growth is not straightforward.

Interesting data regarding bone accretion rates is provided in these studies; the transition from lamellar bone to fibrolamellar complex happens when the primary osteons are approximately 35  $\mu\text{m}$  in diameter, and bone accretion rates are around 20  $\mu\text{m}$  per day in mallards (de Margerie et al., 2002). Maximum growth rates of approximately 80  $\mu\text{m}$  per day are observed in the hind limbs of young emus (Castanet et al., 2000), and up to 171  $\mu\text{m}$  per day in king penguin chicks (de Margerie et al., 2004). However, rates vary widely between taxa, and so any direct transference of the rates to extinct taxa needs to be applied cautiously. Because of these challenges, Erickson (2014) concludes that growth rate estimates based on tissue typing are likely to be inaccurate. Further, it is well accepted that rates of bone apposition vary, not only between taxa, and individuals, but also between skeletal elements. Different types of fibrolamellar bone tissue (those with different vascular canal orientation) can grow at similar rates during ontogeny (de Margerie et al., 2002). Conversely, Starck and Chinsamy (2002) observed a wide range of growth rates from the same tissue type in the Japanese quail (Starck & Chinsamy, 2002). In addition, vertebrate species with large body size tend to grow more quickly than small species (Case, 1978). Therefore, it is recommended that bone matrix types in fossil taxa be described generally as indicating 'fast' or 'slow' rates of apposition or falling within a specified range only. Notwithstanding this complexity, more accurate inferences can still be drawn if we compare homologous skeletal elements, and ideally, organisms of a similar mass and ontogenetic stage, and similar bone fibre matrix types.

### **Cyclical growth marks**

Cyclical growth marks (CGMs) are visible as thin, dark, circumferential lines within the bone cortex and indicate a cessation (as shown by a LAG) or slowing (annuli) of bone growth rate, the area in between growth lines being a 'zone'. Cyclical growth marks are widely reported in ectothermic vertebrates

(Peabody, 1961), although, CGMs are not uncommon in mammal bones (Peabody, 1961; Morris, 2009; Köhler et al., 2012; Kolb et al., 2015). Reid first noted zones and annuli in the pelvis of a sauropod dinosaur (Reid, 1981). Zonal bone and LAGs have now been reported in many non-avian dinosaur taxa, in both fibrolamellar (fast growing) and lamellar (slower growing) bone (Starck & Chinsamy, 2002; Chinsamy, 2005; Padian & Lamm, 2013).

It is generally accepted that lines of arrested growth (LAGs) are deposited on an annual basis (Peabody, 1961; Francillon-Vieillot et al., 1990; Castanet, 1994; Hall, 2015) and, therefore, they can be used as skeletochronological indicators to estimate minimum chronological age (see Castanet, 1994 for a summary of methods of calculating age and longevity in reptiles). Zone widths generally meet expectations for annual tissue deposition (Sander & Tückmantel, 2003), and decrease with age (Chinsamy et al., 1995). Therefore, a rate of osteogenesis can be estimated from the distance between growth lines, where the radial distance is assumed to represent one year's growth. Variations in rates of growth can be used to determine the developmental stages of individuals, and to draw inferences regarding metabolism, life history strategies and phylogeny (Botha & Chinsamy, 2001; de Ricqlès, 1983; Reid, 1981, 2012).

There are several issues relating to the production and presence of LAGs. During remodelling, LAGs are often resorbed as the medullary region expands, or the cortex is remodelled, which leads to an underestimation of age. Consequently, several techniques have been developed to calculate missing LAGs, such as using regression equations, or stacking, whereby younger bone samples are overlaid onto older specimens to estimate missing bone (Chinsamy, 1993). Different bones of the same skeleton may have different numbers of LAGs, or LAGs may be difficult to see, or inconsistently deposited. For the latter reason HOS stages were developed for sauropods and have since been applied to a variety of taxa (see Chapter 1).

Care needs to be taken over the choice of skeletal element, which may be limited in fossil material. Garcia (2011) summarises the relative suitability of

bones for aging reptiles based on a study of the skeletal elements of *Alligator mississippiensis*. The most informative area to section when studying growth is mid-diaphysis where the greatest growth and least periosteal remodelling occurs. The author also compared LAGs over a wide range of skeletal elements to create a 'map' to indicate comparable elements with the least likelihood of loss of LAGs due to remodelling (Garcia, 2011).

### **Growth curves and life history**

When plotted against femoral length and then combined with mass estimates, LAGs have been instrumental in enabling researchers to plot dinosaur growth curves (Chinsamy, 1993; Erickson & Tumanova, 2000). Although there are few challenges to the published work on growth curves, a study by Myhrvold (2013) of 31 data sets used to estimate growth rate, found results difficult to replicate, possibly due to systematic errors and bias towards younger specimens. The author suggests inferences of asymptotic growth in non-avian dinosaurs may have been overestimated as a result. and that "both maximum dinosaur growth rates and maximum dinosaur sizes have little statistical support" (Myhrvold, 2013).

A growth curve for *Psittacosaurus mongoliensis* was constructed using Developmental Mass Extrapolation (DME), which relates the linear measurement from an anatomical structure (such as femoral length) to body mass changes through ontogeny. The specimen shows an unusual, sudden increase in growth indicated by increasing vascularity and longitudinal, then reticular, and finally radial vascular orientation (indicative of high rates of bone apposition) throughout ontogeny (Erickson & Tumanova, 2000). This is the opposite pattern to that usually seen in non-avian dinosaur bones, where vascularity tends to decrease as the animal nears maturity, and, it is suggested, could be due to environmental conditions, diet, or even a move from bipedality to quadrupedality (Erickson & Tumanova, 2000).

The only unequivocal sign of full adult size being reached is the presence of an external fundamental system (EFS, Cormack, 1987), a type of growth line (de Ricqlès, 1983; Erickson, 2014), visible as a series of closely spaced thin,

dark lines at the bone periphery (**Figure 2.2**). An EFS indicates a change from active growth to slow accretion and has been found in Pseudosuchia, Crocodylomorpha, Pterosauria and Dinosauria. It has therefore been suggested that determinate growth may be the primitive state for archosaurs (see Andrade et al., 2015 and references therein).

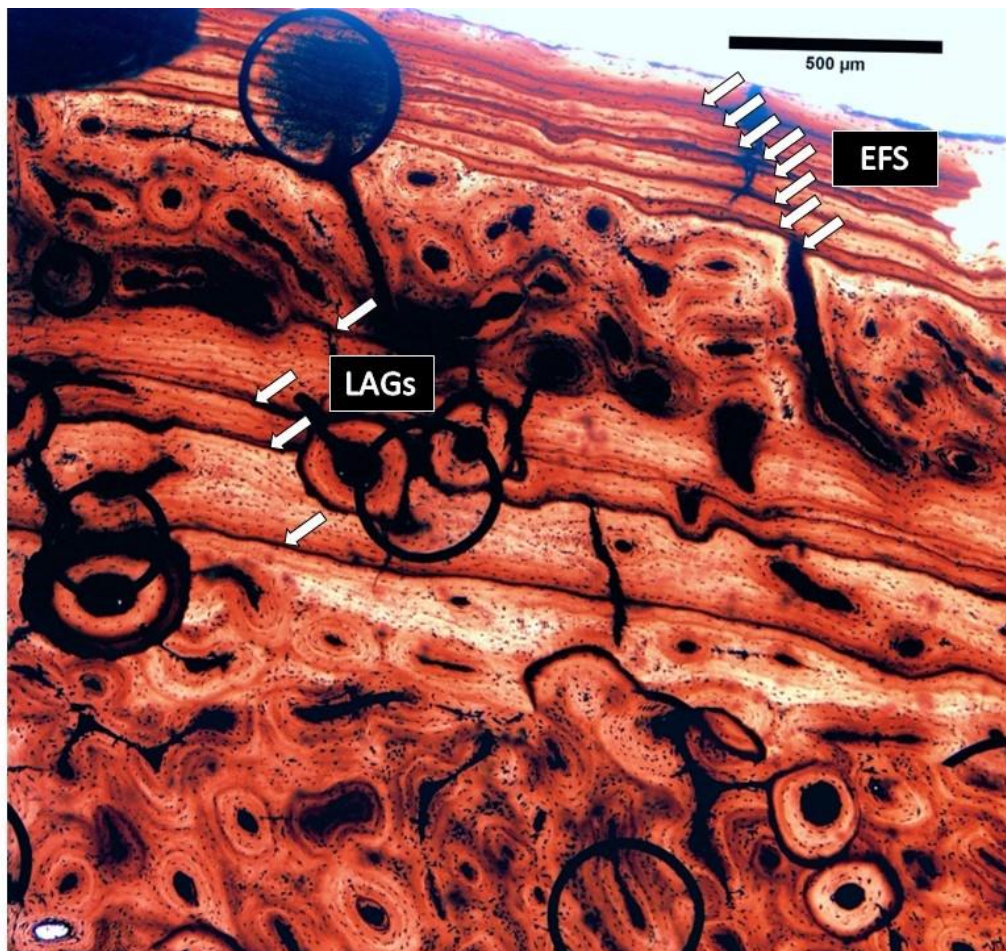


**Figure 2.2 Cyclical growth marks.** A series of tightly packed growth lines (white arrows) in *Camarasaurus* at the bone periphery, indicating the cessation of growth (EFS), and lines of arrested growth (LAGs), PPL. Photograph by S. Strachan.

## 2.3 Mechanics

*“Cortical and trabecular bone remodel throughout life in response to mechanical stress and, as such, can provide more direct insight into the function of a particular bone, joint and/or morphology than can be gleaned from external morphology alone.”* (Tsegai et al., 2013).

A review of the challenges of making behavioural and phylogenetic inferences from hominid fossils proposes that in order to test hypotheses about behavioural or life-history variations, we need to compare features that are very plastic, or have important functional roles (Lieberman, 1997). Bone is a living tissue that replenishes throughout life, and is fundamental in supporting and protecting the body, and is therefore a good choice for making such inferences. It is important to note that there are two meanings of ‘mechanics’ as applied to bone in palaeohistological study: either the innate properties of the material, which may affect its ability to respond to types of stress; or, the resultant observable effects of mechanical stress experienced by the bone, such as increased remodelling as a result of frequent or repetitive movements. Most of the research carried out on fossil specimens explores the latter, as the original bone material and thus its properties have been altered by permineralisation.

### **Remodelling**

The general concept that bone adapts to mechanical stress during life is broadly known as “Wolff’s Law” (Wolff, 1892; but see Ruff et al., 2006). It is well established that bone remodels in response to specific types of stress which can be caused by the environment, locomotor style or lifestyle (Currey, 2002; Habib & Ruff, 2008; van Oers et al., 2014; Hall, 2015). Bones grow by periosteal accretion and remodelling via a basic multicellular unit (BMU). When bone is removed from one area by osteoclasts, and osteoblasts lay down bone in a new area, the shape of the bone changes and this is known as modelling; when this happens in the same place, remodelling takes place (Freemont, 1993; Bonewald & Johnson, 2008).

Remodelling affects the size and shape of the bone periphery and cortex, cortical thickness, and, possibly to a lesser extent, medullary cavity size and shape (Currey, 2002; Starck & Chinsamy, 2002; Habib & Ruff, 2008; Sanchez et al., 2010; Tsegai et al., 2013; Püschel & Benítez, 2014; van Oers et al., 2014; Hall, 2015). Limb bones are subject to the greater mechanical stress than for example, ribs, and experience higher remodelling rates as a result (Goliath et al., 2016). The remodelling effect was demonstrated by adding an asymmetrical mechanical load to one side of a chick; additional bone deposition was observed on the weighted side, creating an irregular bone cross section. The femur responded more noticeably; in contrast the tibiotarsus and tarsometatarsus (which experience less mechanical stress), did not respond with asymmetrical bone formation (Starck & Chinsamy, 2002). Remodelling of bone can, therefore, be used to infer not only locomotor style, but also environment and lifestyle. Homoplasies or convergence of histology are thus useful as they may reveal similarity of movement, behaviour, and environment (de Ricqlès et al., 2004). In addition, biomechanical demands may influence features in bone at the histological level during growth such as: osteonal size and structure (Martin et al., 1996); vascular canal orientation (de Margerie et al., 2002; but see Lee & Simons, 2015); bone fibre organisation (Riggs et al., 1993; Martin et al., 1996; also see Lee 2004); and circularity of vascular canals and resorption cavities (Sanchez et al., 2010). As bones grow and remodel in response to mechanical influence, this mechanical signal often dominates. Indeed, it has been suggested that the prevailing signals in bone histology are those of growth and mechanics, rather than phylogeny (de Ricqlès et al., 2004; Enlow, 1962).

### **Locomotor style and cortical remodelling**

Even slight variations of locomotor style can cause different mechanical loading regimes, which may result in inter-species variation. As the development of locomotor style follows a specific pathway, these differences are potentially specific to a particular taxon. Habib and Ruff (2008) successfully demonstrated that locomotor dynamics in birds can be differentiated based on analysis of cortical thickness ('hollowness') in cross-sections of femora and humeri. Cross-sectional properties proved more informative than relative bone

length in determining locomotor style, and humeral cortical thickness showed particular utility in differentiating between aquatic and non-aquatic taxa (Habib & Ruff, 2008; Houssaye et al., 2016). However, it cannot be assumed that this would apply for all taxa.

Geometric morphometrics were successfully used to differentiate between hunter gatherers and farmers (with known variations in lifestyle relating to locomotor activity), according to femoral morphology (Püschel & Benítez, 2014). The study looked at remodelling in the femoral cortex using micro-CT scans, and variations in the size of the medullary cavity. The two groups could be differentiated based on variations in femoral cortical remodelling using morphometrics, but not on medullary morphology, indicating that femoral cortex morphology is a more robust indicator of lifestyle than medullary cavity morphology.

Data for these studies was gathered by non-destructive micro-CT scan methods and results are consistent. They demonstrate the synergistic nature of structure and function, as limb movement needs to be considered to place bone structure in context. For example, for aquatic taxa, when primary propulsion comes from the forelimbs, these elements better represent adaptations for stress and strain. Hind limbs may demonstrate adaptations primarily to reduce buoyancy such as increased compactness (Houssaye et al., 2016). Therefore, the choice of element and understanding of locomotor dynamics is essential to interpreting patterns of bone remodelling in extant taxa, and comparisons can then be made with bone morphology in fossil taxa (although see Maidment et al., 2012, and Chapter 7).

### **Vascular canal orientation and strain**

Several studies have indicated that bone tissue with predominantly circumferential vascular canals (laminar bone), may be a biomechanical adaptation to greater torsional loads (e.g., caused by flapping flight).

Primary vascular canals in mallards were classified into four categories, according to their individual orientation. Degree of vascular laminarity was

calculated and it was found that in wing bones (where the greatest torsional loads are experienced) laminarity was, as predicted, greater than in leg bones. However, the radius and femur were exceptions and showed higher laminarity than expected (de Margerie et al., 2002). Whether this result is in fact growth related or due to some other factor is unknown. The exception of the radius and femur are difficult to explain, although torsional strength also appears to be important for avian femora (Carrano & Biewener, 1999).

Studies by Lee (2004) and Lee & Simons (2015) do not support the connection between torsional strain and bone vascularity. Differences in bone due to the biomechanical effects of strain were explored by comparing the collagen fibre organisation (bone matrix type) and the distribution and orientation of vascular canals of dorsal, compared to ventral, quadrants in transverse thin sections of alligator femora across ontogeny (Lee, 2004). The results showed weak support for collagen fibre organisation being correlated with bone strain and did not support a significant relationship between vascular canal orientation and strain. The overall conclusion was that the pattern of femoral growth had a greater influence on collagen fibre organisation than mechanics (Lee, 2004). Further, a second study found that bat bone is avascular in small bats of less than 100g (Lee & Simons, 2015). As bats increase in size, their bone becomes (poorly) vascularised, and for large bats some longitudinal and radial canals can be seen. Comparatively sized birds display a very different pattern of vascularity, comprising highly vascularised bone with various degrees of bone laminarity. As both bats and birds would be expected to experience similar torsional loading in the wings, the authors conclude that the difference in bone histology is the result of the slower growth rate of bats (about four times slower than that of birds), and that laminar bone is not a required biomechanical adaptation to torsional loading. Therefore, growth rate, rather than mechanics, is the primary signal. It is suggested that at a small scale, nutrient and waste exchange can be supported by canaliculi alone, but as the mass of bone increases, vascular canals are required to support these processes, hence the increase in vascularity in bat wing bones with body size (Lee & Simons, 2015).

### **Non-locomotor behaviour**

Tsegai et al. (2013) investigated how trabecular bone structure correlates with hand posture and use in Hominidae. The study looked at bone volume and stiffness in the third metacarpal in a range of taxa with different hand usage, such as investigative use by gorilla, and suspensory use by orangutans. It was found that regions of high trabecular bone volume and greatest stiffness correlated with predicted loading of the hand in different behavioural categories (Tsegai et al., 2013). As the authors point out, trabecular bone remodels rapidly in response to strain, either by addition, to add strength where needed, or by removal, where lower levels of strain are experienced. This may, therefore, be particularly useful in indicating habitual posture or modes of locomotion.

## **2.4 Environment**

### **Environment and mechanics**

Information about different environments can be inferred from fossil bone histology from changes in rates of growth resulting from differing levels of mechanical strain experienced. Different environments (e.g., aquatic, or terrestrial) present different physical demands due to differing gravitational loads, or density, and this will “generate specific types of strains on limbs, with the result that aquatic and terrestrial locomotion require different resistances from the bone elements” (Sanchez et al., 2010). Differential loading will result in varying patterns of modelling and remodelling according to Wolff's Law. There is therefore a strong overlap in the signals of growth, mechanics, and the environment, closely linked to lifestyle.

Laurin et al. (2004) applied phylogenetically weighted logistic regression techniques to femoral compactness and body size of lissamphibians, showing that an increase in both parameters is associated with the return to a fully aquatic lifestyle. Lissamphibians were chosen as they have a great diversity of lifestyles and a fairly conservative body shape (Laurin et al., 2004). The femur was chosen partly due to availability, and as it is suggested that the proximal limb elements more strongly reflect a change in lifestyle (reflected in changes

in compactness), than distal elements (Ashley-Ross, 1994). However, an earlier study, using concentrated-changes tests, suggested a closer correlation of axial length (rather than bone compactness) with lifestyle. Although the authors could isolate aquatic taxa (which tended to have a smaller medullary cavity), they were unable to distinguish between amphibious and terrestrial taxa solely based on size or compactness. The degree of compactness relating to lifestyle and ecosystem may also change between sprawling and upright gaits (Girondot & Laurin, 2003).

Using principal components analysis, researchers were able to discriminate between temnospondyls in terrestrial and aquatic environments (Sanchez et al., 2010). They looked at surface area and circularity of circumference, as well as various histological indicators such as circularity of vascular canals and resorption cavities. Gross measurements of various skeletal elements (such as skull and humeral and femoral length) were also included to allow for the effects of scale in calculations, and so that histological results could be compared with expectations of palaeoecological morphotypes. Characteristics of resistance to torsion (empty medullary cavity, greater compactness of cortex and vascular circularity) isolated one specimen as strongly terrestrial in PCA analysis. The histological information was particularly useful in cases where the anatomical proportions were not strongly indicative of adaptation to habitat, distinguishing between shallow water and terrestrial limb-driven locomotion. A lack of significant differences between the organisation of the stylopods of juveniles and adults was interpreted as an indication that locomotor style was probably the same (assuming a similar environment). Further, shaft circularity (expected to be indicative of greater torsional strain) did not explain resistance to torsion, although this could be because temnospondyl bones do not conform to the typical tetrapod cylinder shape, being shorter and fatter (Sanchez et al., 2010).

### **Environment and growth**

It has also been suggested that CGM's are a response to environmental factors such as temperature variation or seasonality, although results are mixed. A global study on extant wild ruminants showed that growth was

arrested in line with a decrease in metabolic rate, body temperature and hormonal changes, as an energy conserving strategy prompted by seasonality (Köhler et al., 2012). It has previously been suggested that photoperiodicity is a critical factor for the deposition of LAGs (Padian & Lamm, 2013). The many observations of zonation in fish suggest a positive correlation between annual zones and regions with more extreme seasonal contrast (Peabody, 1961). However, a change in environmental circumstances simulated by restricting food availability in juvenile quails, resulted in decreased growth rate (reduced cortical thickness), but no formation of LAG's or annuli (Starck & Chinsamy, 2002).

Wilson & Chin (2014) found that migratory behaviour is not recorded in the bone microstructure of pygoscelid penguins, and no LAGs were found in non-migratory gentoos, although this could be due to birds reaching skeletal maturity before overwintering or migration (Wilson & Chin, 2014). A study of polar dinosaur bone histology notes a continuous rate of bone deposition in a hypsilophodontid femur (without LAGs), where migration was discounted due to small size, whereas an ornithomimosaur from the same area has a cyclical pattern of bone formation with at least nine LAGs. The authors interpreted these varying patterns of bone microstructure as reflections of different growth strategies of the two dinosaurs (Chinsamy et al., 1998).

In conclusion, strong overlaps in the signals of mechanics and the environment, closely linked to lifestyle, make it difficult to isolate the effects of bone growth to just one of these factors on bone growth.

## **2.5 Taxonomy and Phylogeny**

On the simplest level, broad differences in bone histology can be observed between fish, reptiles, mammals, and birds. Quekett (1849b) wrote: "in each of the four great classes of animals, the bone-cells present certain peculiarities in their form, which, when once an observer is conversant with, he would be enabled to satisfy himself as to the true affinities of doubtful specimens of organic remains." He observed differences in bone cell size, shape and

presence, as well as the orientation and the size of vascular canals, and the size, number, and organisation of canaliculi, which he summarised across these four groups (Quekett, 1849b). Differences in bone matrix type among taxa were noted by Foote & Hrdlička (1916), and Enlow observed similar variation in his extensive thesis and subsequent studies describing vertebrate bone histology (Enlow, 1955; Enlow & Brown, 1956, 1957, 1958). Most recently, de Buffrénil et al. (2021) summarise the diversity of skeletal tissues found across vertebrates, including a chapter dedicated to phylogenetic signal in bone histology.

There are a number of studies, particularly in the fields of anthropology and forensic science, which explore the use of histological variables for the purpose of species discrimination and determination (Mulhern & Ubelaker, 2001; Dittmann, 2003; Urbanová & Novotný, 2005; Martiniaková et al., 2006; Hillier & Bell, 2007; Crescimanno & Stout, 2012; Skedros et al., 2013; Brits et al., 2014; Cummaudo et al., 2019). Research has emphasised methods that can be used to distinguish between human and non-human bone, a priority in forensic work for example, and have thus necessarily mostly involved extant species. One of the benefits of extant studies is the ability to check results against a priori known taxonomic groups - although this poses a problem where fossil taxa are concerned, where phylogenetic relationships may be unresolved, or where there is too little material to allow for confident assignation. These studies have found it is generally possible to distinguish between human and non-human bone specimens, the latter usually domestic and farm animals (see review by Hillier & Bell, 2007; but see Cattaneo et al., 2009), using secondary osteon circularity (Crescimanno & Stout, 2012), and diameter (Skedros et al., 2013; but see Dittmann, 2003), or osteocyte morphometrics (Cummaudo et al., 2019). These studies were generally not concerned with evolutionary patterns or apportioning differences due to environmental, life-history, phylogenetic or other influences, but simply to determine if there is a difference that can be used to identify or discriminate between species. Nonetheless, the results are useful in providing an indication of potential areas for further exploration. However, we need to be cautious when drawing conclusions from studies involving human bone as humans

display some particular and unusual bone histology characteristics, possibly in part linked to an unusually long life span. Human bone displays a high degree of bone remodelling, and a very wide range of Haversian canal and Haversian systems diameter and density measurements, which can create a large overlap area with some animal species (Urbanová & Novotný, 2005; Skedros et al., 2013). Nevertheless, plexiform bone, typical of large mammals, is uncommon in humans (except rarely in foetal and pathological bone), as is banding (the linear organisation of primary or secondary osteons), and these have successfully been used as distinguishing features to separate human from animal bone (Mulhern & Ubelaker, 2001; Martiniaková et al., 2006; Hillier & Bell, 2007; Brits et al., 2014).

When reviewing non-human animal studies, the majority are conducted at the taxonomic classification level of order and above, and information about how variables differ at the species level is sparse. Qualitative differences in histological variables are generally noted between taxa. These studies indicate some taxonomic utility in histomorphometrics, for example in vascular canals (Martiniaková et al., 2007), osteon size, shape and number of lamellae (Hidaka et al., 1998; Zedda et al., 2008; Giua et al., 2014), and osteocyte lacunal distance and density (Skedros, 2005). However, few of the studies compared homologous elements or controlled for variations in histology due to different rates of growth related to ontogenetic stage, biomechanics, or size, all of which have been shown to impact on bone histological traits (Castanet et al., 2000; de Margerie et al., 2004; Klein & Sander, 2008; Skedros et al., 2013; Felder et al., 2017).

Of the extant studies that compared humeri and/or femora of similarly sized, adult species (Zedda et al., 2008; Giua et al., 2014), secondary osteon size, shape and number of lamellae seem to be the best candidates for species discrimination; osteon circularity may also have some taxonomic utility. When tested for statistical significance, weak to strong support relating to interspecific differences emerges, but this varies across taxa, and according to the variable under investigation.

It is important to appreciate that species differentiation is not the same as identification and does not necessarily equate to a unique characteristic. In addition, not all studies are directly comparable, as imaging techniques, choice of variables, methods of quantifying morphometric data, and statistical analysis vary. Further, in assessing results, one of the disadvantages of null hypothesis testing methods such as ANOVA can be an over-reliance on the  $p$ -value in determining significance, which is influenced by a variety of factors such as sample size (Thiese et al., 2016). The biggest problem, however, is the non-independence of taxa, which means that without further investigation it is not clear whether these differences are due to relatedness, or whether they are influenced by other factors such as mechanics or size. To assess whether variation is in fact due to relatedness, we need to test for the presence and strength of a phylogenetic signal (see 1.3 and Chapter 5).

## 2.6 Summary

- Palaeohistology provides insight into the growth, mechanics, and the evolutionary trajectory of extinct organisms.
- Bone matrix type is informative about general rates of growth. Rates of growth may be indicative of physiology, but bone matrix type is not diagnostic for endothermic or ectothermic physiology.
- Amprino's rule holds, however, intraskeletal variation is high. Ideally in comparative studies, we should compare homologous skeletal elements.
- Cyclical growth marks are a useful tool for age estimation and to produce growth curves and ontogenetic inferences, but poorly reflect lifestyle.
- Statistical analyses suggest that there is a significant phylogenetic signal in some histological structures; bone size and cortical thickness in particular may be informative.
- The dynamic nature of bone growth means that the mechanical signal is generally significant in histological structures, enabling inferences regarding locomotor dynamics, ecology, and lifestyle.

- An under researched area, which this study seeks to explore, is the use of histological traits to inform phylogenetic analyses in palaeontology.

## Chapter 3 Materials and methods

This chapter outlines the basic materials and methodology used in the current study. Methods and materials used for a specific part of the study are described in the methods section of the relevant chapter.

### 3.1 Sauropod specimens

Sauropods were chosen partly due to the availability of material, which is well sampled within non-avian dinosaurs. The chosen taxa are quadrupedal and graviportal, which minimises the influence of different locomotor styles on bone histology. Not all the specimens have been confidently identified at the species level as they are from isolated long bones, and therefore some are at best diagnostic at the level of genus (Griebeler et al., 2013).

A total of 35 specimens from 10 taxonomic groups within Neosauropoda were analysed (**Table 3.1**): *Dicraeosaurus hansemanni*, *D. sattleri* and *Dicraeosaurus* sp.; Apatosaurinae; *Camarasaurus* spp.; *Europasaurus holgeri*; *Giraffatitan brancai*; *Phuwiangosaurus sirindhornae*; *Magyarosaurus dacus*; *Ampelosaurus atacis*. In addition, *Janenschia robusta*, which is most likely a non-neosauropod eusauropod (Mannion et al., 2019).

Most of these specimens are held at Bonn University and have been the subject of several previous histological studies, apart from NHMUK PV R5937 (*Giraffatitan*), and NHMUK PV unreg. (*Dicraeosaurus*) which were core sectioned for this study and are held at the Natural History Museum, London.

**Table 3.1 List of specimens in the current study**

| Taxa                                | Specimen no.                    | Femoral length (mm) | Circum (mm)      | HOS                 |
|-------------------------------------|---------------------------------|---------------------|------------------|---------------------|
| <i>Giraffatitan brancai</i>         | MFN IX 1                        | 880 <sup>a</sup>    | 340 <sup>a</sup> | 9 <sup>c</sup>      |
|                                     | MFN XV                          | 2190 <sup>a</sup>   | 820 <sup>a</sup> | 12 <sup>a</sup>     |
|                                     | MFN dd452                       | 1350                | 620              | 10 <sup>a</sup>     |
|                                     | MFN Nr 305                      | 1560                | 609 <sup>b</sup> | 11 <sup>c</sup>     |
|                                     | MFN St 291                      | 1830                | 713 <sup>b</sup> | 10/11 <sup>c</sup>  |
|                                     | NHMUK PV 5937*                  | 876                 | 294              | 8                   |
| <i>Dicraeosaurus</i>                | <i>D. hansemanni</i> MFN dd3032 | 1140                | -                | 9 <sup>c</sup>      |
|                                     | <i>D. sattleri</i> MFN M1b      | 1120                | -                | 9 <sup>c</sup>      |
|                                     | <i>D. sattleri</i> MFN O2       | 980                 | -                | 8 <sup>c</sup>      |
|                                     | <i>D. sp.</i> NHMUK PV unreg*   | 1065                | -                | 11                  |
|                                     | <i>D. sp.</i> NHMUK PV unreg*   | 1065                | -                | 11                  |
| Apatosaurinae                       | BYU 681-11940                   | 1330                | 535              | 9 <sup>a</sup>      |
|                                     | BYU                             | 1580                | 680              | 12/EFS <sup>a</sup> |
|                                     | 601-17328                       | 2044 <sup>b</sup>   | 910              | 13 <sup>a</sup>     |
|                                     | OMNH 4020                       | 970                 | 370 <sup>a</sup> | 7 <sup>c</sup>      |
|                                     | BYU 681-17014                   |                     |                  |                     |
| <i>Europasaurus holgeri</i>         | DFMMh/FV 495.9                  | 400 <sup>a</sup>    | 181 <sup>a</sup> | 9 <sup>a</sup>      |
|                                     | DFMMh/FV 403.3                  | 475 <sup>a</sup>    | 185 <sup>a</sup> | 10 <sup>a</sup>     |
|                                     | DFMMh/FV 555.2                  | 316 <sup>a</sup>    | 175 <sup>a</sup> | 11 <sup>a</sup>     |
| <i>Camarasaurus</i> spp.            | CM 11393                        | 1566                | 682              | 12 <sup>c</sup>     |
|                                     | CM 36664                        | 1452                | 644 <sup>b</sup> | 12/EFS <sup>c</sup> |
|                                     | BYU 725-12173                   | 1330                | 570              | 8 <sup>a</sup>      |
|                                     | SMA K11-29-1                    | 830 <sup>a</sup>    | 376 <sup>b</sup> | 12 <sup>c</sup>     |
|                                     | SMA 0002                        | 935 <sup>a</sup>    | 421 <sup>b</sup> | 11 <sup>c</sup>     |
| <i>Magyarosaurus dacus</i>          | FGGUB r1992                     | 540                 | 195              | 14 <sup>d</sup>     |
|                                     | FGGUB r1046                     | 525                 | 193              | 14 <sup>d</sup>     |
|                                     | FGGUB r1220                     | 346                 | 176              | 13 <sup>d</sup>     |
|                                     | FGGUB r1511                     | 466                 | 179              | 13 <sup>d</sup>     |
| <i>Phuwiangosaurus sirindhornae</i> | PC.DMR K21                      | 1120                | -                | 11 <sup>c</sup>     |
|                                     | PC.DMR No no.                   | 1030                | -                | 10/11 <sup>c</sup>  |
|                                     | PC.DMR K4-69                    | 1050 <sup>a</sup>   | -                | 12 <sup>c</sup>     |

| Taxa                       | Specimen no. | Femoral length (mm) | Circum (mm) | HOS             |
|----------------------------|--------------|---------------------|-------------|-----------------|
| <i>Janenschia robusta</i>  | NHUB Nr 22   | 1270                | -           | 12 <sup>e</sup> |
| <i>Ampelosaurus atacis</i> | MDE C3 174   | >690                | 480         | 12 <sup>f</sup> |
|                            | MDE C3 203   | 780                 | 270         | 12 <sup>c</sup> |
|                            | MDE C3 1182  | 695                 | 273         | 13 <sup>c</sup> |
|                            | MDE C3 527   | 680 <sup>a</sup>    | -           | 13 <sup>c</sup> |
|                            | MDE C3 261   | 840 <sup>a</sup>    | -           | 12 <sup>c</sup> |

\*Sectioned for this study

<sup>a</sup>Mitchell & Sander (2014)

<sup>b</sup>estimated from linear regression

HOS stages from <sup>a</sup>Mitchell & Sander (2014), <sup>c</sup>Mitchell et al. (2017), <sup>d</sup>Stein et al. (2010),

<sup>e</sup>Sander (2000a), <sup>f</sup>Klein et al. (2012), apart from\*

*Giraffatitan*, *Dicraeosaurus* and *Janenschia* are from the Late Jurassic Tendaguru Formation, Tanzania (Africa) which displays a diverse range of sauropod fauna (Janensch, 1914, 1929) (**Figure 3.1**). *Giraffatitan brancai* (Janensch, 1914) is a large, basal brachiosaurid titanosauriform. Previously known as *Brachiosaurus brancai* but recovered as a separate species (Taylor, 2009), *Giraffatitan* is placed outside Titanosauria (Mannion et al., 2013, 2017) (**Figure 3.1**). Several specimens of the smaller diplodocoid *Dicraeosaurus* (Janensch, 1914; Schwarz-Wings & Böhm, 2014; Wilson, 2002) were studied: *Dicraeosaurus hansemanni* and *D. sattleri*, as described by (Sander, 2000a). An additional specimen, *Dicraeosaurus* sp. (NHMUK PV unreg.), as yet unregistered but confidently ascribed to *Dicraeosaurus*, was included. Named for its very stocky bones, the intermediately sized *Janenschia robusta* (Fraas, 1908; Sternfeld, 1911; Wild, 1991) was originally placed as one of the oldest members of Titanosauria (Wild, 1991). More recent analyses have placed it as a non-titanosauriform (Bonaparte et al., 2000) or even a non-neosauropod (Mannion et al., 2019).

*Camarasaurus* and *Apatosaurinae*, also Late Jurassic, are both from the Morrison Formation in North America (Ayer, 1999; Mateus, 2006). Coeval with the Tendaguru beds, the Morrison Formation boasts a wide range of sauropod fauna, including nesting sites, and the most commonly found sauropod,

*Camarasaurus*. Several specimens of unspecified camarasaurid, *Camarasaurus* spp. (Cope, 1877) were analysed. Positioned outside of Titanosauriformes, *Camarasaurus* is a medium sized basal macronarian (Carballido et al., 2011; D’Emic, 2012).

Four specimens previously attributed to the large diplodocid *Apatosaurus* (Marsh, 1877) were studied. However, Tschopp et al. (2015) called into question the specific assignation of many of the Morrison apatosaurids, and so they are listed here as Apatosaurinae.

Two dwarf taxa, *Europasaurus* and *Magyarosaurus*, are included. The Late Jurassic dwarf sauropod *Europasaurus holgeri* (Sander et al., 2006), is one of the most complete sauropods known from northern Germany. The phylogenetic position of *Europasaurus* is controversial, and it is considered either a brachiosaurid titanosauriform (Mannion et al., 2013, 2017), or a basal camarasauromorph outside Titanosauriformes (Carballido et al., 2020). The similarly sized, Late Cretaceous titanosaur, *Magyarosaurus dacus* (Nopcsa, 1915), originally *Titanosaurus dacus*, is from Romania, and the smallest adult sauropod discovered at 5 m (Jianu & Weishampel, 1999).

The Late Cretaceous titanosaur, *Ampelosaurus atacis* (le Loeuff, 2005), a derived lithostrotian, is from southern France, and was most recently placed as a saltasaurid within Lirainosaurinae (Díez Díaz et al., 2018; Wilson, 2002).

*Phuwiangosaurus sirindhornae* (Martin et al., 1993, 1994) is an Early Cretaceous basal titanosauriforme from the Sao Khua Formation in Thailand, recently recovered within Euthelopodiae (D’Emic, 2012; Mannion et al., 2013; Mocho et al., 2014), although it has previously been placed as a brachiosaurid (Royo-Torres et al., 2009), and titanosaur (Carballido et al., 2011; D’Emic, 2012).

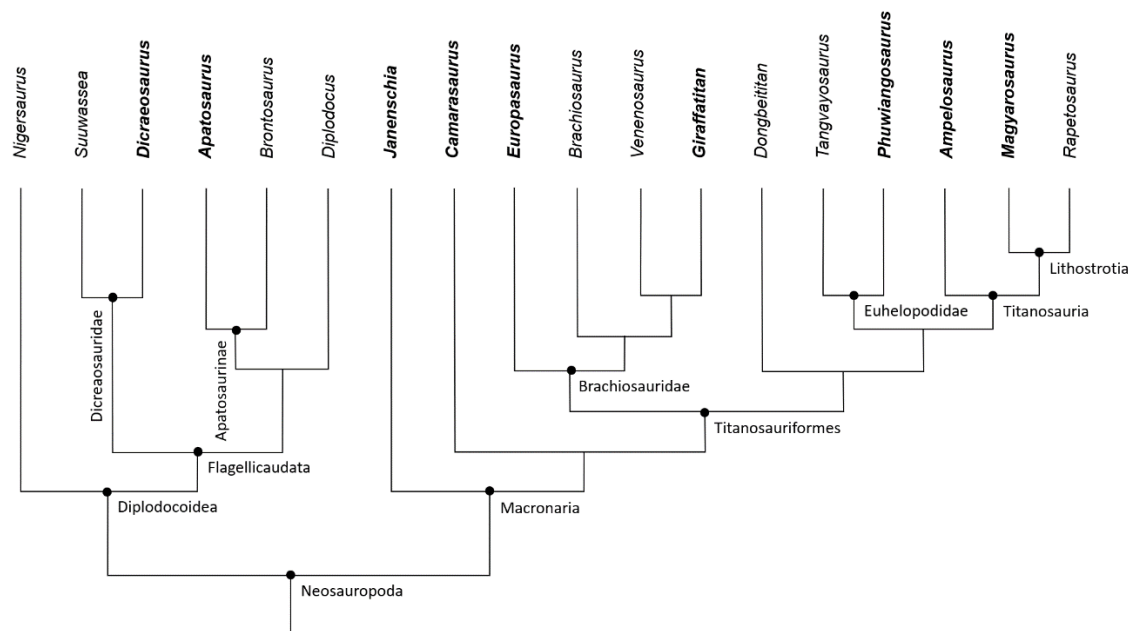


**Figure 3.1 Cladogram of Neosauropoda.** Combined cladogram showing phylogenetic relationships of Neosauropoda, after: Bates et al. (2016); Cashmore et al. (2020); Mannion et al. (2013, 2017, 2019); Tschopp et al. (2015). Taxa used in this study are in bold.

### 3.2 Phylogenetic tree

Tree data was drawn from Cashmore et al. (2020), a super tree combining several sources and time scaled using the Extended Hedman method (Hedman, 2010; Lloyd et al., 2016). Branch lengths were calculated using first and last appearance datums (see S1). Changes to the phylogeny were made using Mesquite (Maddison & Maddison, 2018). Changes made were the position of *Magyarosaurus*, which is under review (P. Upchurch pers. comm. 2022) and was added to the tree in the most recent position as sister to *Repetosaurus* (Curry Rogers, 2005); labels were changed to *Camarasaurus* spp, rather than a specific species; and *Apatosaurus* was re-labelled Apatosaurinae.

Methods of calculating phylogenetic signal are sensitive to the size of the phylogeny, polytomies and the inclusion of branch lengths. The data set included branch lengths and no polytomies. It is not ideal to mix taxonomic levels (for example subfamily and species level data), however, as tip numbers were small, it was considered better to do this to keep as many taxonomic groups as possible. The tree was subsequently pruned to match the data file.

### 3.3 Specimen histology

Titanosaurs such as *Ampelosaurus*, *Phuwiangosaurus* and *Magyarosaurus* display an atypical sauropod primary bone matrix called “modified lamellar bone” (MLB: Klein et al., 2012; although see Woodward & Lehman, 2009; Ghilardi et al., 2016) where the fibrolamellar bone matrix consists of mostly parallel-fibered or lamellar bone rather than woven bone, in addition to early onset of extensive remodelling prior to reaching skeletal maturity (Klein et al., 2012; Stein et al., 2010). This suggests a generally lower growth rate compared to diplodocids and basal macronarians (Klein & Sander, 2008; Klein et al., 2009). This extensive remodelling by secondary osteons was the inspiration for Stein et al.'s (2010) addition of the 14<sup>th</sup> HOS stage and the development of the RS (remodelling stages) technique by Mitchell et al. (2017). As Haversian bone overprints the primary bone fibre matrix and makes it difficult or impossible to compare original histological features, the degree of remodelling, size and shape of secondary osteons, and the osteocytes within them may be good traits for comparison of mature sauropod bone.

The bone histology of *Dicraeosaurus*, *Giraffatitan* (previously listed as *Brachiosaurus*) and *Janenschia* are described in Sander's (2000a) study of the histology of the Tendaguru sauropods. *Giraffatitan* shows typical fibrolamellar bone with a thick cortex, with narrow lumina in adults that contain distinct flattened osteocyte lacunae and extensive remodelling as full size is reached. Unusually, *Giraffatitan* was shown to reach sexual maturity at about only 40% of maximum size (Sander, 2000a). Bone histology of the two *Dicraeosaurus* species, *D. hansemanni* and *D. sattleri*, is similar, but differs from that of other Tendaguru sauropods by displaying a regionalised vascular pattern, where

laminar fibrolamellar bone (with circumferential vascular canals) alternates with regions dominated by longitudinal to plexiform canals. In addition, large erosion cavities with only a thin lamellar lining extend up to the mid-cortex, resulting in high levels of vascularity (Sander, 1999). The cortex of *Janenschia* is very thick, with many erosion spaces and gradual transition between juvenile and adult bone as indicated by the width of the lumina and (unusually for sauropods), a fairly distinct boundary between the spongiosa and cortical bone. Of particular note are the many, well-developed polish lines (Sander, 2000a), considered comparative to annual growth lines but only visible under reflected light, in addition to LAGs. Together these allow for a detailed growth record of *Janenschia* to be constructed, indicating time to sexual maturity estimated as 11 years, and somatic maturity reached at 26 years (Sander, 1999, 2000a; Sander & Tückmantel, 2003).

All three of the *Camarasaurus* specimens available for histological analysis (M1b, O2 and dd3032) were identified as belonging to the same, large morphotype (type 2) by Klein and Sander (2008), and showed growth marks more frequently than in Titanosaurs.

Signs of bone maturity such as a reduction in the spacing of LAGs, extensive remodelling and an EFS, together with reduced bone length, indicate that *Europasaurus* is an insular dwarf species (Sander et al., 2006). The Hațeg Basin, previously an island (Benton et al., 2010), is home to *Magyarosaurus*, another island dwarf sauropod. The presence of extensive remodelling in *Magyarosaurus*, indicates a small adult rather than the juvenile of a larger species (Benton et al., 2010; Stein et al., 2010).

### **3.4 Definition of adult**

Adult specimens were selected to minimise age related differences. However, restricting specimens to those with an EFS, signifying full, somatic maturity has been reached, resulted in a very small data set, in addition, this feature may not appear in all species. In the absence of an EFS in most specimens, and to improve the robustness of statistical analysis, data sets were expanded to

include specimens of HOS 8 and above, which are considered sexually mature, as indicated by a slowing of growth rate (Klein & Sander, 2008). It is important to note that although these specimens can be considered 'adult', they may not have reached full, somatic growth which continues beyond sexual maturity in sauropods (Sander, 2000a), and so it is accepted that an ontogenetic signal may not be eliminated. HOS stages were established for the two specimens sectioned for this study, NHMUK PV R5937 (HOS 8), and NHMUK PV unreg. (HOS 11) according to the standard method (Klein & Sander, 2008; Stein et al., 2010). Diplodocoid specimens of Stage 3 and above on the combined Histo-Morph Ontogeny Scale (H-MOS) of Woodruff et al. (2017) were selected, corresponding to HOS 8 and above.

### **3.5 Skeletal element**

The femur was chosen as it is the largest and most robust appendicular bone, as well as being considered a suitable proxy for body size, and to aid comparison with previously published studies.

Femora are subject to high levels of mechanical stress, which is likely to lead to higher remodelling rates and possibly influence the morphology of histological structures within the bone (Goliath et al., 2016). Several other skeletal elements such as the fibula and ribs were considered, however, lack of specimens, and more limited cortical bone area meant that the fibula was discounted, and less is known about the effects of calcium homeostasis on the morphometrics of bone histology in ribs. Comparison of the same skeletal element across specimens limits variation due to different locomotory styles. Biomechanical variation was also limited due to the study taxa being considered graviportal quadrupeds (Bonnar & Bonnar, 2003).

### **3.6 Measuring phylogenetic signal**

A variety of methods are used to measure phylogenetic signal, such as Bayesian and maximum likelihood methods, or techniques based on spatial autocorrelation that estimate correlation between histological features and

location on a phylogeny. These can be applied to univariate, covariate, or bivariate data. Autocorrelation tests include: Moran's  $I$  (Moran, 1950; Gittleman & Kot, 1990); Abouheif's  $C_{mean}$  (Abouheif, 1999); Phylogenetic Eigenvector Regression (PVR: Diniz-Filho et al., 2012); and regressions on distance matrices based on a Mantel test (Legendre et al. 1994). These tests infer the degree to which a trait is influenced by its phylogenetic position and thus look for correlation of traits in terms of relating to spatial and time series data (Keck et al., 2016). Some of the methods, such as PVR and regressions on distance matrices incorporate branch length information but not an evolutionary model (although see Debastiani & Duarte, 2017). Alternatively, methods that assume an evolutionary model (usually Brownian motion), such as Blomberg's  $K$  (Blomberg et al., 2003) and Pagel's  $\lambda$  (Pagel, 1999), can be used to investigate underlying evolutionary processes (see Münkemüller et al., 2012 for a comparison).

Blomberg's  $K$ -statistic (Blomberg et al., 2003; Revell, 2012) compares the amount of observed trait variance to the trait variance expected under BM. This process is repeated (e.g., reps = 1000) and the randomised values are compared to the observed value of  $K$  to determine its significance. The strength of phylogenetic signal is expressed as a ratio of the mean squared error of the tip data ( $MSE_0$ ) measured from the phylogenetic corrected mean, and the mean squared error derived from the variance-covariance matrix from the given phylogeny ( $MSE$ ) under BM. If trait similarities closely follow a BM model,  $MSE$  will be small and thus the ratio of  $MSE_0$  to  $MSE$  (and hence  $K$ ) will be large. Conversely, if trait similarities do not follow a BM model,  $MSE$  will be large, therefore the ratio of  $MSE_0$  to  $MSE$  (and hence  $K$ ) will be small (Kamilar & Cooper, 2013). Values for Blomberg's  $K$  range from 0 to infinity. For values of  $K = 0$  (the null expectation that there is no phylogenetic signal) we infer no phylogenetic signal (phylogenetic independence);  $K = 1$  indicates strong phylogenetic signal and that species' traits are distributed as would be expected under BM;  $K > 1$  indicates a phylogenetic signal stronger than would be expected under BM.

Pagel's lambda ( $\lambda$ ) (Pagel, 1999; Revell, 2012) is a scaling parameter for the phylogeny, providing a weighting factor that, when fitted to the Brownian phylogenetic covariance, scales it to the observed data. Therefore,  $\lambda$  is the transformation of the phylogeny that ensures the best fit of the trait data to a BM model. Pagel's  $\lambda$  ranges from 0 to 1. For  $\lambda = 0$  we infer that species' traits evolve independent of phylogeny (i.e., no, or weak phylogenetic signal), where  $\lambda = 0$  shrinks the internal branches relative to the tip branches, creating a polytomy - essentially a star phylogeny. For  $\lambda = 1$  we infer "species' traits covary in direct proportion to their shared evolutionary history" (Freckleton et al., 2002), or random genetic drift under a BM model (i.e., strong phylogenetic signal). Intermediate values indicate a phylogenetic effect weaker than that expected under BM, or trait evolution according to some model other than pure BM. Although values of  $\lambda$  can theoretically exceed one (where traits are more similar than would be expected under BM), in practice, values of  $\lambda$  are constrained to be equal to one as covariances cannot exceed variances in a phylogenetic variance-covariance matrix.

In addition, Pagel's  $\lambda$  can be used as an indicator of effect size. Münkemüller et al. (2012) compared four indices of phylogenetic signal using simulated data (Blomberg's  $K$ , Pagel's  $\lambda$ , Abouheif's  $C_{\text{mean}}$  and Moran's  $I$ ). These were compared to a weighting factor ( $w$ ) determined from traitgrams, where continuous traits were simulated under different strengths of BM ( $w$ ), to estimate the strength of the phylogenetic signal. The weighting factor was found to be very similar to Pagel's  $\lambda$  (unsurprisingly, as  $w$  was based on  $\lambda$ ). Therefore,  $w$  can be approximated from Pagel's  $\lambda$ , providing a reliable effect size measure (Freckleton et al., 2002; Münkemüller et al., 2012).

Moran's  $I$  (Moran, 1950) is a measure of spatial autocorrelation based on simultaneous data locations and values, and establishes whether the spatial pattern observed is clustered, random, or dispersed. It was adapted for phylogenies by Gittleman & Kot (1990) and is described as "an autocorrelation coefficient describing the relation of cross-taxonomic trait variation to phylogeny". Deviations from the mean of neighbouring values are multiplied to create a cross-product. Neighbouring values that are either both above or

below the mean, and hence can be said to be clustering together, will generate a positive cross product (Moran's index). Values that are either side of the mean will generate a negative cross product and represent a dispersed pattern. Those randomly arranged, (indicating no autocorrelation) will have a value of zero. The observed value is compared to an expected value and a  $p$ -value is calculated to indicate whether the difference is statistically significant. The null hypothesis is that there is a random distribution across the space (phylogeny), interpreted as low or no phylogenetic signal. Moran's  $I$  usually varies from -1 to 1; values close to 0 indicate species resemble each other as predicted under BM; values  $< 0$  indicates species resemble each other less than predicted by BM; values  $> 0$  indicate species resemble each other more closely than expected under BM.

Abouheif's  $C_{\text{mean}}$  (Abouheif, 1999) is derived from a test for serial independence (TFSI) (von Neumann et al., 1941) and is based on two measures of spatial autocorrelation, Geary's  $c$  tests and Moran's  $I$  (Pavoine et al., 2008). Therefore, Abouheif's  $C_{\text{mean}}$  is similar to Moran's  $I$ , also varying from -1 to 1, but unlike Moran's index, it is calculated using a non-zero diagonal in the matrix of phylogenetic proximities. A further difference, and possible advantage in some cases, is that Abouheif's  $C_{\text{mean}}$  does not require branch lengths. Nodes are rotated, which changes the ranking of the tips whilst maintaining the topology, whilst the mean of the TFSI  $C$ -statistic is calculated for each rotation and compared to the observed mean  $C$ -statistic. The null hypothesis that there is no phylogenetic autocorrelation can be rejected if the probability of the observed mean is less than the chosen alpha value ( $p < 0.05$ ). All four of these methods broadly agree but are calculated following different approaches and thus measure different aspects of phylogenetic signal (see Hjelmen & Johnston, 2017; Münkemüller et al., 2012; Pavoine & Ricotta, 2013 for examples).

All four of these methods broadly agree but are calculated following different approaches and thus measure different aspects of phylogenetic signal (see Hjelmen & Johnston, 2017; Münkemüller et al., 2012; Pavoine & Ricotta, 2013 for examples).

### **The significance and strength of phylogenetic signal**

The significance and strength of phylogenetic signal is influenced by many factors: taxonomic level; sample size; topology; calculation method; skeletal element; and the biological variable under investigation (Losos, 2008; Pearman et al., 2008). De Ricqlès' opinion, expressed in several studies, is that a phylogenetic signal in bone histology is present, but likely to be weakly expressed (de Ricqlès et al., 2004, 2008; de Ricqlès, 2011). However, he does conclude that "bone tissue phenotypes can reflect a phylogenetic signal at supraspecific levels if homologous elements are used, and if ontogenetic trajectories and size-dependent differences are taken into consideration" (de Ricqlès et al., 2008). Padian (2013) also agrees that "the phylogenetic 'signal' in bone is persistent, but it is never the strongest signal". A trait with no or very weak phylogenetic signal is likely to alter randomly across a phylogeny, and relationships between taxa cannot be explored by reference to the presence or lack of that trait in an ancestor. Conversely, a trait with a very strong phylogenetic signal that is highly conserved or subject to inertia, will lack variability and this limits its usefulness as a phylogenetically informative trait. Values accepted as indicating 'strong' (or 'high') phylogenetic signal vary among authors (Losos, 2008), but it is generally accepted as  $K$  or  $\lambda$  near or equal to 1, and a weak phylogenetic signal is where  $K$  or  $\lambda$  is near, or equal to 0 (Cooper et al., 2010). Kamilar and Cooper (2013) consider  $K > 0.5$  as moderate to high.

A very high or strong signal ( $K > 1$ ) may be the result of evolutionary and phylogenetic conservatism, inertia, or constraint (Blomberg & Garland, 2002; Losos, 2008). Phylogenetic conservatism is the retention of traits over time among related species (Wiens et al., 2010) and may be due to: stabilising selection; pleiotropy (for example, a gene influencing two or more seemingly unrelated phenotypic traits); high levels of gene flow; limited genetic variation; low rates of evolution; or physiological or biotic constraints that restrict the evolution of new phenotypes (Harvey & Pagel, 1991; Wiens & Graham, 2005; Losos, 2008; Revell et al., 2008; Ackerly, 2009). Traits evolving to an optimum which itself evolves according to a BM process (Hansen et al., 2008) or genetic drift occurring at different rates across a phylogenetic tree can also result in a

phylogenetic signal greater than that expected under BM (Revell et al., 2008). A low or weak phylogenetic signal ( $K$  or  $\lambda$  near 0) indicates species' traits are more similar in distant relatives and less similar in close relatives or are randomly distributed across a phylogeny. This results in phylogenetic trees that are not always divergent. Weak phylogenetic signal may be due to interspecific hybridization; horizontal gene transfer; convergent evolution; reversion of traits to ancestor states (OU process); limits to evolution; stabilising selection; adaptive radiation (rapidly diversifying to fill new niches); cryptic speciation (different species that look similar); or a variety of processes that lead to high evolutionary lability (highly changeable traits) (Gittleman et al., 1996; Blomberg et al., 2003; Losos, 2008). Therefore, either a very strong signal (which could indicate inertia or constraint), or a very weak signal means that the variable is likely to be unsuitable for use in phylogenetic analysis.

Different causes of strong or weak phylogenetic signal can make results difficult to interpret without further analysis, and evolutionary processes such as random variation or stasis that do not conform to a BM model of evolution, may produce similar  $K$  or  $\lambda$  values, particularly when phylogenetic signal is weak. In addition, Phylogenetic Niche Conservatism (PNC), the “tendency of species to retain ancestral ecological characteristics” (Wiens & Graham, 2005) which has been shown to result in strong phylogenetic signal (Harvey & Pagel, 1991; Wiens & Graham, 2005; Losos, 2008), may, conversely, also lead to very weak phylogenetic signal (Revell et al., 2008). This poses a challenge as to the interpretation and meaning of phylogenetic signal. One solution is to compare the relative fit of different models of evolution to the data, such as a white noise, BM, or a stabilising selection model (e.g., Ornstein-Uhlenbeck model, see Chapter 5). The expectation being that random variation in traits might show a better fit with a white noise model, and stasis may show a better fit with, for example, an OU model that pulls towards a central trait value or tendency.

### 3.7 Imaging and analysis

Transverse petrographic thin sections of sauropod femora from collections held by the Steinmann Institute at Bonn University were examined in situ by the author. Thin section slides were primarily from drill cored sections, but also diaphyseal sections, all prepared in accordance with standard histological practices for fossil bone (Padian & Lamm, 2013; Sander, 2000a). The standard area to sample for histological analysis of the femur is the anterior side, at the area of least circumference, approximately mid-diaphysis. This position records the most complete appositional growth record and least periosteal remodelling (Francillon-Vieillot et al., 1990; Klein & Sander, 2008; Garcia, 2011). All the samples chosen were taken from this location and comparative areas were identified from diaphyseal sections. This area was also used for circumference measurements.

Slides were examined and photographed at the holding institution under a Leica (Wetzler, Germany) DMLP polarising microscope with digital microscope camera attachment (Leica DFC420), using plane polarised (PPL) and cross polarised light (XPL). To visualise the osteons, canals and identify the cortical bone boundary, images of a complete transect from the inner to the outer surface of the bone at x4 magnification were stitched together using Microsoft Image Composite Editor 2.0.3 (ICE).

For the osteocytes, a series of images at x40 magnification was taken at 5  $\mu\text{m}$  intervals, bringing into focus the furthest to the nearest osteocytes in the field of view. An average of 5 images were stacked, meaning that osteocytes from a depth of approximately 25  $\mu\text{m}$  were visualised. This was necessary to measure a reasonable number of cells from each specimen. These images were then stacked to create a 'z-stack' which combines them into one image (**Figure 3.2**). The clarity of the cell outline was improved where necessary by increasing the focus using the 'Stacks' and 'Stack Focuser' plugins in ImageJ to give a clearer outline (Abramoff et al., 2004).

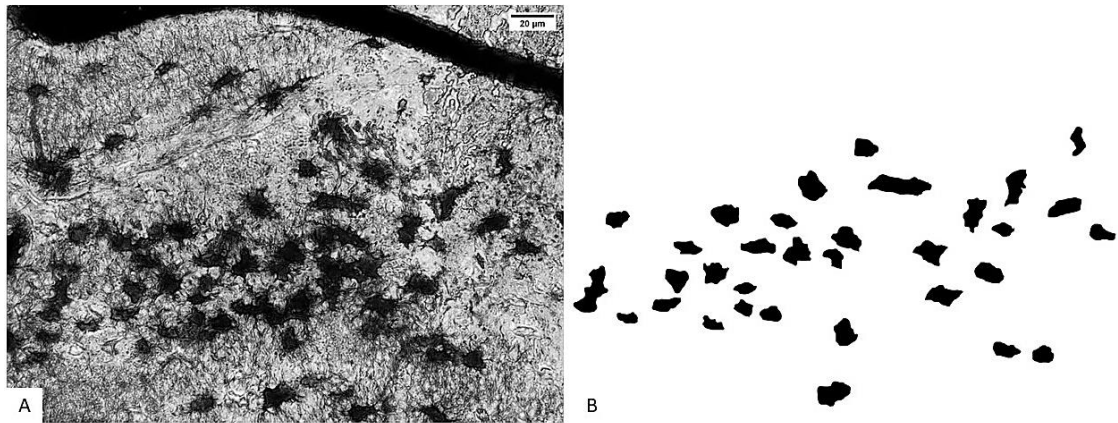


**Figure 3.2 Osteocyte lacunae within the cortical bone of *Dicraeosaurus*.** **A)** Osteocytes (centre) are from within an area of woven bone, osteocytes top left of image are within the lamellae of a secondary osteon and so were excluded. Composite image created from stacking at 5 µm intervals. **B)** Binary image of lacunae following manual outlining and filling, canalicular channels were excluded. Scale bar 20 µm. Images by S. Strachan.

Images were analysed and shape data quantified using ImageJ (Ferreira & Rasband, 2012). Various image recognition software was explored to outline the structures, such as the 'Weka Trainable Segmentation' plugin in ImageJ, which can be programmed in an iterative process to recognise certain images. However, a lack variation in greyscale values between structures and the surrounding bone meant that thresholding could not take place, and so the boundaries of all secondary osteons, canals and osteocytes were manually traced and digitised using a Wacom digitiser (Wacom, Saitama, Japan) using image software (Corel Paint Shop Pro 2019). In total, 2,676 osteons and canals, and 1,758 osteocytes were circled. Traced images were saved as binary images, and morphometric data gathered using the 'Analyse Particles' plugin in ImageJ (**Figure 3.3**). The cortical bone and medullary cavity boundary were identified using the 'Compactness Bar' method (see Chapter 4), the cortical region being defined as containing 50% or less bone as opposed to pore space, which is the usual practice in palaeohistological studies.

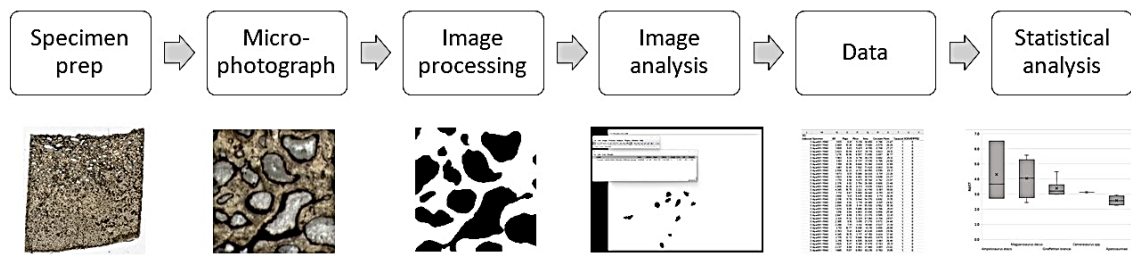


**Figure 3.3 Workflow process for histomorphometric analysis.**

### **Osteons and canals**

As bone microstructure data is very often taken from thin sections (as here), micro morphometric measurements are from a 2D image of a 3D structure. Therefore, the orientation and plane of section of the feature needs to be considered and standardised. To compare longitudinal secondary osteons only, and discount osteons that were bisected at an angle resulting in a more ovate cross section, circularity was calculated. Only those with a value  $> 0.7$  were included, and only minimum diameter measurements of osteons and canals were used. Initially circularity was limited to 0.8, but this resulted in too few measurements for some specimens, and so the condition was relaxed. This is considered reasonable, given that the deviation of Haversian canals from the long axis of the cortical bone (and hence shape variation) may be minimal (Parfitt et al., 1987). Osteons were also excluded if the diameter of the Haversian canal was greater than the radius of the longest axis of the osteon, in which case the structure was considered an erosion cavity. Osteons that fell within the region of interest with a distinct cement line that was at least 90% visible were included. Minimum osteon and canal axis diameters were calculated using the secondary axis of the best fitting ellipse, as well as area. Mean osteon infill area, and the ratio between minimum internal and external diameter of the secondary osteons (KOn), was also calculated (**Table 3.2**).

### **Osteocytes**

There is a relationship between the appositional rate of bone growth, size of osteoblasts, and size of osteocytes that are subsequently formed from them (Marotti et al., 1976; Marotti, 1977). Specifically, bone that is laid down quicker

results in larger osteoblasts and larger osteocytes. Therefore, to compare lacunae across homologous bone types with similar growth rates, three bone fibre matrices were identified, using primarily collagen fibre organisation, examined under XPL with the addition of a lambda filter: woven bone was identified by randomly oriented, generally short collagen fibres in primary bone matrix that is isotropic (dark) under XPL; parallel-fibered bone was identified by a more regular, organised pattern of collagen fibres in primary bone, and anisotropic under XPL; osteocytes from secondary osteons were gathered from within the lamellae of Haversian canals with a distinct cement line. The mean value of osteocyte measurements from each bone matrix type was calculated for each specimen, and mean values used where there was more than one specimen representing a species.

It should be noted that in humans, osteocyte lacunae within secondary osteons decrease in size towards the central canal (Marotti, 1977; Ardizzoni, 2001). Due to limitations on the number of osteocytes clearly visible, osteocytes in the current study were not separated into different zones within the secondary osteon (*sensu* Cummaudo et al., 2019), which may have affected values.

The major axis of an osteocyte is oriented parallel to the collagen fibre orientation in osteons (Marotti, 1979; Kerschitzki et al., 2011). Osteocyte morphology will therefore vary according to where the cell is sectioned. Marotti (1979) demonstrated that differently oriented osteocytes in osteons, may result in a difference in cell area of 55-84% depending on the section axis. The author therefore recommends standardising orientation with respect to sectioning. This was not possible in the current study due to a lack of available material. Therefore, osteocytes within secondary osteons measured here may contain some that are obliquely dissected because of variation in orientation of collagen fibres with respect to the main axis of the osteon. However, the authors found that cell minimum diameter, did not seem to change regardless of line of sectioning and orientation of the cell (Marotti, 1979), and so minimum diameter measurements are included here to mitigate variation.

### 3.8 List of variables

**Table 3.2 List of variables used in current study**

| Variable                             | Description   |
|--------------------------------------|---|
| <b>Macro raw measures</b>            |   |
| <b>fL</b>                            | Femur length (mm)   |
| <b>Circ</b>                          | Mid-shaft circumference (least circumference) (mm)  |
| <b>CT</b>                            | Cortical thickness (mm)   |
| <b>Rd</b>                            | Radius (mm)   |
| <b>Derived measures</b>              |   |
| <b>Mass</b>                          | Body mass estimated from fL:<br>$y = 2.3459x - 0.2935$<br>where $y = \log_{10}$ body mass (g), $x = \log_{10}$ femur length (mm),<br>$r^2 = 0.73$ (O’Gorman & Hone, 2012)   |
| <b>Ar</b>                            | Bone cross sectional area estimated from circumference, $Ar = C^2/4$  |
| <b>RI(Circ)</b>                      | Circumferential Robusticity Index, $RI(Circ) = Circ/L \times 100$<br>(Stock & Shaw, 2007)   |
| <b>RI(CT)</b>                        | Cortical Thickness Robusticity Index, $RI(CT) = CT/L \times 100$<br>(Stock & Shaw, 2007)  |
| <b>TI</b>                            | Relative cortical thickness, or Thickness Index, $(TI) = CT/Circ \times 100$<br>Defined as $CT/CaM$ in Mitchell & Sander (2014)   |
| <b>K</b>                             | Ratio between the internal and external diameter of the bone,<br>$K = (Rd-CT)/Rd$<br>High K = thinner bone, varies from 0 (solid) to 1 (very thin walled)<br>Defined as $K = R-t/R$ in Currey & Alexander (1985)                                  |
| <b>Rd/CT</b>                         | Ratio between the outer radius of the bone, and the cortical thickness, high value = thinner bone, optimal value for impact loading (2.3), values for static strength (3.0), and stiffness (3-9)<br>Defined as $R/t$ in Currey & Alexander (1985) |
| <b>Secondary osteon raw measures</b> |   |
| <b>On.Dm</b>                         | Secondary axis of the best fitting ellipse, short axis diameter (minimum diameter) of secondary osteon ( $\mu\text{m}$ )  |
| <b>On.Ar</b>                         | Secondary osteon area ( $\mu\text{m}^2$ )   |

(List of variables used in current study contd.)

| Vascular canal raw measures |   |
|-----------------------------|---|
| <b>On.Vc.Dm</b>             | Secondary axis of the best fitting ellipse, short axis diameter of canal ( $\mu\text{m}$ )  |
| <b>On.Vc.Ar</b>             | Secondary osteon canal area ( $\mu\text{m}^2$ )   |
| Derived measures            |   |
| <b>On.In.Ar</b>             | Mean Infill area of secondary osteons = $\text{On.Ar} - \text{On.Vc.Ar}$ ( $\mu\text{m}^2$ )  |
| <b>KOn</b>                  | Ratio between the minimum internal and external diameter of secondary osteon<br>$\text{KOn} = ((\text{On.Dm}/2) - (\text{On.Dm} - \text{On.Vc.Dm}/2)) / (\text{On.Dm}/2)$ |
| Osteocyte raw measures      |   |
| <b>Ot.Dm</b>                | Short axis diameter of osteocyte ( $\mu\text{m}$ )  |
| <b>Ot.DM</b>                | Long axis of osteocyte ( $\mu\text{m}$ )  |
| <b>Ot.Ar</b>                | Osteocyte area ( $\mu\text{m}^2$ )  |
| <b>Ot.P</b>                 | Osteocyte perimeter ( $\mu\text{m}$ )   |
| Derived measures            |   |
| <b>Ot.Cr</b>                | Osteocyte circularity, $\text{Ot.Cr} = 4\pi (\text{Ot.Ar}) / (\text{Ot.P})^2$<br>(1 = perfect circle, 0 = elongated polygon)  |
| <b>Ot.AR</b>                | Aspect ratio of osteocyte = $\text{Ot.DM} / \text{Ot.Dm}$<br>(1 = perfect circle, values > 1 indicate increasingly ovate shape)   |

### 3.9 Statistical analysis

Statistical analyses were carried out using SPSS (IBM Statistics 27) and R (R Core Team (2021). R: A language and environment for statistical computing. R Foundation for Statistical Computing, Vienna, Austria. URL <http://www.R-project.org/>) (see individual chapters for details of packages used).

## 3.10 Abbreviations

### List of institutions

**BYU**, Museum of Earth Sciences, Brigham Young University, Provo, Utah, U.S.A.; **CM**, Carnegie Museum of Natural History, Pittsburgh, USA; **DFMMh/FV**, Dinosaurier-Freilichtmuseum Mücke/Museum für Naturkunde, Mücke, Germany; **FGGUB**, Facultatea de Geologie si Geofisica, Universitatea Bucuresti, Bucharest; **MB.R.**, Museum für Naturkunde, Berlin, Germany; **MDE**, Musée des Dinosauriens in Esperaza, Aude, France; **MFN**, Museum für Naturkunde, Berlin, Germany; **NHMUK**, Natural History Museum, London, United Kingdom; **NHUB**, Naturkundemuseum der Humboldt-Universität, Berlin, Germany; **OMNH**, Sam Noble Oklahoma Museum of Natural History, Norman, Oklahoma; **PC.DMR**, Department of Mineral Resources, Khon Kaen Province, Kalasin, Thailand; **SMA**, Sauriermuseum Aathal, Canton Zürich, Switzerland; **TMP**, Royal Tyrrell Museum of Palaeontology, Drumheller, Alberta, Canada; **IPB**, Steinmann Institute of Geology, Mineralogy and Palaeontology, University of Bonn (slides accessioned under original SMA numbers).

### Technical abbreviations

**EFS**, External fundamental system; **FLB**, fibrolamellar bone tissue; **HOS**, Histological ontogenetic stage; **LAG**, line of arrested growth; **PFB**, parallel-fibered bone tissue; **PPL**, plane polarised light; **On**, secondary osteon; **Ot**, osteocyte; **WB**, woven bone tissue; **XPL**, cross polarised light.

## 3.11 Terminology

To review the literature, it is first necessary to decide on the terminology to be used to provide an accurate and consistent reference. Many of the histological concepts and terms in use today were coined by the “founding fathers of microscopy”, Antonie van Leeuwenhoek (1632-1733) and Clopton Havers (1657-1702), after whom the central canal in an osteon which contains nerves and blood vessels is named (de Ricqlès et al., 2004). As palaeohistology has developed as a subject, authors have described the same features in different

ways (synonymy), and sometimes used the same terminology to describe different features (homonymy). In addition, as our understanding of cellular biology has developed, some terms are now misleading, and new terms need to be added (Prondvai et al., 2014). This is important to bear in mind when reviewing the literature. This study uses terminology by Francillon-Vieillot et al. (1990), but as elaborated by Padian and Lamm (2013) and Prondvai and Stein (2014).

# Chapter 4 A Novel Method to Quantify Cortical Thickness

## 4.1 Introduction

Cortical thickness in bone is measured as the width of cortical bone, as distinct from the central medullary cavity. Deciding where the medullary cavity finishes and cortical bone begins is essential for quantitatively comparing cortical bone thickness across specimens and has been used to investigate: sexual size dimorphism (Hidaka et al., 1998; Nieves et al., 2005); functional adaptation (Germain & Laurin, 2005; Mahboubi et al., 2014; Püschel & Benítez, 2014); species identification (Urbanová & Novotný, 2005; Mitchell & Sander, 2014); and phylogeny (Hidaka et al., 1998; Cubo et al., 2005; Houssaye et al., 2014); in addition to being used to calculate various robusticity and thickness indices (Stock & Shaw, 2007; Mitchell & Sander, 2014). Further, Habib and Ruff (2008) successfully demonstrated that locomotor dynamics in birds can be differentiated based on analysis of cortical thickness ('hollowness') in cross-sections of femora and humeri, and humeral cortical thickness showed particular utility in differentiating between aquatic and non-aquatic taxa (Habib & Ruff, 2008).

Typically, cortical bone ('compacta') has a greater proportion of bone to pore space, the pore space of cortical bone primarily including the vascular canals of secondary osteons and resorption cavities. The medullary cavity is usually more porous and has a lining of, or is filled with, less dense cancellous or spongy bone ('spongiosa') (Hall, 2015). Within palaeontology, compacta is most commonly identified as >50% bone and spongiosa (contained within the medullary cavity) as ≤50% bone. Therefore, the place where bone crosses this compactness threshold is used to discriminate between the medullary cavity and cortical bone, and hence identify cortical width or thickness. The proportion of bone to pore space is called 'compactness' or porosity.

Calculating compactness in fossil specimens poses a particular problem as, unlike extant bone, it is not possible to use stains to highlight areas of bone, or ultrasound techniques (Gilbert et al., 2009). Micro-CT scanning can often offer the resolution necessary but is more expensive and time consuming than examining a thin section slide directly. Bone profiler (Girondot & Laurin, 2003) and ImageJ (Ferreira & Rasband, 2012) are both free programs that can be used to calculate changes in bone compactness, and hence cortical width, in images of fossil bone thin section slides. Bone profiler thresholds an image and estimates compactness in concentric circles outwards from the bone centre. The transition from medulla to cortex is indicated by the most abrupt change in compactness. BoneJ (a macro for ImageJ) can calculate and illustrate compactness using chosen pixel values to inform threshold limits. Both programs work well on high contrast images and full, transverse thin section slides. However, images subject to diagenesis, those containing cracks or other visual noise, or awkwardly shaped fragments can be difficult to process. A further technique used is to isolate a region of interest within the bone, and manually trace the pore space, which can then be digitised and quantified as a percentage of the total area using image processing software. However, this is very time-consuming, and the percentage of pore space varies according to the region of interest chosen and is valid for the whole region, rather than identifying a specific point or change from compacta to spongiosa.

Sauropod long bones are characterised by a lack of open medullary cavity, filled with cancellous bone (Sander et al., 2011; Sander, 2000a), which often grades gradually into the more compact cortical bone proper. This makes it difficult to distinguish between the cortex and central core area, and thus measure cortical thickness. In addition, due to their size, sauropod long bones are often cored rather than transversely cut, resulting in a rectilinear thin section which can be difficult to process using standard methods. A novel image processing procedure that produces two visual outputs, a 'compactness profile' and 'compactness bar', is presented here, which the author has developed to deal with this problem. This process is demonstrated using photomicrographs of quadrupedal non-avian dinosaur thin section slides

(thyreophoran and sauropod specimens); the thyreophoran specimens included were an ankylosaur and several stegosaurs.

## 4.2 Materials and methods

The slides were photographed at x4 magnification (see Chapter 4) using either PPL or XPL, according to whichever gave the clearest differentiation between pore space and bone. Overlapping images were taken in sequence from the periosteal surface of the bone as far into the bone centre as possible and were stitched together using Microsoft ICE (Image Composite Editor) to create a strip covering the radius of the bone. A scale bar was added to the stitched image. To save time, a x2.5 objective could be used which would increase the field of view; alternatively, a high-resolution scanned image, or a photograph of the section taken over a light box with a macro lens added to the camera may work as well, as long as canals and resorption cavities are clearly visible.

The stitched image was then processed as follows (**Figure 4.1**): Using Corel Paint Shop Pro (2019) the original image (A), is greyscaled, (B). Next, the luminance value was found for the boundary of the white areas (pore space) using the dropper tool, for example a value of 100. This value is then used to threshold the image, the process being repeated as necessary to find the value that best replicates the distribution of bone and pore space visible in the original image. Computer luminance values range from 0-255, where black is 0% brightness, with an RGB colour value of 0/0/0, and white is 100% brightness with an RGB colour value of 255/255/255. Original image width and height is noted, and the image is then resized to a width of 1 pixel whilst maintaining the same original height. This process averages the luminance values of the pixels within each horizontal line. The image is then resized a second time back to the original width, creating a greyscaled compactness profile (CP) where shades of grey represent the variation in compactness between bone (pure black) to pore space (pure white) (C). The graduated CP is then thresholded a second time, using a value of 127 (i.e., half-way between black and white), to create a monochrome image. This creates a compactness bar (CB), where white areas represent  $\geq 50\%$  pore space and black areas

represent >50% bone (D). The luminance value used to threshold the image at this stage should be recorded, as different values will affect the final image outcome - here it is recorded as a 'T' value. The CB image can then be superimposed on top of the original stitched image to visualise a cut-off point between pore space and bone, indicated by the top of the white bar nearest the periosteal surface (red line) (E). This is the cortico-medullary cavity boundary at 50% compactness with the chosen threshold value, here a value of 100. The image is saved as a JPEG and cortical thickness measured using ImageJ.

Where the difference in greyscale values between bone and pore space could not be differentiated, or where there were features in the bone (such as cracks) that were likely to affect the final result, pore spaces were manually traced and digitised using a Wacom digitiser (Wacom, Saitama, Japan) and image software (Corel Paint Shop Pro 2020).

Some of these processes can be carried out in ImageJ, however, comparisons are easier in a graphics package such as Paint Shop Pro because each image can be saved as a new layer which can be hidden from view, overlaid on top of other layers, or adjusted at any time once saved.

Different proportions of bone to pore space could be calculated by changing the luminance threshold value (T-value). For example, in extant medicine, 5 – 15% pore space is more commonly used to define cortical bone. Changing the T-value to 216 will create a boundary point at 15% porosity.

### **4.3 Results**

For most specimens, the CP showed a greyscale image where the luminance values represent varying degrees of cortical bone to pore space. The CB showed a series of stripes which could be used to quantitatively determine cortical thickness.

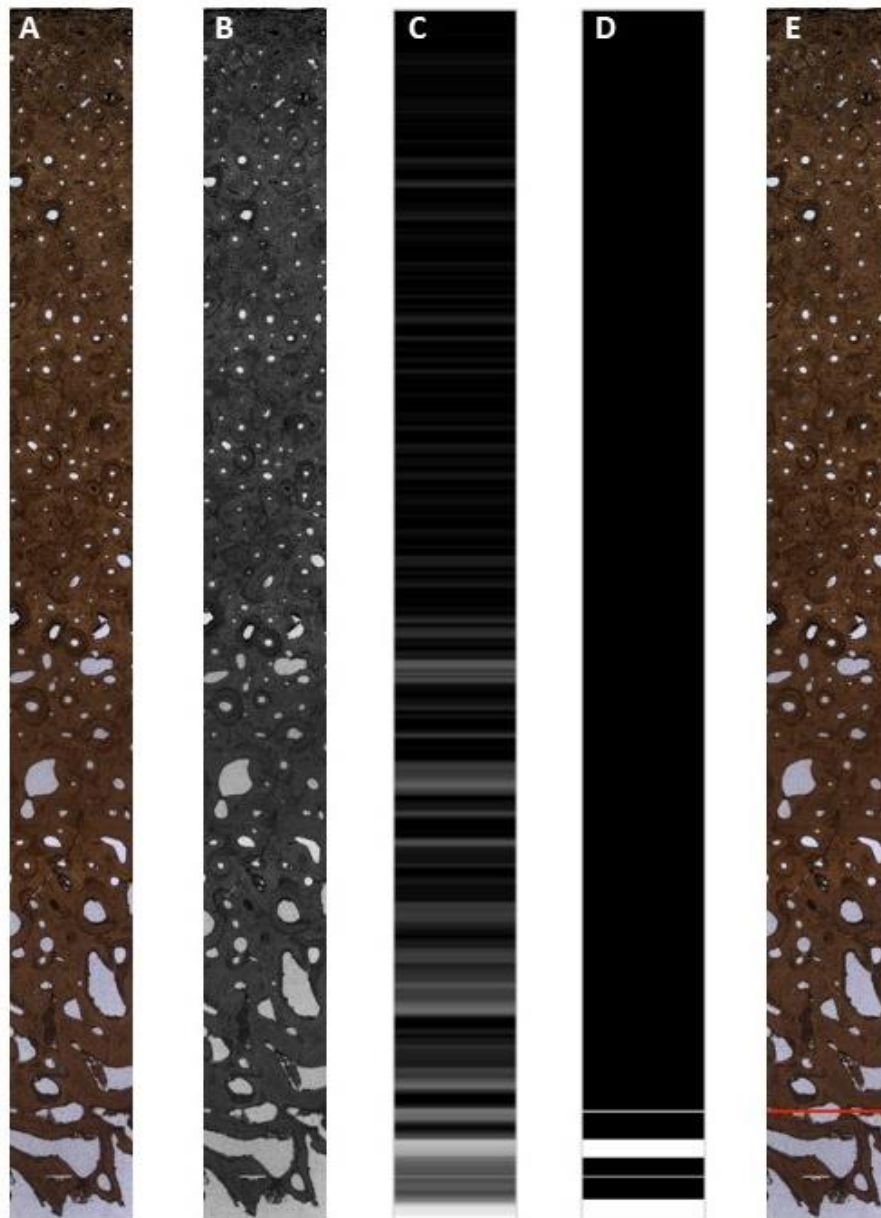


**Figure 4.1 Image processing workflow of CP and CB images. A) - E)** *Anodontosaurus lambei* TMP 1982.9.3. **A)** Stitched image of bone cross section, PPL. **B)** Greyscale image, of A). **C)** CP after resizing. Greyscale luminance value represents varying proportions of cortical bone (dark) to pore space (light). **D)** CB after thresholding again. Black areas represent > 50% cortical bone, white areas represent  $\geq$  50% pore space, achieved by setting  $T=127$ . **E)** Original image with cortico-medullary cavity boundary superimposed (red line). The periosteal surface is at the top of the image, the medullary cavity is at the bottom. Scale bar = 500 $\mu$ m. Images by S. Strachan.

A decision may need to be made as to which stripe to use as the boundary point. Generally, the top (towards the bone surface) of a series of stripes was chosen although it is helpful to refer to the original specimen slide. Isolated

lines that seem to occur mid-cortex by reference to the original specimen were usually caused by an anomalous cluster of vascular canals or resorption cavities and were not selected (**Figure 4.2**).

When examining photographs of specimen C3 1182 (*Ampelosaurus atacis*) (**Figure 4.3**), the XPL images showed better contrast than the PPL images, but neither thresholded well due to lack of contrast resulting from diagenetic alteration and a mineral infilled crack in the upper part of the specimen (the white diagonal line top left in image (A)). This resulted in very similar greyscale values for pore space and cortical bone, and so pore space was manually traced, digitised and flood filled (B), and the crack was ignored. The resulting CB image produced five bars and it was decided by reference to the original thin section (rather than the processed image), to ignore the highest bar and choose the upper part of the fourth bar as the cut-off point for transition between medullary cavity and cortical bone.

The Apatosaurinae specimens showed the thickest cortex with an average thickness of 38.2 mm, compared to *Magyarosaurus* with an average thickness of 8.6 mm. The single ankylosaur specimen, *Anodontosaurus*, had a thick cortex of 21.4 mm, whereas the stegosaur specimens (*Kentrosaurus*), approximately similar in size to the ankylosaur, had an average CT of 9.95 mm. There were intra-species differences, even though all specimens were histologically beyond sexual maturity. For example, within *Magyarosaurus*, specimen r1992 has a CT more than twice that of r1511, and within *Dicraeosaurus*, one specimen had a CT of 12.2 mm and the other a CT of 21.1 mm (**Table 4.1**).

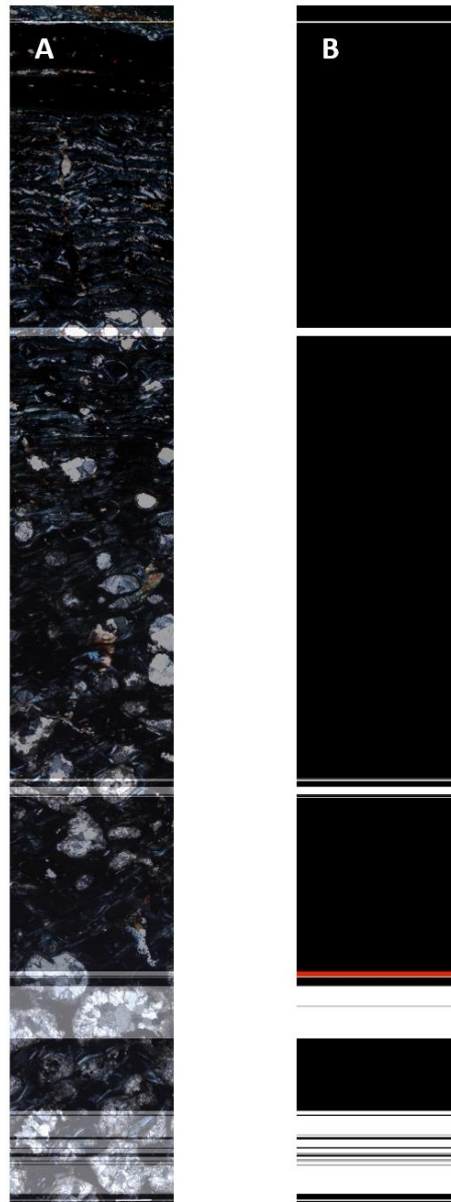


**Figure 4.2 Image processing of compactness bar of *Ampelosaurus atacis* C3 638. A)** CB overlaid on the original image, XPL. **B)** CB showing multiple possible boundary points. The cortico-medullary cavity boundary (red line) was chosen by reference to the original image. The bone surface is at the top of the image. Images by S. Strachan.

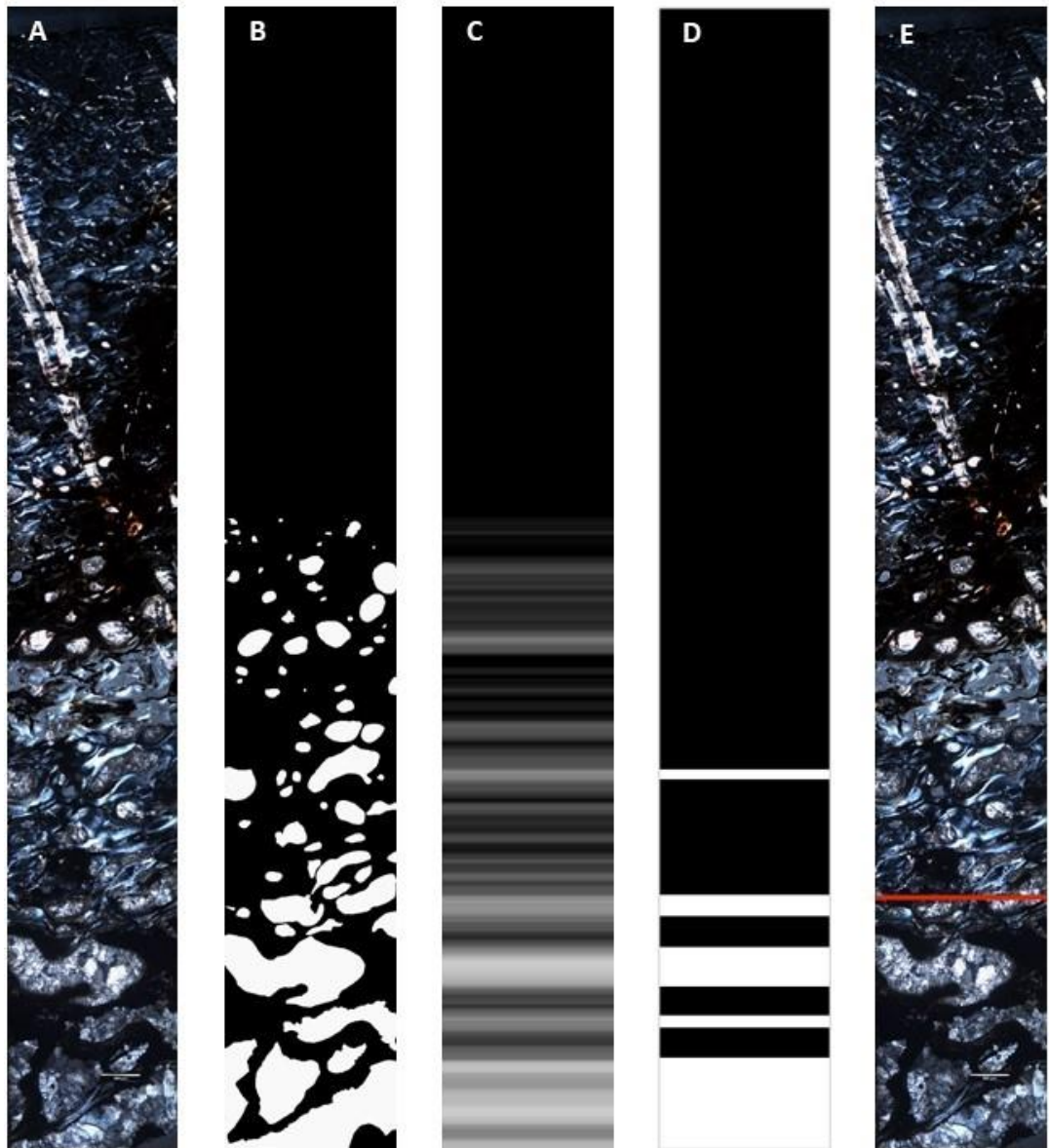


**Figure 4.3 Image processing of CP and CB without thresholding. A) – E)** *Ampelosaurus atacis* C3 1182. **A)** stitched image (XPL) with very poor contrast between bone and pore space which prevented the use of automatic thresholding. **B)** Manual outline and infill of pore space (white areas) - it was not necessary to outline the whole area. **C)** CP after second resizing. **D)** CB after thresholding. **E)** Original image with cortico-medullary cavity boundary superimposed (red line), chosen by reference to original image. The bone surface is at the top of the images. Scale bar = 500 $\mu$ m. Images by S. Strachan.

**Table 4.1 Cortical thickness measurements estimated from CP and CB**

| Taxa                                | Specimen      | CT<br>(mm) | Previously reported<br>CT (mm) |
|-------------------------------------|---------------|------------|--------------------------------|
| Apatosaurinae                       | BYU 681-11940 | 30.75      | 35.0 <sup>a</sup>              |
|                                     | BYU 601-17328 | 47.84      | 37.0 <sup>a</sup>              |
|                                     | OMNH 4020     | 36.06      | 70.0 <sup>a</sup>              |
| <i>Giraffatitan brancai</i>         | MFN dd452     | >30.70     | 33.0 <sup>a</sup>              |
|                                     | MFN Nr. 305   | 21.60      |                                |
|                                     | MFN St 291    | 34.00      |                                |
| <i>Phuwiangosaurus sirindhornae</i> | PC.DMR no No. | 14.80      |                                |
|                                     | PC.DMR K21    | 14.10      |                                |
| <i>Dicraeosaurus sattleri</i>       | MFN M1b       | 12.20      |                                |
|                                     | MFN dd3032    | 21.10      |                                |
| <i>Ampelosaurus atacis</i>          | MDE C3 174    | 11.70      |                                |
|                                     | MDE C3 1182   | 10.98      |                                |
|                                     | MDE C3 203    | 15.70      |                                |
| <i>Magyarosaurus dacus</i>          | FGGUB r1220   | 7.50       |                                |
|                                     | FGGUB r1511   | 5.10       |                                |
|                                     | FGGUB r1046   | 7.00       | 14.0 <sup>a</sup>              |
|                                     | FGGUB r1992   | 12.70      | 16.0 <sup>a</sup>              |
| <i>Kentrosaurus aethiopicus</i>     | MB.R.3572     | 9.40       | 9.4 <sup>b</sup>               |
|                                     | MB.R.3583     | 10.50      | 11.4 <sup>b</sup>              |
| <i>Anodontosaurus lambei</i>        | TMP 1982.9.3  | 21.40      |                                |

(-) indicates pore space was manually drawn round and infilled.

The value used to separate pore space from bone was 50% (T=127).

Previously reported measurements from <sup>a</sup>(Mitchell & Sander, 2014), <sup>b</sup>(Redelstorff et al., 2013).

## 4.4 Discussion

### Comparison with previous recorded measures

Calculations of cortical thickness (CT) using this method compared well with previously recorded measures for *Kentrosaurus*, *Giraffatitan*, and most of the Apatosaurs (**Table 4.1**). However, *Magyarosaurus* R.1046 was recorded as 7.0 mm using the CB technique, but previously as 14.0 mm, and Apatosaurinae OMNH 4020, in which the thickness recorded in this study was half the previously recorded cortical thickness (Mitchell & Sander, 2014). Some variation is to be expected due to the choice of positioning of the radial area sampled, and it is likely (although not detailed) that cortical thickness measurements previously reported are mean values from several points throughout the cortex. This emphasises the necessity to compare homologous regions of bone and use consistent techniques where possible in comparative studies.

### Comparison of CPs

Positioning various CPs side by side enables a quick visual comparison of compactness variation across the chosen cortical bone region of interest (**Figure 4.4**). The *Ampelosaurus* and *Magyarosaurus* specimens compared are all mature adults according to Histological Ontogenetic Stages (Klein & Sander, 2008; Stein et al., 2010) and show interesting variation in femoral bone compactness and cortical thickness. *Magyarosaurus* being generally more compact than *Ampelosaurus*. A thicker cortex suggesting a more robust animal, or the necessity to support increased mass. It is important here to compare homologous regions of homologous bones. When comparing CPs visually, it is helpful to adjust the length proportional to other specimens.

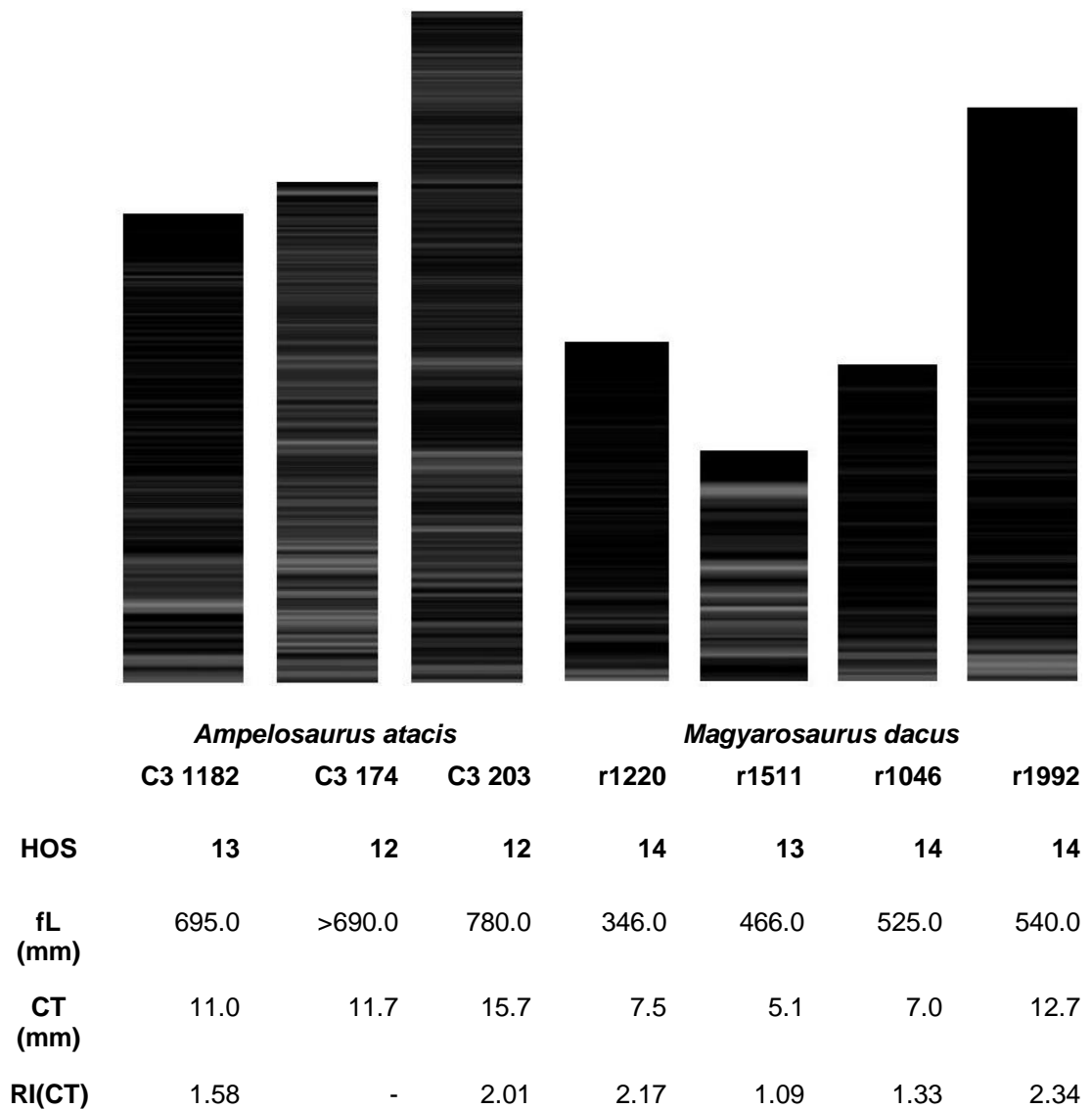


**Figure 4.4 Comparison of CPs across two sauropod taxa.** Cortical bone CPs for sauropods *Ampelosaurus* (C3 1182, C3 174, C3 203) and *Magyarosaurus* (r1220, r1511, r1046, r1992). All specimens are adults, with HOS stages ranging from 12-14. CP image height shown is proportional to relative cortical thickness. Lighter areas represent pore space, and darker areas > 50% bone. Apart from r1511, *Magyarosaurus* typically has a more compact cortex than the *Ampelosaurus* specimens, shown by fewer light grey areas. According to the robusticity index RI(CT), there is no clear relationship between compactness (shown here as darker CP) and greater robusticity, indicated by a higher RI(CT) value. Bone surface is at the top, medullary cut-off point is at the bottom.

#### **Caveats and potential problems**

Usually, the medullary cavity contains predominately spongiosa, and cortical bone contains predominately compacta; however, this is not always the case.

The cortex can consist of fine cancellous bone and the medulla region can sometimes consist largely of secondary compacta (Francillon-Vieillot et al., 1990). If there is a sufficient difference in compactness between the bone regions, the method proposed here can be adapted for bones of this nature.

Occasionally a specimen will be too degraded or contain too much visual noise for the first stage of thresholding to be carried out. Cracks could be mistakenly thresholded as pore space, or the mineral infill in the resorption cavities could have a greyscale value very close to or even below that of the surrounding cortical bone. In these cases, pore space needs to be manually outlined before the image is processed as above. Of the 20 specimens analysed, 7 gave good results from thresholding, and 13 involved manual outlining of pore space to some degree - although it is important to bear in mind that these specimens were chosen as they were challenging to analyse using other methods. Manual outlining is time consuming, however, it is not always necessary to outline and fill the pore space for the whole section if it can be determined by eye roughly in which region of the bone the boundary point is likely to lie. Partial outlining still enables the identification of a clear boundary and therefore quantification of cortical thickness. It also results in a CP and CB for the region of interest, but care must be taken if comparing CP and CB images of complete and partially processed images side by side as areas that have not been processed will look black, similar to compact bone in a fully processed image.

## **4.5 Conclusion**

Variations in compactness across a section of cortical bone can be represented using a greyscale compactness profile (CP) for visual analysis and comparison between specimens. With further processing, a monochrome compactness bar (CB) can be produced that clearly and quantitatively separates predominantly pore space from predominantly bone within a chosen area, and which can be used to estimate the cortico-medullary cavity boundary point, and hence determine the cortical thickness of the bone.

Positioning various CPs side by side enables a quick visual comparison of variation in compactness across the cortical bone region of interest and highlighted surprising intraspecific variation in bone compactness and cortical thickness at comparable histologic stages of development.

# Chapter 5 Phylogenetic Signal of Bone Microstructure traits Within Sauropoda

## 5.1 Introduction

### Overview

The phylogenetic dependence of morphological characters is well established (Gould, 1977). The inclusion of bone microstructure (including histological) morphological traits may improve the resolution of phylogenetic analyses for extinct taxa, similar to the method used for extant species (Cordie & Budd, 2016; Best & Kamilar, 2018), providing critical information on the evolutionary development of these traits and additional data to help resolve problem taxa. However, bone microstructure data is rarely included in phylogenetic analyses and therefore a potentially informative data source in evolutionary studies is largely absent.

In this chapter, we explore whether there is a significant phylogenetic signal in femoral bone microstructure within Sauropoda. We consider whether these variables are suitable to include in phylogenetic analyses to further our understanding of evolutionary relationships in deep time, and how might this be achieved. We are not aware of any studies that have compared homologous sections of homologous bones of closely related taxa at a similar developmental stage.

Sauropods are giant, herbivorous, quadrupedal non-avian dinosaurs, famous for their long necks and size, with body mass estimates of between 6 to over 60 tonnes (Carballido et al., 2017; Sander et al., 2011; Upchurch et al., 2004). Sauropods are well sampled within non-avian dinosaurs histologically (Company, 2011; Curry, 1999; de Buffrénil et al., 2021; Díez Díaz et al., 2018; Enlow & Brown, 1956, 1957, 1958; Erickson, 2005; Erickson et al., 2001; Klein et al., 2009; Klein & Sander, 2008; Lehman & Woodward, 2008; Sander et al., 2004; 2006; 2011; Rogers & Erickson, 2005; Sander, 1999, 2000a; Sander &

Tückmantel, 2003). The availability of specimens, taxonomic diversity, and large bone size makes them suitable choices for comparative bone histology study (see Chapter 3).

### **Phylogenetic signal**

For a trait to be phylogenetically informative, particularly when working in deep time, a strong phylogenetic signal is desirable as an inverse relationship is generally expected between the strength of phylogenetic signal and degree of homoplasy in morphometric data (although see Klingenberg & Gidaszewski, 2010).

Phylogenetic signal is the “tendency for related species to resemble each other more than they resemble species drawn at random from the tree” (Blomberg & Garland, 2002). When a phylogenetic signal is present and said to be strong, closely related taxa are more similar than distantly related taxa, and as phylogenetic distance increases, similarity decreases, resulting in divergent phylogenetic trees. This is expected under genetic drift and natural selection, as these processes should approximate a Brownian Motion model of evolution (Revell et al., 2008).

A variety of methods are used to measure phylogenetic signal, such as Bayesian and maximum likelihood methods, or techniques based on spatial autocorrelation (see 3.63.6). Autocorrelation tests include: Moran's  $I$  (Moran, 1950; Gittleman & Kot, 1990); Abouheif's  $C_{mean}$  (Abouheif, 1999); Phylogenetic Eigenvector Regression (PVR: Diniz-Filho et al., 2012); and regressions on distance matrices based on a Mantel test (Legendre et al. 1994). These tests estimate correlation between histological features and location on a phylogeny and infer the degree to which a trait is influenced by its phylogenetic position (see Keck et al., 2016). Some of the methods, such as PVR and regressions on distance matrices incorporate branch length information but not an evolutionary model (although see DeBastiani & Duarte, 2017). Alternatively, methods that assume an evolutionary model (usually Brownian motion), such as Blomberg's  $K$  (Blomberg et al., 2003) and Pagel's  $\lambda$  (Pagel, 1999), can be used to investigate underlying evolutionary processes

(see Münkemüller et al., 2012 for a comparison). Pagel's  $\lambda$  can also be used as an indicator of effect size ( $w$ , see 3.6) (Freckleton et al., 2002; Münkemüller et al., 2012). All four of these methods broadly agree but are calculated following different approaches, and thus measure different aspects of phylogenetic signal (see Hjelman & Johnston, 2017; Münkemüller et al., 2012; Pavoine & Ricotta, 2013 for examples).

### **Previous studies**

Phylogenetic signal has been observed in a variety of microanatomical and palaeohistological traits, including: vascular density and canal orientation; bone size; cortical thickness; compactness; secondary osteon area; osteocyte lacunae size and cell density (Cubo et al., 2005; Felder et al., 2017; Houssaye et al., 2016; Legendre et al., 2013; Legendre et al., 2014; Marín-Moratalla et al., 2014; Mitchell et al., 2017; Ponton et al., 2007; Stein & Werner, 2013). One of the few studies which used palaeohistological data in phylogenetic analysis included the orientation of primary osteons in tibiotarsi in the character suite for palaeognathus birds (Houde, 1986, 1987). This study demonstrated that phylogeny plays a significant role in how this trait varies among taxa and placed ratite origination within the '*Lithornis*-cohort' (Houde, 1986, 1987). It was possible because there is an observable and consistent difference between neognathus birds and the palaeognathus birds (tinamous and ratites) in vascular canal type and arrangement. In addition, other factors, such as the effects of biomechanics (flightlessness), ontogeny, fossilisation, and size, were controlled for. However, these vascular patterns are not unique and appear in many other taxa (Enlow & Brown, 1958), and so are informative only at particular taxonomic levels.

Only three studies to date have looked specifically at the phylogenetic signal in bone microstructure traits. Cubo et al. (2005) investigated the variation of macro, microanatomical and histological traits in the femora of 35 species of adult sauropsids. The authors concluded that a phylogenetic signal is weakly expressed in histological traits, explaining 18.7% of the variation of vascular density in archosaurs using the Mantel test. Variation in bone size and relative cortical thickness ( $K$ ) were well supported in archosaurs, explaining 81.8% and

86.2% of variation respectively, but not in the other taxa. The authors concluded that phylogenetic signal was highly significant at the morphological and microstructural level, but significant at the histological level for only some traits (such as vascular density) and may be easily 'overwritten' or crowded out by biomechanical, ontogenetic, and environmental signals (Cubo et al., 2005). Legendre et al. (2013) looked at seven bone histology characters, across 25 amniote taxa, which included extinct and extant taxa. A significant phylogenetic signal was found in 15 out of 21 of the characters according to at least one of the three tests, with 20-60% of the variation in histological characters explained by phylogeny using PVR (Legendre et al., 2013). Adjustment was made for different ontogenetic stages by comparing the outer cortical region (recent growth) of younger specimens, with the inner cortical region (laid down in earlier growth stages) of more mature specimens. Additionally, cortical bone area was divided into four transects so that homologous regions of the cortex could be compared as well as mean values for the whole bone area (Legendre et al., 2013). Both of these studies used regression methods and the same data set, and sample sizes were small which may have affected statistical significance.

In a later study with a more extensive data set, Legendre et al. (2014) looked at phylogenetic signal in 62 bone histology features in 21 species of palaeognathus birds. Different topologies were compared, using four different methods of calculating phylogenetic signal (Pagel's  $\lambda$ , Blomberg's  $K$ , Abouheif's  $C_{mean}$  and PVR). Approximately 20-50% of the variables (depending on the topology used) indicated a significant signal using at least three out of four methods. Bone size (cross sectional area), vascular density and osteocyte lacunae size consistently showed the strongest signal (Legendre et al., 2014).

In addition, several studies have tested for phylogenetic signal in bone histology traits prior to statistical analysis when testing for correlation of histological data with other traits. Generally, a weak phylogenetic signal is discovered, which even when significant, does not affect results (Houssaye et al., 2014; Felder et al., 2017). A strong significant signal was found, however,

when testing for flight style correlates in the micro-anatomy of the furcula in birds. Phylogenetic signal in whole bone area (Pagel's  $\lambda = 0.964$ , Blomberg's  $K = 0.958$ ) and Haversian bone density ( $K = 0.451$ ,  $\lambda = 0.40$ , although  $\lambda$  values were not significant) justified the subsequent use of phylogenetic methods (Mitchell et al., 2017). Further studies have found a significant phylogenetic signal in femoral compactness (relating to size of the medullary cavity) in adult lissamphibians (Laurin et al., 2004), the proportion of longitudinal and circular primary canals and osteocyte density in adult wild ruminants (Marín-Moratalla et al., 2014), and osteocyte density was found to be greater in sauropodomorphs “than scaled up or comparably sized mammals” in a study which incorporated extant and extinct tetrapods (Stein & Werner, 2013).

These studies illustrate that bone microstructure has phylogenetic utility. In addition, phylogenetic signal is present, but may vary across different histological variables, taxa, and levels of the taxonomic hierarchy (see Kamilar & Cooper, 2013).

## 5.2 Materials and Methods

### Data sources

Thin sections prepared from the anterior mid-diaphysis of 31 sauropod femora were photographed, and morphometric data was digitised and processed as described in Chapter 3. All specimens were at, or beyond, sexual maturity (HOS 8, or equivalent), thus limiting, although not eliminating, variation due to ontogeny.

### Variables

For full list of variables and calculations see **Table 3.2** and S1.

As osteocytes vary in size and shape within different bone matrix types, osteocyte measurements from woven bone, parallel-fibered bone (which may also cross over with lamellar bone), and from within the lamellae of secondary osteons were assessed separately. Osteocyte measurements were not available for all bone matrix types (On, PFB and WB) for all the specimens,

which lowered the number of taxa (and hence tips) in the phylogeny for some analyses.

To minimise the inclusion of resorption cavities, only osteons with circularity > 0.7, and with a canal diameter less than the radius of the longest axis of the osteon, were included.

Two indices of robusticity were calculated: RI(Circ) and RI(CT) (Stock & Shaw, 2007). To further explore differences in scale, a 'thickness index' (TI) of cortical thickness divided by circumference (Mitchell & Sander, 2014), and two ratios that describe the bone wall thickness using radius, as opposed to circumference, were also included: K, and Rd/CT (Currey & Alexander, 1985). Although radius varies across a transverse thin section of bone, these ratios are comparable across specimens as homologous regions of the femur (anterior) were compared.

Missing data for *Camarasaurus*, *Giraffatitan* and *Apatosaurus* was imputed via linear regression using SPSS (IBM Statistics 27) to increase the number of taxa for which robusticity indices could be incorporated. Circumference was calculated using fL; and fL and CT were calculated using circumference for each taxon, where there was adequate data available. Data were supplemented with specimen measurements from the literature (**Table 3.1**). All regressions satisfied a linear relationship, and the model was statistically significant with high values of adjusted R<sup>2</sup> which classified as 'very good' (Cohen, 1988).

As most of the specimens were core sampled and only slides from the cored sections were available for study, bone area could not be measured directly. Bone area was therefore calculated from circumference where available. This assumes all the shapes approximate to a circle, which they do not, but it is an acceptable method if used consistently and for the purpose of establishing a ratio between specimens (see **Table 3.2**).

Cortical thickness was estimated using the 'Compactness Bar' method (see Chapter 4).

### **Statistical analysis**

Statistical analyses, including a principal components analysis (PCA, see S1 for details) were carried out using SPSS (IBM Statistics 27).

Outliers can affect the robustness of various statistical tests, however, outliers in this data set were examined and considered the result of natural variation in the dataset (rather than errors), and the preference for univariate data sets was to leave them in where mean values only were used and the effect would be negligible. In addition, calculations for  $K$ ,  $\lambda$ , and the evolutionary models tested, are fairly robust to outliers (Gittleman & Kot, 1990; Martins, 1996).

Data were log<sub>10</sub> transformed prior to analysis. Where there was more than one specimen from a taxonomic group, mean values were used.

### **Phylogenetic signal**

Univariate data were tested for evidence of phylogenetic signal using R (R Core Team (2020)). Four methods were compared: Blomberg's  $K$ ; Pagel's  $\lambda$ ; Moran's  $I$ ; and Abouheif's  $C_{\text{mean}}$  (see 3.6).

Blomberg's  $K$  is the most used method of testing for phylogenetic signal, and has the advantage that it can go above 1, indicating stronger trait similarity between species than expected under BM. This was an important feature as it was predicted as a potential outcome for at least some of the biological variables tested. Pagel's  $\lambda$  and Abouheif's  $C_{\text{mean}}$  have been shown to perform better for discriminating random and BM patterns of trait distribution (Freckleton et al., 2002; Münkemüller et al., 2012). Of the four, Abouheif's  $C_{\text{mean}}$  does not incorporate branch lengths. To aid comparison with previous studies and to provide more comprehensive results, all four methods are reported here.

Blomberg's  $K$  and Pagel's  $\lambda$  were calculated using `phylosig` from `phytools` in R (R Core Team, 2020). Moran's  $I$  and Abouheif's  $C_{\text{mean}}$  values were calculated using the function `abouheif.moran` (package `adephylo` in R), using Monte Carlo simulations and the default value of 999 randomisations. The null hypothesis ( $H_0$ ) is that trait values are distributed independently across the phylogeny, therefore a statistically significant value of  $p$  ( $\alpha < 0.05$ ) indicates that the null hypothesis (effectively, no discernible pattern) can be rejected.

For the purposes of this study the strength of phylogenetic signal is defined for Blomberg's  $K < 0.4$  as weak;  $0.4 < K < 0.7$  as moderate;  $0.7 < K < 1$  strong; and  $K > 1$  as a very strong phylogenetic signal. A signal using Pagel's  $\lambda$  is defined as:  $\lambda < 0.4$ , weak;  $0.4 < \lambda < 0.7$  as moderate;  $\lambda > 0.7$  as a strong phylogenetic signal.

### **Evolutionary models**

Different evolutionary models were compared, and likelihood ratio test statistics calculated using the `fitContinuous` package `GEIGER v2.0` in R (Pennell et al., 2014) which compares different maximum likelihood models for continuous trait evolution to the data. The function uses random starting points and various optimization methods, meaning that the optimal solution is data and model dependent. Model 'goodness of fit' is calculated using maximum likelihood values.

Evolutionary models tested:

Brownian Motion (BM) - expects trait evolution to follow a random walk. The rate of evolution is constant and variance in the distribution of trait values is directly proportional to branch lengths (here, time since divergence) (Cavalli-Sforza & Edwards, 1967; Felsenstein, 1985).

Lambda0 (L0) - rescales internal branch lengths to zero, replicating a star-like phylogeny where all hierarchical relationships are removed.

Lambda (L) - rescales internal branch lengths by a linear fraction. The phylogeny predicts covariance among trait values for species, lambda = 1 recovers BM (Pagel, 1999).

Ornstein-Uhlenbeck (OU) - (Hansen, 1997) is a random walk around a central tendency or value, as expected under stabilizing selection. The central tendency may be towards an optimum (Lande, 1976; Felsenstein, 1988), indicating a biological constraint (Harmon & Glor, 2010). Attraction strength is proportional to parameter  $\alpha$ , the “strength of the pull towards a central trait value” (Cooper et al., 2016). Values range from zero to infinity (although in GEIGER this is limited to 150);  $\alpha = 0$  describes pure Brownian motion and as  $\alpha$  increases, the expectation is that phylogenetic signal decreases, and recently diverged species are no more or less likely to be similar than distant ones (Revell et al., 2008).

Rate trend (RT) - a diffusion model that fits a linear trend through larger or smaller rates in time.

Delta (D) - a tree transformation, time-dependent model of trait evolution which indicates a slow down or speeding up of the rate of character evolution over time (Pagel, 1999). Values of  $\delta = 1$  indicate BM; values of  $\delta > 1$  indicate recent evolution has been relatively fast;  $\delta < 1$ , indicates recent evolution is relatively slow.

White noise (WN) - a derivative of a BM model, WN is a random, non-phylogenetic model and corresponds to a Lambda = 0 model. It assumes data are from a single, normal distribution with mean = 0 and variance  $\sigma^2$  and no covariance structure exists between species.

Early Burst model (EB) - (Harmon & Glor, 2010), also called accelerating-decelerating (ACDC) model (Blomberg et al., 2003), is a random walk model where the rate of evolution exponentially increases or decreases through time. Values of  $r$  = initial rate;  $\alpha$  is the rate change parameter;  $t$  = time;  $\alpha = 0$

describes pure BM; and negative  $\alpha$  indicates rates of evolution decreasing through time.

Log-likelihood values (LnLik) were calculated using maximum likelihood estimation as a measure of goodness of fit for the models - the higher the value the better fit (values range from - to + infinity). The maximum likelihood value is proportional to the probability of observing the data given the model tested (Pagel, 1999), and thus indicates the model that gives the most probable description of the data.

Akaike's information Criterion values were calculated using R (Akaike, 1974) to compare different models of evolution for the traits. Akaike's information Criterion (AIC) uses a model's maximum likelihood estimation (log-likelihood) as a measure of fit for each model and indicates how likely one is to see the observed data (phylogeny) given the model. As sample sizes were small, AIC values corrected for small sample sizes (AICc) were calculated. A lower AICc value indicates greater support for a particular model. When comparing models, it is generally accepted that a difference of  $> 4$  is acceptable, and  $> 2$  in some cases is considered acceptable, although there is no universally agreed difference between AIC scores that is considered significant. In practice therefore, models within 2 AICc values of the lowest AICc value are considered equivalent (Burnham & Anderson, 2002). As this can lead to inconclusive results,  $\Delta\text{AICc}$  (delta) and  $\text{AICc}(w)$  weights were calculated as an alternative to identify the relative best fit model, using GEIGER function `aicw` in R. The model with  $\Delta\text{AICc} = 0$ , or  $\text{AICc}(w)$  closest to 1 indicates the best fit to the data.

It is important to remember that LnLik and AIC are comparative processes. They do not definitively show one model to be the correct one but indicate which of the models tested is a better fit, which of course will change depending on the models included.

## 5.3 Results

The calculation of the  $p$ -value of Blomberg's  $K$  involves a randomisation process, and therefore may alter slightly with each run, however, this did not have any material effect on the results. The best fit evolutionary model was assessed using the lowest AICc(w) values, where AICc(w) is nearest to 1 and  $\Delta\text{AICc} = 0$  (which here gave the same results). For full results, including AIC values, see S1.

### Osteocytes

Of the 18 osteocyte variables tested according to Blomberg's  $K$ , 10 were statistically significant for phylogenetic signal, if including PFB.Ot.Dm ( $K = 1.365$ ,  $p = .058$ ) (**Error! Reference source not found.**, also see S1). Across the three bone matrix types (On, PFB and WB), osteocyte measurements of aspect ratio, circularity and minimum diameter (Ot.AR, Ot.Cr, Ot.Dm) showed high values ( $K > 1$ ), indicating a phylogenetic signal greater than that expected under BM) (**Error! Reference source not found.**). As circularity decreases with an increase in aspect ratio, it is expected that a phylogenetic signal would be present in both or neither of these variables, as was found here.

Generally, a high signal for  $K$  was also indicated for  $\lambda$ ; a particular exception was PFB.Ot.Dm which indicated very high phylogenetic signal using Blomberg's  $K$ , but no phylogenetic signal using Pagel's  $\lambda$ . In addition, On.Ot.Ar showed a strong significant phylogenetic signal ( $K = 1.148$ ,  $p = .034$ ), but a weaker effect size according to Pagel's  $\lambda$  ( $\lambda = 0.545$ ).

Moran's  $I$  and Abouheif's  $C_{\text{mean}}$  showed non-significant results and low values near to zero for 17 of the 18 osteocyte variables tested, except for WB.Ot.AR which indicated significant phylogenetic signal according to Moran's  $I$  ( $I = 0.230$ ,  $p = 0.049$ ). Osteocyte results were non-significant for Pagel's  $\lambda$ .

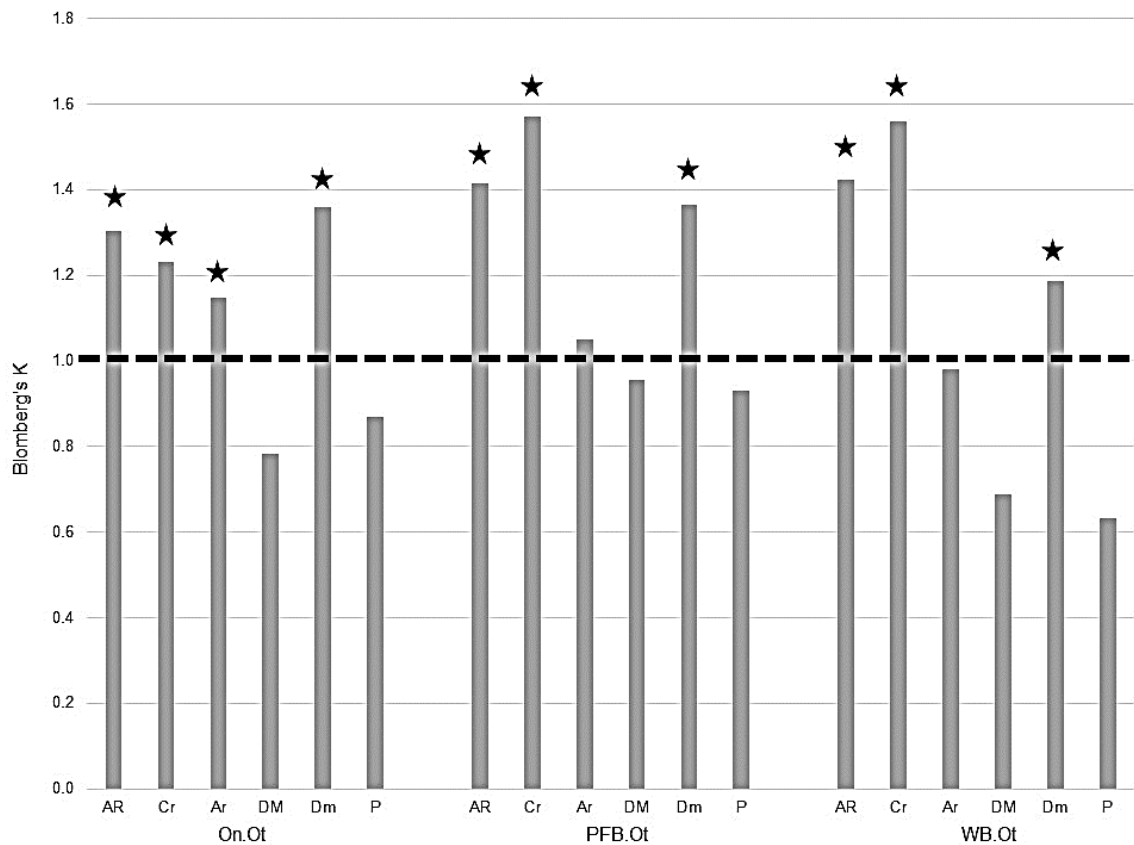


**Figure 5.1 Phylogenetic signal in osteocyte morphometrics.** Dotted line indicates Blomberg's  $K = 1$ , above which a phylogenetic signal is greater than expected under Brownian motion. Star indicates statistically significant values ( $\alpha = .05$ ).

Eleven of the eighteen osteocyte variables were best represented by a BM model of evolution according to AICc(w). For these variables, either a white noise or lambda0 model (or both) was an equivalent best according to AICc, with the addition of the delta model as an equivalent for On.Ot.Cr. For the remaining variables, a lambda0 or white noise model was a best fit according to AICc(w), with a BM, lambda zero and white noise models an equivalent best according to AICc (see S1).

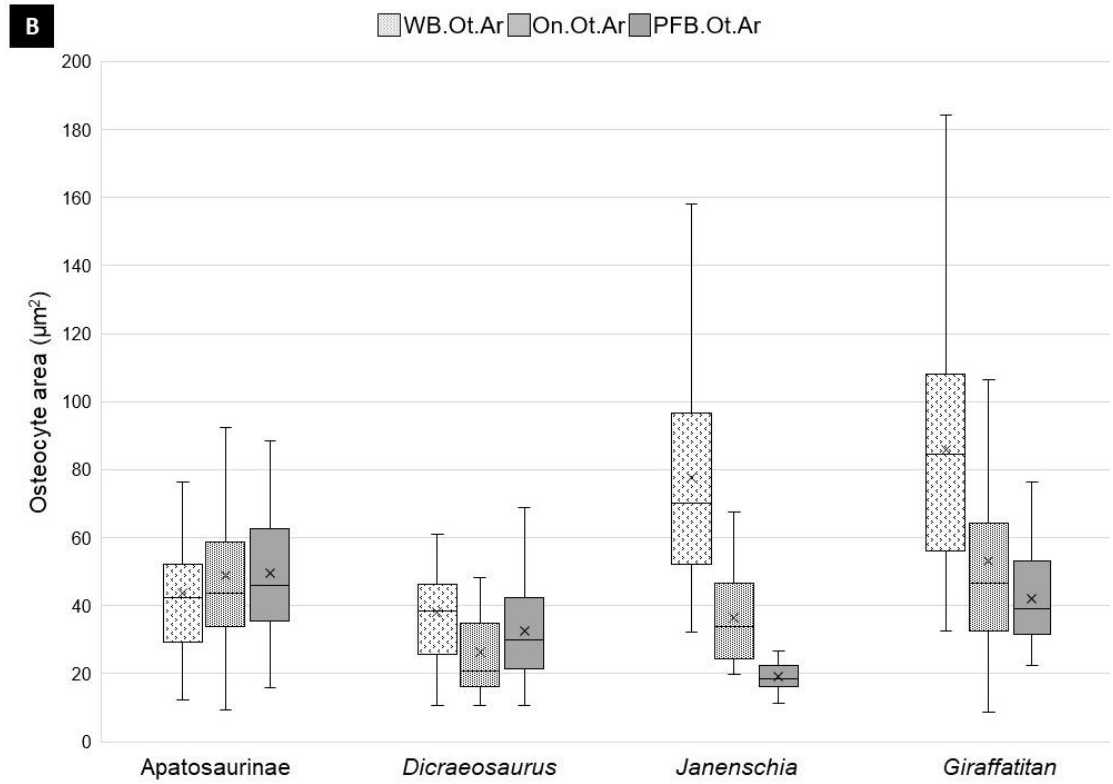
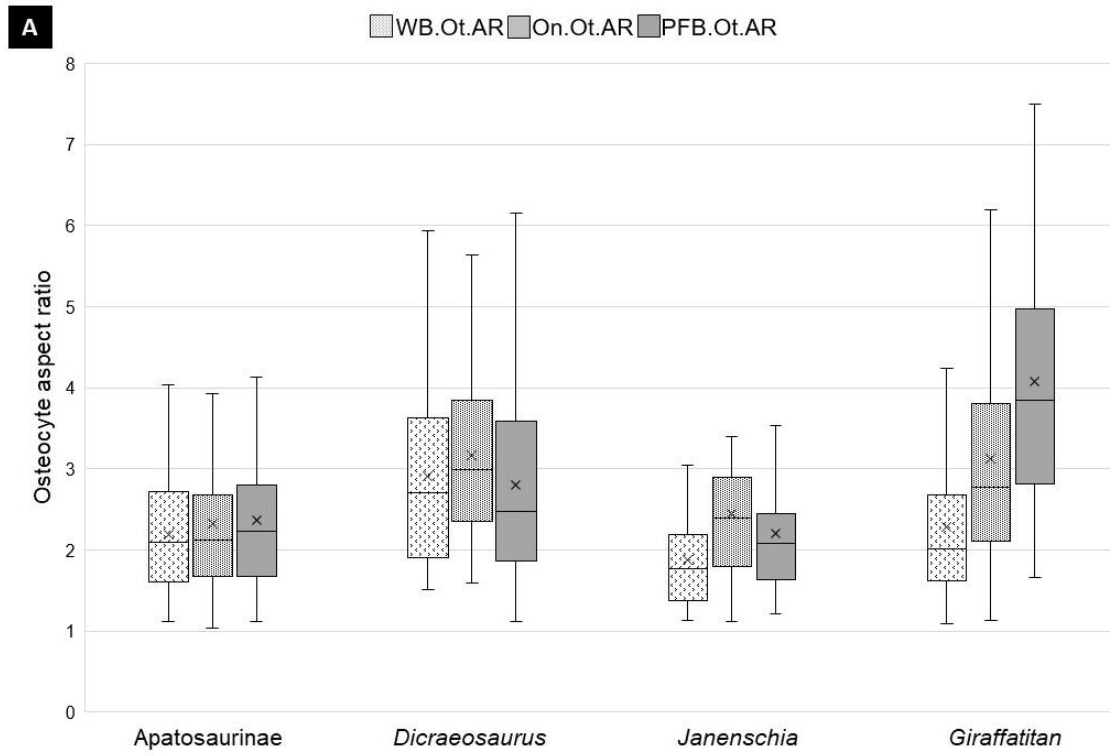
Although not consistent across taxa, variation in osteocyte morphometry from different bone matrix types and secondary osteons justified the statistical separation of these cells (**Figure 5.2**).

**Table 5.1 Phylogenetic signal in osteocyte morphometrics**

| Variable  | n | Blomberg's<br>$K$ | $\rho$      | Pagels<br>$\lambda$ | $\rho$ | Moran's<br>$I$ | $\rho$      | Abouheif's<br>$C_{mean}$ | $\rho$ |
|-----------|---|-------------------|-------------|---------------------|--------|----------------|-------------|--------------------------|--------|
| On.Ot.AR  | 9 | 1.304             | <b>.024</b> | 1.000               | .393   | -0.112         | .405        | -0.073                   | .636   |
| On.Ot.Cr  | 9 | 1.230             | <b>.040</b> | 1.000               | .418   | -0.131         | .497        | -0.090                   | .672   |
| On.Ot.Ar  | 9 | 1.148             | <b>.034</b> | 0.545               | .760   | 0.003          | .207        | 0.056                    | .368   |
| On.Ot.DM  | 9 | 0.782             | .256        | 0.579               | .883   | -0.002         | .251        | 0.078                    | .347   |
| On.Ot.Dm  | 9 | 1.360             | <b>.008</b> | 1.000               | .526   | -0.070         | .326        | -0.029                   | .547   |
| On.Ot.P   | 9 | 0.868             | .164        | 0.670               | .700   | 0.079          | .142        | 0.156                    | .214   |
| PFB.Ot.AR | 6 | 1.414             | <b>.017</b> | 1.000               | .458   | -0.031         | .221        | 0.220                    | .182   |
| PFB.Ot.Cr | 6 | 1.570             | <b>.009</b> | 1.000               | .317   | 0.054          | .135        | 0.273                    | .136   |
| PFB.Ot.Ar | 6 | 1.049             | .176        | 0.000               | 1.000  | -0.262         | .495        | 0.026                    | .440   |
| PFB.Ot.DM | 6 | 0.955             | .318        | 1.000               | .482   | -0.177         | .550        | 0.294                    | .169   |
| PFB.Ot.Dm | 6 | 1.365             | <b>.058</b> | 0.000               | 1.000  | -0.143         | .343        | -0.002                   | .513   |
| PFB.Ot.P  | 6 | 0.931             | .317        | 1.000               | .527   | -0.212         | .610        | 0.246                    | .174   |
| WB.Ot.AR  | 8 | 1.423             | <b>.033</b> | 1.000               | .245   | 0.230          | <b>.049</b> | 0.286                    | .086   |
| WB.Ot.Cr  | 8 | 1.559             | <b>.034</b> | 1.000               | .307   | 0.072          | .134        | 0.108                    | .280   |
| WB.Ot.Ar  | 9 | 0.981             | .115        | 1.000               | .652   | -0.074         | .290        | 0.036                    | .404   |
| WB.Ot.DM  | 8 | 0.689             | .527        | 0.000               | 1.000  | -0.322         | .851        | -0.221                   | .875   |
| WB.Ot.Dm  | 8 | 1.185             | <b>.038</b> | 1.000               | .305   | 0.084          | .122        | 0.176                    | .189   |
| WB.Ot.P   | 8 | 0.632             | .686        | 0.000               | 1.000  | -0.232         | .642        | -0.074                   | .628   |

n = no. of taxonomic groups.

Statistically significant values are shown in bold ( $\alpha = .05$ ).



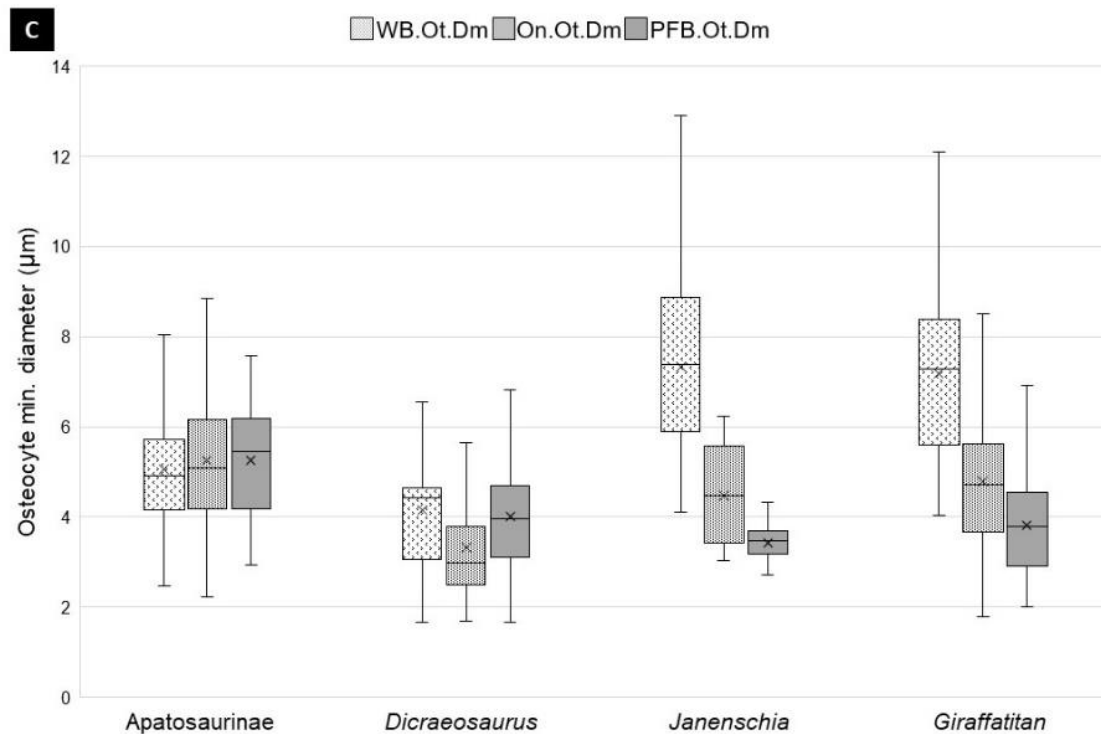


**Figure 5.2 Box and whisker plots showing comparison of osteocyte morphometry. A) – C),** Comparison of osteocyte aspect ratio (Ot.AR), area (Ot.Ar), and minimum diameter (Ot.Dm) in specimens for which comparable data were available from woven bone (WB), secondary osteons (On), and parallel-fibered bone (PFB). Specimens included: BYU 681-11940, BYU 601-17328 (*Apatosaurinae*); MFN dd3032 (*Dicraeosaurus hansemanni*), NHMUK PV unreg. (*Dicraeosaurus* sp.); NHUB Nr 22 (*Janenschia robusta*); MFN dd452, MFN Nr 305, MFN St 291 (*Giraffatitan brancai*). **A)** Osteocyte aspect ratio, note the wider range of values of *Dicraeosaurus* and *Giraffatitan* and considerable overlap in aspect ratio from the different bone areas in the *Apatosaurinae* specimens. **B)** Osteocyte area varies widely particularly for osteocytes from woven bone in *Janenschia* and *Giraffatitan*, which are generally larger than osteocytes from within secondary osteons and parallel-fibered bone in these taxa. **C)** Osteocyte minimum diameter is greater and more varied in size for woven bone cells in *Janenschia* and *Giraffatitan*. Cell minimum diameter in the *Apatosaurinae* specimens is similar across the different bone matrix types. Osteocyte morphometrics were therefore analysed separately according to bone matrix type.

### Robusticity

A moderate, significant phylogenetic signal was identified in three indices of robusticity (RI(CT), Rd/CT and TI) using Abouheif's  $C_{mean}$  (0.392 - 0.404), indicating taxa resemble each other more closely than expected under BM. All

other measures were non-significant (**Error! Reference source not found.** and S1).

A white noise model was the best fit according to AICc(w) for K, Rd/CT and TI. However, using AICc values, a BM model was an equivalent best for all three, and lambda0 was also equivalent for Rd/CT and TI. According to AICc(w), RI(Circ) was best represented by a lambda0 model, and a white noise model was a best equivalent using AICc. A delta model was a best fit for RI(CT), delta values indicate a slowing of character trait evolution through time ( $\delta = 0.115$ ), although four models (D, BM, EB, W) were equivalent best according to AICc.

**Table 5.2 Phylogenetic signal in femoral robusticity**

| Variable | n  | Blomberg's<br><i>K</i> | <i>p</i> | Pagels<br>$\lambda$ | <i>p</i> | Moran's<br><i>I</i> | <i>p</i> | Abouheif's<br><i>C</i> <sub>mean</sub> | <i>p</i>    |
|----------|----|------------------------|----------|---------------------|----------|---------------------|----------|--|-------------|
| K        | 6  | 0.506                  | .471     | 1.000               | .412     | -0.422              | .882     | 0.097                                  | .365        |
| Rd/CT    | 6  | 0.702                  | .259     | 0.729               | .472     | 0.098               | .071     | 0.404                                  | <b>.010</b> |
| RI(Circ) | 6  | 0.446                  | .631     | 0.000               | 1.000    | -0.191              | .425     | -0.088                                 | .672        |
| RI(CT)   | 10 | 0.995                  | .096     | 1.000               | .107     | 0.070               | .136     | 0.392                                  | <b>.012</b> |
| TI       | 6  | 0.702                  | .296     | 0.729               | .472     | 0.098               | .066     | 0.404                                  | <b>.022</b> |

Statistically significant values are shown in bold ( $\alpha = .05$ )

### **Osteons and canals**

No significant phylogenetic signal was detected for secondary osteons or their canals according to the four measures tested.

A white noise model was a best fit for secondary osteons and canals according to AICc(w) and AICc apart from On.Vc.Ar which was equivalent best fit with a lambda0 model, and On.Vc.Dm which was equivalent best fit with BM, white noise and lambda0.

### **Micro and macro variables**

No phylogenetic signal was detected in cortical thickness, bone size, femoral length, circumference or mass according to the four measures tested.

A white noise model or white noise and lambda0 model were an equivalent best fit according to AICc(w) and AICc values.

## **5.4 Discussion**

The presence and strength of phylogenetic signal in various palaeohistological and micro-level traits within sauropod femora was assessed using Blomberg's  $K$ ; Pagel's  $\lambda$ ; Moran's  $I$ ; and Abouheif's  $C_{\text{mean}}$ . Additionally, whether traits follow a particular evolutionary model was tested. Homologous regions of homologous bones were compared, and all specimens were at or beyond sexual maturity. A strong, significant phylogenetic signal was found within osteocyte morphometrics (AR, Cr, Dm) in osteocyte call lacunae measured from within parallel-fibered bone, woven bone, and the lamellae of secondary osteons in sauropod femora according to Blomberg's  $K$ . A phylogenetic signal was also revealed in robusticity indices RI(CT), Rd/CT and TI according to Abouheif's  $C_{\text{mean}}$ . Models where phylogenetic signal was identified generally followed a BM evolutionary pattern. We conclude that these variables could therefore be considered suitable to include in phylogenetic analyses.

Bone size, cortical thickness, secondary osteon, and Haversian canal measurements from across the cortex did not display a phylogenetic signal, and so are not recommended for inclusion in phylogenetic analysis.

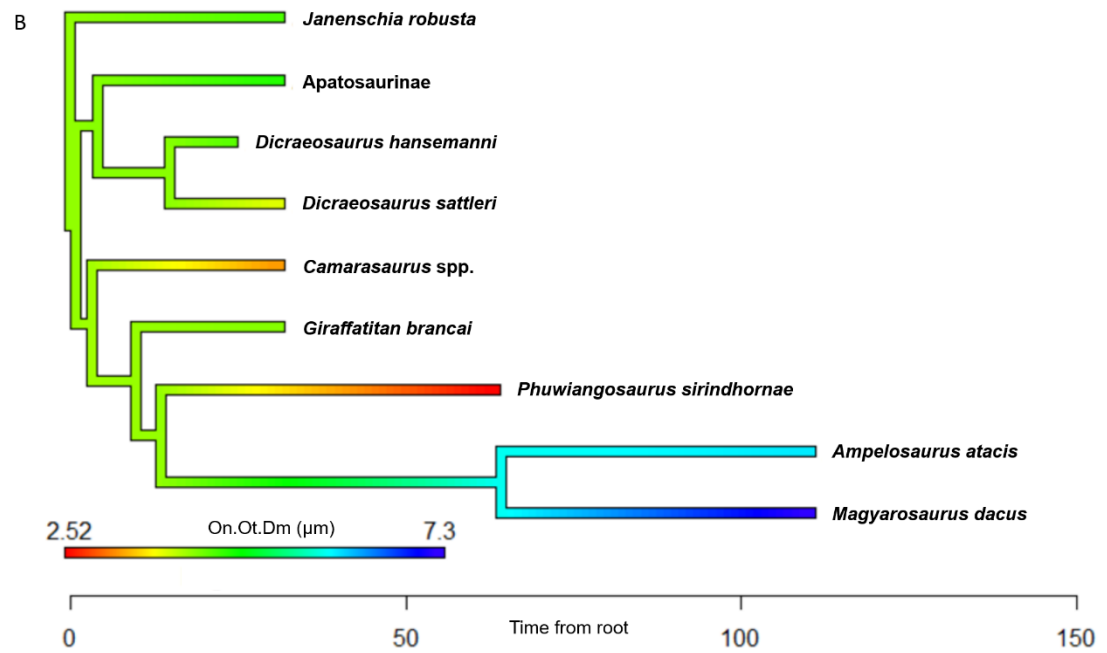
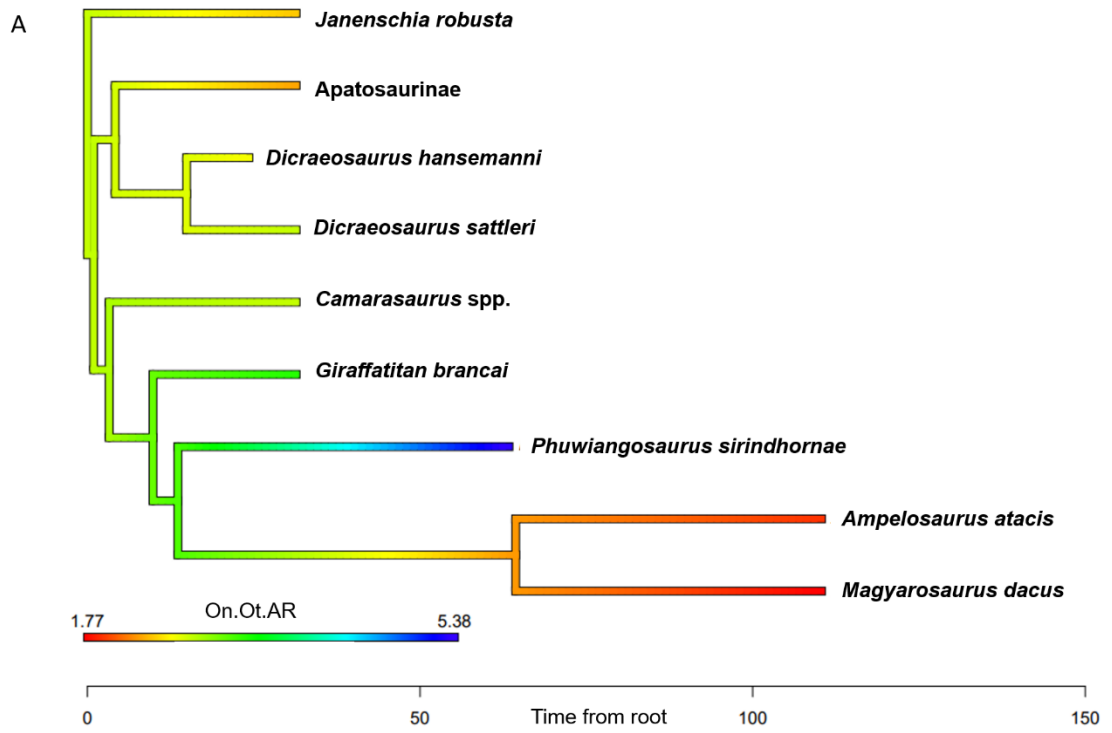
### **Osteocytes**

Finding statistically significant phylogenetic signal in the osteocytes of primary bone (woven bone and parallel-fibered bone) is important as not all bone contains secondary osteons; however, sauropods in particular display high levels of bone remodelling and finding areas of primary bone for interspecific comparison may be difficult in mature specimens. Sauropods often display extensive remodelling, therefore osteocyte morphology in secondary osteons

may be a particularly useful trait to incorporate into phylogenetic analysis for this taxon.

When osteocyte aspect ratio from secondary osteons is mapped onto the species phylogeny used in this study, variation across taxonomic groups and consistency within clades can be seen (**Figure 5.3**). Overlaying minimum diameter onto the phylogeny also shows variation across taxonomic groups, and similarity within clades, although slightly less than for aspect ratio. It can be seen that the titanosaurs *Ampelosaurus* and *Magyarosaurus* have more ovate and narrower osteocytes in both woven bone and secondary osteons. Aspect ratio of osteocytes in woven bone was the only variable that was found to be significant according to more than one measure (Moran's *I* and Blomberg's *K*), adding further support to the conclusion that there is a strong phylogenetic signal within this variable.

However, strong signal in osteocyte morphology ( $K > 1$ ) (**Error! Reference source not found.**), may be symptomatic of inertia, conservatism, or constraint (Blomberg & Garland, 2002; Losos, 2008), in which case a lack of variability would make osteocytes a poor choice for incorporating into phylogenies. The fit continuous tests indicate that a BM model gives the most probable description of the data for osteocytes, which may have resulted in increased sensitivity according to Blomberg's *K* and therefore higher values (Münkemüller et al., 2012). It is important to remember that LnLik and AIC are comparative models, and therefore results should be interpreted as indicative of areas for potential further exploration. Values of  $1.148 > K < 1.570$  are not considered extremely high, and a value of  $K = 1.8$  was found to be commensurate with a BM model (Münkemüller et al., 2012). Moreover, under conditions of constraint, the OU model might be expected to be a best fit (which it was not), indicating a pull towards a central value. Overall, Blomberg's *K* is considered suitable to interpret here and osteocyte aspect ratio useful to incorporate into phylogenetic analyses.



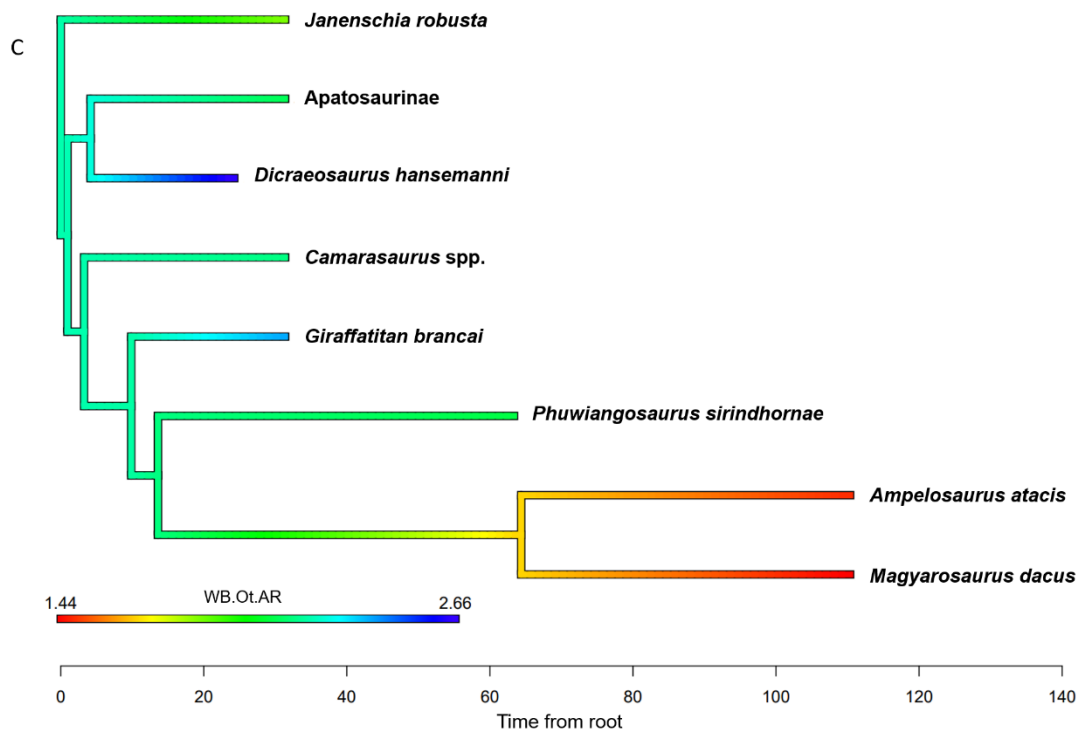


**Figure 5.3 Osteocyte morphometrics mapped onto phylogeny. A)** Aspect ratio of osteocytes from secondary osteons mapped onto phylogeny, showing close relationship with clade membership. Values > 1 indicate increasingly ovate shape. **B)** Minimum diameter ( $\mu\text{m}$ ) of osteocytes from secondary osteons mapped onto phylogeny. **C)** Aspect ratio of osteocytes from woven bone mapped onto phylogeny. In general, variation across taxonomic groups and consistency within clades can be seen.

The conclusions here of a phylogenetic signal in osteocyte aspect ratio supports previous results found in palaeognathous birds by Legendre et al. (2014) where a moderate significant phylogenetic signal in mean cell shape (aspect ratio) was found according to Pagel's lambda ( $\lambda = 0.651$ ,  $p = .013$ ), although not significant for Blomberg's  $K$  ( $K = 0.200$ ,  $p = .130$ ). A significant phylogenetic signal in the osteocyte lacunae size (area) in the caudal and medial femoral transects of transverse thin sections was also found for almost every topology and method used (Legendre et al., 2014). Cells were measured from the fastest growing primary bone in the 2014 study, however, and so are most directly comparable with the WB or PFB measurements in the current study. Although significant signal was found in On.Ot.Ar in the current study, results for osteocyte area in WB and PFB were non-significant.

It is likely that osteocyte size is influenced by other factors. In an earlier study, phylogeny was found to explain only 24.7% of femoral cell size in amniotes ( $p = .020$ ) and 39.7% in archosaurs ( $p = .011$ ), and 37.8% of femoral cell shape ( $p = .012$ ) in amniotes using PVR, suggesting factors other than phylogeny influence osteocyte size and shape (Legendre et al., 2013).

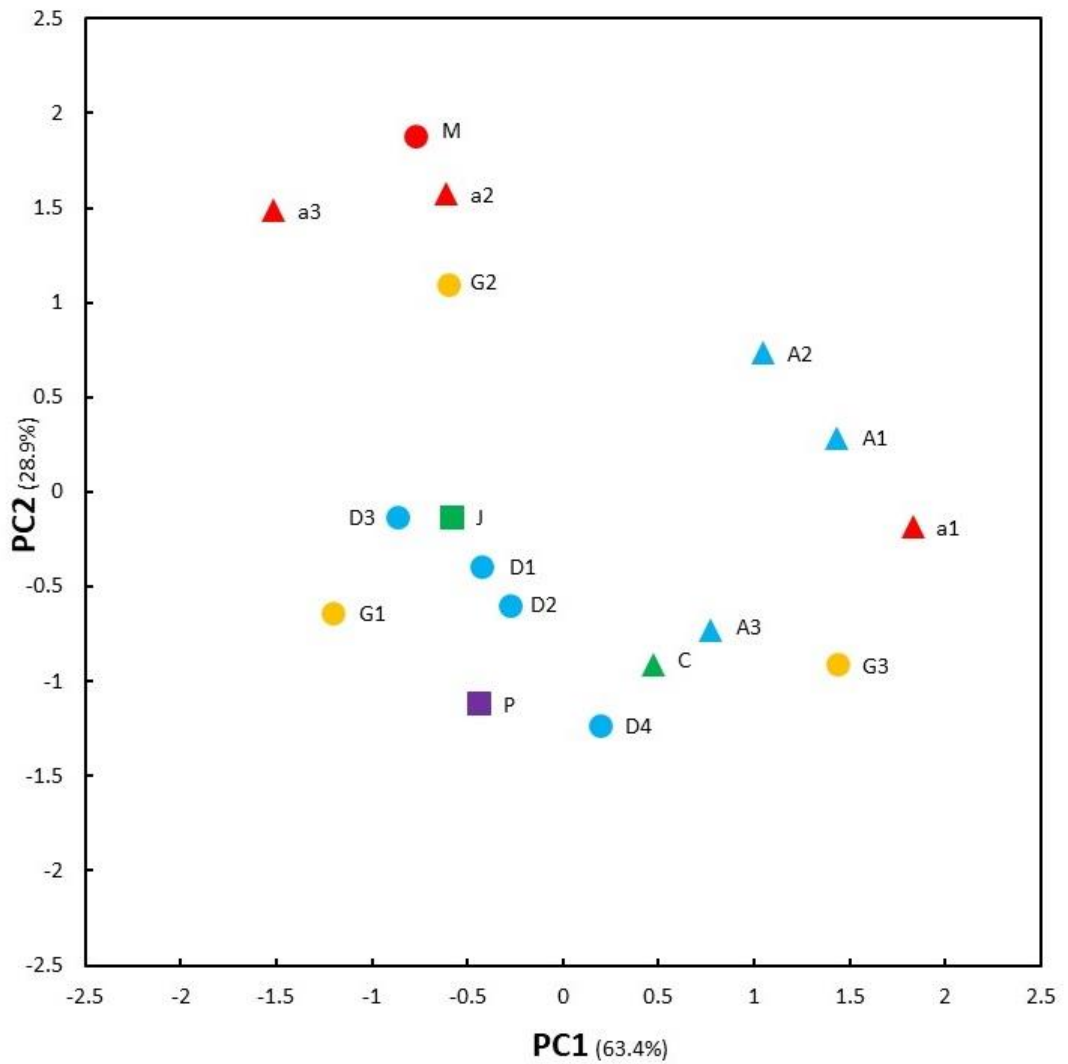
Whole genome size, or DNA C-value, is generally positively correlated with cell volume in plants and animals (Gregory, 2000, 2002, 2005; Hardie & Hebert, 2003; Horner & Macgregor, 1983; Martin & Fisher, 1966; Mirsky & Ris, 1951). Genome size was found to be correlated with osteocyte lacunae volume in birds (D'Emic & Benson, 2013; Grunmeier & D'Emic, 2019) and other extant vertebrates (Gregory, 2001; Davesne et al., 2020). In addition, osteocyte lacunae volume has been used to estimate genome size in fossil specimens (Organ et al., 2007, 2009), and draw conclusions regarding evolutionary relationships (Montanari et al., 2011; Organ et al., 2011). If osteocyte volume is correlated with genome size, it is critical to know whether genome size itself is correlated with phylogeny. If so, it would be predicted that osteocyte volume would also correlate with phylogeny. It is generally accepted that there is a phylogenetic component to genome size variation. However, genome size varies widely across different organisms (Gregory, 2001; Dufresne & Jeffery, 2011), and has not been widely tested for the presence of phylogenetic signal, although a strong signal has been identified in insects (Sessegolo et al., 2016; Hjelmen & Johnston, 2017; Yuan et al., 2021). In addition, although genome size (and hence osteocyte volume) may correlate with phylogeny, a consistent and predictable pattern of genome size variation has yet to be found. Genome size varies between closely related species, between sexes, and is influenced by other factors, such as adaptations to flight (Leitch et al., 1998; Boulesteix et al., 2006; Andrews et al., 2009; Wright et al., 2014; Hjelmen et al., 2019). This means that osteocyte volume, and 2D morphometric measures closely correlated with volume, such as cell area, may make good candidates for inclusion in phylogenetic analyses, but need to be considered on a taxon-by-taxon basis, as the relationship with phylogeny is by no means ubiquitous.

We conclude that some measures of osteocyte morphometry (aspect ratio, circularity, minimum diameter, and area), display a phylogenetic signal and could be useful to code and incorporate into phylogenetic analyses. If osteocyte traits are utilised in this way, it is important to separate cells according to bone matrix type. In addition, as phylogenetic signal is not ubiquitous across taxa, variables should be compared to a known phylogeny to establish the extent of phylogenetic signal. This could create a cyclical process of only using histological traits in a phylogeny where phylogenetic signal has been established by correlation with a phylogeny. Notwithstanding these problems, we still conclude that osteocyte morphology can play a critical role in phylogenetic analyses.

### **PCA analysis**

A principal component analysis (PCA, see S1 for details) was conducted to explore correlations between variables. The number and choice of variables was limited due to lack of data available across all taxonomic groups, however, the analysis revealed two components which together explained 92.3% of the total variance (**Figure 5.4**). Secondary osteon size loaded strongly on Component 1, and osteocyte size within secondary osteons loaded strongly on Component 2 (see S1 for details).

There is considerable overlap of taxa particularly along PC1 (secondary osteon size) indicating that it may be difficult to distinguish taxonomic groups according to these variables. The *Giraffatitan* and *Ampelosaurus* specimens are particularly widely spaced. Some clustering of the diplodocids, *Dicraeosaurus* and the Apatosaurinae specimens (shown in blue), can be seen along PC2 (osteocytes within secondary osteons). In addition, the Apatosaurinae and *Dicraeosaurus* specimens cluster separately along PC1. The position of *Janenschia*, clustering within the *Dicraeosaurus* specimens is interesting as this specimen was originally attributed to *Dicraeosaurus*. Of the titanosaurs (shown in red), *Magyarosaurus*, despite its much smaller size, also clusters with two of the three *Ampelosaurus* specimens. A wider data set of known taxonomic affinity would be required to draw further conclusions.



- M: *Magyarosaurus* r1046
- ▲ a: 1) *Ampelosaurus* C3 174; 2) *Ampelosaurus* C3 203; 3) *Ampelosaurus* C3 1182
- ▲ A: 1) *Apatosaurinae* 681-11940; 2) *Apatosaurinae* 601-17328; 3) *Apatosaurinae* 4020
- D: 1) *Dicraeosaurus* M1b; 2) *Dicraeosaurus* O2; 3) *Dicraeosaurus* dd3032; 4) *Dicraeosaurus* PV unreg
- G: 1) *Giraffatitan* Nr 305; 2) *Giraffatitan* St 291; 3) *Giraffatitan* PV 5937
- ▲ C: *Camarasaurus* 36664
- J: *Janenschia* Nr 22
- P: *Phuwiangosaurus* K21

**Figure 5.4 PCA analysis of bone histology morphometrics.** PC1 (secondary osteon size) and PC2 (osteocyte size). Diplodocids (blue) are widely spread along PC1, but some clustering can be seen along PC2. Some clustering of titanosaurs (red) can be seen, with the exception of a1.

## Robusticity

Significant phylogenetic signal was uncovered in three of the measures of robusticity in the current study using Abouheif's  $C_{\text{mean}}$ . Variations in locomotor style and development result in interspecific differences in bone modelling and remodelling, and hence variation in robusticity of long bones (Currey, 2002; Starck & Chinsamy, 2002; Habib & Ruff, 2008; Sanchez et al., 2010; Tsegai et al., 2013; Püschel & Benítez, 2014; van Oers et al., 2014; Hall, 2015). These variations may generate unique or distinctive patterns that could be used to differentiate between species.

Results in the current study are consistent with previous studies that have indicated there are species level differences observed in the robusticity of sauropod femora (Bonnar, 2004; Sander, 2000a; Taylor, 2009), even in comparably sized sauropods (Sander, 2000a). *Diplodocus humeri* and femora were found to be more gracile, and *Apatosaurus* more robust, when comparing homologous landmarks of humeri and femora in Morrison sauropods using morphometrics and thin-plate splines (Bonnar, 2004). *Camarasaurus* had more robust femora, similar to *Apatosaurus*, but gracile humeri, suggesting differing locomotor styles (Bonnar, 2004). In a re-evaluation of *Brachiosaurus altithorax* and *Giraffatitan brancai*, when comparing the humeri and femora using GI, *Giraffatitan* was found to be more gracile than *Brachiosaurus*, and both had more gracile humeri than other sauropods examined (Taylor, 2009). On comparing the Tendaguru sauropods, although similarly size, *Barosaurus* was found to be more gracile than the stout *Janenschia* (Sander, 2000a).

Considering that Abouheif's  $C_{\text{mean}}$  generally performed well against the other three measures when tested (Münkemüller et al., 2012) and a non-random evolutionary model was recovered as a best fit for RI(CT), the conclusion here is that RI(CT), Rd(CT) and TI have phylogenetic signal, and may be useful to incorporate into evolutionary analyses.

As far as we are aware, only the robusticity variable K has previously been tested for phylogenetic signal, where a strong significant signal was identified in diapsids and archosaurs using regressions on distance matrices, although

a signal was not found in Lepidosauria or Neognathae (Cubo et al., 2005). Results indicated (as also found here) that phylogenetic signal is inconsistent across taxonomic groups. Results for K presented in this study were non-significant for sauropods, although sample size may have been an influencing factor on  $p$ -values (see 'Limitations' below).

### **Bone size**

Results here do not support a phylogenetic signal at the species to subfamily level in bone size (area) of sauropod femora, and so bone size is not recommended for inclusion in sauropod phylogenies without further testing with a larger sample size. However, taxon numbers were low in this study for bone size, and the lack of a significant signal at this taxonomic level does not preclude a signal at higher taxonomic levels or in different species.

A signal in bone area seems to be highly clade specific. (Cubo et al., 2005) found that phylogeny explains 81.8% of variation in femoral bone size in archosaurs, although not in five other sauropsid clades. In birds, furcula bone area showed a strong significant phylogenetic signal (Mitchell et al., 2017); and a high and significant signal was reported in the femora and tibiotarsi of palaeognathous birds (Legendre et al., 2014). The strong signal in birds may be due to the adaptations of flight, including the secondary loss of flight, where high levels of morphological bone plasticity and thus variation over time exists between taxa. Under these conditions it is perhaps unsurprising that a phylogenetic signal is present where such variation exists. This highlights the importance of considering the function and biological context of the skeletal element.

Bone size in the current study was estimated from circumference and as such does not reflect unique variations in shape. We do not discount the possibility that a more sophisticated and accurate method of shape analysis may uncover variations between taxa that may have taxonomic or phylogenetic utility.

### **Cortical thickness**

Previous authors have observed a stronger phylogenetic signal in traits at the micro level rather than histological (Castanet et al., 2010; Cubo et al., 2005; Laurin et al., 2004; Legendre et al., 2014), indicating that microanatomical characters such as cortical thickness and morphological characters are likely to be better choices for phylogenetic analysis. However, in the current study, this did not seem to be the case. This may be because phylogenetic signal also varies at different taxonomic levels; for example, a strong signal may be found in a variable at one taxonomic level, but not at a higher or lower level (Kamilar & Cooper, 2013). This study focussed on the taxonomic levels of species to subfamily, whereas the studies mentioned generally explored phylogenetic signal at higher taxonomic levels. The results presented here, supporting only a low, or no phylogenetic signal in cortical thickness, are in line with previous research by Houssaye et al. (2016), who found only a weak phylogenetic signal in cortical thickness in mammals and reptiles.

Cortical thickness is influenced by locomotor style, for example varying between aquatic and non-aquatic taxa (Habib & Ruff, 2008; Houssaye et al., 2016), and it is likely that response to biomechanical stress resulting from varying locomotor style is a greater influence on cortical thickness than phylogeny. All the specimens in the current study are considered graviportal (Bonnar & Bonnar, 2003) and so variation due to locomotor style is likely to be limited.

It is also difficult to measure cortical thickness in many sauropod specimens, as the medullary cavity is typically filled with cancellous bone surrounded by a wide transition zone of highly vascular bone that grades into the denser cortical bone. This makes identifying the cortico-medullary cut-off point difficult and a more subjective matter dependent on the researcher's choice of method and results therefore may not be directly comparable. It could be argued that for these reasons, cortical thickness is not a good choice of comparative trait in sauropods. However, we propose that results are comparable if consistent estimation techniques are used, as in the current study (see Chapter 4). In addition, cortical thickness is useful when combined with measurements such

as bone length, circumference, or bone radius to calculate various indices of robusticity which may display a phylogenetic signal. As such it is worth investigating, although from the results here, cortical thickness is not recommended as a useful trait to incorporate into phylogenetic analyses on its own.

### **Osteons and canals**

Results in this study, indicating a weak or no phylogenetic signal in the size of secondary osteons and Haversian canals, are consistent with findings by Felder et al., (2017) who studied these structures in a wide range of mammal femora and humeri. This was a surprising result as several studies have observed taxonomic differences between species in secondary osteon size (Zedda et al., 2008; Skedros et al., 2013; Giua et al., 2014), and shape (Hidaka et al., 1998; Zedda et al., 2008; Crescimanno & Stout, 2012). However, these studies did not test for correlation with other factors or incorporate a phylogeny, and it is likely that body size (as demonstrated by Felder et al., 2017), or mechanics are the dominant signal and primary cause of the variation between the taxonomic groups, rather than phylogeny.

Although no phylogenetic signal was detected in their morphology, secondary osteons play a variety of roles in bone development, primarily related to bone replacement and repair instigated by ageing or mechanical stress. As such, the pattern and extent of remodelling (not assessed here) may reflect variations in ontogeny or locomotor style and hence a unique pattern which can be used to identify taxa, as observed in sauropods by (Sander, 2000a).

Therefore, although secondary osteon and Haversian canal morphometrics are of limited value in phylogenetic analyses, the degree and organisation of these structures throughout ontogeny offers taxonomic utility, and pattern recognition approaches may offer a way of quantifying variation between taxa.

## 5.5 Limitations

### Model comparison

Estimating phylogenetic signal using four different measures enables comparison, and the sometimes-contrasting results revealed in this study demonstrate that identifying and interpreting phylogenetic signal is not straightforward. Results varied according to the method used to measure phylogenetic signal. In general, the different methods of estimating phylogenetic signal are known to be strongly correlated and congruent with each other (Diniz-Filho et al., 2012; Pavoine & Ricotta, 2013). Münkemüller et al. (2012) found Pagel's  $\lambda$  and Blomberg's  $K$  sometimes result in divergent conclusions (contra Revell et al., 2008), although this was not generally the case here, apart from PFB.Ot.Dm which indicated a strong significant signal in  $K$ , but no signal according to Pagel's  $\lambda$ .

When branch length is available and accurate, Blomberg's  $K$  and Pagel's  $\lambda$  tend to outperform autocorrelation methods (Martins, 1996; Münkemüller et al., 2012). Due to the availability of branch lengths, and as it follows an evolutionary model, Blomberg's  $K$  is considered an acceptable measure to interpret here, with the additional benefit of being able to indicate phylogenetic signal stronger than expected under BM and being more widely comparable with existing studies. However, Blomberg's  $K$  has been found to be particularly sensitive to traits that follow a BM model (Münkemüller et al., 2012) which may have affected values.

### Sample size

The effect of sample size is one of the main limitations of this study. Ideally a minimum of 20 taxonomic groups would have been included, however, due to an extended period of global travel restrictions, this was not possible. The decision was made to proceed with the specimens available and make statistical adjustments for small sample size where possible, small sample size being a not uncommon problem in palaeontological studies.

None of the Pagel's  $\lambda$  results were significant, and lack of statistical significance reported here may in part be due to small taxa numbers. In all four of the tests used, type II errors (not identifying a phylogenetic signal when one is present) have been found to increase at small sample size (Legendre et al., 2013; Legendre et al., 2014; Münkemüller et al., 2012). Blomberg's  $K$  in particular showed higher type II errors for intermediate values of BM (up to  $w = 0.8$ ), and the means of all four indices used here were found to increase with increasing numbers in tests of between 5 and 30 taxa (Hjelmen & Johnston, 2017). Therefore, Münkemüller et al. (2012) suggest concentrating on effect size measures (using  $\lambda$  for this purpose), as reported in the current study, rather than significance.

### **Scale**

Choosing specimens at, or beyond, sexual maturity only, and that are graviportal, and sampling homologous sections of the same skeletal element, limits ontogenetic, intraskeletal and biomechanical variation to some degree. However, scale has not been accounted for and varies widely among the specimens chosen and may be an influencing factor. This is addressed in Chapter 6.

## **5.6 Conclusion**

According to Blomberg's  $K$ , a strong, significant phylogenetic signal exists within osteocyte morphometrics (AR, Cr, Dm) in lacunae measured from within parallel-fibered bone, woven bone, and the lamellae of secondary osteons in sauropod femora. In addition, Abouheif's  $C_{\text{mean}}$  identified a phylogenetic signal within robusticity indices RI(CT), Rd/CT and TI. Therefore, we conclude that these variables may be potential candidates for incorporation into phylogenetic analyses. The inclusion of these histological traits and indices of robusticity may increase the resolution and accuracy of phylogenetic trees, increase understanding of evolutionary relationships within these taxa, and may provide additional data to help resolve problem taxa.

## 5.7 Recommendations

### Data preparation and assessing phylogenetic signal in palaeohistological traits

- All terms should be defined to avoid synonymy and homonymy, preferably with examples of the characters used
- Use consistent measurement protocols
- Incorporate as many species (taxonomic groups) as possible, ideally 20 or more
- Calculate and report standard error (or CI), or some measure of effect size (e.g., Pagel's  $\lambda$ )
- Compare homologous regions of bone
- Compare homologous orientations of vascular canals
- Compare homologous bone fibre matrix types for osteocytes
- Preferably compare more than one method of calculating phylogenetic signal. If only using one, we recommend Blomberg's  $K$
- Test for correlation with other variables, such as mass

### Incorporating phylogenetic signal in phylogenetic analysis

For a character state to be informative within phylogenetic analyses, traits should, as far as possible, be synapomorphies (Hennig, 1965). This can be explored using for example ancestral state reconstruction methods (ASR; see Williams et al., 2006 for a summary). However, accuracy of ASR methods is affected by missing data, such as initial character states, states of extinct species, accuracy of phylogenetic trees and relative rate of evolutionary change. In addition, different methods of ASR generate different results (Williams et al., 2006). If enough data is available, it is recommended to test for synapomorphy using ASR, but in the absence or uncertainty of the data available, testing for phylogenetic signal as described above provides an acceptable alternative basis on which to decide whether a palaeohistological trait may have phylogenetic utility.

Histological variables are often continuous and ideally should be left as such, as categorisation into discrete characters involves discarding data. The use of continuous traits can improve morphological phylogenetics (Parins-Fukuchi, 2018). However, for some phylogenetic analyses, data will need to be discretised. One of the challenges of coding histological data is that it is often hierarchical, for example, coding for the morphology of osteocytes in secondary osteons is contingent on the presence of both secondary osteons and osteocytes in the chosen bone or bone region. This can result in uninformative states and pseudo-ordering, where a compound character includes absent or present plus 'present but variable' states (Brazeau, 2011). A recommendation is to use contingent or 'reductive coding' to introduce ordering in this situation (Strong & Lipscomb, 1999).

Therefore, rather than 'osteocytes in woven bone in bone X: absent (0); present, min diameter less than Y (1); present, min diameter greater than or equal to Y (2)', instead, use:

1. Woven bone in bone X: absent (0); present (1)
2. Osteocytes in woven bone when present in bone x: min diameter less than Y (0); min diameter greater than or equal to Y (1)

This assumes that woven bone will always have osteocytes present, if this is not the case, an extra state needs to be added:

1. Woven bone in bone X: absent (0); present (1)
2. Osteocytes in woven bone when present in bone X: absent (0); present (1)
3. Min diameter of osteocytes in woven bone when present in bone X: less than Y (0); greater than or equal to Y (1)

Similar character lists would need to be written to include osteocytes in organised bone and secondary osteons.

Note that the condition of absence of a structure should only appear once (e.g., woven bone absent or present) in a data matrix. It is recommended to collapse zero-length branches to avoid creating groupings that share the non-applicable state.

Distinctive patterns in degree and organisation of bone remodelling at various stages of development could also be discretised and coded for phylogenetic analyses. Descriptions such as the degree of remodelling as a proportion of cortical bone in adult specimens could be coded. For example: 'minimal' (fewer than 25% of the cortical bone overprinted by secondary osteons); 'moderate' (secondary osteons up to 50% of cortical bone); or 'extensive' (70-100% remodelling, multiple generations); or with the addition of qualifiers such as 'uneven', or 'scattered'. Alternatively, the number of generations of overlapping secondary osteons could be coded.

In terms of cortical thickness, an alternative suggestion may be to instead discretise a qualitative description of the cortico-medullary boundary. For example, describing the transition or boundary area by the proportion and patterning of this area relative to the cortical bone proper. The terminology 'sharp', 'uneven', 'gradual' or 'intermediate' could also be used and coded for phylogenetic analysis. Similar HOS stages would need to be compared for consistency.

# Chapter 6 Correlation of Bone Histology Traits with Body Mass

## 6.1 Introduction

Having established the presence of phylogenetic signal in some traits within femoral bone microstructure (Chapter 5), further analysis is needed to test for covariance with other factors indicative of scale, such as body mass, before concluding that differences in microscopic traits between species are substantially due to relatedness. Therefore, various bone microstructure traits are tested for correlation with body mass, femoral length and circumference as proxies for scale, using a phylogenetic (PGLS) and non-phylogenetic (Spearman's) test.

Body mass is strongly linked to aspects of physiology, biology and life history. It enables inference of a variety of species' traits such as metabolism, biomechanics, ecology, growth rate and reproductive strategy (Knut Schmidt-Nielsen, 1984; Brown et al., 1993; Gillooly et al., 2001, 2002; Campione & Evans, 2012; Benson et al., 2014). A relationship with body mass has been found in some bone micro-anatomical traits; differences in Haversian system morphology between adult species originally noted in raw data by Jowsey (1966), were later found to be positively related to body weight (Mishra & Knothe Tate, 2004). More recently, secondary osteon and Haversian canal area were "significantly related to body mass, independent of phylogeny" in an extensive study of mammals (Felder et al., 2017). Further, canal circularity and cell density were found to be related to body mass (rather than environment) in wild bovids (Marín-Moratalla et al., 2014), and micro-anatomical traits such as vertebral cortical thickness, were found to be more strongly correlated with body size than habitat in amniotes (Houssaye et al., 2014).

## 6.2 Materials and Methods

### Data sources

Thin sections prepared from the anterior mid-diaphysis of 31 sauropod femora were photographed, and morphometric data was digitised and processed as described in Chapter 3. All specimens were at, or beyond, sexual maturity (HOS 8, or equivalent), thus limiting, although not eliminating, variation due to ontogeny.

### Variables

For full list of variables and calculations see **Table 3.2** and S1.

### Body mass estimation

Either volumetric reconstructions or skeletal scaling relationships are used to estimate body mass. Volumetric reconstructions are more complex and involve a physical or computer-generated reconstruction and estimation of body shape, soft tissues and skeletal properties to estimate mass from volume. In skeletal scaling methods, regression equations plotting body mass against a chosen skeletal element (such as femur length) derived from extant taxa are used to create a predictive model that can estimate body mass using a simple allometric approach (Campione & Evans, 2012). Although wide discrepancies have been noted by some authors (Brassey, 2016), this is an appropriate method where only single elements are available, as in the current study, and both methods were found to be generally consistent when estimating body mass in non-avian dinosaurs (Campione & Evans, 2020). In addition, Campione and Evans (2012) found that “the relationship between proximal (stylopodial) limb bone circumference and body mass is highly conserved in extant terrestrial mammals and reptiles”. Further, measurements of length in sauropods tend to scale isometrically with body mass, and limb bone circumference of sauropods tends to scale with positive allometry (Campione & Evans, 2012), making bone length and circumference suitable proxies for size.

As only femoral measurements were available, body mass was estimated from femoral length using a regression equation based on reported estimations of Sauropodomorpha body mass using femoral length:

$$y = 2.3459x - 0.2935$$

Where  $y = \log_{10}$  body mass (g),  $x = \log_{10}$  femur length (mm),  $r^2 = 0.73$  (O’Gorman & Hone, 2012)

### **Phylogenetic test**

Analyses involving different species sharing a common ancestry violate the assumption of independent data points required by many statistical tests (Felsenstein, 1985; Harvey & Pagel, 1991) and risk inflating type I error rates. To avoid this problem, phylogenetic comparative methods (PCM’s) are used to test for character correlations using maximum likelihood. A measure of the statistical dependence of those traits which are due to phylogenetic relationships can be generated by mapping histological trait values onto known phylogenies, providing insight into a taxon’s evolutionary history (Garland et al., 2005; Revell et al., 2008). Phylogenetic generalised least squares (PGLS: Grafen, 1989; see also Mundry, 2014; Symonds & Blomberg, 2014 for reviews) is an example of a PCM and uses phylogenetic regression to estimate trait correlation among characters by weighting according to shared evolutionary history. The process estimates the slope and intercept values for the regression model and probability using a t-test (among other output), given the chosen phylogenetic tree.

PGLS was calculated using the Caper function in R. This method was chosen over the alternative method, phylogenetically independent contrasts (PIC) as PGLS tends to outperform PIC when evolution does not follow a BM model. Tree data was drawn from Cashmore et al. (2020) (3.2). Mean values for each taxonomic group were used. Body mass was used as the predictor variable, and the histological variables as response variables. Femoral length and circumference were also independently used as predictor variables as further proxies for scale (for data sources see Chapter 3 and S1). As femoral length

was used to calculate mass, results using femoral length and mass as predictor variables were expected to be very similar if not the same. Bivariate data were not tested where the response variable was used to calculate the predictor variable and was therefore likely to be unduly influential.

The phylogeny and data were combined using the function `comparative.data`, and data were  $\log_{10}$  transformed during the analysis to improve normality and homogeneity. Outliers were identified by examination of a scatter plot, and extreme outliers (outside  $Q1 - 3 \cdot IQR$ , or  $Q3 + 3 \cdot IQR$ ) were removed when running the analysis. Deviations of each species from the regression line were assumed to evolve under BM.

A maximum likelihood (ML),  $\lambda$  value, and probability values were calculated which show the optimal value of phylogenetic signal of the residuals (not the individual variables), and tailors the calculation to this value. The ML value can indicate a measure of fit, i.e., the parameter values that make the observed data most likely to have happened; that is, the process tests for the degree of response in the dependent variable  $Y$  (e.g., cell size) to changes in the predictor or independent variable  $X$  (e.g., mass), although no causation is implied. Bounds were set to  $1e-05 \geq \lambda \leq 1$  (apart from `On.Vc.Dm` and `On.Vc.Ar` which required  $1e-03 \geq \lambda \leq 1$ ). The regression coefficient was calculated, which indicates the amount of change in the dependent variable when the independent variable (predictor) changes by one unit (values can therefore exceed  $\pm 1$ ). Additionally,  $R^2$  values were calculated, indicating the percentage of variance explained between a null model and the actual model ( $0 > R^2 < 1$ ). This can be used to illustrate the proportion of the variance of the dependent variable (e.g., cell size) explained by the independent variable (e.g., mass) (although see Ives 2019). Likelihood profile plots for  $\lambda$  and  $t$ -values were also generated as well as model diagnostic plots to check data met the assumptions of the model.

Body mass was also tested independently for phylogenetic signal using `phylosig` from `phytoolsR` and `abouheif.moran` (package `adephylo` in R) (R Core

Team (2020), using Monte Carlo simulations and the default value of 999 randomisations.

### **Non-phylogenetic test**

A non-phylogenetic test was included as it may be more appropriate to interpret if no phylogenetic signal is detected in the residuals (Revell, 2010). Spearman’s rank-order correlation was conducted using SPSS (IBM Statistics 27). This was chosen over Pearson’s correlation as it is less sensitive to strong outliers and deviations from normality than Pearson’s, (which was a consideration for some of the data), and can measure monotonic, rather than strictly linear relationships. Data for individual specimens were compared (as opposed to average measurements for each species as used in PGLS) as taxonomic groupings are not considered in this test. This gave more data pairs and hence results less affected by small sample size. Data were log10 transformed to improve normality and homogeneity of the data. Bivariate plots were assessed for a linear, and specifically monotonic relationship (an assumption of the Spearman’s test), by looking at a scatter plot for each pair. Spearman’s correlation coefficient ranges from  $-1 > r_s < 1$ , with values nearer  $\pm 1$  indicating a stronger correlation.

## **6.3 Results**

For full results see supplementary information, S1.

### **Spearman’s results**

Results for correlation with body mass and femoral length were identical, which is unsurprising as the regression equation used to calculate body mass was based on femoral length. Therefore, only results for body mass are reported here (fL) and Ar, CT and Circ; a moderate correlation with TI; and a moderate,

**Table 6.1 Spearman’s correlation of variables with scale**

| Variable | Body mass (and fL) |       |     | Circ |       |     |
|----------|--------------------|-------|-----|------|-------|-----|
|          | n                  | $r_s$ | $p$ | n    | $r_s$ | $p$ |

|           |    |        |             |    |        |             |
|-----------|----|--------|-------------|----|--------|-------------|
| Ar        | 24 | 0.988  | <b>.000</b> | -  | -      | -           |
| CT        | 26 | 0.888  | <b>.000</b> | 21 | 0.930  | <b>.000</b> |
| Circ      | 24 | 0.988  | <b>.000</b> | -  | -      | -           |
| TI        | 20 | 0.444  | <b>.050</b> | -  | -      | -           |
| K         | 22 | -0.388 | .075        | 23 | -0.285 | .187        |
| Rd/CT     | 20 | -0.444 | <b>.050</b> | -  | -      | -           |
| KOn       | -  | -      | -           | -  | -      | -           |
| On.Ar     | 18 | 0.490  | <b>.039</b> | 14 | 0.437  | .118        |
| On.Dm     | 27 | 0.312  | .113        | 20 | 0.385  | .094        |
| On.In.Ar  | 18 | 0.406  | .095        | 14 | 0.442  | .114        |
| On.Vc.Ar  | 18 | 0.522  | <b>.026</b> | 14 | 0.547  | <b>.043</b> |
| On.Vc.Dm  | 18 | 0.499  | <b>.035</b> | 14 | 0.503  | .067        |
| On.Ot.AR  | 16 | 0.318  | .230        | 12 | 0.608  | <b>.036</b> |
| On.Ot.Cr  | 16 | -0.442 | .087        | 12 | -0.636 | <b>.026</b> |
| On.Ot.Ar  | -  | -      | -           | -  | -      | -           |
| On.Ot.Dm  | -  | -      | -           | -  | -      | -           |
| On.Ot.P   | -  | -      | -           | -  | -      | -           |
| PFB.Ot.AR | 9  | -0.433 | .244        | 5  | -0.500 | .391        |
| PFB.Ot.Cr | 9  | 0.300  | .433        | 5  | 0.100  | .873        |
| PFB.Ot.Ar | 9  | 0.817  | <b>.007</b> | 5  | 0.800  | .104        |
| PFB.Ot.Dm | -  | -      | -           | -  | -      | -           |
| PFB.Ot.P  | 9  | 0.633  | .067        | 5  | 0.200  | .747        |
| WB.Ot.AR  | 15 | 0.293  | .289        | 11 | 0.327  | .326        |
| WB.Ot.Cr  | 15 | -0.082 | .771        | 11 | -0.291 | .385        |
| WB.Ot.Ar  | -  | -      | -           | -  | -      | -           |
| WB.Ot.Dm  | 15 | -0.004 | .990        | 11 | -0.136 | .689        |
| WB.Ot.P   | -  | -      | -           | -  | -      | -           |

Values for body mass and fL were identical

n = no. of specimens

Pairs uncorrelated from looking at the scatter plot (-) are not reported

Statistically significant values are shown in bold ( $\alpha = .05$ )

negative correlation with Rd/CT. A strong, significant, positive correlation was also found between Circ and CT.

Spearman’s correlation identified a strong positive correlation between body mass (and fL) and PFB.Ot.Ar. A moderate correlation was found between body mass and On.Ar, On.Vc.Ar and also On.Vc.Dm and also between Circ and On.Ot.AR, On.Vc.Ar and On.Ot.Cr. Several pairs showed no monotonic relationship and results are therefore not interpretable.

**PGLS results**

Model diagnostics confirmed that the data met model assumptions.

Results when testing against body mass were very similar to those for fL (**Table 6.2**). A positive correlation was observed between body mass and bone Ar, CT and Circ. Femoral length was positively correlated with Ar and CT. A positive correlation was also found between Circ and CT, and between fL and Circ. A greater proportion of variance in CT is explained by Circ ( $R^2 = 0.948$ ) than by mass ( $R^2 = 0.581$ ), or fL ( $R^2 = 0.578$ ). The robusticity index TI showed a positive correlation with mass and fL, and the indices K and Rd/Ct both showed a negative correlation with mass and fL, indicating that with increasing mass (and fL), bones become more solid, and the cortex becomes thicker.

Correlation of secondary osteons and canals with mass and fL were non-significant in all cases. ). Data pairs that were uncorrelated according to the scatter plot and therefore fail the assumptions of the test are not reported here as results are unreliable.

A strong, significant, positive correlation was found between body mass (and fL) and Ar, CT and Circ; a moderate correlation with TI; and a moderate,

**Table 6.1 Spearman’s correlation of variables with scale**

| Variable | Body mass (and fL) |                |   | Circ |                |   |
|----------|--------------------|----------------|---|------|----------------|---|
|          | n                  | r <sub>s</sub> | p | n    | r <sub>s</sub> | p |

|           |    |        |             |    |        |             |
|-----------|----|--------|-------------|----|--------|-------------|
| Ar        | 24 | 0.988  | <b>.000</b> | -  | -      | -           |
| CT        | 26 | 0.888  | <b>.000</b> | 21 | 0.930  | <b>.000</b> |
| Circ      | 24 | 0.988  | <b>.000</b> | -  | -      | -           |
| TI        | 20 | 0.444  | <b>.050</b> | -  | -      | -           |
| K         | 22 | -0.388 | .075        | 23 | -0.285 | .187        |
| Rd/CT     | 20 | -0.444 | <b>.050</b> | -  | -      | -           |
| KOn       | -  | -      | -           | -  | -      | -           |
| On.Ar     | 18 | 0.490  | <b>.039</b> | 14 | 0.437  | .118        |
| On.Dm     | 27 | 0.312  | .113        | 20 | 0.385  | .094        |
| On.In.Ar  | 18 | 0.406  | .095        | 14 | 0.442  | .114        |
| On.Vc.Ar  | 18 | 0.522  | <b>.026</b> | 14 | 0.547  | <b>.043</b> |
| On.Vc.Dm  | 18 | 0.499  | <b>.035</b> | 14 | 0.503  | .067        |
| On.Ot.AR  | 16 | 0.318  | .230        | 12 | 0.608  | <b>.036</b> |
| On.Ot.Cr  | 16 | -0.442 | .087        | 12 | -0.636 | <b>.026</b> |
| On.Ot.Ar  | -  | -      | -           | -  | -      | -           |
| On.Ot.Dm  | -  | -      | -           | -  | -      | -           |
| On.Ot.P   | -  | -      | -           | -  | -      | -           |
| PFB.Ot.AR | 9  | -0.433 | .244        | 5  | -0.500 | .391        |
| PFB.Ot.Cr | 9  | 0.300  | .433        | 5  | 0.100  | .873        |
| PFB.Ot.Ar | 9  | 0.817  | <b>.007</b> | 5  | 0.800  | .104        |
| PFB.Ot.Dm | -  | -      | -           | -  | -      | -           |
| PFB.Ot.P  | 9  | 0.633  | .067        | 5  | 0.200  | .747        |
| WB.Ot.AR  | 15 | 0.293  | .289        | 11 | 0.327  | .326        |
| WB.Ot.Cr  | 15 | -0.082 | .771        | 11 | -0.291 | .385        |
| WB.Ot.Ar  | -  | -      | -           | -  | -      | -           |
| WB.Ot.Dm  | 15 | -0.004 | .990        | 11 | -0.136 | .689        |
| WB.Ot.P   | -  | -      | -           | -  | -      | -           |

Values for body mass and fL were identical

n = no. of specimens

Pairs uncorrelated from looking at the scatter plot (-) are not reported

Statistically significant values are shown in bold ( $\alpha = .05$ )

negative correlation with Rd/CT. A strong, significant, positive correlation was also found between Circ and CT.

Spearman's correlation identified a strong positive correlation between body mass (and fL) and PFB.Ot.Ar. A moderate correlation was found between body mass and On.Ar, On.Vc.Ar and also On.Vc.Dm and also between Circ and On.Ot.AR, On.Vc.Ar and On.Ot.Cr. Several pairs showed no monotonic relationship and results are therefore not interpretable.

### **PGLS results**

Model diagnostics confirmed that the data met model assumptions.

Results when testing against body mass were very similar to those for fL (**Table 6.2**). A positive correlation was observed between body mass and bone Ar, CT and Circ. Femoral length was positively correlated with Ar and CT. A positive correlation was also found between Circ and CT, and between fL and Circ. A greater proportion of variance in CT is explained by Circ ( $R^2 = 0.948$ ) than by mass ( $R^2 = 0.581$ ), or fL ( $R^2 = 0.578$ ). The robusticity index TI showed a positive correlation with mass and fL, and the indices K and Rd/Ct both showed a negative correlation with mass and fL, indicating that with increasing mass (and fL), bones become more solid, and the cortex becomes thicker.

Correlation of secondary osteons and canals with mass and fL were non-significant in all cases. Generally, correlation of osteocyte morphology with mass, fL and Circ was also non-significant. The exception was a significant negative correlation between Circ and WB.Ot.Dm (coeff = -0.324,  $p = .023$ ),  $R^2$  values suggest 86% of the variation in this variable is explained by Circ.

Correlation between Circ and WB.Ot.AR was nearly significant (coeff = 0.341,  $p = .070$ ). Insufficient data was available to test for osteocytes from PFB bone for correlation with Circ (S1).

### **Table 6.2 PGLS correlation of macro and micro variables with scale**

| Indep. | Dep.  | n | Coeff. | St. error<br>± | t-test | p           | R <sup>2</sup> |
|--------|-------|---|--------|----------------|--------|-------------|----------------|
| Mass   | TI    | 6 | 0.074  | 0.022          | 3.35   | <b>.029</b> | 0.737          |
| Mass   | K     | 6 | -0.031 | 0.011          | -2.69  | .054        | 0.645          |
| Mass   | Rd/CT | 6 | -0.074 | 0.022          | -3.35  | <b>.029</b> | 0.737          |
| Mass   | Ar    | 5 | 0.990  | 0.083          | 11.92  | <b>.001</b> | 0.979          |
| Mass   | CT    | 9 | 0.606  | 0.195          | 3.11   | <b>.017</b> | 0.581          |
| Mass   | Circ  | 5 | 0.448  | 0.048          | 9.32   | <b>.003</b> | 0.967          |
| fL     | TI    | 6 | 0.173  | 0.052          | 3.35   | <b>.029</b> | 0.737          |
| fL     | K     | 6 | -0.072 | 0.027          | -2.69  | .054        | 0.645          |
| fL     | Rd/CT | 6 | -0.173 | 0.052          | -3.35  | <b>.029</b> | 0.737          |
| fL     | Ar    | 5 | 2.322  | 0.195          | 11.92  | <b>.001</b> | 0.979          |
| fL     | CT    | 9 | 1.482  | 0.478          | 3.10   | <b>.017</b> | 0.578          |
| fL     | Circ  | 6 | 0.883  | 0.037          | 24.04  | <b>.000</b> | 0.993          |
| Circ   | CT    | 5 | 1.319  | 0.178          | 7.406  | <b>.005</b> | 0.948          |

Statistically significant values are shown in bold ( $\alpha = .05$ )

n = no. of taxonomic groups

For complete data set, see S1

### Phylogenetic signal

No phylogenetic signal was found in body mass independently ( $K = 0.327$ ,  $p = .922$ ;  $\lambda = 0$ ,  $p = 1$ ). Bivariate data, particularly for osteocytes, showed high residual values ( $\lambda = 1$ ) using PGLS; however, all  $p$ -values for the upper bound ( $\lambda = 1$ ) were non-significant.

## 6.4 Discussion

Histological variables were tested for correlation with body mass, femoral length and circumference as proxies for scale, using a phylogenetic (PGLS) and non-phylogenetic (Spearman's) test. Results from both tests broadly agree, finding that macro-level variables are correlated with body mass (estimated from femoral length) but moving towards smaller scale structures

in the biological hierarchy, this correlation weakens and is rarely present in the histological level variables tested.

Covariance between circumference, femoral length and body mass are well established, and results in the current study add further support to this relationship. Both PGLS and Spearman's test indicated that CT, Circ and Ar positively correlate with both body mass and fL, in addition Circ is positively correlated with CT. It is unsurprising that the strong correlation identified between Circ and bone length (which was used to estimate mass) would also generate covariance with Ar and mass, as bone area in this study was estimated from Circ.

Cortical thickness showed a significant and strong correlation with body mass, which confirms that this variable is positively related to, and a suitable proxy for scale. This may be of particular importance when estimating size from partial long bone fragments for which CT can be measured. Findings in this study agree with Houssaye et al. (2014) where (vertebral) cortical thickness in amniotes was found to be strongly correlated with body size.

Variations in robusticity are strongly linked with biomechanics, and in particular, locomotor style, but also mass (Pintore et al., 2021). Both PGLS and Spearman's test identified, as predicted, that as mass increases, the femur becomes more robust according to the robusticity indices K, TI, and Rd/CT. A significant, negative correlation between mass and Rd/CT indicates thicker bones as mass increases, with lower values of Rd/CT indicating bone more suited to impact loading and static strength than stiffness (Currey & Alexander 1985). A positive correlation of mass with TI (higher values denote thicker bones), and Ar, and a negative correlation with K (nearly significant,  $p = 0.75$ ), are also consistent with femoral Circ and CT both increasing with body mass. Covariance of mass with femoral robusticity has previously been established (Campione & Evans, 2012), and results accord with generally accepted principles whereby increases in cross-sectional area and thickness of the walls of tubular structures (such as long bones), are a biomechanical

requirement in response to increased loading (Currey & Alexander, 1985; Hart et al., 2017).

The decision as to whether Spearman's test or the PGLS results are more appropriate to interpret depends on whether a phylogenetic signal is identified in the residuals of the bivariate data (Revell, 2010). Positive correlations found using Spearman's test between body mass and On.Ar, On.Vc.Ar, and On.Vc.Dm; also, between Circ and On.Vc.Ar and On.Vc.Dm, were not found to be significant using PGLS. As all  $p$ -values for the upper bound ( $\lambda = 1$ ) were non-significant for PGLS, we cannot reject the null hypothesis that lambda of the residuals is not 1 and cannot conclude a phylogenetic signal is present in the residuals. However, sample sizes for PGLS were small (6-9 taxa) and this is likely to have affected values, as statistical significance increases with sample size (see Chapter 5 for further discussion). Spearman's test does not require that specimens are combined within species, resulting in a greater number of groups, therefore the significance of results is likely to be less affected by sample sizes and is suitable to interpret where phylogenetic signal of residuals is non-significant or very low. However, Spearman's test does not take 'account' of the phylogeny. The general recommendation, if in doubt, is to use phylogenetic methods, but as sample sizes are small, consideration is given to a range of data in deciding whether to interpret Spearman's or PGLS to avoid an over-reliance on  $p$ -values.

Body mass correlates with phylogeny in some taxa. As stated by Kamilar and Cooper (2013) when studying a range of traits in primates, "Generally, high phylogenetic signal in morphological traits is attributed to their strong correlation with body mass". However, body mass did not show a phylogenetic signal in the current study. This was a surprising result, possibly affected by small sample size.

### **Osteons and canals**

Spearman's test results are appropriate to interpret if the phylogenetic signal in the residuals of mass when tested against mean osteon and canal measurements is indeed zero, as indicated by the PGLS analysis in the current

study. This would indicate a moderate, positive correlation between mass and On.Ar, On.Vc.Ar, On.Vc.Dm, and On.Dm. No significant phylogenetic signal was identified in individual osteon morphometrics, or, in the current study, in body mass, adding further support to the interpretability of the Spearman's results.

These results, of a correlation between osteon and canal size, and scale, support findings by previous authors (Mishra & Knothe Tate, 2004; Felder et al., 2017; Jessica Mitchell et al., 2017). A positive increase in sauropod osteon size with femoral length has previously been observed (Mitchell et al 2017). Further, a positive allometric relationship was found between weight and osteon and Haversian canal diameter, which was greater for canal diameter (Mishra & Knothe Tate, 2004). Felder et al. (2017), however, found a negative allometric relationship between mass and mean secondary osteon area, canal area and osteon infill in a wide range of taxa using PIC. The authors found that although absolute osteon size increased with mass, size decreased proportionately, suggesting a biomechanical limitation on the size of osteons.

It has been suggested that osteon size may be related to strain, which is expected to increase for weight bearing bones with increasing mass, although the exact relationship is unclear. Smaller osteons, rather than larger, were found to be associated with areas of greater strain in a simulation study by van Oers et al. (2008). It should be noted that, contra to expectation, in humans no significant difference in osteon size or infill was noted between ribs and limb bones (femora), as would be expected if osteon size is correlated with strain (Skedros et al., 2013).

A more complex relationship with mass and strain may influence osteon size, connected to the process of osteocyte mechanosensation. Osteocytes translate mechanical strain into signals that promote bone formation and resorption (Lanyon, 1993). The prevailing view is that osteocyte mechanosensation and transduction is, at least in part, signalled by changes in the pressure of fluid through the lacunocanalicular network. Fluid pressure is influenced by the degree of connectivity between osteocytes, provided by

the canalicular network pervading the surrounding bone, which in turn is affected by cell density, dendritic organisation, and distance from the Haversian canal (Bonewald, 2006; Härle & Boudrieau, 2012; van Tol et al., 2020). In one approach used, lengthening the fluid path increased fluid velocity and therefore, mechanosensitivity (van Tol et al., 2020). Larger osteons offer a potentially longer fluid path, and we tentatively propose, this may be a response to maintain, or increase, efficient osteocytic mechanotransduction, a process which diminishes with age. However, the efficiency of fluid and solute transport between osteocytes and the osteonal blood supply in the central canal reduces as distance from the central channel increases, placing a limit on the viable diameter of the osteon (Mishra & Knothe Tate, 2004).

### **Osteocytes**

Spearman's test indicated correlations between body mass and PFB.Ot.Ar and PFB.Ot.P, and Circ and On.Ot.AR, but once phylogeny is incorporated, these were found to be non-significant. However, a significant negative correlation between Circ and WB.Ot.Dm was revealed using PGLS (coeff = -0.324,  $p = .023$ ), as well as a correlation close to significant between Circ and WB.Ot.AR. A strong phylogenetic signal was found in the individual variables Ot.AR, Ot.Cr and Ot.Dm, and On.Ot.Ar, and high residual values ( $\lambda = 1$ ) for bivariate data in 22 of the 40 pairs tested, even though non-significant, suggest that PGLS should be interpreted here in preference to Spearman's correlation. Overall, we conclude that a correlation between the osteocyte morphometrics tested here, and mass is not well supported, or is likely to be weak. However, WB.Ot.Dm seems to be negatively correlated with Circ (and hence related to scale), which explains a large proportion of variance in this variable.

Previous studies have found only a weak correlation with osteocyte lacunae volume and body mass in woven and parallel-fibered bone in birds (D'Emic & Benson, 2013; Grunmeier & D'Emic, 2019). Osteocyte volume was not found to be linked to overall body size or mass in dinosaurs, including sauropodomorphs (Organ et al., 2009). Notwithstanding the fact that osteocyte area rather than volume was examined, in the current study, our findings are consistent with previous results.

The reduction in minimum diameter of woven bone osteocytes as circumference increases may be influenced by a biomechanical response to loading in the development of primary bone fibre matrix. More elongate and ovate osteocytes are associated with areas subject to greater unidirectional loading such as long bones, as opposed to being more spherical in bones subject to bidirectional loading, such as cranial bones (Vatsa et al., 2008; Montanari et al., 2011; van Oers et al., 2015), possibly due to alignment with collagen fibres running transverse to the long bone axis (McMahon et al., 1995; Bromage et al., 2003; Skedros et al., 2013). Even though osteocytes from homologous bone matrices were compared, this may explain the negative correlation between Circ and WB.Ot.Dm found here, which suggests that increases in circumference, and presumably greater weight and therefore compressive loading, correlates with a narrower osteocyte in woven bone. This also explains why aspect ratio increases (indicating a more ovate shape), with an increase in circumference.

## **6.5 Conclusion**

Bone area and cortical thickness are strongly positively correlated with body mass, femoral length, and circumference. As body mass increases, the femur becomes more robust according to all the measures of robusticity tested, indicating these variables are strongly influenced by biomechanics and the need to maintain weight bearing limb bone strength. Secondary osteons and their canals in sauropod femora were found to be positively correlated with scale, possibly a response to increased strain, or the requirement to increase fluid path length to maintain effective mechanotransduction. Generally, osteocyte morphometrics tested did not show covariance with scale, apart from a negative significant correlation between circumference and minimum diameter of osteocytes from woven bone, possibly relating to increased loading. This further supports the proposal to incorporate osteocyte morphometrics in phylogenetic analysis, but not secondary osteons due to the correlation with scale.

# Chapter 7 Theoretical Framework

## 7.1 Introduction

To visualise the synergistic nature of influences on bone histology, we introduce a theoretical framework, which illustrates the relationship between form, function, behaviour, and morphology. The four signals (*sensu* Padian & Lamm, 2013) of palaeohistology are then mapped onto this framework. It is hoped that this pluralistic approach will provide an initial reference point to both better understand and position palaeohistology research within the key themes of evolutionary biology, and prompt further discussion on the ability of palaeohistology to inform on evolutionary patterns and contribute to discussions around a unified theory.

## 7.2 Interrelatedness of signals

The classical pluralistic view proposes that the causes of evolution of a trait incorporate developmental, genetic, and historical influences and constraints, as well as natural selection (Seilacher, 1970; Gould & Lewontin, 1979; Lehner, 1987; Bertossa, 2011; Seilacher & Gishlick, 2015). This is in contrast to an adaptationist view where natural selection of a trait that confers increased fitness is viewed as the most important or primary cause of trait evolution in organisms, often interpreted as ‘Darwinian adaptation’ (Darwin, 1859; Fisher, 1999; Wright, 1931, 1977; for summaries see Mayr, 1982; Ruse, 2003). However, as Gould and Lewontin point out in their 1979 ‘Spandrels’ paper (Gould & Lewontin, 1979), traits may be ‘non-heritable’, such as cultural adaptation in humans; or may arise without selection via genetic drift; as by-products of other genes, the product of multiple genes or duplicate gene families (Kimura, 1968, 1983; Stoltzfus, 1999), or as a result of developmental correlation (Lauder et al., 1993). In addition, traits are constrained by genetics and anatomy (Gritsenko et al., 2016). It is difficult to explain the persistence of nonadaptive or problematic traits, or those that seem to have no function, in a pure adaptationist light. Therefore, a more popular view is that neutral

evolution (without an adaptive assumption) is the null hypothesis used to explain complex traits (Kimura, 1968, 1983).

The interrelatedness of the various influences on morphology (which applies at the histological level) was the focus of Seilacher's (1970) functional morphology (Konstruktions-Morphologie) framework, which expanded the thinking that morphological features were primarily adaptive, developed as a response to natural selection. The framework connects three aspects: the historical or phylogenetic aspect; the adaptational or biological aspect; and the architectural aspect, which includes growth (Seilacher, 1970). Morphology can be understood from the point of view that one, or several, of these aspects may have a more dominant influence. The framework was later developed by adding a fourth aspect, environment, and further, the concept that influences on morphology were a dynamic process, constantly changing over time in response to different degrees of influence of the four aspects, called 'Morphodynamics' (Gould, 2002; Seilacher & Gishlick, 2015) (**Figure 7.1**). In fact, many histologists have commented on the synergistic nature of development and evolution. As mentioned by de Ricqlès et al. (2008a), "We have long advocated a pluralistic approach to biological causality, where phylogenetic, ontogenetic, and functional factors are integrated."

Cubo et al. (2008) attempted to quantify the relative signals (phylogenetic, functional, and structural) that contribute to biological features in extant amniotes using partitioning analysis. This technique "involves the extension from the *qualitative* analysis of phenotypes of given organisms, to the *quantitative* analysis of character variation within clades." (Cubo et al., 2008). The study involved looking at periosteal bone growth using fluorescent labelling and the analysis provided information on the significance of each of the signals as a whole, but most usefully, separated out the 'pure' signal from an overlap, of, for example, functional and structural signals, as opposed to a purely functional signal (**Figure 7.2**).

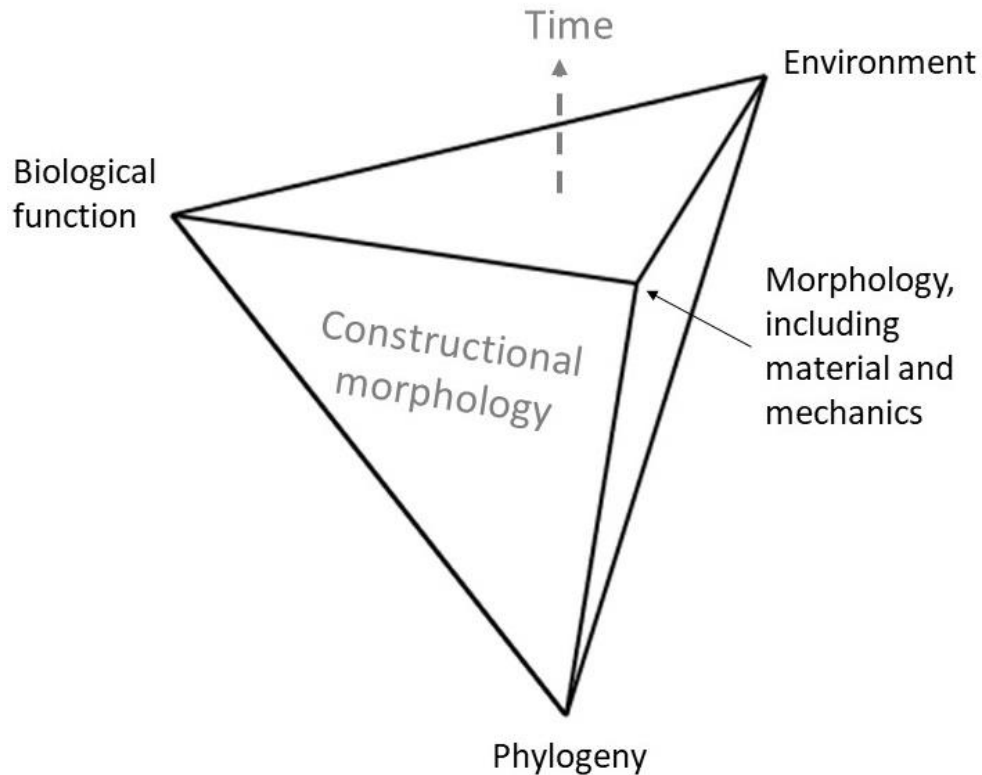


**Figure 7.1 Constructional morphology.** Concept of morphodynamics, illustrating that features of an organism are not merely adaptive, but influenced by a combination of phylogenetic, biological, environmental, and morphological factors that change over time. Adapted from Seilacher and Gishlick (2015). See Briggs (2014) for a review.

The authors found that variation of bone growth rate showed a significant phylogenetic signal globally, but the pure component is not significant, i.e., the "phylogenetic component of bone growth rate variation overlaps to a great extent...with the functional and structural components." The relationship between bone growth rate and function was significant and positively correlated; the pure component was also significant. Results were similarly significant and positively correlated for relative surface of bone apposition and bone growth rate (Cubo et al., 2008).

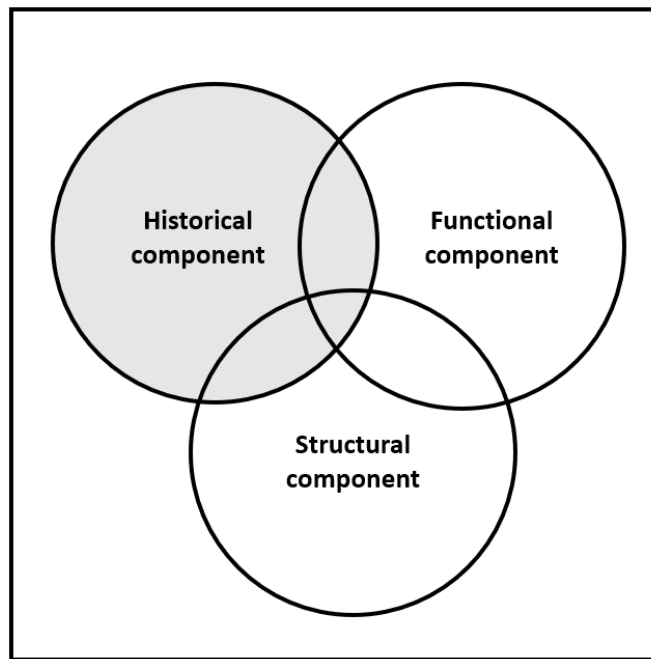


**Figure 7.2 Three principal components of bone growth rate.** The historical (phylogenetic) component can be seen to overlap the structural and functional components. Adapted from Cubo et al. (2008).

De Ricqlès et al. (2004 and references therein) mentions that later histologists such as Amprino and Enlow demonstrated that bone histological diversity primarily “expresses local circumstances of its deposition and further functions” such as growth, ontogeny and mechanics. Therefore, appreciation of the interrelatedness of influences on bone morphology at different levels of the biological hierarchy is critical in order to understand and utilise bone microstructure data.

### **7.3 Theoretical framework**

To create a theoretical framework, it is necessary to define the principal concepts, of which there are varying definitions. The ones used here are taken from those generally accepted in the field of biology (although necessarily simplified), unless otherwise stated. However, it is accepted that alternative definitions may not necessarily fit into the framework.

The concepts and premise under which they are used here are as follows:

Morphology is a structure which is used in a specific way to carry out any sort of behaviour, at any level of the biological hierarchy (sensu Bertossa, 2011). Morphology (including histological structures) therefore enables behaviour. The definition of behaviour used here is “Movement, social interaction, cognition and learning” (Breed & Moore, 2016), and as such incorporates behaviour at the histological level, for example, the movement of osteocytic dendrites within cell lacunae. The broad categories of behaviour can be broken down into behavioural acts and their component parts, separating the objective description from the functional interpretation. For example, the objective description of galloping might involve stride length, speed and other biomechanical descriptors, the functional interpretation possibly being ‘fleeing’. The objective description requires us to look at the morphology and material properties of the structures involved (and therefore overlaps form and phenotype). The functional interpretation involves looking at general categories, behaviour types and social interaction, and involves interpretation of the context. Further, functional behaviour can be broken down into simple and complex behaviours. Simple behaviours are those involving motoric patterns such as feeding or walking. Complex behaviours involve decision making, choice and communication, such as roles, or simultaneous activities (Delgado & Delgado, 1962).

Form is the spatial arrangement of something as distinct from its substance, therefore both behaviour and morphology have form (which can be dynamic or static), and behaviour overlaps both form and function (sensu Bertossa, 2011). Form, of necessity requires morphology, and via behaviour, carries out a particular function. Form alters plastically in response to intrinsic influences (such as ontogeny), and extrinsic influences (such as the environment), within historical constraints. Intrinsic influences are those that are internally either controlled by, or influenced from within, the body (such as ageing), whereas extrinsic influences are external factors that can influence behaviour and morphology, such as temperature or food availability. A phenotype is an individual's observable traits, and therefore encompasses morphology,

development, form, and behaviour. The genotype is the genetic contribution to the phenotype. Phenotypic traits can be determined by the genotype, extrinsic influences, or by selection pressures. Therefore, morphology is influenced not only by historical factors (for example genotypical limitations), but also by extrinsic and intrinsic factors, highlighting the intricate interplay of multiple influences on the phenotypic outcome (**Figure 7.3**). The framework thus represents a pluralistic view.

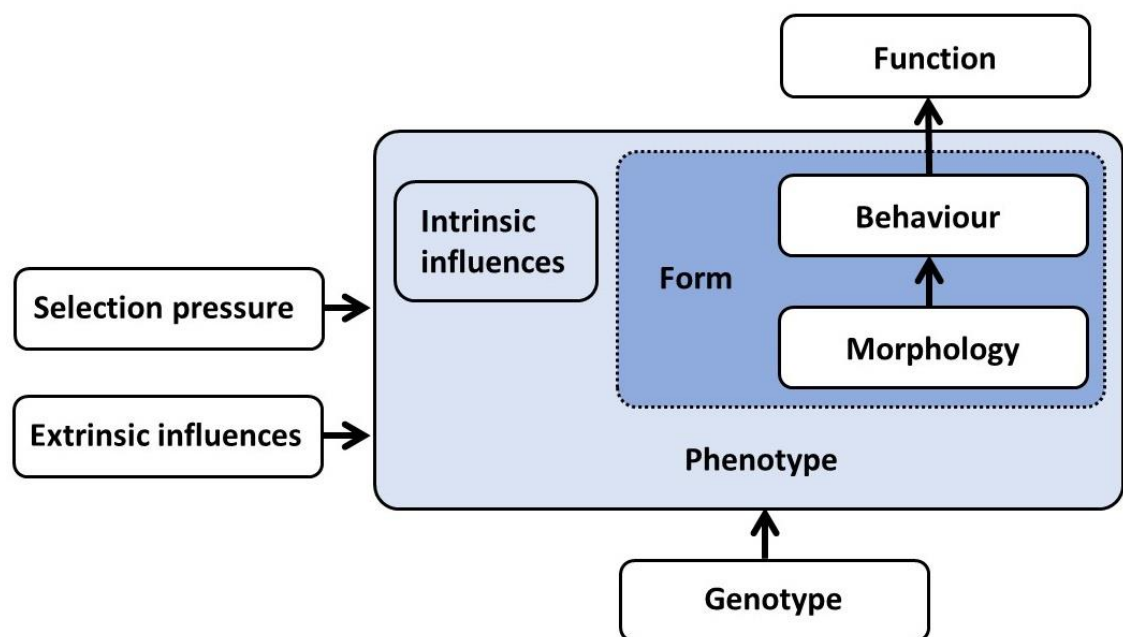


**Figure 7.3 Theoretical framework linking form, function, behaviour, and morphology.** Morphology, which includes histological level structures, is nested within form, and influenced by external and intrinsic factors, ultimately constrained by the phenotype. Morphology enables behaviour, in order to carry out a particular function.

Further, the framework can be extended to illustrate the same morphology being co-opted for different functions (**Figure 7.4**). For example, using a wing to flap during flight, and the same movement (and morphology) being used as part of a courtship display. Osteocyte lacunocanalicular morphology is an example at the histological level. Osteocyte dendritic processes form a

network, enabling nutrients and biochemical signals to be passed between osteocytes, to osteoblasts and bone-lining cells. This allows the cell to perform multiple functions, such as regulate osteoblast and osteoclast activity and therefore orchestrate bone remodelling, in addition to hormonal regulation and mineral homeostasis (Dallas et al., 2013; Florencio-Silva et al., 2015).

Conversely, the same behaviour may result from different morphologies, such as a bird and a bat wing both enabling flight (**Figure 7.4**). Maidment et al. (2012) looked at various convergent osteological characteristics related to locomotor style and stance in ornithischians, following the transition from bipedality to quadrupedality. Variations in osteo morphology were found in taxa with similar stance and the authors concluded "Skeletal morphology alone is therefore not a particularly good predictor of function in ornithischians" (Maidment et al., 2012). This indicates, as illustrated here, that a variety of morphologies could lead to the same behaviour (such as locomotor style). This has important implications to consider when making assumptions about behaviour and function from bone microstructure alone.

Complex behaviours, such as those involved in sexual selection, are difficult to infer for extinct taxa as they require context, and so function is often interpreted as functional adaptation, the "development of a trait that is useful for survival during the process of evolution" (Lehner, 1987) (**Figure 7.4**). Moreover, Arnold (1983) highlights that variations in morphology can directly impact an organism's fitness. Certain morphological features may confer advantages in specific ecological contexts or enhance performance in critical tasks related to survival and reproduction. The concept of fitness, in this context, encompasses the organism's ability to thrive and successfully transmit its genes to subsequent generations. This can be represented on the framework as a connection between function and selection pressure (**Figure 7.4**). However, from a pluralistic viewpoint, traits are not necessarily adaptive or the result of selection (Gould & Lewontin, 1979). Traits may have arisen through correlation or genetic drift, or through selection for some other advantage and been secondarily adapted for the present function, and therefore not technically fit the definition of an adaptation (the 'exaptation' of

Gould & Vrba, 1982), or seemingly have no function. In these cases, there would be no connection between function and selection within the framework (Figure 7.4).

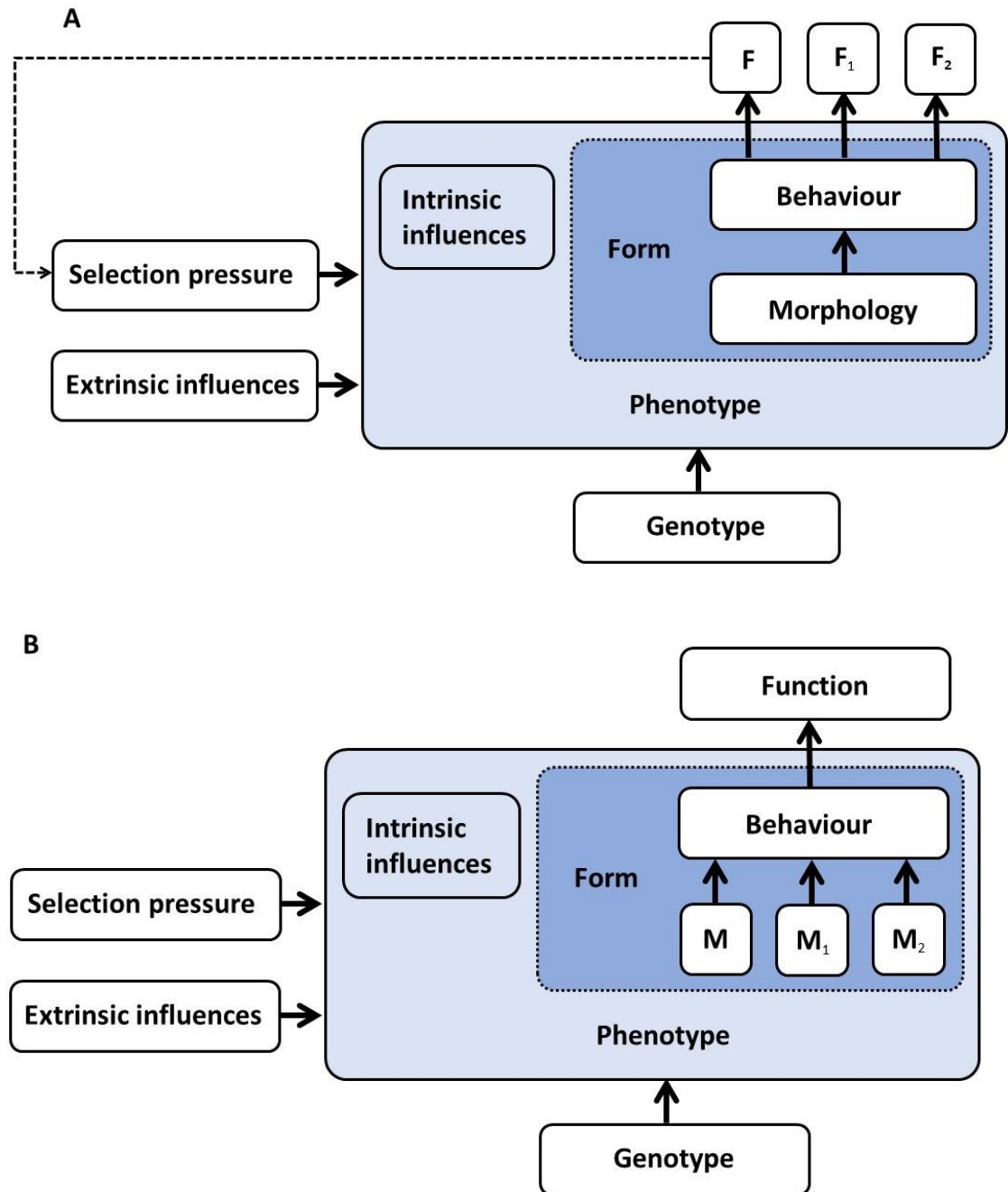


**Figure 7.4 Theoretical framework extended.** **A)** Behaviour can serve a variety of functions (F, F<sub>1</sub>, F<sub>2</sub>) and may, or may not, be adaptive via selection pressure (adaptation shown by dotted line). **B)** Multiple morphologies (M, M<sub>1</sub>, M<sub>2</sub>) can be utilised to enact the same behaviour and may achieve the same function.

Further, in terms of modern theory, the framework can be adapted to represent, and is consistent with, the concepts of constraint and correlations. Constraints refer to factors that limit or restrict the range of possible phenotypic outcomes during evolution (Pigliucci, 2008; Losos, 2011). For example, constraints can influence the evolution of bone histology by imposing limits on the range of available phenotypic variation, or by favouring certain developmental pathways over others. This results in certain morphological features or histological structures being more prevalent or limited in their variation (Badyaev, 2005; Goswami et al., 2014). Constraints may arise from various sources, including genetic, developmental, and ecological factors (Arnold, 1992; Hansen, 1997; Schluter, 2000). These are represented in the framework as genotype (genetic), intrinsic (developmental) and extrinsic (ecological) influences. A restriction or limitation is represented as a constraining field within a defined area of the framework (**Figure 7.5**). For example, in addition to size and shape, for bone to provide viable skeletal support, the relative composition of mineral and collagen must fall within certain parameters or constraints, neither too soft nor too brittle (Rho et al., 1998; Currey, 2002). These material constraints are illustrated as an additional morphospace subset within morphology on the framework (**Figure 7.5**).

Traits are rarely independent entities but are interconnected through genetic, developmental, and functional relationships (Cheverud, 1988; Klingenberg, 2008; Pigliucci, 2010). Correlations between traits, often referred to as trait associations or covariation, can arise due to shared genetic pathways, functional integration, or environmental interactions (Cheverud, 1988; Stepan et al., 2002; Hansen, 2006; Melo et al., 2016). Understanding these trait associations is crucial for unravelling the evolutionary mechanisms underlying bone histology and its functional implications, as changes in one trait can have cascading effects on others, influencing the overall structure and function of the skeletal system (Polly, 2008; Goswami et al., 2015). Correlations between traits can be illustrated within our framework as a directional field that encompasses two (or more) traits. For example, genetic factors play a significant role in the covariance between height and bone length (Sanna et

al., 2008). This is shown as a connecting field linking genotype to two morphological traits on the framework (**Figure 7.5**).

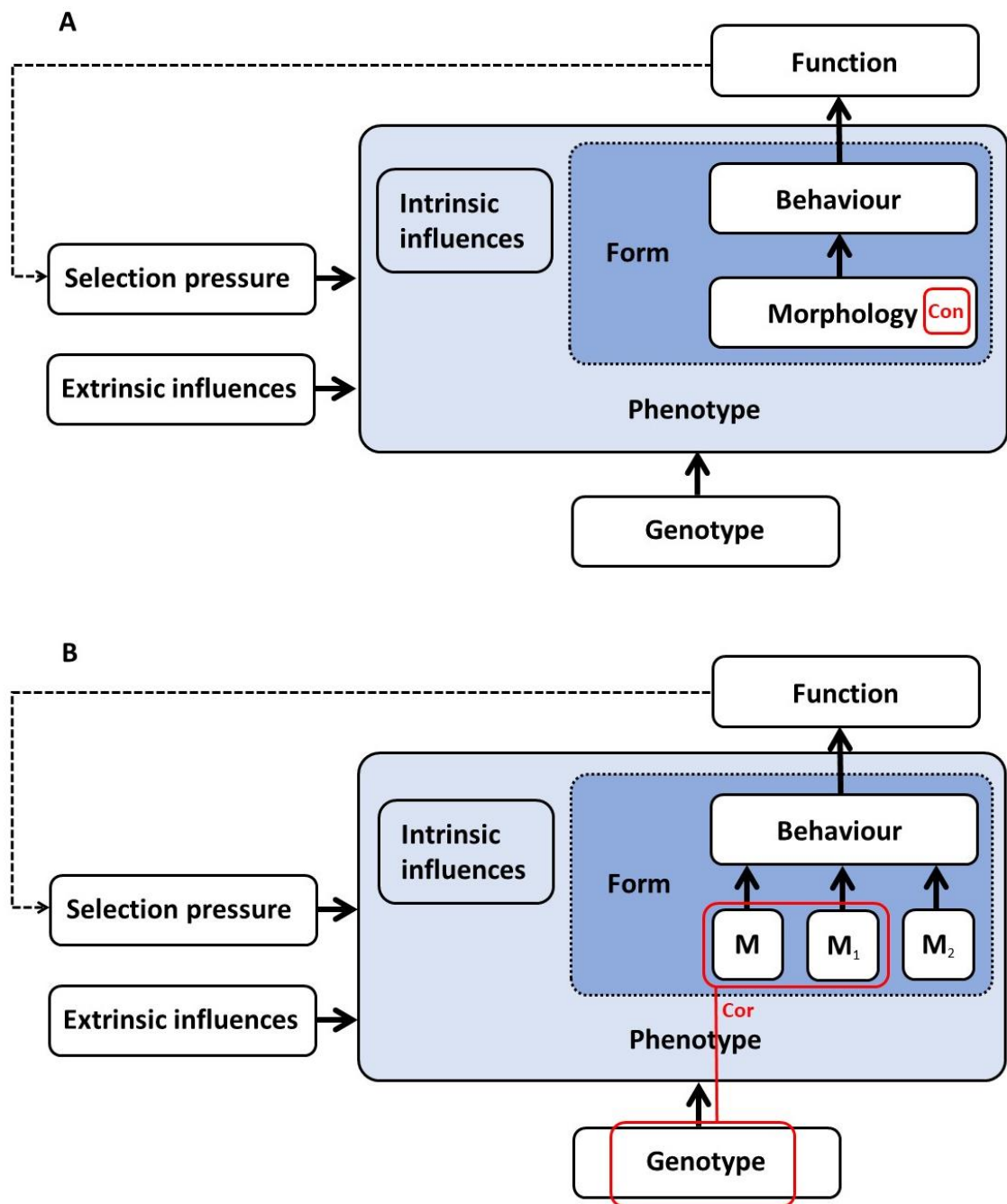


**Figure 7.5 Constraints and correlations within the framework. A)** The balance of collagen and mineral which influences bone strength, places a constraint ('Con') upon bone as a viable structure (shown as the red box within morphology). **B)** Two (or more) morphological traits may be linked and covary ('Cor') due to genetic factors (shown in red).

Constraints, as discussed earlier, can limit or favour certain phenotypic variations (Pigliucci, 2008), which may directly influence an organism's performance and, consequently, its fitness. Furthermore, correlations between traits, as highlighted by Arnold (1983), can also contribute to the overall fitness of an organism. Trait associations and covariation can influence the coordination and efficiency of different morphological features, affecting an organism's ability to carry out complex behaviours and adapt to its environment (Cheverud, 1988; Klingenberg, 2008; Pigliucci, 2010). Whilst acknowledging the potential influence of morphology, constraints and correlations on performance and fitness, our framework also acknowledges that not all of these influences may be adaptive.

## 7.4 Adding the four 'signals'

The four 'signals' of palaeohistology are overlaid onto the theoretical framework to illustrate their relationship with the concepts within (**Figure 7.6**). Through growth, bone histology provides a static record of the bone's plastic response to intrinsic influences (e.g., ontogeny), and extrinsic influences (e.g., environment), within the constraints imposed by the genotype. 'Mechanics' is harder to place as the term is used in two ways in the literature. Firstly, mechanics refers to strain, the observable response of bone to the effects of mechanical stress resulting from some extrinsic influence, such as physical activity. Secondly, it refers to the material properties of the bone, which is therefore a subset of morphology, relating to implied properties and mechanical potential (ultimately restricted by the genotype). Therefore, mechanics would appear as an extrinsic influence as well as related to morphology. For clarity, when talking about 'signals' influencing bone microstructure in the sense of affecting change, we propose using the term mechanics in the former sense, relating to mechanical stress. As phenotypic traits are used to construct phylogenies for fossil taxa where genetic data is limited or not available, 'phylogeny' is placed alongside phenotype on the framework, although it could as easily be associated with the genotype if genetic data is available (**Figure 7.6**).

Not all signals are 'equal' in the sense of overlapping or temporal order. Extrinsic influences affect resulting bone structure, whereas developmental changes can be influenced by selection pressure, and extrinsic influences such as the environment.

Looking at any one of the four signals, it is clear to see the many influences and interrelationships between them, and the relationship with the broader biological concepts illustrated. For example, in terms of bone histological traits, a phylogenetic signal is present, but may be influenced, or 'overwritten', by extrinsic influences, whilst variation is ultimately limited by the genotype. Alternatively, intrinsic influences such as those experienced during ontogeny may dominate, constrained by the material properties of the bone.

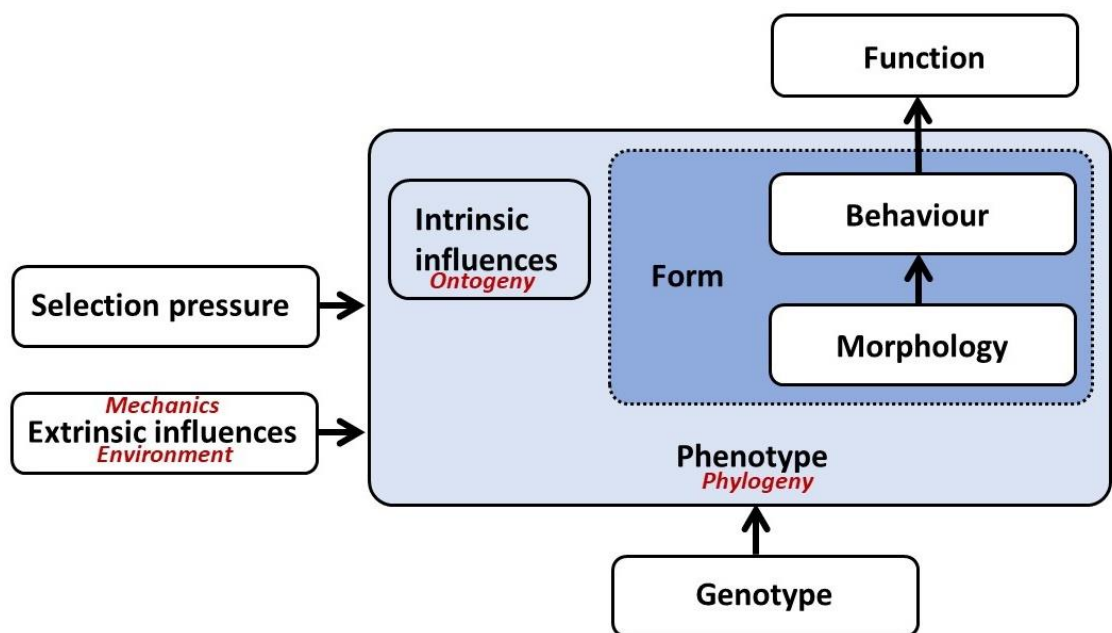


**Figure 7.6 Theoretical framework with four 'signals' overlaid.** Ontogeny, as a developmental process, is an intrinsic influence on bone microstructure. Mechanics here is the observable, morphological response of bone to the (external) effects of stress. The environment is a further extrinsic influence. These influences affect the phenotype which is ultimately constrained by the genotype.

## 7.5 Conclusion

The theoretical framework proposed illustrates the synergistic and interrelated nature of various influences on bone microstructure, and positions these 'signals' within broader evolutionary themes of form, function, behaviour, and morphology. Although we advocate a pluralistic approach, the framework can also be used to illustrate a more traditional adaptationist view. The challenges of quantifying and separating out individual influences on bone microstructure, particularly for fossilised material (notwithstanding the excellent work of authors such as Cubo), we propose, lends support to a more integrated consideration of bone microstructure in palaeobiology, as suggested in Chapter 8.

# Chapter 8 Taxonomic Utility; a Combined Approach

## 8.1 Introduction

The conclusion in the current study is that some aspects of osteocyte morphology and possibly indices of robusticity, display phylogenetic signal at the level of species and subfamily. However, phylogenetic signal is not ubiquitous across traits, taxa, and the various levels of the biological (organismal) hierarchy. This makes it difficult to find bone microstructure traits that can usefully be coded and compared across a wide range of taxa. Due to the complexity and interrelatedness of bone histology features with other influences (as illustrated in Chapter 7), a more effective use of bone microstructure data may be to consider it in conjunction with a range of evidence, in what is here called a 'combined approach'.

### Combined studies

Combining histomorphometric measurements with macro or micro-level data improves the ability to discriminate between taxonomic groups (Hillis, 1987; Urbanová & Novotný, 2005; Martiniaková et al., 2006, 2007; Hillier & Bell, 2007; Habib & Ruff, 2008). Incorporating additional data such as gross morphology or stratigraphy with histological observations creates a combined approach which can be used to classify material from unknown taxa. This is achieved using the presence of either unique, or conversely, typical histological characteristics, often in conjunction with a 'process of elimination', to discriminate between, discount, or alternatively, identify taxa.

The first Norwegian dinosaur bone was identified using bone size, the presence of fibrolamellar bone, and a particularly distinctive array of radial vascular canals in the outer cortex delineated by LAG's. Together, this suggested assignation to a prosauropod, most likely *Plateosaurus* (Hurum et al., 2006). In a later study, an absence of open medullary cavity, thick cortex,

extreme Haversian remodelling, and laminar organisation of primary osteons (all typical of sauropods and particularly titanosaurs) was used to assign fragmented material to Titanosauria, and possibly a dwarf taxon (Nikolov et al., 2020). Thyreophoran affinity was discounted due to higher vascularity, laminar vascular canal orientation, high degree of remodelling and rarity of growth lines, all less typical of thyreophoran bone histology (Nikolov et al., 2020). Garilli et al. (2009) identified the first Sicilian dinosaur bone from the late Cenomanian using a combination of gross morphology and histology. Size was used to discount mammals and birds, the presence of a large, open medullary cavity discounted marine reptiles and is less suggestive of a sauropod, as sauropods typically display a cancellous medullary infill. The extensive presence of laminar fibrolamellar bone and high levels of vascularisation support a theropod assignment, as stegosaurs and ankylosaurs typically display less vascularisation and non-laminar organisation of bone fibre matrix (Garilli et al., 2009). Finally, using a combination of HOS stage comparison, remodelling, degree and organisation of vascularity and growth marks, some disassociated individual bones could be matched or alternatively discounted as belonging to individual sauropod specimens from the Morrison Formation (Wiersma-Weyand et al., 2021). The authors recommend combining histological data with taphonomy and morphology for optimum results.

Given the synergistic, complex, and species-specific nature of development of histological variables, a combined approach is proposed as the most effective way of utilising bone microstructure data for taxonomic purposes - combining gross morphology, sedimentary and stratigraphic data, with histological and microanatomical qualitative and quantitative observations to draw taxonomic conclusions. This cements the use of palaeohistology as a valuable tool with taxonomic utility.

## **8.2 A case study**

An example, demonstrating the taxonomic utility of palaeohistology, is the discovery of the oldest ankylosaur to date, and the first from Africa (Maidment et al., 2021, see S2 for full paper). The material, NHMUK PV R37142, consists

of a series of spines, which (unusually) seemed to be extending directly from a T-shaped bone, reminiscent of a rib in shape. Histological analysis of the specimen (by S. Strachan) was critical in identifying which parts of the structure were likely external osteodermal armour, and which were internal bone, as well as narrowing down possible taxonomic affinity.

### **General methodology**

The base was sectioned transversely, and two horizontal sections were cut from the spine (**Figure 8.1**). Thin sections were prepared to study the histology following standard histological practices for fossil bone (Padian & Lamm, 2013; Sander, 2000a), and examined under a polarising microscope (**Figure 8.2**). To determine whether the 'T' shaped section was likely positioned internally, or externally (including within the dermis), and thus could be considered an osteoderm, the histology was compared to existing slides and osteohistological descriptions of thyreophoran ribs, considered the most likely internal bone that could have formed the lower part of such a structure, and osteoderms. The term osteoderm is used here to refer to dermal skeletogenesis regardless of morphology.

### **Results**

The spine histology of PV R37142 consists of a uniform cortex of well-vascularised fibrolamellar bone surrounding a cancellous core. Several long channels or pipes (de Buffrenil et al., 1986) open to the surface, and extend towards the central core. At least nine growth lines, visible as thin, dark undulating lines parallel to the bone surface, are visible towards the outer surface. Many, small, irregularly arranged osteocytes with poorly developed canaliculi are scattered throughout the primary bone.

The 'T' shaped base consists of two distinct histologies. An upper 'bar', and lower section, perpendicular to the bar and splaying out beneath it. The upper bar is heavily dominated by an ordered pattern of structural fibres (sensu Scheyer & Sander, 2004), visible as dark strands or bundles under polarised light, and arranged approximately perpendicular and parallel to the bone surface, following the curvature of the bone towards the outer edges (**Figure**

**8.1).** The fibres are arranged in a 3D orthogonal plywood-like pattern (Weiss & Ferris, 1954), with successive layers rotated by approximately  $90^{\circ}$ , and vertical inter-fibrillar bundles in between. Small, irregular osteocytes with few or no canaliculi are present in this section (**Figure 8.2**). The lower section displays no structural fibres and is composed of highly vascularised fibrolamellar bone, very similar to the histology of the spike, but heavily remodelled. The two are separated by a strip of structural fibres running the width of the section (**Figure 8.1**).

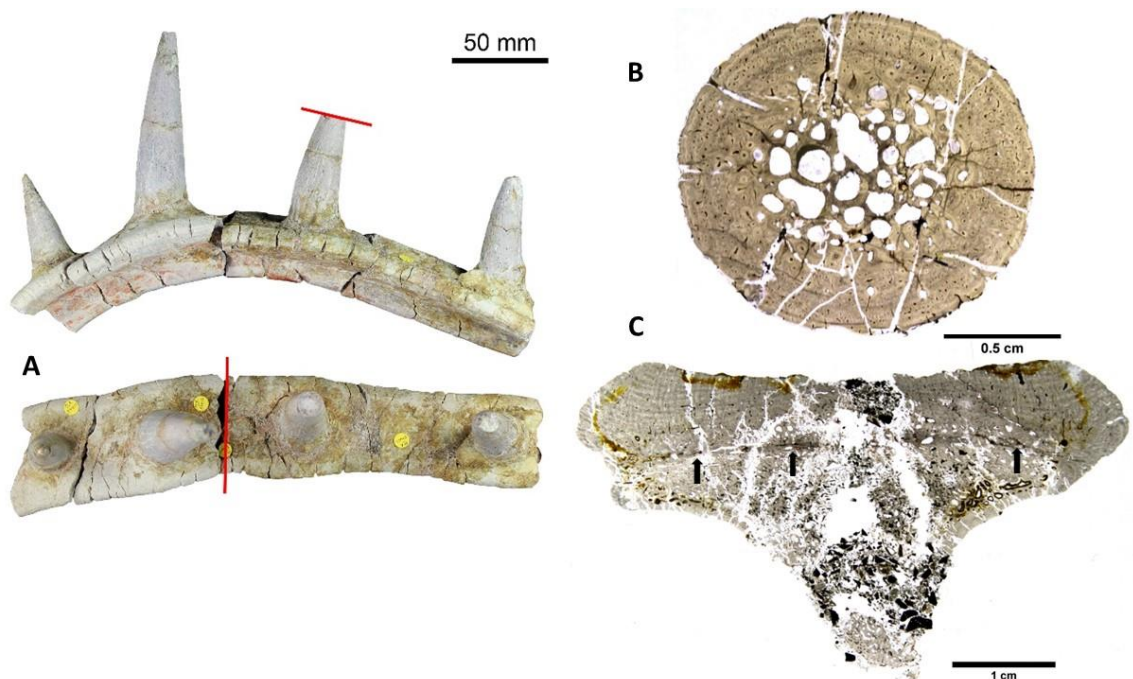


**Figure 8.1 Images of *Spicomellus afer*.** **A)** Side and top view of *Spicomellus afer* (NHMUK PV R37412). Red lines indicate sectioning points of spine (top) and 'T' shaped bar (below). **B)** Photograph of thin section of spike (PVR37412) showing high levels of vascularity in the central core, fibrolamellar bone matrix, and vascular channels opening to the surface. **C)** Photograph of thin section of PVR37412 showing organised structural fibre bundle pattern indicative of metaplastic bone, visible in the upper section of the 'T' shaped bar as alternating light and dark stripes. Black arrows indicate strip of structural fibres dividing the osteoderm, above, from the rib, below. Images: A) Maidment et al. (2021); B) – C), S. Strachan.

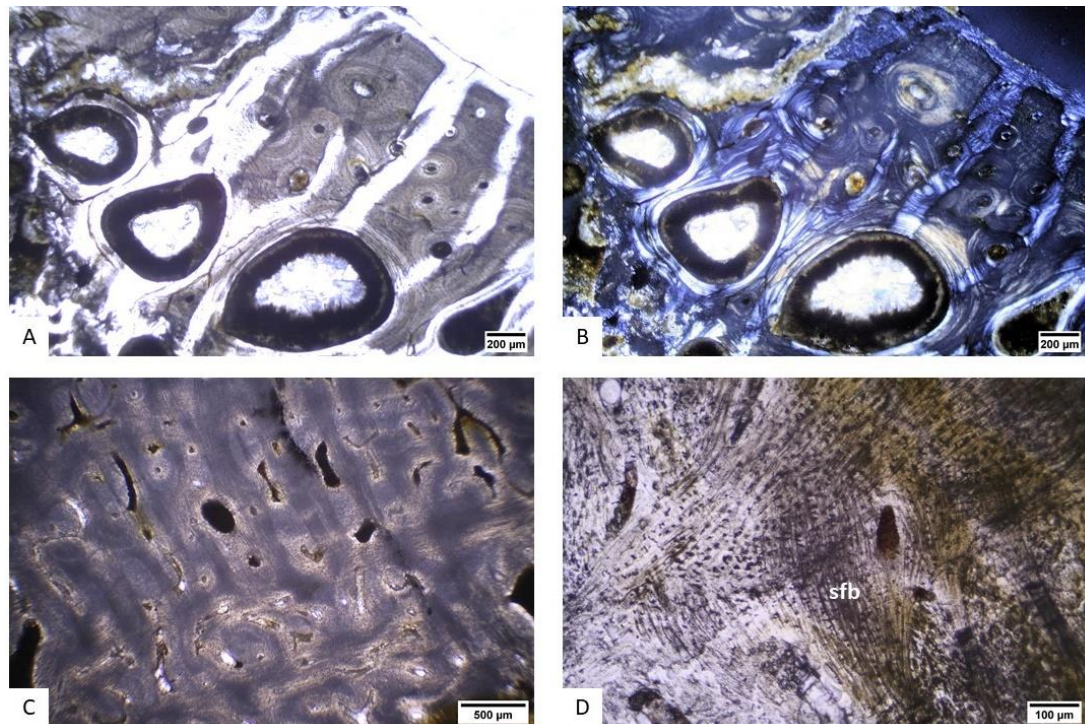


**Figure 8.2 Histology of *Spicomellus afer*.** **A)** Circumferential rows of vascular canals near the surface of the rib. Bone surface top right, PPL. **B)** Same as A) but XPL. Heavy remodelling with several generations of overlapping secondary osteons can be seen top right of image. **C)** Organised structural fibre bundle pattern visible in upper section of the 'T' (osteoderm). Grey 'cast' is likely the result of diagenetic alteration. **D)** Structural fibre bundles (sfb) visible as dark lines pervading the osteoderm. Small, irregular osteocytes with few or no visible processes are scattered throughout, PPL. Images S. Strachan.

## 8.3 Discussion

### Spine

The spine histology of PV R37412 is highly typical of thyreophoran osteoderms, and that of previously reported stegosaur spike and plate histology (Barrett et al., 2002; Burns & Currie, 2014; de Buffrenil et al., 1986; Farlow et al., 2010; Hayashi et al., 2009; Scheyer & Sander, 2004; Stein et al., 2013). Pipes and vascular channels opening to the surface and growth lines are also typical of known specimens (Farlow et al., 2010; Hayashi et al., 2009; Main et al., 2005; McWhinney et al., 2001; Scheyer & Sander, 2004; Stein et al., 2013). The suggestion that the spines were fish teeth was discounted due

to the terrestrial environment, and the histology being dissimilar to the orthodontine present in most fish teeth.

### **Upper bar**

The extensive fibres present in the upper bar section of the 'T' are more appropriately called 'structural fibres' sensu Scheyer & Sander (2004) as they extend across the bone section and are not associated with insertion points. Bone formed via metaplasia from the dermis often exhibits extensive fibre patterns that reflect the incorporation of the collagen fibres from the original extracellular matrix (Scheyer & Sander, 2004; Main et al., 2005; Scheyer et al., 2007). This suggests that the bar is an osteoderm, formed via intramembranous ossification and probably of metaplastic origin.

Dense structural fibres, whether in an organised or random orientation have been observed in all ankylosaur osteoderms, and seem to be a derived characteristic, absent in basal thyreophorans, and stegosaurs (Barrett et al., 2002; Blows, 1987; Hayashi et al., 2010; Scheyer & Sander, 2004; Stein et al., 2013). Differences in the organisational pattern of structural fibres between taxa may be of systematic value (Scheyer & Sander, 2004; Burns, 2008; Burns & Currie, 2014). Fibres have been noted at the base and lower surface of some stegosaur plates and spikes (de Buffrenil et al., 1986; Hayashi et al., 2009, 2012); however, from their angled orientation and position, it is suggested they anchor the plate to the dermis and are therefore more appropriately called Sharpey's fibres (Sharpey et al., 1867) rather than structural fibres. Stratigraphy and gross morphology were used to discount other taxa known to have structural fibres, such as turtles (Barrett et al., 2002; Burns & Currie, 2014; Maidment et al., 2021).

Therefore, although the histology of the spike is typical of thyreophoran osteoderms in general, the structural fibres in the upper bar are characteristic of ankylosaur rather than stegosaur osteoderms.

### **Lower section - rib or osteoderm?**

In terms of basic structure, ribs, as flat bones, typically contain a central cancellous bone layer (diploë) sandwiched between outer layers of compact bone (Hall, 2015) in both extant and extinct vertebrates. Thyreophoran ribs display a similar pattern (Hayashi et al., 2009; Stein et al., 2013; Waskow & Mateus, 2017), and T-shaped ribs are a synapomorphy of Euryopoda (Vickaryous, 2004). However, there are some subtle differences that are typically observed between ribs and osteoderms of fossil and extant taxa.

Long bones, and ribs are formed via endochondral ossification on a cartilaginous precursor (Hall, 2015) whereas osteoderms, as dermal tissue, are accepted as forming as a result of the direct transformation of non-bone cells into bone cells within the mesenchymal tissue in a process called intramembranous ossification (Haines & Mohuiddin, 1968). Additionally, it has been suggested that ankylosaur osteoderms are formed via metaplasia (Reid, 1996; Scheyer & Sander, 2004; Main et al., 2005; Vickaryous & Hall, 2008), a specific case of intramembranous ossification. Although the mechanism cannot be observed in fossil material, metaplastic fossilised bone typically has low levels of vascularity and small or no osteocytes with no visible processes (Haines & Mohuiddin, 1968; Horner et al., 2016; Main et al., 2005; Reid, 1996). The osteocytes in the lower section differ from those in the upper bar by being larger, more ovate and with longer and more visible processes, indicative of a flat bone rather than an osteoderm. Further, although structural fibres have been reported in the ribs of *Euoplocephalus* and two nodosaurids (Stein et al., 2013), plywood-like, thick fibre bundles are unknown in thyreophoran ribs or long bones. Osteoderms also often display a sharp distinction between cortical bone and the cancellous core, whereas ribs may show a gradation from the medullary cavity to the cortex.

Therefore, the histology of the lower T-shaped section is strongly reminiscent of a rib, rather than an osteoderm, the fusion of an osteoderm to a rib being a unique feature among armoured dinosaurs.

In summary, histological data was combined with gross morphology, sedimentary, and stratigraphic data in a combined approach to support an ankylosaurian assignment, and a new species, *Spicomellus afer*.

## **8.4 Conclusion**

Histological data was combined with gross morphology, sedimentary, and stratigraphic data in a combined approach to support an ankylosaurian assignment, and a new species, *Spicomellus afer*.

The development of histological variables is complex and the result of multiple simultaneous influences. Therefore, a combined approach is proposed as the most effective way of utilising bone microstructure data for taxonomic purposes. This approach involves combining gross morphology, sedimentary and stratigraphic data, with histological and microanatomical qualitative and quantitative observations to draw taxonomic conclusions, thus cementing the use of palaeohistology as a valuable tool with taxonomic utility.

# Chapter 9 Conclusions and future work

## **Taxonomic and phylogenetic utility**

An important distinction is proposed between phylogenetic utility, whereby a trait contains a suitably strong phylogenetic signal and is suitable to code and include in phylogenetic analyses, and taxonomic utility, whereby the traits can be used to discriminate between or potentially classify organisms.

## **Phylogenetic utility in macro and micro variables**

In sauropod femora, no significant phylogenetic signal was found in the variables CT, Circ, Ar, RI(Circ) or K individually (Chapter 5). As they are strongly correlated with size (Chapter 6), and do not display a phylogenetic signal for the taxa under investigation, it is suggested they have limited or no phylogenetic utility and would not be useful to include in phylogenetic analyses. However, in combination with information such as femoral length or HOS stage, it may be possible to discriminate between, or discount species using these variables, and so a degree of taxonomic utility may be present.

A phylogenetic signal was detected in Rd/CT, TI, and RI(CT) individually using Abouheif's  $C_{\text{mean}}$ , and these indices are comparable across taxa, suggesting they would have phylogenetic utility. However, strong covariance with mass, as found in the current study, means that scale and a link to biomechanics may be more influential. Partitioning analysis (such as that carried out by Cubo et al. 2008), and testing with a larger data set is recommended before incorporating these indices of robusticity into phylogenetic analyses. However, when used in a combined approach, Rd/CT, TI, and RI(CT), may have taxonomic utility.

## **Secondary osteons and canals**

A significant correlation with mass, lack of phylogenetic signal, and a biomechanical limitation on size, means that secondary osteon morphometrics are not a useful variable to include in phylogenetic analyses for sauropods. However, secondary osteon size varies between human and non-human

species, and so we do not discount that osteon morphology may have taxonomic utility in other species, or at higher levels of the taxonomic hierarchy.

### **Osteocytes**

Generally, the osteocyte variables tested showed a strong, significant phylogenetic signal individually and were not correlated with scale. Although phylogenetic signal is high, it is within reasonable limits. Therefore, we conclude that osteocyte morphometrics have phylogenetic and taxonomic utility and would also be suitable to include in phylogenetic analyses for sauropods. It is predicted that this could be a useful variable to incorporate into phylogenetic analyses for other taxa.

Although minimum diameter in woven bone osteocytes did show a phylogenetic signal, this variable showed a correlation with circumference and perhaps may be more strongly influenced by biomechanics. Partitioning analysis is recommended to explore the relative influences on this variable. Alternatively, osteocytes from secondary osteons or parallel-fibered bone could be used.

### **Combined approach**

As discussed in Chapter 2 and illustrated in the theoretical framework (Chapter 8), there are many overlapping influences on micro and histological level structures in bone. This makes it challenging to extract the portion of the signal that is due to relatedness. In addition, phylogenetic signal is not consistent across variables, taxonomic groups, and levels of the biological hierarchy. Therefore, a combined approach is recommended, whereby micro and histological observations are combined with a variety of data for the purposes of taxonomic identification. Indeed, given the challenges of data preparation, and subsequent interpretation of phylogenetic signal, the author's view is that a combined approach is highly effective and should be more widely adopted.

## **Conclusion**

The current study aimed to explore the phylogenetic signal in various macro, micro, and in particular, histological traits in sauropod femoral bone, and draw conclusions as to the best way to incorporate bone microstructure data into phylogenetic and evolutionary studies. Several osteocyte measurements and possibly indices of robusticity, were identified as suitable for coding and incorporating into phylogenetic analyses, and suggestions made as to how this might be done. Size dependent variation was also explored. Some variables tested that were not considered suitable for incorporating into phylogenetic analyses (such as osteon size), it is proposed, may have taxonomic utility, particularly when used in combination with other data. The use of bone microstructure data in a 'combined approach' is recommended for species discrimination and identification. A new technique is described to estimate cortical thickness, and a theoretical framework is provided to position the four signals of palaeohistology within a broader evolutionary context.

We hope that the use of bone microstructure data continues to develop and becomes a standard consideration in the evolutionary analysis, description, and identification of specimens in the future.

## References

- Aarden, E. M., Burger, E. H. & Nijweide, P. J. (1994) 'Function of Osteocytes in Bone', *Journal of Cellular Biochemistry*, 55, pp. 287–299.
- Abouheif, E. (1999) 'A method for testing the assumption of phylogenetic independence in comparative data', *Evolutionary Ecology Research*, 1, pp. 895–909.
- Abramoff, M. D., Magalhaes, P. J. & Ram, S. J. (2004) 'Image Processing with ImageJ', *Biophotonics International*, 11(7), pp. 36–42.
- Ackerly, D. (2009) 'Conservatism and diversification of plant functional traits: Evolutionary rates versus phylogenetic signal', *PNAS*, 106(2), pp. 19699–19706.
- Akaike, H. (1974) 'A New Look at the Statistical Model Identification', *IEEE Transactions on Automatic Control*, 19(6), pp. 716–723.
- Alexander, R. N. (1997) 'Encyclopedia of Dinosaurs', in Currie, P. J. and Padian, K. (eds) 665-668. Academic Pres, San Diego, California.
- Amprino, R. (1947) 'La structure du tissu osseux envisagee comme expression de differences dans la vitesse de l'accroissement', *Archives de Biologie*, 58, pp. 315–330.
- Anderson, J. F., Hall-Martin, A. & Russell, D. A. (1985) 'Long-bone circumference and weight in mammals, birds and dinosaurs', *Journal of Zoology*, 207(1), pp. 53–61.
- Andrade, R. C., Bantim, R. A. M., Lima, F. J. de, et al. (2015) 'New Data About the Presence and Absence of the External Fundamental System in Archosaurs', *Cadernos de Cultura e Ciência*, 14(1).

- Andrews, C. B., Mackenzie, S. A. & Gregory, T. R. (2009) 'Genome size and wing parameters in passerine birds', *Proceedings of the Royal Society B: Biological Sciences*, Royal Society, 276(1654), pp. 55–61.
- Annè, J., Garwood, R. J., Lowe, T., et al. (2015) 'Interpreting pathologies in extant and extinct archosaurs using micro-CT', *PeerJ*, 3, p. e1130.
- Arbour, V. M. (2009) 'Estimating impact forces of tail club strikes by ankylosaurid dinosaurs', *PLoS ONE*, 4(8).
- Ardizzoni, A. (2001) 'Osteocyte lacunar size-lamellar thickness relationships in human secondary osteons', *Bone*, 28(2), pp. 215–219.
- Arnold, S. J. (1983) 'Morphology , Performance and Fitness', *American Zoologist*, 23(2), pp. 347–361.
- Arnold, S. J. (1992) 'Constraints on Phenotypic Evolution', *The American Naturalist*, 140, pp. S85–S107.
- Ashley-Ross, M. (1994) 'Hindlimb Kinematics During Terrestrial Locomotion in a Salamander (*Dicamptodon Tenebrosus*)', *The Journal of experimental biology*, 193, pp. 255–83.
- Ayer, J. (1999) *Un os, deux os, dinos...: les dinosaures, histoire d'un gisement au Wyoming, Muséum d'histoire naturelle (Neuchâtel)*. Muséum d'histoire naturelle.
- Badyaev, A. V. (2005) 'Stress-Induced Variation in Evolution: From Behavioural Plasticity To Genetic Assimilation', *Proceedings: Biological Sciences*, 272(1566), pp. 877–886.
- Bailleul, A. M., O'Connor, J. & Schweitzer, M. H. (2019) 'Dinosaur paleohistology: Review, trends and new avenues of investigation', *PeerJ*, (9), pp. 1–45.

Barrett, P. M., Clarke, J. B., Brinkman, D. B., et al. (2002) 'Morphology, histology and identification of the "granicones" from the Purbeck Limestone Formation (Lower Cretaceous: Berriasian) of Dorset, southern England', *Cretaceous Research*, 23(2), pp. 279–295.

Bates, K. T., Mannion, P. D., Peter, L., et al. (2016) 'Temporal and phylogenetic evolution of the sauropod dinosaur body plan', *Royal Society Open Science*, 3, p. 150636.

Benson, R. B. J., Campione, N. E., Carrano, M. T., et al. (2014) 'Rates of Dinosaur Body Mass Evolution Indicate 170 Million Years of Sustained Ecological Innovation on the Avian Stem Lineage', *PLoS Biology*, 12(5).

Bentolila, V., Boyce, T. M., Fyhrie, D. P., et al. (1998) 'Intracortical remodeling in adult rat long bones after fatigue loading', *Bone*, 23(3), pp. 275–281.

Benton, M. J., Csiki, Z., Grigorescu, D., et al. (2010) 'Dinosaurs and the island rule: The dwarfed dinosaurs from Hațeg Island', *Palaeogeography, Palaeoclimatology, Palaeoecology*. Elsevier B.V., 293(3–4), pp. 438–454.

Bertossa, R. C. (2011) 'Morphology and behaviour: functional links in development and evolution', *Philosophical Transactions of the Royal Society B: Biological Sciences*, 366(1574), pp. 2056–2068.

Best, A. & Kamilar, J. M. (2018) 'The evolution of eccrine sweat glands in human and nonhuman primates', *Journal of Human Evolution*. Academic Press, 117, pp. 33–43.

Blomberg, S. P. & Garland, T. (2002) 'Tempo and mode in evolution: Phylogenetic inertia, adaptation and comparative methods', *Journal of Evolutionary Biology*, 15(6), pp. 899–910.

Blomberg, S. P., Theodore Garland Jr. & Ives, A. R. (2003) 'Testing for Phylogenetic Signal in Comparative Data : Behavioral Traits Are More Labile', *Evolution*, 57(4), pp. 717–745.

Blows, W. T. (1987) 'The Armoured Dinosaur *Polacanthus Foxi* from the Lower Cretaceous of the Isle of Wight'. *Palaeontology*, Vol. 30, Part 3, The Palaeontological Association, pp. 557–580.

Bonaparte, J. F., Heinrich, W. D. & Wild, R. (2000) 'Review of *Janenschia* Wild, with the description of a new sauropod from the Tendaguru beds of Tanzania and a discussion on the systematic value of procoelous caudal vertebrae in the sauropoda', *Palaeontographica Abt.a*, 256, pp. 25–76.

Bonewald, L. F. (2006) 'Mechanosensation and Transduction in Osteocytes', *Bonekey Osteovision*, 3(10), pp. 7–15.

Bonewald, L. F. (2011) 'The amazing osteocyte', *Journal of Bone and Mineral Research*, 26(2), pp. 229–238.

Bonewald, L. F. & Johnson, M. L. (2008) 'Osteocytes, mechanosensing and Wnt signaling', *Bone*, 42(4), pp. 606–615.

Bonnan, M. E. (2004) 'Morphometric Analysis of Humerus and Femur Shape in Morrison Sauropods: Implications for Functional Morphology and Paleobiology', *Paleobiology*, 30(3), pp. 444–470.

Bonnan, M. F. & Bonnan, M. E. (2003) 'The Evolution of Manus Shape in Sauropod Dinosaurs: Implications for Functional Morphology, Forelimb Orientation, and Phylogeny', *Source: Journal of Vertebrate Paleontology*, 23(3), pp. 595–613.

Boskey, A. L. & Coleman, R. (2010) 'Critical reviews in oral biology & medicine: Aging and bone', *Journal of Dental Research*, 89(12), pp. 1333–1348.

Botha, J. & Chinsamy, A. (2001) 'Growth patterns deduced from the bone histology of the cynodonts *Diademodon* and *Cynognathus*', *Journal of Vertebrate Paleontology*, 20(4), pp. 705–711.

Boulesteix, M., Weiss, M. & Biéumont, C. (2006) 'Differences in genome size between closely related species: The *Drosophila melanogaster* species subgroup', *Molecular Biology and Evolution*. Oxford University Press, 23(1), pp. 162–167.

Brassey, C. A. (2016) 'Body-Mass Estimation in Paleontology: A Review of Volumetric Techniques', *The Paleontological Society Papers*, 22, pp. 133–156.

Brazeau, M. D. (2011) 'Problematic character coding methods in morphology and their effects', *Biological Journal of the Linnean Society*, 104(3), pp. 489–498.

Breed, M. J. & Moore, J. (2016) *Animal Behaviour*. 2nd edn. London: Academic Press.

Briggs, D. E. G. (2014) 'Adolf Seilacher's fossil record', *Geology Today*, 30(6), pp. 227–231.

Brits, D., Steyn, M. & L'Abbé, E. N. (2014) 'A histomorphological analysis of human and non-human femora', *International Journal of Legal Medicine*, 128(2), pp. 369–377.

Bromage, T. G., Goldman, H. M., McFarlin, S. C., et al. (2003) 'Circularly polarized light standards for investigations of collagen fiber orientation in bone.', *Anatomical record. Part B, New anatomist*, 274B(1), pp. 157–168.

Brown, J. H., Marquet, P. A. & Taper, M. L. (1993) 'Evolution of Body Size: Consequences of an Energetic Definition of Fitness', *Source: The American Naturalist*, 142(4), pp. 573–584.

de Buffrenil, V., Farlow, J. O. & de Ricqlès, A. (1986) 'Growth and Function of Stegosaurus Plates : Evidence from Bone Histology', *Paleontological Society*, 12(4), pp. 459–473.

de Buffrénil, Vivian, de Ricqlès, A. J., Zylberberg, Louise, et al. (2021) *Vertebrate Skeletal Histology and Paleohistology*. 1st edn. Edited by V. de Buffrénil, A. de Ricqlès, L. Zylberberg, et al. Boca Raton and London: CRC Press.

Burnham, K. P. & Anderson, D. R. (2002) *Model selection and multimodel inference: a practical information-theoretic approach*. 2nd ed. New York; London: Springer.

Burns, M. E. (2008) 'Taxonomic utility of ankylosaur (Dinosauria, Ornithischia) osteoderms: *Glyptodontopelta mimus* Ford, 2000: a test case', *Journal of Vertebrate Paleontology*, 28(4), pp. 1102–1109.

Burns, M. E. & Currie, P. J. (2014) 'External and internal structure of ankylosaur (Dinosauria, Ornithischia) osteoderms and their systematic relevance', *Journal of Vertebrate Paleontology*, 34(4), pp. 835–851.

Cadena, E. A. & Schweitzer, M. H. (2012) 'Variation in osteocytes morphology vs bone type in turtle shell and their exceptional preservation from the Jurassic to the present', *Bone*. Elsevier Inc., 51(3), pp. 614–620.

Campione, N. E. & Evans, D. C. (2012) 'A universal scaling relationship between body mass and proximal limb bone dimensions in quadrupedal terrestrial tetrapods', *BMC Biology*, 10.

Campione, N. E. & Evans, D. C. (2020) 'The accuracy and precision of body mass estimation in non-avian dinosaurs', *Biological reviews*, 95, pp. 1759–1797.

Canè, V., Marotti, G., Volpi, G., et al. (1982) 'Size and density of osteocyte lacunae in different regions of long bones', *Calcified Tissue International*, 34(1), pp. 558–563.

Carballido, J. L., Pol, D., Cerda, I., et al. (2011) 'The osteology of *Chubutisaurus insignis* del corro, 1975 (Dinosauria : Neosauropoda) from the

“Middle” Cretaceous of Central Patagonia, Argentina’, *Journal of Vertebrate Palaeontology*, 31(1), pp. 93–110.

Carballido, J. L., Pol, Di., Otero, A., et al. (2017) ‘A new giant titanosaur sheds light on body mass evolution among sauropod dinosaurs’, *Proceedings of the Royal Society B: Biological Sciences*. Royal Society Publishing, 284(1860).

Carballido, J. L. & Sander, P. M. (2014) ‘Postcranial axial skeleton of *Europasaurus holgeri* (Dinosauria, Sauropoda) from the Upper Jurassic of Germany: Implications for sauropod ontogeny and phylogenetic relationships of basal Macronaria’, *Journal of Systematic Palaeontology*, 12(3), pp. 335–387.

Carballido, J. L., Scheil, M., Knötschke, N., et al. (2020) ‘The appendicular skeleton of the dwarf macronarian sauropod *Europasaurus holgeri* from the Late Jurassic of Germany and a re-evaluation of its systematic affinities’, *Journal of Systematic Palaeontology*. Taylor & Francis, 18(9), pp. 739–781.

Carrano, M. T. (2001) ‘Implications of limb bone scaling, curvature and eccentricity in mammals and non-avian dinosaurs’, *The Zoological Society of London*, 254, pp. 41–55.

Carrano, M. T. & Biewener, A. A. (1999) ‘Experimental alteration of limb posture in the chicken (*Gallus gallus*) and its bearing on the use of birds as analogs for dinosaur locomotion’, *Journal of Morphology*, 240(3), pp. 237–249.

Case, T. J. (1978) ‘A General Explanation for Insular Body Size Trends in Terrestrial Vertebrates’, *Ecology*, 59(1), pp. 1–18.

Cashmore, D. D., Mannion, P. D., Upchurch, P., et al. (2020) ‘Ten more years of discovery: revisiting the quality of the sauropodomorph dinosaur fossil record’, *Palaeontology*, pp. 1–28.

Castanet, J. (1994) ‘Age Estimation and Longevity in Reptiles’, *Gerontology*, 40, pp. 174–192.

Castanet, J., Cubo, J. & Montes, L. (2010) 'Relationship between bone growth rate and bone tissue organization in amniotes: first test of Amprino's rule in a phylogenetic context', *Animal Biology*. Brill, 60(1), pp. 25–41.

Castanet, J., Grandin, A., Abourachid, A., et al. (1996) 'Expression de la dynamique de croissance de l'os périostique chez *Anas platyrhynchos*', *C.R. Acad. Sci. (Paris)*, 319, pp. 301–308.

Castanet, J., Rogers, K. C., Cubo, J., et al. (2000) 'Periosteal bone growth rates in extant ratites (ostriche and emu). Implications for assessing growth in dinosaurs.', *Comptes rendus de l'Academie des sciences. Serie III, Sciences de la vie*, 323(6), pp. 543–550.

Cattaneo, C., Porta, D., Gibelli, D., et al. (2009) 'Histological determination of the human origin of bone fragments', *Journal of Forensic Sciences*, 54(3), pp. 531–533.

Cavalli-Sforza, L. L. & Edwards, A. W. (1967) 'Phylogenetic analysis. Models and estimation procedures', *American Journal of Human Genetics*, 19(3), pp. 233–257.

Cerda, I. A., Chinsamy, A., Pol, D., et al. (2017) 'Novel insights into the origin of the growth dynamics of sauropod dinosaurs', *PloS one*, 12(6), p. e0179707.

Chan, N. R. (2017) 'Phylogenetic variation in hind-limb bone scaling of flightless theropods', *Paleobiology*, 43(1), pp. 129–143.

Cheverud, J. M. (1988) 'A Comparison of Genetic and Phenotypic Correlations', *Evolution*, 42(5), pp. 958–968.

Chinsamy, A. (1993) 'Bone Histology and Growth Trajectory of the Prosauropod Dinosaur *Massospondylus carinatus* Owen', in *Modern Geology*. 18th edn, pp. 319–29.

Chinsamy, A. (2005) *The Microstructure of Dinosaur Bone*. 1st edn. Maryland: John Hopkins University Press.

Chinsamy, A., Chiappe, L. M., Marugán-Lobón, J., et al. (2013) 'Gender identification of the Mesozoic bird *Confuciusornis sanctus*.', *Nature communications*, 4, p. 1381.

Chinsamy, A., Hanrahan, S. A., Neto, R. M., et al. (1995) 'Skeletochronological Assessment of Age in *Angolosaurus skoogi*, a Cordylid Lizard Living in an Aseasonal Environment', *Journal of Herpetology*, 29(3), pp. 457–460.

Chinsamy, A., Rich, T. & Vickers-Rich, P. (1998) 'Polar dinosaur bone histology', *Journal of Vertebrate Paleontology*, 18(2), pp. 385–390.

Christiansen, P. (2007) 'Long-bone geometry in columnar-limbed animals: Allometry of the proboscidean appendicular skeleton', *Zoological Journal of the Linnean Society*, 149(3), pp. 423–436.

Cohen, J. (1988) *Statistical power analysis for the behavioral sciences*. 2nd edn. Hillsdale, N.J. : L. Erlbaum Associates.

Company, J. (2011) 'Bone histology of the titanosaur *Lirainosaurus astibiae* (Dinosauria: Sauropoda) from the Latest Cretaceous of Spain', *Naturwissenschaften*, 98(1), pp. 67–78.

Cooper, N., Jetz, W. & Freckleton, R. P. (2010) 'Phylogenetic comparative approaches for studying niche conservatism', *Journal of Evolutionary Biology*, 23(12), pp. 2529–2539.

Cooper, N., Thomas, G. H., Venditti, C., et al. (2016) 'A cautionary note on the use of Ornstein Uhlenbeck models in macroevolutionary studies', *Biological Journal of the Linnean Society*, 118, pp. 64–77.

Cope, E. D. (1877) 'On a gigantic saurian from the Dakota epoch of Colorado', *Paleontological Bulletin*, 25, pp. 5–10.

Cordie, D. R. & Budd, A. F. (2016) 'Histological data in a combined phylogenetic analysis of scleractinian reef corals', *Journal of Morphology*. John Wiley and Sons Inc., 277(4), pp. 494–511.

Cormack, D. (1987) *Ham's Histology*. New York: Lippincott.

Crescimanno, A. & Stout, S. D. (2012) 'Differentiating Fragmented Human and Nonhuman Long Bone Using Osteon Circularity', *Journal of Forensic Sciences*, 57(2), pp. 287–294.

Cubo, J., Legendre, L. & Laurin, M. (2021) 'Phylogenetic Signal in Bone Histology', in *Vertebrate Skeletal Histology and Paleohistology*, pp. 617–625.

Cubo, J., Legendre, P., de Ricqlès, A., et al. (2008) 'Phylogenetic, functional, and structural components of variation in bone growth rate of amniotes', *Evolution & development*, 10(2), pp. 217–227.

Cubo, J., Ponton, F., Laurin, M., et al. (2005) 'Phylogenetic signal in bone microstructure of sauropsids', *Systematic biology*, 54(4), pp. 562–574.

Cubo, J., Roy, N. le, Martinez-maza, C., et al. (2012) 'Paleohistological estimation of bone growth rate in extinct archosaurs', *Paleobiology*, 38(2), pp. 335–349.

Cullinane, D. M. (2002) 'The role of osteocytes in bone regulation: Mineral homeostasis versus mechanoreception', *Journal of Musculoskeletal Neuronal Interactions*, 2(3), pp. 242–244.

Cummaudo, M., Cappella, A., Giacomini, F., et al. (2019) 'Histomorphometric analysis of osteocyte lacunae in human and pig: exploring its potential for species discrimination', *International Journal of Legal Medicine*. International Journal of Legal Medicine, 133(3), pp. 711–718.

Currey, J. D. (1964) 'Some Effects of Ageing in Human Haversian Systems', *Journal of anatomy*, 98, pp. 69–75.

Currey, J. D. (2002) *Bones: Structure and Mechanics*. 1st edn. Princeton University Press.

Currey, J. D. & Alexander, R. (1985) 'The thickness of the walls of tubular bones', *J. Zool. London*, 206, pp. 453–468.

Curry, K. A. (1999) 'Ontogenetic Histology of Apatosaurus (Dinosauria : Sauropoda): New Insights on Growth Rates and Longevity Published by : Taylor & Francis , Ltd . on behalf of The Society of Vertebrate Paleontology Stable URL : <http://www.jstor.org/stable/4524036> Access', *Journal of Vertebrate Paleontology*, 19(4), pp. 654–665.

Curry Rogers, K. (2005) 'Titanosauria: A Phylogenetic Overview', in Curry Rogers, K. and Wilson, J. A. (eds) *The Sauropods: Evolution and Paleobiology*. University of California Press, pp. 50–103.

Curry Rogers, K., Whitney, M., D'Emic, M., et al. (2016) 'Precocity in a Tiny Titanosaur from the Cretaceous of Madagascar', *Science*, 352(6284), pp. 450–454.

Curtin, A. J., Macdowell, A. a., Schaible, E. G., et al. (2012) 'Noninvasive histological comparison of bone growth patterns among fossil and extant neonatal elephantids using synchrotron radiation X-ray microtomography', *Journal of Vertebrate Paleontology*, 32(4), pp. 939–955.

Dallas, S. L., Prideaux, M. & Bonewald, L. F. (2013) 'The osteocyte: An endocrine cell . . . and more', *Endocrine Reviews*, 34(5), pp. 658–690.

Darwin, C. R. (1859) *On the origin of species by means of natural selection, or the preservation of favoured races in the struggle for life*. 1st edn. Edited by J. Murray. London.

Davesne, D., Schmitt, A. D., Fernandez, V., et al. (2020) 'Three-dimensional characterization of osteocyte volumes at multiple scales, and its relationship

with bone biology and genome evolution in ray-finned fishes', *Journal of Evolutionary Biology*, 33(6), pp. 808–830.

Debastiani, V. J. & Duarte, L. da S. (2017) 'Evolutionary Models and Phylogenetic Signal Assessment via Mantel Test', *Evolutionary Biology*. Springer Verlag, 44(1), pp. 135–143.

Delgado, R. & Delgado, J. M. R. (1962) 'An Objective Approach to Measurement of Behavior', *Philosophy of Science*, 29(3), pp. 253–268.

D'Emic, M. D. (2012) 'The early evolution of titanosauriform sauropod dinosaurs', *Zoological Journal of the Linnean Society*, 166(3), pp. 624–671.

D'Emic, M. D. & Benson, R. B. J. (2013) 'Measurement, variation, and scaling of osteocyte lacunae: A case study in birds', *Bone*. Elsevier Inc., 57(1), pp. 300–310.

Díez Díaz, V., Garcia, G., Pereda-Suberbiola, X., et al. (2018) 'The titanosaurian dinosaur *Atsinganosaurus velauciensis* (Sauropoda) from the Upper Cretaceous of southern France: New material, phylogenetic affinities, and palaeobiogeographical implications', *Cretaceous Research*, 91, pp. 429–456.

Diniz-Filho, J. A. F., Santos, T., Rangel, T. F., et al. (2012) 'A comparison of metrics for estimating phylogenetic signal under alternative evolutionary models', *Genetics and Molecular Biology*, 35(3), pp. 673–679.

Dittmann, K. (2003) *Histomorphometrische Untersuchung der Knochenmikrostruktur von Primaten und Haustieren mit dem Ziel der Speziesidentifikation unter Berücksichtigung von*.

Dufresne, F. & Jeffery, N. (2011) 'A guided tour of large genome size in animals: What we know and where we are heading', *Chromosome Research*, 19(7), pp. 925–938.

Enlow, D. H. (1955) *A comparative Histological Study of Fossil and Recent Bone Tissues*.

Enlow, D. H. (1962) 'Functions of the Haversian System', *American Journal of Anatomy*, 110(May), pp. 269–305.

Enlow, D. H. (1969) 'The bone of reptiles', in Gans, C. and Bellairs, A. d'A. (eds) *Biology of the Reptilia, vol. 1*. London, New York: Academic Press, pp. 45–80.

Enlow, D. H. & Brown, S. O. (1956) 'A comparative histological study of fossil and recent bone tissues. Part 1.', *The Texas Journal of Science*, 8(4), pp. 405–443.

Enlow, D. H. & Brown, S. O. (1957) 'A comparative histological study of fossil and recent bone tissues. Part II.', *The Texas Journal of Science*, 9(2), pp. 186–214.

Enlow, D. H. & Brown, S. O. (1958) 'A comparative histological study of fossil and recent bone tissues. Part II.', *The Texas Journal of Science*, 10(2), pp. 187–230.

Erickson, G. M. (2005) 'Assessing dinosaur growth patterns: a microscopic revolution.', *Trends in ecology & evolution*, 20(12), pp. 677–84.

Erickson, G. M. (2014) 'On Dinosaur Growth', *Annual Review of Earth and Planetary Sciences*, 42(1), pp. 675–697.

Erickson, G. M., Rauhut, O. W. M., Zhou, Z., et al. (2009) 'Was dinosaurian physiology inherited by birds? Reconciling slow growth in archaeopteryx.', *PloS one*, 4(10), p. e7390.

Erickson, G. M., Rogers, K. C. & Yerby, S. A. (2001) 'Dinosaurian growth patterns and rapid avian growth rates', *Nature*, 412(6845), pp. 429–433.

Erickson, G. & Tumanova, T. (2000) 'Growth curve of *Psittacosaurus mongoliensis* Osborn (Ceratopsia: Psittacosauridae) inferred from long bone histology', *Zoological Journal of the Linnean Society*, 130(4), pp. 551–566.

Farlow, J. O., Hayashi, S. & Tattersall, G. J. (2010) 'Internal vascularity of the dermal plates of *Stegosaurus* (Ornithischia, Thyreophora)', *Swiss Journal of Geosciences*, 103(2), pp. 173–185.

Felder, A. A., Phillips, C., Cornish, H., et al. (2017) 'Secondary Osteons Scale Allometrically In Mammalian Humerus And Femur', *R. Soc. open sci*, 4, p. 170431.

Felsenstein, J. (1985) 'Phylogenies and the Comparative Method', *The American naturalist*, 125(1), pp. 1–15.

Felsenstein, J. (1988) 'Phylogenies and Quantitative Characters', *Annual Review of Ecology and Systematics*, 19, pp. 445–471.

Ferreira, T. & Rasband, W. (2012) 'ImageJ User Guide User Guide ImageJ', *Image J user Guide*, 1.46r.

Ferretti, M. & Palumbo, C. (2021) 'Static Osteogenesis versus Dynamic Osteogenesis: A Comparison between Two Different Types of Bone Formation', *Applied Sciences*. MDPI AG, 11(5), p. 2025.

Ferretti, M., Palumbo, C., Contri, M., et al. (2002) 'Static and dynamic osteogenesis: Two different types of bone formation', *Anatomy and Embryology*, 206(1–2), pp. 21–29.

Fisher, R. A. (1999) *The Genetical Theory of Natural Selection*. Edited by J. H. Bennett. Oxford: Oxford University Press.

Florencio-Silva, Ri., Sasso, G. R. D. Silva., Sasso-Cerri, E., et al. (2015) 'Biology of Bone Tissue: Structure, Function, and Factors That Influence Bone Cells', *BioMed Research International*, 2015, pp. 1–17.

Foote, J. S. & Hrdlička, A. (1916) *A Contribution to the Comparative Histology of the Femur*. Edited by A. Hrdlička. Washington, Smithsonian Institution.

Fraas, E. (1908) 'Ostafrikanische Dinosaurier', *Palaeontographica*, 55, pp. 105–144.

Francillon-Vieillot, H., Buffrenil, V., Castanet, J., et al. (1990) 'Microstructure and Mineralization of Vertebrate Skeletal Tissues', *Skeletal Biomineralization: Patterns, Processes and Evolutionary Trends*. Edited by J. G. Carter. New York: Van Nostrand Reinhold, 5, pp. 471–530.

Freckleton, R. P., Harvey, P. H. & Pagel, M. (2002) 'Phylogenetic analysis and comparative data: A test and review of evidence', *American Naturalist*, 160(6), pp. 712–726.

Freemont, A. J. (1993) 'Basic bone cell biology.', *International journal of experimental pathology*, 74(4), pp. 411–6.

Garcia, B. J. (2011) *Skeletochronology of the American Alligator (Alligator Mississippiensis): Examination of the Utility of Elements for Histological Study*. Florida State University.

Garilli, V., Klein, N., Buffetaut, E., et al. (2009) 'First dinosaur bone from Sicily identified by histology and its palaeobiogeographical implications', *Neues Jahrbuch fur Geologie und Palaontologie - Abhandlungen*, 252(2), pp. 207–216.

Garland, T., Bennett, A. F. & Rezende, E. L. (2005) 'Phylogenetic approaches in comparative physiology', *Journal of Experimental Biology*, 208(16), pp. 3015–3035.

Germain, D. & Laurin, M. (2005) 'Microanatomy of the radius and lifestyle in amniotes (Vertebrata, Tetrapoda)', *Zoologica Scripta*, 34(4), pp. 335–350.

Ghilardi, A. M., Aureliano, T., Duque, R. R. C., et al. (2016) 'A new titanosaur from the Lower Cretaceous of Brazil', *Cretaceous Research*. Elsevier Ltd, 67, pp. 16–24.

Gilbert, R. P., Liu, Y., Groby, J. P., et al. (2009) 'Computing porosity of cancellous bone using ultrasonic waves, II: The muscle, cortical, cancellous bone system', *Mathematical and Computer Modelling*. Elsevier Ltd, 50(3–4), pp. 421–429.

Gillooly, J. F., Brown, J. H., West, G. B., et al. (2001) 'Effects of Size and Temperature on Metabolic Rate', *New Series*, 293(5538), pp. 2248–2251.

Gillooly, J. F., Charnov, E. L., West, G. B., et al. (2002) 'Effects of Size and Temperature on Developmental Time', *Nature*, 417, pp. 70–73.

Girondot, M. & Laurin, M. (2003) 'Bone profiler: a tool to quantify, model, and statistically compare bone-section compactness profiles', *Journal of Vertebrate Paleontology*, 23(June), pp. 458–461.

Gittleman, J. L., Anderson, C. G., Kot, M., et al. (1996) 'Comparative Tests of Evolutionary Lability and Rates Using Molecular Phylogenies', in Harvey, P. H. and Britain, R. S. (eds) *New uses for new phylogenies*. Oxford ; New York: Oxford University Press, pp. 289–307.

Gittleman, J. L. & Kot, M. (1990) 'Statistics and a Null Model for Estimating Phylogenetic Effects', *Systematic Zoology*, 39(3), pp. 227–241.

Giua, S., Farina, V., Cacchioli, A., et al. (2014) 'Comparative histology of the femur between mouflon (*Ovis aries musimon*) and sheep (*Ovis aries aries*)', *Journal of Biological Research (Italy)*, 87(2), pp. 74–77.

Goliath, J. R., Stewart, M. C. & Stout, S. D. (2016) 'Variation in osteon histomorphometrics and their impact on age-at-death estimation in older individuals', *Forensic Science International*. Elsevier Ireland Ltd, 262, pp. 282.e1-282.e6.

González, R., Cerda, I. A., Filippi, L. S., et al. (2020) 'Early growth dynamics of titanosaur sauropods inferred from bone histology', *Palaeogeography, Palaeoclimatology, Palaeoecology*. Elsevier B.V., 537.

Goswami, A., Binder, W. J., Meachen, J., et al. (2015) 'The fossil record of phenotypic integration and modularity: A deep-time perspective on developmental and evolutionary dynamics', *Proceedings of the National Academy of Sciences of the United States of America*, 112(16), pp. 4891–4896.

Goswami, A., Smaers, J. B., Soligo, C., et al. (2014) 'The macroevolutionary consequences of phenotypic integration: From development to deep time', *Philosophical Transactions of the Royal Society B: Biological Sciences*, 369(1649).

Gould, S. J. (1977) *Ontogeny and Phylogeny*. Edited by S. J. Gould. London: Belknap Press of Harvard University Press.

Gould, S. J. (2002) 'The Integration of Constraint and Adaptation (Structure and Function) in Ontogeny and Phylogeny: Structural Constraints, Spandrels, and the Centrality of Exaptation in Macroevolution', in *The Structure of Evolutionary Theory*, pp. 1179–1295.

Gould, S. J. & Lewontin, R. C. (1979) 'The Spandrels of San Marco and the Panglossian Paradigm: A Critique of the Adaptationist Programme', *Proceedings of the Royal Society of London. Series B, Biological Sciences*, 205(1161), pp. 581–598.

Gould, S. J. & Vrba, E. S. (1982) 'Exaptation-A Missing Term in the Science of Form', *Paleobiology*, 8(1), pp. 4–15.

Grafen, A. (1989) 'The Phylogenetic Regression', *Phil. Trans.*, 326, pp. 119–157.

Gregory, T. R. (2000) 'Nucleotypic effects without nuclei: Genome size and erythrocyte size in mammals', *Genome*, 43(5), pp. 895–901.

Gregory, T. R. (2001) 'The bigger the C-value, the larger the cell: genome size and red blood cell size in vertebrates.', *Blood cells, molecules & diseases*, 27(5), pp. 830–43.

Gregory, T. R. (2002) 'A Bird's Eye View of the C-Value Enigma : Genome Size , Cell Size , and Metabolic Rate in the Class Aves', *Evolution*, 56(1), pp. 121–130.

Gregory, T. R. (2005) 'The C-value enigma in plants and animals: A review of parallels and an appeal for partnership', *Annals of Botany*, 95(1), pp. 133–146.

Griebeler, E. M., Klein, N. & Sander, P. M. (2013) 'Aging, Maturation and Growth of Sauropodomorph Dinosaurs as Deduced from Growth Curves Using Long Bone Histological Data: An Assessment of Methodological Constraints and Solutions', *PLoS ONE*, 8(6).

Gritsenko, V., Hardesty, R. L., Boots, M. T., et al. (2016) 'Biomechanical constraints underlying motor primitives derived from the musculoskeletal anatomy of the human arm', *PLoS ONE*, 11(10), pp. 1–18.

Grunmeier, O. & D'Emic, M. D. (2019) 'Scaling of statically derived osteocyte lacunae in extant birds: Implications for palaeophysiological reconstruction', *Biology Letters*. Royal Society Publishing, 15(4).

Habib, M. B. & Ruff, C. B. (2008) 'The effects of locomotion on the structural characteristics of avian limb bones', *Zoological Journal of the Linnean Society*, 153(3), pp. 601–624.

Haines, R. W. & Mohuiddin, A. (1968) 'Metaplastic bone', *Journal of anatomy*, 103, pp. 527–538.

Hall, B. K. (2015) *Bones and Cartilage, Development and Evolutionary Skeletal Biology*. 2nd edn. London: Elsevier Inc.

Hansen, T. E. (2006) 'The evolution of genetic architecture', *Annual Review of Ecology, Evolution, and Systematics*, 37, pp. 123–157.

Hansen, T. F. (1997) 'Stabilizing Selection and the Comparative Analysis of Adaptation', *Evolution*, 51(5), pp. 1341–1351.

Hansen, T. F., Pienaar, J. & Orzack, S. H. (2008) 'A comparative method for studying adaptation to a randomly evolving environment', *Evolution*, 62(8), pp. 1965–1977.

Hardie, D. C. & Hebert, P. D. N. (2003) 'The nucleotypic effects of cellular DNA content in cartilaginous and ray-finned fishes', *Genome*, 46(4), pp. 683–706.

Härle, F. & Boudrieau, R. J. (2012) 'Maxillofacial bone healing', in *Oral and Maxillofacial Surgery in Dogs and Cats*. Elsevier Ltd., pp. 7–13.

Harmon, L. J. & Glor, R. E. (2010) 'Poor statistical performance of the Mantel test in phylogenetic comparative analyses', *Source: Evolution*, 64(7), pp. 2173–2178.

Hart, N. H., Nimphius, S., Rantalainen, T., et al. (2017) 'Mechanical basis of bone strength: influence of bone material, bone structure and muscle action', *J Musculoskelet Neuronal Interact*, 17(3), pp. 114–139.

Harvey, P. H. & Pagel, M. D. (1991) *The comparative method in evolutionary biology*. Oxford: Oxford University Press.

Hayashi, S., Carpenter, K., Scheyer, T. M., et al. (2010) 'Function and Evolution of Ankylosaur Dermal Armor', *Acta Palaeontologica Polonica*, 55(2), pp. 213–228.

Hayashi, S., Carpenter, K. & Suzuki, D. (2009) 'Different Growth Patterns between the Skeleton and Osteoderms of Stegosaurus (Ornithischia: Thyreophora)', *Journal of Vertebrate Paleontology*, 29(1), pp. 123–131.

Hayashi, S., Carpenter, K., Watabe, M., et al. (2012) 'Ontogenetic histology of Stegosaurus plates and spikes', *Palaeontology*, 55(1), pp. 145–161.

Hedman, M. M. (2010) 'Constraints on Clade Ages from Fossil Outgroups', *Paleobiology*, 36(1), pp. 16–31.

Hennig, W. (1965) 'PHYLOGENETIC SYSTEMATICS', *Entomol*, 10, pp. 97–116.

Hidaka, S., Matsumoto, M., Ohsako, S., et al. (1998) 'A Histometrical Study on the Long Bones of Raccoon Dogs, *Nyctereutes procyonoides* and Badgers, *Meles meles*', *The Journal of veterinary medical science / the Japanese Society of Veterinary Science*, 60(3), pp. 323–326.

Hillier, M. L. & Bell, L. S. (2007) 'Differentiating human bone from animal bone: A review of histological methods', *Journal of Forensic Sciences*, 52(2), pp. 249–263.

Hillis, D. M. (1987) 'Molecular Versus Morphological Approaches to Systematics', *Ann. Rev. Ecol. Syst.*, 18(1987), pp. 23–42.

Hjelman, C. E., Garrett, M. A., Holmes, V. R., et al. (2019) 'Genome size evolution within and between the sexes', *Journal of Heredity*. Oxford University Press, 110(2), pp. 219–228.

Hjelman, C. E. & Johnston, J. S. (2017) 'The mode and tempo of genome size evolution in the subgenus *Sophophora*', *PLoS ONE*. Public Library of Science, 12(3), pp. 1–14.

Horner, H. A. & Macgregor, H. C. (1983) 'C value and cell volume: their significance in the evolution and development of amphibians.', *Journal of Cell Science*, 63, pp. 135–146.

Horner, J. R. & Padian, K. (2004) 'Age and growth dynamics of *Tyrannosaurus rex*.', *Proceedings. Biological sciences / The Royal Society*, 271(1551), pp. 1875–80.

Horner, J. R., Woodward, H. N. & Bailleul, A. M. (2016) 'Mineralized tissues in Dinosaurs interpreted as having formed through metaplasia: A preliminary evaluation', *Comptes Rendus - Palevol. Academie des sciences*, 15(1–2), pp. 176–196.

Houde, P. (1986) 'Ostrich ancestors found in the Northern Hemisphere suggest new hypothesis of ratite origins', *Nature*, 324(11), pp. 563–565.

Houde, P. (1987) 'Histological Evidence for the Systematic Position of *Hesperornis* (Odontornithes: Hesperornithiformes)', *The Auk*, 104(1), pp. 125–129.

Houssaye, A. (2014) 'Advances in vertebrate palaeohistology: Recent progress, discoveries, and new approaches', *Biological Journal of the Linnean Society*, 112(4), pp. 645–648.

Houssaye, A., Lindgren, J., Pellegrini, R., et al. (2013) 'Microanatomical and Histological Features in the Long Bones of Mosasaurine Mosasaurs (Reptilia, Squamata) - Implications for Aquatic Adaptation and Growth Rates', *PLoS ONE*, 8(10), pp. 1–12.

Houssaye, A., Sander, M. P. & Klein, N. (2016) 'Adaptive patterns in aquatic amniote bone microanatomy - More complex than previously thought', *Integrative and Comparative Biology*, 56(6), pp. 1349–1369.

- Houssaye, A., Tafforeau, P. & Herrel, A. (2014) 'Amniote vertebral microanatomy – what are the major trends?', *Biological Journal of the Linnean Society*, 112, pp. 735–746.
- Houssaye, A., Waskow, K., Hayashi, S., et al. (2016) 'Biomechanical evolution of solid bones in large animals: A microanatomical investigation', *Biological Journal of the Linnean Society*, 117(2), pp. 350–371.
- Hubner, T. R. (2012) 'Bone Histology in *Dysalotosaurus lettowvorbecki* (Ornithischia: Iguanodontia) - Variation, Growth, and Implications', *PLoS ONE*, 7(1).
- Hurum, J. H., Bergan, M., Müller, R., et al. (2006) 'A Late Triassic dinosaur bone, offshore Norway', *Norsk Geologisk Tidsskrift*, 86(2), pp. 117–123.
- Huttenlocker, A. K., Woodward, H. N. & Hall, B. K. (2013) 'The Biology of Bone', in Padian, K. and Lamm, E.-T. (eds) *Bone Histology of Fossil Tetrapods: Advancing Methods, Analysis, and Interpretation*. 1st edn. University of California Press, pp. 13–34.
- Ives, A. R. (2019) 'R 2 s for Correlated Data: Phylogenetic Models, LMMs, and GLMMs', *Systematic Biology*, 68(2), pp. 234–251.
- Janensch, W. (1914) 'Bericht über den Verlauf der Tendaguru-Expedition', *für Biontologie*, 3(1), pp. 15–58.
- Janensch, W. (1929) 'Material und Formgehalt der Sauropoden in der Ausbeute der Tendaguru-Expedition, 1909-1912', *Palaeontographica (Supplement VII)*, 2, pp. 3–34.
- Janvier, P. (1996) *Early vertebrates*. Edited by P. Janvier. Oxford: Oxford University Press.
- Jianu, C. M. & Weishampel, D. B. (1999) 'The smallest of the largest: A new look at possible dwarfing in sauropod dinosaurs', *Geologie en*

*Mijnbouw/Netherlands Journal of Geosciences*. Stichting Netherlands Journal of Geosciences, 78(3–4), pp. 335–343.

Jowsey, J. (1966) 'Studies of Haversian systems in man and some animals', *Journal of anatomy*, 100(Pt 4), pp. 857–864.

Kamilar, J. M. & Cooper, N. (2013) 'Phylogenetic signal in primate behaviour, ecology and life history', *Philosophical Transactions of the Royal Society B: Biological Sciences*, 368(1618).

Keck, F., Rimet, F., Bouchez, A., et al. (2016) 'Phylosignal: An R package to measure, test, and explore the phylogenetic signal', *Ecology and Evolution*, 6(9), pp. 2774–2780.

Kerschnitzki, M., Wagermaier, W., Roschger, P., et al. (2011) 'The organization of the osteocyte network mirrors the extracellular matrix orientation in bone', *Journal of Structural Biology*, 173(2), pp. 303–311.

Kilbourne, B. M. & Makovicky, P. J. (2010) 'Limb bone allometry during postnatal ontogeny in non-avian dinosaurs', *Journal of Anatomy*, 217(2), pp. 135–152.

Kimura, M. (1968) 'Evolutionary Rate at the Molecular Level', *Nature*, 217, pp. 624–626.

Kimura, M. (1983) *The Neutral Theory of Molecular Evolution*. Cambridge: Cambridge University Press.

Klein, N. & Sander, M. (2008) 'Ontogenetic stages in the long bone histology of sauropod dinosaurs', *Paleobiology*, 34(2), pp. 247–263.

Klein, N., Sander, M. & Suteethorn, V. (2009) 'Bone histology and its implications for the life history and growth of the Early Cretaceous titanosaur *Phuwiangosaurus sirindhornae*', *Geological Society, London, Special Publications*, 315(1), pp. 217–228.

Klein, N., Sander, P. M., Stein, K., et al. (2012) 'Modified laminar bone in *Ampelosaurus atacis* and other Titanosaurs (Sauropoda): implications for life history and physiology.', *PloS one*, 7(5), p. e36907.

Klingenberg, C. P. (2008) 'Morphological integration and developmental modularity', *Annual Review of Ecology, Evolution, and Systematics*, 39, pp. 115–132.

Klingenberg, C. P. & Gidaszewski, N. A. (2010) 'Testing and Quantifying Phylogenetic Signals and Homoplasy in Morphometric Data', *Systematic Biology*, 59(3), pp. 245–261.

Knut Schmidt-Nielsen (1984) *Why is Animal Size so Important?* Cambridge: Cambridge University Press.

Köhler, M., Marín-Moratalla, N., Jordana, X., et al. (2012) 'Seasonal bone growth and physiology in endotherms shed light on dinosaur physiology.', *Nature*, 487(7407), pp. 358–61.

Kokshenev, V. B. & Christiansen, P. E. R. (2010) 'Salient features in the locomotion of proboscideans revealed via the differential scaling of limb long bones', *Biological Journal of the Linnean Society*, 100(1), pp. 16–29.

Kolb, C., Scheyer, T. M., Veitschegger, K., et al. (2015) 'Mammalian Bone Palaeohistology: a Survey and New Data with Emphasis on Island Forms', *PeerJ*, 3, p. e1358.

Lande, R. (1976) 'Natural Selection and Random Genetic Drift in Phenotypic Evolution', *Society for the Study of Evolution*, 30(2), pp. 314–334.

Landis, W. J., Hodgens, K. J., Arena, J., et al. (1996) 'Structural relations between collagen and mineral in bone as determined by high voltage electron microscopic tomography', *Microscopy Research and Technique*, 33(2), pp. 192–202.

- Lanyon, L. E. (1993) 'Calcified Tissue International Osteocytes, Strain Detection, Bone Modeling and Remodeling', *Calcif Tissue Int*, 53(1), pp. 102–107.
- Lauder, G. V., Leroi, A. M. & Rose, M. R. (1993) 'Adaptations and History', *Trends in ecology & evolution*, 8(8), pp. 107–143.
- Launey, M. E., Buehler, M. J. & Ritchie, R. O. (2010) 'On the mechanistic origins of toughness in bone', *Annual Review of Materials Research*, 40, pp. 25–53.
- Laurin, M., Girondot, M. & Loth, M.-M. (2004) 'The evolution of long bone microstructure and lifestyle in lissamphibians', *Paleobiology*, 30(4), pp. 589–613.
- Lee, A. H. (2004) 'Histological organization and its relationship to function in the femur of Alligator mississippiensis Histological organization and its relationship to function in the femur of Alligator mississippiensis', *Journal of Anatomy*, 204, pp. 197–207.
- Lee, A. H. & Simons, E. L. (2015) 'Wing bone laminarity is not an adaptation for torsional resistance in bats', *PeerJ*, 3, p. e823.
- Legendre, L. J., Bourdon, E., Scofield, R. P., et al. (2014) 'Bone Histology, Phylogeny, and Palaeognathous Birds (Aves: Palaeognathae)', *Biological Journal of the Linnean Society*, 112(4), pp. 688–700.
- Legendre, L. J., Gucrossed D Signnard, G., Botha-Brink, J., et al. (2016) 'Palaeohistological Evidence for Ancestral High Metabolic Rate in Archosaurs', *Systematic Biology*. Oxford University Press, 65(6), pp. 989–996.
- Legendre, L., le Roy, N., Martinez-Maza, C., et al. (2013) 'Phylogenetic signal bone histology of amniotes revisited', *Zoologica Scripta*, 42(1), pp. 44–53.

Lehman, T. M. & Woodward, H. N. (2008) 'Modeling Growth Rates for Sauropod Dinosaurs', *Paleobiology*, 34(2), pp. 264–281.

Lehner, P. N. (1987) 'Design and Execution of Animal Behaviour Research : An Overview', *J Anim Sci*. 80523, 65(5), pp. 1213–1219.

Leitch, I. J., Chase, M. W. & Bennett, M. D. (1998) 'Phylogenetic Analysis of DNA C-values Provides Evidence for a Small Ancestral Genome Size in Flowering Plants', *Annals of Botany*, 82, pp. 85–94.

Lieberman, D. E. (1997) 'Making Behavioral and Phylogenetic Inferences from Hominid Fossils: Considering the Developmental Influence of Mechanical Forces', *Annual Review of Anthropology*, 26(1), pp. 185–210.

Lloyd, G. T., Bapst, D. W., Friedman, M., et al. (2016) 'Probabilistic divergence time estimation without branch lengths: dating the origins of dinosaurs, avian flight and crown birds', *Biology letters*, 12(11).

le Loeuff, J. (2005) 'Romanian late cretaceous dinosaurs: Big dwarfs or small giants?', *Historical Biology*, 17(1999), pp. 15–17.

Losos, J. B. (2008) 'Phylogenetic niche conservatism, phylogenetic signal and the relationship between phylogenetic relatedness and ecological similarity among species', *Ecology Letters*, 11(10), pp. 995–1003.

Losos, J. B. (2011) 'Convergence, Adaptation, and Constraint', *Evolution*, 65(7), pp. 1827–1840.

Maddison, W. P. & Maddison, D. R. (2018) 'Mesquite: a modular system for evolutionary analysis Version 3.51 28 June 2018 <http://www.mesquiteproject.org>'.

Mahboubi, S., Bocherens, H., Scheffler, M., et al. (2014) 'Was the Early Eocene proboscidean *Numidotherium koholense* semi-aquatic or terrestrial?

Evidence from stable isotopes and bone histology', *Comptes Rendus - Palevol. Academie des sciences*, 13(6), pp. 501–509.

Maidment, S. C. R., Barrett, P. M., Maidment, S. C. R., et al. (2012) 'Does morphological convergence imply functional similarity? A test using the evolution of quadrupedalism in ornithischian dinosaurs', *Proceedings of the Royal Society B*, 279(1743), pp. 3765–3771.

Maidment, S. C. R., Strachan, S. J., Ouarhache, D., et al. (2021) 'Bizarre dermal armour suggests the first African ankylosaur', *Nature Ecology and Evolution*.

Main, R. P., de Ricqlès, A., Horner, J. R., et al. (2005) 'The evolution and function of thyreophoran dinosaur scutes: implications for plate function in stegosaurs', *Paleobiology*, 31(2), pp. 291–314.

Mannion, P. D., Allain, R. & Moine, O. (2017) 'The earliest known titanosauriform sauropod dinosaur and the evolution of Brachiosauridae', *PeerJ*, 5, p. e3217.

Mannion, P. D., Upchurch, P., Barnes, R. N., et al. (2013) 'Osteology of the Late Jurassic Portuguese sauropod dinosaur *Lusotitan atalaiensis* (Macronaria) and the evolutionary history of basal titanosauriforms', *Zoological Journal of the Linnean Society*, 168(1), pp. 98–206.

Mannion, P. D., Upchurch, P., Mateus, O., et al. (2012) 'New information on the anatomy and systematic position of *Dinheirosaurus lourinhanensis* (Sauropoda: Diplodocoidea) from the Late Jurassic of Portugal, with a review of European diplodocoids', *Journal of Systematic Palaeontology*, 10(3), pp. 521–551.

Mannion, P. D., Upchurch, P., Schwarz, D., et al. (2019) 'Taxonomic affinities of the putative titanosaurs from the Late Jurassic Tendaguru Formation of Tanzania: Phylogenetic and biogeographic implications for eusauropod

dinosaur evolution', *Zoological Journal of the Linnean Society*, 185(3), pp. 784–909.

de Margerie, E., Cubo, J. & Castanet, J. (2002) 'Bone typology and growth rate: testing and quantifying "Amprino's rule" in the mallard (*Anas platyrhynchos*)', *Comptes Rendus Biologies*, 325(3), pp. 221–230.

de Margerie, E., Robin, J.-P., Verrier, D., et al. (2004) 'Assessing a relationship between bone microstructure and growth rate: a fluorescent labelling study in the king penguin chick (*Aptenodytes patagonicus*).', *The Journal of experimental biology*, 207(Pt 5), pp. 869–879.

Marín-Moratalla, N., Cubo, J., Jordana, X., et al. (2014) 'Correlation of quantitative bone histology data with life history and climate: A phylogenetic approach', *Biological Journal of the Linnean Society*, 112(4), pp. 678–687.

Marotti, G. (1977) *Decrement in Volume of Osteoblasts in Osteon Formation and its Effect on the Size of the Corresponding Osteocytes, Bone Histomorphometry*. Edited by P. J. Meunier. Paris: Armur-Montagu.

Marotti, G. (1979) 'Osteocyte orientation in human lamellar bone and its relevance to the morphometry of periosteocytic lacunae', *Metabolic Bone Disease and Related Research*, 1(4), pp. 325–333.

Marotti, G., Ledda, M., Delrio, N., et al. (1976) 'Distribution and size of osteocytic lacunae in secondary osteons of the dog', in Courvoisier, B. and Donath, A. (eds) *Exploration Morphologique et fonctionnelle du squelette, Symposium CEMO*. Genève: Médecine & Hygiène, pp. 225–230.

Marsh, O. C. (1877) 'Notice of Some New Dinosaurian Reptiles From the Jurassic Formation', *Am. J. Sci.*, 3(14), pp. 514–516.

Martin, P. G. & Fisher, R. A. (1966) 'Variation in the Amounts of Nucleic Acids in the Cells of Different Species of Higher Plants', *Experimental Cell Research*, 44, pp. 81–94.

- Martin, R. B., Gibson, V. A., Stover, S. M., et al. (1996) 'Osteonal structure in the equine third metacarpus', *Bone*, 19(2), pp. 165–171.
- Martin, R. & Saller, K. (1957) 'Gustav Fischer Verlag', in *Lehrbuch der Anthropologie*. Stuttgart.
- Martin, V., Buffeataut, E. & Suteethorn, V. (1993) 'Jurassic sauropod dinosaurs of Thailand: a preliminary report', in Thanasutipita, T. (ed.) *Proceedings of the International Symposium on Biostratigraphy of mainland Southeast Asia*. Chiang Mai University, pp. 415–425.
- Martin, V., Buffeataut, E. & Suteethorn, V. (1994) 'A new genus of sauropod dinosaur from the Sao Khua formation (Late Jurassic or early Cretaceous) of northeastern Thailand', *Comptes rendus de l'Académie des Sciences de Paris*, 319(2), pp. 1085–1092.
- Martiniaková, M., Grosskopf, B., Omelka, R., et al. (2006) 'Differences among species in compact bone tissue microstructure of mammalian skeleton: Use of a discriminant function analysis for species identification', *Journal of Forensic Sciences*, 51(6), pp. 1235–1239.
- Martiniaková, M., Grosskopf, B., Omelka, R., et al. (2007) 'Histological study of compact bone tissue in some mammals: A method for species determination', *International Journal of Osteoarchaeology*, 17(1), pp. 82–90.
- Martins, E. P. (1996) 'Phylogenies, Spatial Autoregression, and the Comparative Method: A Computer Simulation Test', *Evolution*, 50(5), pp. 1750–1765.
- Mateus, O. (2006) 'Late Jurassic dinosaurs from the Morrison Formation (USA), the Lourinhã and Alcobaça Formations (Portugal), and the Tendaguru beds (Tanzania): a comparison', *New Mexico Museum of Natural History and Science Bulletin*, 36(2003), pp. 223–231.

Mayr, E. (1982) *The growth of biological thought: diversity, evolution, and inheritance*. Cambridge: Belknap Press.

McMahon, J. M., Boyde, A. & Bromage, T. G. (1995) 'Pattern of Collagen Fiber Orientation in the Ovine Calcaneal Shaft and Its Relation to Locomotor-Induced Strain', *The Anatomical Record*, 242, pp. 147–158.

McWhinney, L. A., Rothschild, B. M. & Carpenter, K. (2001) 'Post traumatic chronic osteomyelitis in Stegosaurus dermal spikes', in Carpenter K. (ed.) *The Armored Dinosaurs*. Indiana: Indiana University Press, pp. 141–156.

Melo, D., Porto, A., Cheverud, J. M., et al. (2016) 'Modularity: genes , development and evolution', *Annual Review of Ecology, Evolution, and Systematics*, 47, pp. 463–486.

Meunier (2011) 'The Osteichthyes, from the Paleozoic to the extant time, through histology and palaeohistology of bony tissues', *Comptes Rendus - Palevol*. Elsevier Masson SAS, 10(5–6), pp. 347–355.

Mirsky, A. E. & Ris, H. (1951) 'The Desoxyribonucleic Acid Content of Animal Cells and its Evolutionary Significance', *The Journal of General Physiology*, 34(4), pp. 451–462.

Mishra, S. & Knothe Tate, M. L. (2004) 'Allometric scaling relationships in microarchitecture of mammalian cortical bone', *50th Annual Meeting of the Orthopaedic Research Society, San Francisco*, 29, p. 231.

Miskiewicz, J. J. & Mahoney, P. (2016) 'Ancient Human Bone Microstructure in Medieval England: Comparisons between Two Socio-Economic Groups', *Anatomical Record*, 299(1), pp. 42–59.

Mitchell, J., Legendre, L. J., Lefèvre, C., et al. (2017) 'Bone histological correlates of soaring and high-frequency flapping flight in the furculae of birds', *Zoology*. Elsevier GmbH., 122, pp. 90–99.

Mitchell, J. & Sander, P. M. (2014) 'The three-front model: a developmental explanation of long bone diaphyseal histology of Sauropoda', *Biological Journal of the Linnean Society*, 112(4), pp. 765–781.

Mitchell, Jessica, Sander, P. M. & Stein, K. (2017) 'Can Secondary Osteons be Used as Ontogenetic Indicators in Sauropods? Extending the Histological Ontogenetic Stages into Senescence', *Paleobiology*, 43(May), pp. 1–22.

Mocho, P., Royo-Torres, R. & Ortega, F. (2014) 'Phylogenetic reassessment of *Lourinhasaurus alenquerensis*, a basal Macronaria (Sauropoda) from the Upper Jurassic of Portugal', *Zoological Journal of the Linnean Society*, 170(4), pp. 875–916.

Montanari, S., Brusatte, S. L., de Wolf, W., et al. (2011) 'Variation of osteocyte lacunae size within the tetrapod skeleton: Implications for palaeogenomics', *Biology Letters*, 7(5), pp. 751–754.

Moran, P. A. P. (1950) 'Notes on Continuous Stochastic Phenomena', *Biometrika*, 37(1), pp. 17–37.

Morris, P. (2009) 'A Method for Determining Absolute Age in the Hedgehog', *Journal of Zoology*, 161(2), pp. 277–281.

Moss, M. L. (1961) 'Osteogenesis of acellular teleost fish bone', *American Journal of Anatomy*, 108(1), pp. 99–109.

Mulhern, D. M. & Ubelaker, D. H. (2001) 'Differences in Osteon Banding Between Human and Nonhuman Bone', *Journal of Forensic Sciences*, 46(2), p. 14952J.

Mundry, R. (2014) 'Statistical Issues and Assumptions of Phylogenetic Generalized Least Squares', in Garamszegi, L. Z. (ed.) *Modern Phylogenetic Comparative Methods and their Application in Evolutionary Biology*. Berlin, Heidelberg: Springer-Verlag, pp. 131–153.

Münkemüller, T., Lavergne, S., Bzeznik, B., et al. (2012) 'How to measure and test phylogenetic signal', *Methods in Ecology and Evolution*, 3(4), pp. 743–756.

Myhrvold, N. P. (2013) 'Revisiting the estimation of dinosaur growth rates', *PLoS ONE*, 8(12).

von Neumann, J., Kent, R. H., Bellinson, H. R., et al. (1941) 'The Mean Square Successive Difference', *Source: The Annals of Mathematical Statistics*, 12(2), pp. 153–162.

Nganvongpanit, K., Siengdee, P., Buddhachat, K., et al. (2017) 'Anatomy, histology and elemental profile of long bones and ribs of the Asian elephant (*Elephas maximus*)', *Anatomical Science International*. Springer Japan, 92(4), pp. 554–568.

Nieves, J. W., Formica, C., Ruffing, J., et al. (2005) 'Males have larger skeletal size and bone mass than females, despite comparable body size', *Journal of Bone and Mineral Research*, 20(3), pp. 529–535.

Nikolov, V., Yaneva, M., Dochev, D., et al. (2020) 'Bone histology reveals the first record of titanosaur (Dinosauria: Sauropoda) from the late cretaceous of Bulgaria', *Palaeontologia Electronica*, 23(1), pp. 1–38.

Nopcsa, F. (1915) 'Die Dinosaurier der siebenburgischen Landesteile Ungarns', *Geol. Reichsanst.*, 23, pp. 1–26.

van Oers, R. F. M., Klein-Nuland, J. & Bacabac, R. G. (2014) 'The Osteocyte as an Orchestrator of Bone Remodeling : An Engineer ' s Perspective', *Clinic Rev Bone Miner Metab*, 12, pp. 2–13.

van Oers, R. F. M., Ruimerman, R., van Rietbergen, B., et al. (2008) 'Relating osteon diameter to strain', *Bone*, 43(3), pp. 476–482.

van Oers, R. F. M., Wang, H. & Bacabac, R. G. (2015) 'Osteocyte Shape and Mechanical Loading', *Current Osteoporosis Reports*, 13(2), pp. 61–66.

O’Gorman, E. J. & Hone, D. W. E. (2012) 'Body Size Distribution of the Dinosaurs', *PLoS ONE*, 7(12).

Organ, C. L., Brusatte, S. L. & Stein, K. (2009) 'Sauropod dinosaurs evolved moderately sized genomes unrelated to body size', *Proceedings of the Royal Society B: Biological Sciences*. Royal Society, 276(1677), pp. 4303–4308.

Organ, C. L., Canoville, A., Reisz, R. R., et al. (2011) 'Paleogenomic data suggest mammal-like genome size in the ancestral amniote and derived large genome size in amphibians', *Journal of Evolutionary Biology*, 24(2), pp. 372–380.

Organ, C. L., Shedlock, A. M., Meade, A., et al. (2007) 'Origin of avian genome size and structure in non-avian dinosaurs.', *Nature*, 446(7132), pp. 180–184.

Oxnard, C. E. (1993) 'Bone and bones, architecture and stress, fossils and osteoporosis', *Journal of Biomechanics*, 26(SUPPL. 1), pp. 63–79.

Padian, K. (2013) 'Why Study the Bone Microstructure of Fossil Tetrapods?', in Padian, K. and Lamm, E. (eds) *Bone Histology of Fossil Tetrapods*. 1st edn. University of California Press, Berkeley, pp. 1–11.

Padian, K., Horner, J. R. & de Ricqlès, A. (2004) 'Growth in Small Dinosaurs and Pterosaurs : The Evolution of Archosaurian Growth Strategies', *Journal of Vertebrate Paleontology*, 24(3), pp. 555–571.

Padian, K. & Lamm, E. (2013) *Bone Histology Of Fossil Tetrapods*. 1st edn. University of California Press, Berkeley.

Padian, K., de Ricqlès, A. & Horner, J. R. (2001) 'Dinosaurian growth rates and bird origins', *Nature*, 412, pp. 405–408.

Pagel, M. (1999) 'Inferring the historical patterns of biological evolution', *Nature*, 401(6756), pp. 877–884.

Parfitt, A. M. (1994) 'Osteonal and Hemi-Osteonal Remodeling: The spatial and Temporal Framework for Signal Traffic in Adult Human Bone', *Journal of Cellular Biochemistry*, 55(3), pp. 273–286.

Parfitt, M., Drezner, M. K., Glorieux, F. H., et al. (1987) 'Bone Histomorphometry: Standardization of Nomenclature, Symbols, and Units', *Journal of bone and mineral research: the official journal of the American Society for Bone and Mineral Research*, 2(6).

Parins-Fukuchi, C. (2018) 'Use of Continuous Traits Can Improve Morphological Phylogenetics', *Systematic Biology*, 67(2), pp. 328–339.

Pavoine, S., Ollier, S., Pontier, D., et al. (2008) 'Testing for phylogenetic signal in phenotypic traits: New matrices of phylogenetic proximities', *Theoretical Population Biology*, 73(1), pp. 79–91.

Pavoine, S. & Ricotta, C. (2013) 'Testing for phylogenetic signal in biological traits: The ubiquity of cross-product statistics', *Evolution*, 67(3), pp. 828–840.

Pawlina, W. (2016) *Histology A Text and Atlas*. 7th edn. Philadelphia: Wolters Kluwer Health.

Peabody, F. E. (1961) 'Annual growth zones in living and fossil vertebrates', *Journal of Morphology*, 108(1), pp. 11–62.

Pearman, P. B., Guisan, A., Broennimann, O., et al. (2008) 'Niche dynamics in space and time', *Trends in Ecology and Evolution*, 23(3), pp. 149–158.

Pennell, M. W., Eastman, J. M., Slater, G. J., et al. (2014) 'Geiger v2.0: An expanded suite of methods for fitting macroevolutionary models to phylogenetic trees', *Bioinformatics*, 30(15), pp. 2216–2218.

Petrtyl, M., Heřt, J. & Fiala, P. (1996) 'Spatial organization of the haversian bone in man', *Journal of Biomechanics*, 29(2), pp. 161–167.

Phatsara, M., Nganvongpanit, K. & Mahakkanukrauh, P. (2016) 'Comparative morphometric study for distinguishing between human and non-human mammalian (cow, dog, horse, monkey and pig) long bones', *Chiang Mai Veterinary Journal*, 14(May), pp. 23–38.

Pigliucci, M. (2008) 'Is evolvability evolvable?', *Nature Reviews Genetics*, 9(1), pp. 75–82.

Pigliucci, M. (2010) 'Okasha's evolution and the levels of selection: toward a broader conception of theoretical biology', *Biology & Philosophy*, 25(3), pp. 405–415.

de Pinna, M. C. C. (1991) 'Concepts and tests of homology in the cladistics paradigm', *Cladistics*, 7(4), pp. 367–394.

Pintore, R., Houssaye, A., Nesbitt, S. J., et al. (2021) 'Femoral specializations to locomotor habits in early archosauriforms', *Journal of Anatomy*. John Wiley and Sons Inc.

Polly, P. D. (2008) 'Developmental dynamics and G-Matrices: Can morphometric spaces be used to model phenotypic evolution?', *Evolutionary Biology*, 35(2), pp. 83–96.

Ponton, F., Montes, L., Castanet, J., et al. (2007) 'Bone histological correlates of high-frequency flapping flight and body mass in the furculae of birds: a phylogenetic approach', *Biological Journal of the Linnean Society*, 91, pp. 729–738.

Prondvai, E., Stein, K. H. W., de Ricqlés, A., et al. (2014) 'Development-based revision of bone tissue classification: the importance of semantics for science', *Biological Journal of the Linnean Society*, 112(4), pp. 799–816.

Püschel, T. A. & Benítez, H. A. (2014) 'Femoral Functional Adaptation: A Comparison Between Hunter Gatherers and Farmers Using Geometric Morphometrics', *International Journal of Morphology*, 32(2), pp. 627–633.

Quekett, J. (1849a) 'Additional Observations on the intimate Structure of Bone', *Transactions of the Microscopical Society of London*, 2(1), pp. 59–64.

Quekett, J. (1849b) 'On the intimate Structure of Bone, as composing the Skeleton in the four great Classes of Animals, viz., Mammals, Birds, Reptiles, and Fishes, with some Remarks on the great Value of the Knowledge of such Structure in determining the Affinities of Minute F', *Transactions of the Microscopical Society of London*, 2(1), pp. 46–58.

Redelstorff, R., Hübner, T. R., Chinsamy, A., et al. (2013) 'Bone histology of the stegosaur Kentrosaurus aethiopicus (Ornithischia: Thyreophora) from the Upper Jurassic of Tanzania.', *Anatomical record (Hoboken, N.J. : 2007)*, 296(6), pp. 933–52.

Reid, R. E. H. (1981) 'Lamellar-zonal Bone with Zones and Annuli in the Pelvis of a Sauropod Dinosaur', *Nature*, 292, pp. 49–51.

Reid, R. E. H. (1983) 'High vascularity in bones of dinosaurs, mammals and birds', *Geological Magazine*, 120(02), pp. 191–194.

Reid, R. E. H. (1984) 'Primary bone and dinosaurian physiology', *Geological Magazine*, 121(April), pp. 589–598.

Reid, R. E. H. (1996) 'Bone histology of the Cleveland-Lloyd dinosaurs and of dinosaurs in general, Part I: Introduction: Introduction to bone tissues', *Geology Studies, Brigham Young University*, 41, pp. 25–72.

Reid, R. E. H. (2012) 'How Dinosaurs Grew', in Brett-Surman, M. K., Holtz, T. R., and Farlow, J. O. (eds) *The Complete Dinosaur*. Indiana University Press, pp. 419–421.

Remaggi, F., Palumbo, C. & Ferretti, M. (1998) 'Histomorphometric study on the osteocyte lacuno-canalicular network in animals of different species. I. Woven-fibered and parallel-fibered bones', *Italian Journal of Anatomy and Embryology*, 103(4), pp. 145–155.

Revell, L. J. (2010) 'Phylogenetic signal and linear regression on species data', *Methods in Ecology and Evolution*. Wiley, 1(4), pp. 319–329.

Revell, L. J. (2012) 'phytools: An R package for phylogenetic comparative biology (and other things)', *Methods in Ecology and Evolution*, 3(2), pp. 217–223.

Revell, L. J., Harmon, L. J., Collar, D. C., et al. (2008) 'Phylogenetic Signal, Evolutionary Process, and Rate', *Systematic Biology*, 57(4), pp. 591–601.

Rho, J. Y., Kuhn-Spearing, L. & Zioupos, P. (1998) 'Mechanical properties and the hierarchical structure of bone', *Medical Engineering and Physics*, 20(2), pp. 92–102.

de Ricqlès, A. (1975) 'Recherches Paléohistologiques sur les os Longs des Tétrapodes VII. Sur la Classification, la Signification Fonctionnelle et L'histoire des Tissus Osseux des Tétrapodes. Première Partie', *Annales de Paléontologie*, 61, pp. 51–129.

de Ricqlès, A. (1976) 'Recherches Paléohistologiques sur les os Longs des Tétrapodes VII. Sur la Classification, la Signification Fonctionnelle et L'histoire des Tissus Osseux des Tétrapodes', *Annales de Paléontologie*, 62, pp. 71–126.

de Ricqlès, A. (1977) 'Recherches Paléohistologiques sur les os Longs des Tétrapodes VII. Sur la Classification, la Signification Fonctionnelle et L'histoire des Tissus Osseux des Tétrapodes. Première Partie 2/ Fonctions.', *Annales de Paléontologie*, 63, pp. 33–56, 133–160.

de Ricqlès, A. (1978) 'Recherches Paléohistologiques sur les os Longs des Tétrapodes VII. Sur la Classification, la Signification Fonctionnelle et L'histoire des Tissus Osseux des Tétrapodes 3: Evolution', *Annales de Paléontologie*, 64, pp. 85–111, 153–184.

de Ricqlès, A. (1983) 'Cyclical Growth in the long Limb Bones of a Sauropod Dinosaur', *Acta Palaeontologica Polonica*, 28(1–2), pp. 225–232.

de Ricqlès, A., Castanet, J. & Francillon-Vieillot, H. (2004) 'The “message” of bone tissue in paleoherpetology', *Italian Journal of Zoology*, 71(sup2), pp. 3–12.

de Ricqlès, A. & Horner, J. R. (2003) 'L'histologie osseuse de quelques archosauriens pseudosuchiens triasiques et formes apparentées', *Annales de Paleontologie*, 89(2), pp. 67–101.

de Ricqlès, Armand, Padian, K., Knoll, F., et al. (2008) 'On the origin of high growth rates in archosaurs and their ancient relatives: Complementary histological studies on Triassic archosauriforms and the problem of a “phylogenetic signal” in bone histology', *Annales de Paleontologie*, 94(2), pp. 57–76.

de Ricqlès, A., Padian, K., Knoll, F., et al. (2008) 'On the origin of high growth rates in archosaurs and their ancient relatives: Complementary histological studies on Triassic archosauriforms and the problem of a “phylogenetic signal” in bone histology', *Annales de Paleontologie*, 94(2), pp. 57–76.

de Ricqlès, A. J. (2011) 'Vertebrate palaeohistology: Past and future', *Comptes Rendus - Palevol*, 10(5–6), pp. 509–515.

de Ricqlès, A. J. (2021) 'Paleohistology: An historical - bibliographical introduction', in de Buffrénil, V., de Ricqlès, A. J., Zylberberg, L., et al. (eds) *Vertebrate Skeletal Histology and Paleohistology*. 1st edn. Boca Raton: CRC Press, pp. 3–26.

Riesenfeld, A. (1972) 'Metatarsal robusticity in bipedal rats', *American Journal of Physical Anthropology*, 36(2), pp. 229–233.

Riggs, C. M., Lanyon, L. E. & Boyde, A. (1993) 'Functional associations between collagen fibre orientation and locomotor strain direction in cortical bone of the equine radius', *Anatomy and Embryology*, 187(3), pp. 231–238.

Rogers, C. & Erickson, G. M. (2005) 'Sauropod Histology: Microscopic Views on the lives of Giants', in Rogers, A. C. and Wilson, J. A. (eds) *The Sauropods*. University of California Press, pp. 303–362.

Royo-Torres, R., Cobos, A., Luque, L., et al. (2009) 'High European sauropod dinosaur diversity during Jurassic-Cretaceous transition in riodeva (teruel, Spain)', *Palaeontology*, 52(5), pp. 1009–1027.

Ruff, C. B., Holt, B. & Trinkaus, E. (2006) 'Who's Afraid of the Big Bad Wolff?: "Wolff's Law" and Bone Functional Adaptation', *American Journal of Physical Anthropology*, 129, pp. 484–498.

Ruse, M. (2003) *Darwin and Design: Does Evolution Have a Purpose?* New Brunswick: Harvard University Press.

Sanchez, S., Ahlberg, P. E., Trinajstić, K. M., et al. (2012) 'Three-dimensional synchrotron virtual paleohistology: A new insight into the world of fossil bone microstructures', *Microscopy and Microanalysis*, 18(5), pp. 1095–1105.

Sanchez, S., Dupret, V., Tafforeau, P., et al. (2013) '3D Microstructural Architecture of Muscle Attachments in Extant and Fossil Vertebrates Revealed by Synchrotron Microtomography', *PLoS ONE*, 8(2), pp. 1–16.

Sanchez, S., Germain, D., de Ricqlès, A., et al. (2010) 'Limb-bone histology of temnospondyls: Implications for understanding the diversification of palaeoecologies and patterns of locomotion of Permo-Triassic tetrapods', *Journal of Evolutionary Biology*, 23(10), pp. 2076–2090.

Sander, M. P., Klein, N., Buffetaut, E., et al. (2004) 'Adaptive radiation in sauropod dinosaurs: bone histology indicates rapid evolution of giant body size through acceleration', *Organisms Diversity & Evolution*, 4(3), pp. 165–173.

Sander, P. M. (1999) 'Life history of Tendaguru sauropods as inferred from long bone histology', *Fossil Record*, 2(1), pp. 103–112.

Sander, P.M. (2000) 'Longbone Histology of the Tendaguru Sauropods: Implications for Growth and Biology', *Paleobiology*, 26(3), pp. 466–488.

Sander, P. M. (2000) 'Prismless enamel in amniotes: terminology, function, and evolution', in Teaford, M. F., Smith, M. M., and Ferguson, M. W. J. (eds) *Development, Function and Evolution of Teeth*. Cambridge University Press, pp. 92–106.

Sander, P Martin, Christian, A., Clauss, M., et al. (2011) 'Biology of the sauropod dinosaurs: the evolution of gigantism.', *Biological reviews of the Cambridge Philosophical Society*, 86(1), pp. 117–55.

Sander, P. M. & Clauss, M. (2008) 'Sauropod Gigantism', *Science*. Royal Society, 322(5899), pp. 200–201.

Sander, P. M. & Klein, N. (2005) 'Developmental plasticity in the life history of a prosauropod dinosaur.', *Science (New York, N.Y.)*, 310(5755), pp. 1800–1802.

Sander, P.M., Klein, N., Stein, K., et al. (2011) 'Sauropod Bone Histology and Its Implications for Sauropod Biology', in Klein, Nicole, Remes, K., Gee, C. T., et al. (eds) *Biology of the Sauropod Dinosaurs*. Indiana University Press.

Sander, P. M., Mateus, O., Laven, T., et al. (2006) 'Bone histology indicates insular dwarfism in a new Late Jurassic sauropod dinosaur', *Nature*, 441(7094), pp. 739–741.

Sander, P. M. & Tückmantel, C. (2003) 'Bone lamina thickness, bone apposition rates, and age estimates in sauropod humeri and femora', *Paläontologische Zeitschrift*, 77(1), pp. 161–172.

Sanna, S., Jackson, A. U., Nagaraja, R., et al. (2008) 'Common variants in the GDF5-BFZB region are associated with variation in human height', *Nature Genetics*, 40(2), pp. 198–203.

Scheyer, T. M., Klein, N. & Sander, P. M. (2010) 'Developmental palaeontology of Reptilia as revealed by histological studies', *Seminars in Cell and Developmental Biology*. Elsevier Ltd, 21(4), pp. 462–470.

Scheyer, T. M. & Sander, P. M. (2004) 'Histology of ankylosaur osteoderms : implications for systematics and function', *Journal of Vertebrate Paleontology*, 24(4), pp. 874–893.

Scheyer, T. M., Sander, P. M., Joyce, W. G., et al. (2007) 'A plywood structure in the shell of fossil and living soft-shelled turtles (Trionychidae) and its evolutionary implications', *Organisms Diversity and Evolution*, 7(2), pp. 136–144.

Schluter, D. (2000) 'Ecological character displacement in adaptive radiation', *American Naturalist*, 156(S4), pp. S4–S16.

Schwarz-Wings, D. & Böhm, N. (2014) 'A morphometric approach to the specific separation of the humeri and femora of Dicraeosaurus from the Late Jurassic of Tendaguru, Tanzania', *Acta Palaeontologica Polonica*, 59(1), pp. 81–98.

Schweitzer, M. H., Wittmeyer, J. L. & Horner, J. R. (2005) 'Gender-Specific Reproductive Tissue in Ratites and Tyrannosaurus rex', *Science*, 308(5727), pp. 1456–1460.

Seilacher, A. (1970) 'Arbeitskonzept zur Konstruktions-Morphologie', *Lethaia*, 3(1), pp. 393–396.

Seilacher, A. & Gishlick, A. D. (2015) *Morphodynamics* . 1st edn. CRC Press.

Sessegolo, C., Burlet, N. & Haudry, A. (2016) 'Strong phylogenetic inertia on genome size and transposable element content among 26 species of flies', *Biology Letters*. Royal Society, 12(8).

Sharpey, W., Thompson, A. & Cleland, J. (1867) *Quain's Elements of Anatomy*. 7th Ed. Edited by W. Sharpey, A. Thompson, and J. Cleland. London: James Walton.

Skedros, J. G. (2005) 'Osteocyte lacuna population densities in sheep, elk and horse calcanei', *Cells Tissues Organs*, 181(1), pp. 23–37.

Skedros, J. G., Knight, A. N., Clark, G. C., et al. (2013) 'Scaling of Haversian canal surface area to secondary osteon bone volume in ribs and limb bones', *American Journal of Physical Anthropology*, 151(2).

Starck, J. M. & Chinsamy, A. (2002) 'Bone microstructure and developmental plasticity in birds and other dinosaurs', *Journal of Morphology*, 254(3), pp. 232–246.

Stein, K., Csiki, Z., Rogers, K. C., et al. (2010) 'Small body size and extreme cortical bone remodeling indicate phyletic dwarfism in *Magyarosaurus dacus* (Sauropoda: Titanosauria).', *Proceedings of the National Academy of Sciences of the United States of America*, 107(20), pp. 9258–9263.

Stein, K. & Prondvai, E. (2013) 'Rethinking the nature of fibrolamellar bone: an integrative biological revision of sauropod plexiform bone formation.', *Biological reviews of the Cambridge Philosophical Society*, 89(1), pp. 24–47.

Stein, K. W. H. & Werner, J. (2013) 'Preliminary analysis of osteocyte lacunar density in long bones of tetrapods: all measures are bigger in sauropod dinosaurs', *PLoS one*, 8(10), p. e77109.

Stein, M., Hayashi, S. & Sander, P. M. (2013) 'Long bone histology and growth patterns in ankylosaurs: implications for life history and evolution', *PloS one*, 8(7), p. e68590.

Steppan, S. J., Phillips, P. C. & Houle, D. (2002) 'Comparative quantitative genetics: evolution of the Gmatrix', *Trends in Ecology & Evolution*, 17(7), pp. 320–327.

Sternfeld, R. (1911) 'Zur Nomenklatur der Gattung Gigantosaurus Fraas', *Sitzungsberichte der Gesellschaft Naturforschender Freunde zu Berlin*, 8, p. 398.

Stock, J. & Shaw, C. (2007) 'Which Measures of Diaphyseal Robusticity Are Robust? A Comparison of External Methods of Quantifying the Strength of Long Bone Diaphyses to Cross-Sectional Geometric Properties', *American Journal of Physical Anthropology*, 134, pp. 412–423.

Stoltzfus, A. (1999) 'On the possibility of constructive neutral evolution', *Journal of Molecular Evolution*, 49(2), pp. 169–181.

Strong, E. E. & Lipscomb, D. (1999) 'Character Coding and Inapplicable Data', *Cladistics*, 15, pp. 363–371.

Swanepoel, E. (2003) *Analysis of the faunal remains of Kemp's Caves and an investigation into possible computerized classification of bones*. University of Pretoria.

Swanepoel, E. & Steyn, M. (2011) 'Robusticity of Bovidae skeletal elements from southern Africa and their potential in species identification', *Annals of the Ditsong National Museum of Natural History*, 1, pp. 41–52.

Symonds, M. & Blomberg, S. (2014) *A Primer on Phylogenetic Generalised Least Squares, Modern Phylogenetic Comparative Methods and their Application in Evolutionary Biology*.

Taylor, M. P. (2009) 'A re-evaluation of *Brachiosaurus altithorax* Riggs 1903 (Dinosauria, Sauropoda) and its generic separation from *Giraffatitan brancai* (Janensch 1914)', *Journal of Vertebrate Paleontology*, 29(3), pp. 787–806.

Teti, A. & Zallone, A. (2009) 'Do osteocytes contribute to bone mineral homeostasis? Osteocytic osteolysis revisited', *Bone*. Elsevier Inc., 44(1), pp. 11–16.

Thiese, M. S., Ronna, B. & Ott, U. (2016) 'P value interpretations and considerations', *Journal of Thoracic Disease*, 8(9), pp. E928–E931.

van Tol, A. F., Roschger, A., Repp, F., et al. (2020) 'Network architecture strongly influences the fluid flow pattern through the lacunocanicular network in human osteons', *Biomechanics and Modeling in Mechanobiology*. Springer, 19(3), pp. 823–840.

Tschopp, E., Mateus, O. & Benson, R. B. J. (2015) 'A specimen-level phylogenetic analysis and taxonomic revision of Diplodocidae (Dinosauria, Sauropoda)', *PeerJ*, 3, p. e857.

Tsegai, Z. J., Kivell, T. L., Gross, T., et al. (2013) 'Trabecular bone structure correlates with hand posture and use in hominoids', *PLoS ONE*, 8(11).

Tumarkin-deratzian, A. R. (2007) 'Fibrolamellar Bone in Wild Alligator mississippiensis', *Journal of Herpetology*, 41(2), pp. 341–345.

Upchurch, P., Barrett, P. M., Dodson, P., et al. (2004) 'Sauropoda: The Dinosauria', in WEISHAMPEL, D. B., DODSON, P., and OSMÓLSKA, H. (eds). University of California Press.

Urbanová, P. & Novotný, V. (2005) 'Distinguishing between human and non-human bones: Histometric method for forensic anthropology', *Anthropologie*, 43, pp. 77–85.

Urino, D. A. I., Anti, M. D., Walter, S., et al. (2013) 'Modern techniques for ancient bones: Vertebrate Palaeontology and medical CT analysis', *New Advances in Italian Paleontology*, 2, pp. 24–26.

Vatsa, A., Breuls, R. G., Semeins, C. M., et al. (2008) 'Osteocyte morphology in fibula and calvaria - Is there a role for mechanosensing?', *Bone*, 43(3), pp. 452–458.

Verborgt, O., Gibson, G. J. & Schaffler, M. B. (2000) 'Loss of osteocyte integrity in association with microdamage and bone remodeling after fatigue in vivo', *Journal of Bone and Mineral Research*, 15(1), pp. 60–67.

Vickaryous, M. K. & Hall, B. K. (2008) 'Development of the dermal skeleton in *Alligator mississippiensis* (Archosauria, Crocodylia) with comments on the homology of osteoderms', *Journal of Morphology*, 269(4), pp. 398–422.

Vickaryous, M. K., Maryanska, T., Weishampel, D. B. 363-392 (2004) 'Ankylosauria', in Weishampel, D.B., Dodson, P., Osmolska, H. (ed.) *The Dinosauria*. 2nd edn. University of California Press, Berkeley, pp. 363–392.

Waskow, K. & Mateus, O. (2017) 'Dorsal rib histology of dinosaurs and a crocodile from western Portugal: Skeletochronological implications on age determination and life history traits', *Comptes Rendus - Palevol. Académie des sciences*, 16(4), pp. 1–15.

Wedel, M. J. (2003) 'Vertebral Pneumaticity, Air Sacs, and the Physiology of Sauropod Dinosaurs', *Paleobiology*, 29(2), pp. 243–255.

Weiss, P. & Ferris, W. (1954) 'Electromicrograms of Larval Amphibian Epidermis', *Experimental Cell Research*, 549, pp. 546–549.

Wiens, J. J., Ackerly, D. D., Allen, A. P., et al. (2010) 'Niche conservatism as an emerging principle in ecology and conservation biology', *Ecology Letters*, 13(10), pp. 1310–1324.

Wiens, J. J. & Graham, C. H. (2005) 'Niche conservatism: Integrating evolution, ecology, and conservation biology', *Annual Review of Ecology, Evolution, and Systematics*, 36, pp. 519–539.

Wiersma-Weyand, K., Canoville, A., Siber, H., et al. (2021) 'Testing hypothesis of skeletal unity using bone histology: The case of the sauropod remains from the Howe-Stephens and Howe Scott quarries (Morrison Formation, Wyoming, USA)', *Palaeontologia Electronica*. Coquina Press, 24(1), pp. 1–33.

Wild, R. (1991) 'Janenschia n.g. robusta (E. Fraas 1908) pro Tornieria robusta (E. Fraas 1908) (Reptilia, Saurischia, Sauropodomorpha)', *Stuttgarter Beiträge zur Naturkunde. Serie B. Geologie und Paläontologie*, 173, pp. 1–4.

Williams, P. D., Pollock, D. D., Blackburne, B. P., et al. (2006) 'Assessing the accuracy of ancestral protein reconstruction methods', *PLoS Computational Biology*, 2(6), pp. 0598–0605.

Wilson, J. A. (2002) 'Sauropod dinosaur phylogeny: critique and cladistic analysis', *Zoological Journal of the Linnean Society*, 136(2), pp. 215–275.

Wilson, J. A., Curry Rogers, K., Editor, B., et al. (2012) 'Sauropoda', in *The Complete Dinosaur*. Indiana University Press, pp. 444–481.

Wilson, L. E. & Chin, K. (2014) 'Comparative osteohistology of Hesperornis with reference to pygoscelid penguins: the effects of climate and behaviour on avian bone microstructure', *Royal Society Open Science*, 1(3), pp. 140245–140245.

Wolff, J. (1892) *The Law of Bone Remodeling*. New York: Springer Berlin Heidelberg (translated by P. Maquet and R. Furlong).

Wood, J. R. & de Pietri, V. L. (2015) 'Next-generation paleornithology: Technological and methodological advances allow new insights into the evolutionary and ecological histories of living birds', *The Auk*, 132(2), pp. 486–506.

Woodruff, D. C., Fowler, D. W. & Horner, J. R. (2017) 'A new multi-faceted framework for deciphering diplodocid ontogeny.', *Palaeontologica Electronica*, 20.3.43A(September), pp. 1–53.

Woodward, H. N., Horner, J. R. & Farlow, J. O. (2014) 'Quantification of intraskeletal histovariability in *Alligator mississippiensis* and implications for vertebrate osteohistology.', *PeerJ*, 2, p. e422.

Woodward, H. N. & Lehman, T. M. (2009) 'Bone histology and microanatomy of *Alamosaurus sanjuanensis* (Sauropoda: Titanosauria) from the maastrichtian of Big Bend National Park, Texas', *Journal of Vertebrate Paleontology*, 29(3), pp. 807–821.

Wright, N. A., Gregory, T. R. & Witt, C. C. (2014) 'Metabolic “engines” of flight drive genome size reduction in birds', *Proceedings of the Royal Society B: Biological Sciences*. Royal Society, 281(1779).

Wright, S. (1931) 'Evolution in Mendelian Populations', *Genetics*, 16, pp. 97–159.

Wright, S. (1977) *Evolution and the Genetics of Populations, Volume 3 Experimental Results and Evolutionary Deductions*. University of Chicago Press.

Yuan, H., Huang, Y., Mao, Yi., et al. (2021) 'The Evolutionary Patterns of Genome Size in Ensifera (Insecta: Orthoptera)', *Frontiers in Genetics*. Frontiers Media S.A., 12, pp. 1–13.

Zedda, M., Lepore, G., Manca, P., et al. (2008) 'Comparative bone histology of adult horses (*Equus caballus*) and cows (*Bos taurus*)', *Journal of Veterinary Medicine Series C: Anatomia Histologia Embryologia*, 37(6), pp. 442–445.

# Supplementary information

**S1** - Data spreadsheet

**S2** - Maidment, S. C. R., Strachan, S. J., Ouarhache, D., Scheyer, T. M., Brown, E. E., Fernandez, V., Johanson, Z., Raven, T. J., & Barrett, P. M. (2021). Bizarre dermal armour suggests the first African ankylosaur. *Nature Ecology and Evolution*.